Phosphate (P_i) is an essential nutrient for all living organisms and plays a crucial role in modern agriculture. Most of the P_i used by humans is derived from mined P_i rock and processed into agricultural fertilizers. However, the currently established linear P_i economy faces challenges such as geopolitical dependence on limited reserves, rising fertilizer prices, heavy metal contamination, and ecological damage caused by extensive P_i application. These challenges are expected to intensify due to population growth and increasing meat consumption. Sustainable P_i management therefore requires a transition toward a circular P_i economy.

This thesis contributes to this transition by advancing biotechnological polyphosphate (polyP) production using *Saccharomyces cerevisiae (S. cerevisiae)*. The previously established polyP hyperaccumulation protocol was adapted for high-throughput screening and combined with the JC-D7 fluorescence assay to analyze yeast strains for altered polyP content, chain length, and growth performance. The JC-D7 assay demonstrated high robustness against various abiotic factors and extraction conditions, enabling rapid classification of yeast strains based on their polyP production levels. Furthermore, systematic evaluation of trace elements and vitamins during the starvation phase revealed zinc and inositol as key factors enhancing polyP accumulation in *S. cerevisiae*. Zinc stimulates the P_i-responsive signaling pathway during P_i starvation. The role of inositol was examined using phospholipid mutants and strains carrying deletions of genes involved in inositol synthesis or transport. In this context, the minimal medium requirements for both the starvation and feeding phases of the polyP hyperaccumulation process were redefined. Collectively, these findings contribute to reduced nutrient consumption, improved product purification efficiency, and a deeper understanding of polyP metabolism in *S. cerevisiae*.

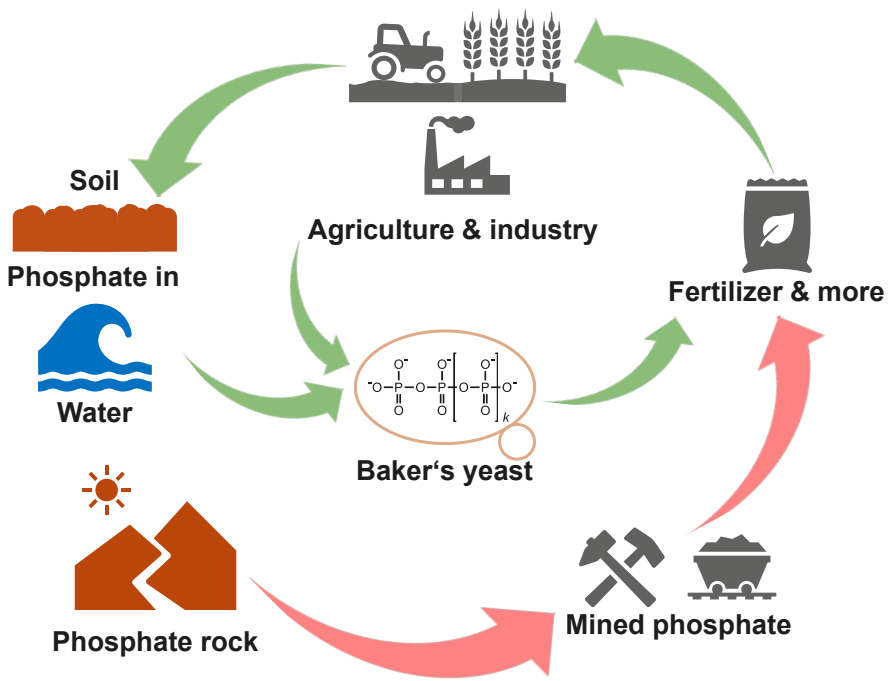
The results of this dissertation, combined with process-guided strain engineering, provide an opportunity to promote the industrial implementation of biotechnological polyP production with *S. cerevisiae* and contribute to the transition toward a circular P_i economy. To fully realize its potential, informed decisions regarding raw materials, strain development, product applications, and process design, supported by collaboration between research, industry, policy, and society, are essential.

ISBN 978-3-98555-358-7

Contributions to a circular phosphate economy – Polyphosphate production in *Saccharomyces cerevisiae*
Alexander Deitert

Alexander Deitert

Contributions to a circular phosphate economy – Polyphosphate production in *Saccharomyces cerevisiae*



iAMB Institute of Applied Microbiology | ABBt Aachen Biology and Biotechnology | RWTH AACHEN UNIVERSITY
Edition Wissenschaft Apprimus

Contributions to a circular phosphate economy – Polyphosphate production in *Saccharomyces cerevisiae*

Von der Fakultät für Mathematik und Naturwissenschaften der
RWTH Aachen University zur Erlangung des akademischen Grades eines Doktors
der Naturwissenschaften genehmigte Dissertation

vorgelegt von

Alexander Deitert
Molekulare und Angewandte Biotechnologie, M.Sc.

aus
Bonn, Nordrhein-Westfalen, Deutschland

Berichter:
Univ.-Prof. Dr.-Ing. Lars Mathias Blank
Univ.-Prof. Dr. rer. nat. Andrij Pich

Tag der mündlichen Prüfung: 08.07.2026

Diese Dissertation ist auf den Internetseiten der Universitätsbibliothek verfügbar.

Bibliografische Information der Deutschen Nationalbibliothek
Die Deutsche Nationalbibliothek verzeichnet diese Publikation in der Deutschen Nationalbibliografie; detaillierte bibliografische Daten sind im Internet über https://portal.dnb.de abrufbar.

Alexander Deitert:

Contributions to a circular phosphate economy – Polyphosphate production in *Saccharomyces cerevisiae*

1. Auflage, 2026

Gedruckt auf holz- und säurefreiem Papier, 100% chlorfrei gebleicht.

Copyright Apprimus Verlag, Aachen, 2026
Wissenschaftsverlag des Instituts für Industriekommunikation und Fachmedien
an der RWTH Aachen
Steinbachstr. 25, 52074 Aachen, Deutschland
Internet: www.apprimus-verlag.de, E-Mail: info@apprimus-verlag.de

Alle Rechte, auch das des auszugsweisen Nachdruckes, der auszugsweisen oder vollständigen Wiedergabe, der Speicherung in Datenverarbeitungsanlagen und der Übersetzung, vorbehalten.

Printed in Germany

ISBN 978-3-98555-358-7

Eidesstattliche Erklärung

Ich, Alexander Deitert, erkläre hiermit, dass diese Dissertation und die darin dargelegten Inhalte die eigenen sind und selbstständig, als Ergebnis der eigenen originären Forschung, generiert wurden.

Hiermit erkläre ich an Eides statt

1. Diese Arbeit wurde vollständig oder größtenteils in der Phase als Doktorand dieser Fakultät und Universität angefertigt;
2. Sofern irgendein Bestandteil dieser Dissertation zuvor für einen akademischen Abschluss oder eine andere Qualifikation an dieser oder einer anderen Institution verwendet wurde, wurde dies klar angezeigt;
3. Wenn immer andere eigene oder Veröffentlichungen Dritter herangezogen wurden, wurden diese klar benannt;
4. Wenn aus eigenen oder aus Veröffentlichungen Dritter zitiert wurde, wurde stets die Quelle hierfür angegeben. Diese Dissertation ist vollständig meine eigene Arbeit, mit der Ausnahme solcher Zitate;
5. Alle wesentlichen Quellen von Unterstützung wurden benannt;
6. Wenn immer ein Teil dieser Dissertation auf der Zusammenarbeit mit anderen basiert, wurde von mir klar gekennzeichnet, was von anderen und was von mir selbst erarbeitet wurde;
7. Ein Teil oder Teile dieser Arbeit wurden zuvor veröffentlicht:
   Deitert, A., Fees, J., Mertens, A., Nguyen Van, D., Maares, M., Haase, H., Blank, L. M., and Keil, C. Rapid Fluorescence Assay for Polyphosphate in Yeast Extracts Using JC-D7. *Yeast*, 41, 593-604, 2024, doi: 10.1002/yea.3979.[1]
   Deitert, A., Baier, M., Eerlings, R., Fees, J., Österlein Kück, A., Repin, J., Demling, P., and Blank, L. M. Polyphosphate Accumulation Is Determined by Zinc and Inositol in *Saccharomyces cerevisiae*. *Yeast*, 0, 1–12, 2025, doi: 10.1002/yea.70006.[2]

Aachen, 08.01.2026

Alexander Deitert

[1]Reprinted (adapted) with permission from John Wiley & Sons Ltd. Open Access CC BY-NC-ND 4.0. © The Authors 2024.

[2]Reprinted (adapted) with permission from John Wiley & Sons Ltd. Open Access CC BY-NC-ND 4.0. © The Authors 2025.

Funding

The Bundesministerium für Bildung und Forschung (BMBF) is gratefully acknowledged for providing financial support (funding code 031B1143A).

Bundesministerium für Bildung und Forschung

The Werner Siemens-Stiftung is gratefully acknowledged for providing financial support within the WSS Research Center catalaix.

WSS
WERNER SIEMENS-STIFTUNG

Contributions

Science, particularly the fields of molecular and applied biotechnology, is characterized by its interdisciplinary nature. Collaborations are intended to leverage the expertise of each party and to advance joint projects. Accordingly, some of the results in this thesis were obtained through collaborations with other research institutions or through supervising student theses. At the beginning of each chapter, the contributions and assistance of others are acknowledged. In addition, this work builds on the expertise and practical experience gained at the Institute of Applied Microbiology (RWTH Aachen University, Aachen, Germany) through many years of research in the field of circular bioeconomy, for which I express my gratitude.

Tools

Digital tools such as ChatGPT (OpenAI) and Grammarly were employed exclusively for linguistic refinement and improvement of the English language style of this dissertation. These tools were used solely for language-related purposes and did not influence or contribute to the scientific content, results, or interpretations presented herein.

Danksagung

Zu Beginn möchte ich mich bei Prof. Dr.-Ing. Lars M. Blank für die Möglichkeit, meine Dissertation am Institut für Angewandte Mikrobiologie anfertigen zu können, und für die Übernahme der Erstbetreuung bedanken. Ich bin sehr froh, meine Dissertation an so einem modernen, kompetenten und offenen Lehrstuhl angefertigt zu haben. Vielen Dank für dein Vertrauen, dein offenes Ohr, deine unermüdliche Unterstützung sowie deinen wissenschaftlichen und persönlichen Rat. Besonders dankbar bin ich dir für all das, was du mir im Verlauf meiner Promotion ermöglicht hast. Das DAAD-Austauschprojekt und damit die einmalige Gelegenheit, nach sieben Jahren meine Schwester in Neuseeland zu besuchen, haben für mich sowohl fachlich als auch privat große Bedeutung gehabt. Deine Begeisterung für alles, was auch nur entfernt mit Mikrobiologie zu tun hat, war stets ansteckend, ebenso wie die legendären Kickerrunden am Abend, bei denen der Tisch jedes Mal mit ganzem Körpereinsatz bearbeitet wurde.

Des Weiteren möchte ich Prof. Dr. rer. nat. Andrij Pich für die Übernahme der Zweitkorrektur meiner Doktorarbeit danken.

Mein besonderer Dank gilt zudem der Werner Siemens-Stiftung für die großzügige Förderung im Rahmen des WSS Research Center catalaix sowie dem Bundesministerium für Bildung und Forschung (BMBF) für die Unterstützung im Rahmen des Projekts „Anwendung neuartiger Technologiekonzepte für die Phosphor-Rückgewinnung aus Biomasse zur Herstellung von Bio-Polyphosphaten“. Freie Forschung ist der Grundpfeiler unserer demokratischen Gesellschaft und eine wesentliche Voraussetzung für Innovationen am Wirtschaftsstandort Deutschland.

Philipp, ich möchte dir für deine herausragende Betreuung in der Polyphosphatarbeitsgruppe danken. Du hattest immer ein offenes Ohr, warst selbst bei den kleinsten Problemen sofort zur Stelle und hast mich insbesondere bei der Erstellung von Manuskripten und dieser Arbeit sehr unterstützt. Deine offene, ehrliche und lockere Art hat entscheidend zur großartigen Arbeitsatmosphäre beigetragen. Zum Schluss habe ich sogar angefangen, deine Witze ein wenig zu mögen. Roy, auch dir möchte ich für deine Unterstützung bei der Koordination des Screenings in Leuven und darüber hinaus herzlich danken. Es war immer einfach und angenehm, mit Fragen oder Herausforderungen auf dich zuzukommen. Ein großer Dank gilt auch meinen Kolleg*innen der Polyphosphat-Arbeitsgruppe: Makarius Baier, Jana Fees und Tobias Karmainski. Ohne euch hätte die Arbeit an diesem Themenfeld bei Weitem nicht so viel Freude bereitet. Besonders schätze ich unseren offenen und vertrauensvollen Austausch in den vergangenen Jahren. Dieser war stets von Unterstützung, Verständnis und Kollegialität geprägt. Ich bin überzeugt, dass wir genau deshalb das PolyP-Arbeitsfeld am iAMB gemeinsam spürbar vorangebracht haben. Ein besonderer Dank geht an dich, Jana. Du warst meine erste Ansprechpartnerin für PolyP im Labor und hast mir

den Übergang vom Studium zur Promotion ungemein erleichtert. Unvergessen bleibt unsere gemeinsame Zeit in Neuseeland. Dass meine Eltern dir regelmäßig liebe Grüße ausrichten, obwohl sie dich nie persönlich getroffen haben, spricht für sich. Makarius und Tobias, ihr wart nicht nur großartige Kollegen im Labor, sondern auch im Büro. Von eurer Expertise konnte ich enorm profitieren. Danke für eure Unterstützung, eure Geduld und die vielen gemeinsamen Stunden im Projekt. Ein herzliches Dankeschön geht außerdem an meine Studierenden: Ailin Österlein, Julia Repin, Anna Mertens, Lennart Brans, Paula Teucher, Alina Maas und Angelina Henk. Ihr habt mit eurer engagierten Mitarbeit entscheidend zu dieser Arbeit beigetragen. Die Zusammenarbeit mit euch hat mir nicht nur fachlich, sondern auch persönlich große Freude bereitet. Vielen Dank für euren unermüdlichen Einsatz und eure Begeisterung.

Darüber hinaus möchte ich mich bei allen derzeitigen und ehemaligen Mitarbeitenden sowie Studierenden des iAMB herzlich bedanken. Besonders hervorheben möchte ich an dieser Stelle Dr. Martin Zimmermann, Annette Scheer, Gisela Beisel und Isabel Reuter. Euer unermüdlicher Einsatz für das Institut hat mich von Anfang an beeindruckt. Ich weiß eure tatkräftige Unterstützung sehr zu schätzen. Die Atmosphäre und die Zusammenarbeit am iAMB sind etwas ganz Besonderes. Das Arbeitsklima ist geprägt von Unterstützung, Zusammenhalt und gegenseitigem Verständnis. Es hat mir immer sehr viel Freude bereitet, zur Arbeit zu kommen, da ich dort Freund*innen statt Kolleg*innen begegnet bin. Dazu haben auch die vielfältigen Aktivitäten außerhalb der Arbeitszeit beigetragen: das iAMB-Oktoberfest, der iAMB-Karneval, der iAMB-Institutstrip, die iAMB-Weihnachtsfeier und das gemeinsame Feierabendbier. Und ganz ehrlich: Ein eigener Kühlschrank im Severraum ist einfach der Hammer!

Mein größter Dank gilt jedoch meiner Familie. Ihr habt mich von klein auf stets unterstützt, mir Rückhalt gegeben und ich konnte mich immer auf euch verlassen. Ihr habt mir den Weg zur Universität erst ermöglicht und damit eine Chance geschaffen, von der viele nur träumen können. Papa, du warst es, der mein Interesse an der Biologie bereits früh geweckt und damit meinen weiteren Karriereweg entscheidend geprägt hat. Mama, du hast mir immer vermittelt, dass sich Fleiß und Ehrgeiz auszahlen. Franny, dir danke ich für deinen schwesterlichen Beistand. Nachdem du mit 18 Jahren nach Neuseeland gegangen bist, war es etwas ganz Besonderes, dass meine Promotion uns in diesem wunderbaren Land wieder zusammengeführt hat. Fabienne, dir gilt mein besonderer Dank. Seit mehr als 12 Jahren stehst du felsenfest an meiner Seite und bist immer für mich da. Meine Promotion war nicht immer einfach und oft sehr stressig. Du hast mir stets Verständnis entgegengebracht, mich unermüdlich unterstützt und mir an vielen Stellen den Rücken freigehalten. Dafür bin ich dir zutiefst dankbar. Ich hatte das große Glück, mit 17 Jahren dem Menschen zu begegnen, den viele ihr Leben lang suchen. Ich liebe dich und freue mich sehr auf unsere gemeinsame Zukunft.

“As many know, the Chinese expression for "crisis" consists of two characters side by side. The first is the symbol for "danger," the second the symbol for "opportunity".”

-Al Gore-

Table of Contents

Table of Contents I

Summary V

Zusammenfassung VII

Nomenclature XI

List of Figures XV

List of Tables XIX

Chapter 1 1

1 General Introduction 3

1.1 The natural phosphate cycle 3
1.2 The human phosphate cycle and phosphate problematic 4
1.3 Phosphorous removal strategies 7
1.4 Phosphorus recovery strategies 8
1.5 Biological phosphorus removal strategies 9
1.6 Inorganic polyphosphates: structure, applications, and production 10
1.7 Phosphate homeostasis in *Saccharomyces cerevisiae* 13
1.8 Polyphosphate metabolism in *Saccharomyces cerevisiae* 16
1.9 Scope and outline of this thesis 18

Chapter 2 21

2 Material and Methods 23

2.1 General Methods 23
2.2 Material and Methods for Chapter 3 26
2.3 Material and Methods for Chapter 4 27
2.4 Material and Methods for Chapter 5 29
2.5 Material and Methods for Chapter 6 32
2.6 Material and Methods for Chapter 7 34

Chapter 3 39

3 Rapid fluorescence assay for polyphosphate in yeast extracts using JC-D7 41

3.1 Abstract 41
3.2 Introduction 41

3.3 Results ... 43
3.4 Discussion ... 50
3.5 Conclusion ... 53

Chapter 4 ... 55

4 Screening of the Yeast Knockout collection to identify new engineering targets in polyphosphate metabolism ... 57

4.1 Abstract ... 57
4.2 Introduction ... 57
4.3 Results ... 59
4.4 Discussion ... 64
4.5 Conclusion ... 66

Chapter 5 ... 69

5 Screening of an industrial *Saccharomyces cerevisiae* library to identify polyphosphate hyperaccumulating strains ... 71

5.1 Abstract ... 71
5.2 Introduction ... 71
5.3 Results ... 73
5.4 Discussion ... 82
5.5 Conclusion ... 85

Chapter 6 ... 87

6 Influence of trace elements and vitamins on polyphosphate hyperaccumulation in *Saccharomyces cerevisiae* ... 89

6.1 Abstract ... 89
6.2 Introduction ... 89
6.3 Results ... 90
6.4 Discussion ... 100
6.5 Conclusion ... 102

Chapter 7 ... 105

7 Characterizing the starvation and feed phase in the hyperaccumulation protocol for polyphosphate production ... 107

7.1 Abstract ... 107
7.2 Introduction ... 107

7.3 Results 109
7.4 Discussion 121
7.5 Conclusion 125

Chapter 8 127

8 General Discussion 129

8.1 The role of polyP in achieving the UN Sustainable Development Goals 129
8.2 Industrial application of polyP-rich yeast extract or pure bio-polyP 136
8.3 Concluding remarks and outlook 140

Appendix 145

A.1 Appendix for Chapter 3 147
A.2 Appendix for Chapter 4 150
A.3 Appendix for Chapter 5 157
A.4 Appendix for Chapter 6 161
A.5 Appendix for Chapter 7 165

References 175

Curriculum Vitae 211

Summary

Phosphate (PO_4^{3-}, P_i) is an essential nutrient for all living organisms and plays a crucial role in modern agriculture. Most of the P_i used by humans is derived from mined P_i rock and processed into agricultural fertilizers. However, the currently established linear P_i economy faces challenges such as geopolitical dependence on limited reserves, rising fertilizer prices, heavy metal contamination, and ecological damage caused by extensive P_i application. It is expected that these challenges will worsen due to population growth, increasing meat consumption, and the envisaged bioeconomy. Sustainable P_i management requires a transition to a circular P_i economy.

This thesis supports the transition to a circular P_i economy by developing biotechnological polyphosphate (polyP) production applying *Saccharomyces cerevisiae* (*S. cerevisiae*). The polyP hyperaccumulation protocol previously established by Christ and Blank (2019) [1] was modified for high-throughput screening and combined with the JC-D7 fluorescence assay to analyze *S. cerevisiae* strain collections for altered polyP content, chain length, and growth performance. The JC-D7 assay proved robust against numerous abiotic factors and extraction agents, enabling rapid and sensitive classification of yeasts based on polyP content. The investigation of *S. cerevisiae* strain collections identified several novel yeast deletion mutants and industrial strains as promising candidates for metabolic engineering and polyP production. Furthermore, a systematic evaluation of the influence of individual trace elements and vitamins during the starvation phase identified zinc and inositol as key factors for enhanced polyP production by *S. cerevisiae*. Zinc stimulates the P_i-responsive signaling pathway during P_i starvation. The role of inositol was examined using phospholipid mutants and strains carrying deletions of genes involved in inositol synthesis or transport. In this context, the minimal medium requirements for both the starvation and feeding phases of the polyP hyperaccumulation process were redefined. These findings reduce nutrient consumption, improve product purification efficiency, and provide a deeper understanding of polyP metabolism in *S. cerevisiae*.

The results of this dissertation, combined with process-guided strain engineering, provide an opportunity to promote the industrial implementation of biotechnological polyP production with *S. cerevisiae* and contribute to the transition towards a circular P_i economy. However, to ensure that *S. cerevisiae* can make such a significant contribution, it is crucial to make well-informed decisions regarding raw material selection, strain development, application of biotechnologically produced bio-polyP, and process design. This requires coordinated efforts from research, policy-making, industry, and society.

Zusammenfassung

Phosphat (PO_4^{3-}, P_i) ist ein essenzieller Nährstoff für alle Lebewesen und spielt in der modernen Landwirtschaft eine entscheidende Rolle. Der größte Teil des von Menschen genutzten P_i stammt aus abgebautem P_i-Gestein und wird zu landwirtschaftlichen Düngemitteln verarbeitet. Die derzeit vorherrschende lineare P_i-Wirtschaft sieht sich jedoch Herausforderungen wie der geopolitischen Abhängigkeit von begrenzten Reserven, steigenden Düngemittelpreisen, Schwermetallbelastungen sowie ökologischen Schäden durch ineffiziente P_i-Anwendung ausgesetzt. Es wird erwartet, dass sich diese Entwicklung aufgrund von Bevölkerungswachstum, steigendem Fleischkonsum und der angestrebten Bioökonomie weiter verschärft. Ein nachhaltiges P_i-Management erfordert den Übergang zu einer zirkulären P_i-Wirtschaft.

Diese Arbeit leistet einen Beitrag zur Entwicklung der biotechnologischen Polyphosphat (PolyP)-Produktion mit *Saccharomyces cerevisiae* (*S. cerevisiae*), um den Übergang zu einer zirkulären P_i-Wirtschaft zu unterstützen. Das von Christ und Blank. (2019) [1] etablierte PolyP-Hyperakkumulationsprotokoll wurde für Hochdurchsatz-Screenings modifiziert und mit dem JC-D7-Fluoreszenz-Assay kombiniert, um *S. cerevisiae*-Stammsammlungen hinsichtlich veränderter PolyP-Gehalte, Kettenlängen und Wachstumsleistungen zu untersuchen. Der JC-D7-Assay erwies sich als robust gegenüber zahlreichen abiotischen Faktoren und Extraktionsmitteln. Er ermöglichte eine schnelle und sensitive Klassifizierung der Stämme auf Grundlage des PolyP-Gehalts der Hefeextrakte. Die Untersuchung von *S. cerevisiae*-Stammsammlungen identifizierte neuartige Hefedeletionsmutanten sowie Industriestämme als vielversprechende Kandidaten für das Metabolic Engineering und die PolyP-Produktion. Darüber hinaus ermittelte eine systematische Untersuchung des Einflusses einzelner Spurenelemente und Vitamine in der Hungerphase Zink und Inositol als Schlüsselfaktoren für eine erhöhte PolyP-Produktion in *S. cerevisiae*. Zink stimuliert den P_i-abhängigen Signalweg während der P_i-Hungerphase. Die Rolle von Inositol wurde unter Verwendung von Phospholipid-Mutanten sowie von Stämmen mit Deletionen von Genen der Inositolsynthese oder des Inositoltransports untersucht. In diesem Zusammenhang wurden die Minimalmedienanforderungen sowohl für die Hunger- als auch für die Fütterungsphase des PolyP-Hyperakkumulationsprozesses neu definiert. Dies reduziert den Nährstoffeintrag, verbessert die Effizienz der Produktaufarbeitung und liefert ein tieferes Verständnis des PolyP-Stoffwechsels in *S. cerevisiae*.

Die Ergebnisse dieser Dissertation, zusammen mit prozessgestützter Stammentwicklung, bieten die Möglichkeit, der industriellen Etablierung einer biotechnologischen PolyP-Produktion mit *S. cerevisiae* näherzukommen und zur Abkehr von der linearen P_i-Wirtschaft beizutragen. Um jedoch sicherzustellen, dass *S. cerevisiae* diesen Beitrag leisten kann, ist es entscheidend, die

richtigen Entscheidungen in Bezug auf Rohstoffauswahl, Stammentwicklung, die Anwendung von biotechnologisch hergestelltem Bio-PolyP und die Prozessgestaltung zu treffen. Dies erfordert gemeinsame Anstrengungen von Forschung, Politik, Wirtschaft und Gesellschaft.

Nomenclature

Abbreviations

Abbreviation	Description
aCGH	array comparative genomic hybridization
ADI	acceptable daily intake
AICAR	5-aminoimidazole-4-carboxamide ribonucleotide
APP	ammonium polyphosphate
ATP	adenosine triphosphate
BMBF	German Federal Ministry for Education and Research
CCNV	chromosomal copy number variation
CDW	cell dry weight
CHEF	contour-clamped homogeneous electric field
CTR	carbon dioxide transfer rate [mmol/l/h]
CWW	cell wet weight
DAG	diacylglycerol
DAPI	4′,6-diamidino-2-phenylindole
DCP	dicalcium phosphate
DMSO	dimethyl sulfoxide
DNA	deoxyribonucleic acid
DSP	downstream processing
EBPR	Enhanced Biological Phosphorus Removal
EDTA	ethylenediaminetetraacetic acid
EFSA	European Food Safety Authority
e.g.	*exempli gratia*
EU	European Union
G418	geneticin
GMO	genetically modified organism
GRAS	Generally Recognized As Safe
GRH	Growth Rate Hypothesis
gRNA	guide RNA
HPLC	high-performance liquid chromatography
iAMB	Institute of Applied Microbiology
i.e.	*id est*

Abbreviation	**Description**
INPHORS	intracellular phosphate reception and signaling
InsPP	inositol pyrophosphate
LCA	life-cycle assessment
LPA	lysophosphatidic acid
MAG	monoacylglycerol
MTP	microtiter plate
n	variable for the polyP chain length
NAD	nicotinamide adenine dinucleotide
n.d.	not detectable
NE	negative control
NGS	next-generation sequencing
NP-40	Nonidet P-40
OD_{600}	optical density measured at 600 nm
OTR	oxygen transfer rate in mmol [mmol/l/h]
ORF	open reading frame
P	phosphorus
PA	phosphatidate
PAO	polyphosphate-accumulating organisms
PC	positive control
PEBPR	Photo-Enhanced Biological Phosphorus Removal
pH	pH value [-]
PHA	polyhydroxyalkanoate
PHC	phosphatidylcholine
PHO	phosphate signal transduction pathway
P_i	phosphate (PO_4^{3-}, synonym: orthophosphate)
PLS	phospholipid synthesis
polyP	inorganic polyphosphate
$polyP_n$	inorganic polyphosphate with a chain length of n
qPCR	quantitative real-time PCR
rpm	revolutions per minute
rRNA	ribosomal ribonucleic acid
SAM	S-adenosylmethionine
S. cerevisiae	*Saccharomyces cerevisiae*
SD	synthetic defined

Abbreviation	Description
SDAP	spray-dried animal plasma
SDGs	UN's Sustainable Development Goals
SDS	sodium dodecyl sulfate
SEM	standard error of the mean
sfGFP	superfolder green fluorescent protein
SPX domain	(Syg1p/Pho81p/XPR1p) receptor domains
TAG	triacylglycerol
TE	Verduyn trace elements
TEA	techno-economic analysis
TOM	transfer-rate online measurement
TPA	Tris(2-pyridylmethyl)amine
TPEN	N,N,N′,N′-tetrakis(2-pyridylmethyl)ethylenediamine
TV	Verduyn vitamins
μ_{max}	maximum growth rate [1/h]
USP	upstream processing
VH	Versuchsanstalt der Hefeindustrie e.V.
VTC	vacuolar transporter chaperone
w/o	without
WT	wild type
WWTP	wastewater treatment plant
YEP	yeast extract peptone
YEP-Nat	YEP medium supplemented with nourseothricin
YKO	yeast knockout

List of Figures

Figure 1: Natural and human-derived phosphate cycle. 4
Figure 2: Schematic presentation of Enhanced Biological Phosphorus Removal (EBPR). 9
Figure 3: Molecular structure of P_i and polyP. 10
Figure 4: Central metabolic pathway of polyP production in *S. cerevisiae*. 14
Figure 5: PolyP concentration and chain length dependence of the JC-D7 fluorescence signal. 43
Figure 6: PolyP-mediated JC-D7 fluorescence in the presence of inorganic metal salts. 44
Figure 7: The effect of EDTA on metal salt quenching of polyP JC-D7 fluorescence. 45
Figure 8: Effect of common polyP extraction agents on polyP JC-D7 fluorescence. 46
Figure 9: Optimization of JC-D7 application on yeast extracts. 47
Figure 10: Comparison of JC-D7 fluorescence measurements and enzymatic analysis of polyP in yeast extracts. 49
Figure 11: Protein interaction network of hypo- and hyperaccumulating deletions in the YKO collection. 61
Figure 12: Protein interaction network including functional clustering of hypo- and hyperaccumulating deletions in the YKO collection. 62
Figure 13: PolyP screening of the VH-strain collection in the non-adapted protocol for highest relative polyP signal. 73
Figure 14: PolyP screening of the Top 20 strains of the VH-strain collection for the best relative producer in the non-adapted protocol. 75
Figure 15: PolyP screening of the Top 5 strains of the VH-strain collection for the best relative producer in the adapted and non-adapted protocol. 76
Figure 16: PolyP screening of the Top 20 strains of the VH-strain collection for the best absolute producer in the non-adapted protocol. 78
Figure 17: PolyP screening of the Top 5 strains of the VH-strain collection for the best absolute producer in the non-adapted protocol. 80
Figure 18: Influence of trace elements on polyP hyperaccumulation of VH2.200. 91
Figure 19: Influence of individual vitamins on polyP hyperaccumulation of VH2.200. 93
Figure 20: Influence of zinc and inositol on polyP hyperaccumulation of VH2.200. 94
Figure 21: 3D-surface diagrams for the effect of inositol and zinc on polyP hyperaccumulation of diverse yeast strains. 95
Figure 22: TOM cultivation with various yeast strains in starvation medium without or only with inositol and zinc. 97

Figure 23: PHO pathway activation by *S. cerevisiae* in the starvation phase of the polyP hyperaccumulation protocol. 99
Figure 24: Evaluating the impact of glucose, KCl, $CaCl_2$, and succinate in the starvation medium on polyP production with VH2.200. 110
Figure 25: Evaluating the impact of glucose and phosphate in the feed medium on polyP production with VH2.200. 111
Figure 26: Evaluating the impact of completely reduced starvation and feed media on polyP production with VH2.200. 113
Figure 27: Evaluating the impact of reduced $MgCl_2$ concentrations in the feeding medium on polyP production with VH2.200. 115
Figure 28: Investigating the effect of phospholipid metabolism-associated genes on polyP accumulation in BY4742 deletion mutants. 117
Figure 29: PolyP accumulation in CEN.PK WT and CEN.PK *pah1*Δ under various supplemented starvation media. 119
Figure 30: Investigating the effect of inositol metabolism-associated genes on polyP accumulation in CEN.PK deletion mutants. 120
Figure 31: 17 UN Sustainable Development Goals adopted by all United Nations Members. 129

Figure A1: Fluorescence spectra of mono/polyP-treated JC-D7. 147
Figure A2: Normalized fluorescence intensity data of mono/polyP-treated JC-D7. 148
Figure A3: Fluorescence spectra of JC-D7 pretreated with polyP and inorganic metal salts. 148
Figure A4: Application of the fluorescent dye JC-D7 to extracts of VH2.200. 149
Figure A5: Holding device for sonication of 96-well MTPs applied for screening of the YKO collection and VH-strain collection. 150
Figure A6: PolyP screening of yeast control strains Ethanol Red, VH2.200, CEN.PK WT and BY4741 WT in the non-adapted protocol via JC-D7. 150
Figure A7: Protein interaction network of hypoaccumulating deletions with an OD_{600}-corrected JC-D7 signal of 0.5x in the YKO collection. 152
Figure A8: Protein interaction network of hyperaccumulating deletions with an OD_{600}-corrected JC-D7 signal of 2.0x in the YKO collection. 154
Figure A9: Protein interaction network of hypo- and hyperaccumulating deletions with an OD_{600}-corrected JC-D7 signal of 0.5x and 2.0x in the YKO collection. 155
Figure A10: PolyP screening of the complete VH-strain collection in the non-adapted protocol for highest absolute polyP signal. 158

Figure A11: Analysis of yeast ploidy of the Top 5 highest relative polyP producing strains in the VH-strain collection using flow cytometry. 160
Figure A12: Influence of individual trace elements of Group 3 on polyP hyperaccumulation of VH2.200. 162
Figure A13: Effect of inositol and zinc on polyP hyperaccumulation of VH2.200. 162
Figure A14: PolyP content of various yeast strains after TOM cultivation in starvation medium w/o any trace elements and vitamins (NE_{TE+TV}) or only with inositol and $ZnSO_4$. 163
Figure A15: Plasmid map of pPr_{Pho5}-sfGFP to assay PHO pathway activation. 163
Figure A16: PolyP content of CEN.PK WT and CEN.PK pPr_{Pho5}-sfGFP after BioLector cultivation. 164
Figure A17: Evaluation of the impact of reduced starvation media and adapted glucose levels in the feed medium on polyP production with VH2.200. 165
Figure A18: Evaluating the impact of $(NH_4)_2SO_4$ in the starvation medium on polyP production with VH2.200. 166
Figure A19: Investigating the effect of additional phospholipid metabolism-associated genes on polyP accumulation in BY4742 deletion mutants. 167
Figure A20: Investigating the effect of *ino1*Δ, *itr2*Δ, and *itr1*Δ*itr2*Δ on polyP accumulation in CEN.PK deletion mutants. 168

List of Tables

Table 1: Clusters of trace elements applied for screening. 32
Table 2: Gene deletions identified in this screening and by Freimoser et al. (2006) [152]. 63
Table 3: Average polyP chain length and maximal growth rate (μ_{max}) of the best-performing VH-collection strains..... 81
Table 4: Metabolic impact of inositol and zinc on *S. cerevisiae* during P_i starvation. 98
Table 5: Composition of all starvation and feed media used to define the minimal nutritional requirements of VH2.200 for polyP hyperaccumulation. 112

Table A1: Two-way ANOVA table of the experiment on the polyP-responsibility of the fluorescent dye JC-D7. 147
Table A2: Hypoaccumulating deletions with an OD_{600}-corrected JC-D7 signal of 0.5x in the YKO collection. 151
Table A3: Hyperaccumulating deletions with an OD_{600}-corrected JC-D7 signal of 2.0x in the YKO collection. 153
Table A4: Functional clustering of hypo- and hyperaccumulating deletions with an OD_{600}-corrected JC-D7 signal of 0.5x and 2.0x in the YKO collection. 156
Table A5: Background information on the best-producing strains identified in the screening of the VH-strain collection. 157
Table A6: Cell size of best-producing strains in the VH-strain collection. 158
Table A7: Ranking the Top 20 highest absolute polyP-producing strains of the VH-strain collection in terms of their relative polyP production level. 159
Table A8: Concentration of vitamin stock solutions. 161
Table A9: Concentration of trace element stock solutions. 161
Table A10: *S. cerevisiae* strains used to test the influence of inositol on polyP production. 168
Table A11: *S. cerevisiae* strains employed in the phospholipid screening experiments. 169
Table A12: Cost of raw materials applied in the starvation and feeding phase of the polyP hyperaccumulation protocol. 172
Table A13: Cost assessment of starvation and feeding media used in the polyP hyperaccumulation protocol. 173

Chapter 1

General Introduction

Contributions:

This chapter was written by Alexander Deitert and critically reviewed by Philipp Demling and Lars Mathias Blank.

1 General Introduction

1.1 The natural phosphate cycle

The biochemist Frank Westheimer wrote in his paper: “Granted that the phosphates are ubiquitous in biochemistry, what do they do? The answer is that they can do almost everything.” [2]. Phosphorus (P), as part of phosphate (P_i/PO_4^{3-}), is an irreplaceable element for life [3-5]. It fulfills diverse cellular functions by providing structure, enabling energy storage, and allowing information delivery [4]. For instance, phospholipids are the primary building blocks of cellular membranes. They contain about 4 % P by mass and account for 5-10 % of cellular biomass [3, 6]. Adenosine triphosphate (ATP) is particularly crucial for short-term energy storage and is highly enriched in P (18 % by mass). However, the combined contribution of ATP, ADP, and AMP to the total cellular biomass is minimal (0.1 %) [3]. Nucleic acids contain roughly 9 % P by mass and play a fundamental role in genetic information storage and processing, particularly in the form of ribosomal ribonucleic acid (rRNA) [6]. The relevance of rRNA led to the formulation of the Growth Rate Hypothesis (GRH), which links organismal growth rates to P demand via rRNA production [7, 8]. In vertebrates, the hypothesis's application is limited since P is predominantly stored in bones rather than in rRNA, mainly in the form of calcium hydroxyapatite ($Ca_{10}(PO_4)_6(OH)_2$) [7, 9].

Compared to its biological significance and cellular predominance, the environmental abundance of P is relatively scarce, as the Earth’s crust is dominated by elements like Si, O, and Fe [3]. The P in the Earth's crust is mainly available as apatite minerals (e.g., fluorapatite, chlorapatite, hydroxyapatite), with fluorapatite being the most abundant [10, 11]. In the natural P cycle (Figure 1), the supply of new P to ecosystems is determined by the release of P trapped in these minerals through slow rock weathering rates. P_i then erodes into water streams and soils. The P_i in soils is taken up by plants and transferred through food networks. Decomposition and excretion return it to the soil, where it is recycled multiple times before leaching into aquatic systems. Eventually, P-containing substances flow to the ocean via rivers and coastal waters. Other sources of oceanic P include hydrothermal inputs and low-temperature reactions between seawater and the seafloor. In water bodies, P cycles between the water column and sediments before ultimately being buried in ocean sediments [3, 10, 12]. Over geological timescales (10^8-10^9 years) [13, 14], a set of low-temperature processes compacts, cements, and chemically alters sedimented P into solid P_i rocks, a transformation known as diagenesis. This makes the P cycle one of the slowest among all biogeochemical cycles [10, 13].

1.2 The human phosphate cycle and phosphate problematic

Long before the elemental discovery of P by Hennig Brandt in 1669, P had played a central role in human development, as mankind depended on the natural P in soils for food production [15]. Since then, anthropogenic activities have intervened with the natural P cycle and massively released P from geological sources (Figure 1). Throughout human history, three revolutions - namely the Industrial Revolution, the Sanitation Revolution, and the Green Revolution - transformed the use of P [15]. The Industrial Revolution triggered a mass movement of populations to cities. It thereby disrupted the small-scale nutrient recycling scheme at the level of farms and villages. The Sanitation Revolution shifted waste disposal from land-based to water-based systems, disrupting P recycling cycles and replacing them with throughput systems. Liebig's "mineral theory" in 1840 identified for the first time the fertilizing effect of P on plant growth [16, 17]. This led to the adoption of agricultural practices and, ultimately, to the Green Revolution. The Green Revolution established industrial agriculture, demanding large quantities of mineral P-rich fertilizer and essentially abandoning the traditional use of naturally P-rich organic fertilizers [15]. These revolutions disrupted traditional, closed-loop P cycles and replaced them with linear systems, finally contributing to P scarcity and environmental pollution [3, 15, 18, 19].

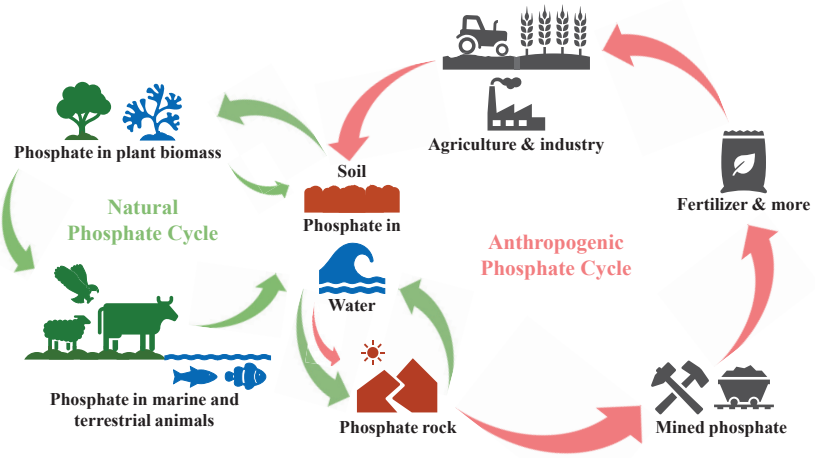


Figure 1: Natural and human-derived phosphate cycle.
The natural P_i cycle is depicted in green, and the anthropogenic P_i cycle is shown in red. In the natural P_i cycle, P_i from ore erodes into water streams and soils. The absorption of P_i by plants and algae is followed by the subsequent uptake of fixed P_i by animals, both terrestrial and marine. P_i returns to the environment through excretion or die-off. Over millions of years, this process leads to the formation of new P_i ore. Large-scale mining of P_i significantly alters the dynamics of the global P_i cycle. Mined P_i is primarily used as a fertilizer to enhance crop and livestock yields. The utilization of diverse products returns P_i to the natural cycle via soil and water. The magnitude of the arrows indicates the intensity of the P_i flow. The information is based on [10,12]. The figure was created via PowerPoint.

P is one of industrial agriculture's key macronutrients for plant growth, alongside nitrogen and potassium [20]. However, due to its tendency to bind with soil minerals, such as aluminum, the applied P becomes inaccessible to plants and remains in the soil [3, 21, 22]. To still cover the substantial P demand of high-yield crops and ensure sufficient productivity, heavy fertilization is required [15, 23]. P flows have increased by 400 % since the mid-20th century due to human activity, surpassing changes in the carbon and nitrogen cycles [24]. Approximately 90 % of the P_i rock mined annually is utilized for food production, primarily as fertilizers (82 %), with smaller amounts used for animal feed (5 %) and food additives (2 %) [19, 25]. Crop production is expected to increase by 51-86 % by 2050 to meet future global food demand from a growing population, especially for meat-focused diets, and for bioenergy. Inevitably, the demand for P_i fertilizer is expected to rise further [3, 22, 26-28]. The remaining 10 % of mined and processed P_i rock is utilized in detergents and various industrial applications, including high-value applications such as electronics and pharmaceuticals [25, 29]. P_i rock is classified by its P_2O_5 content into low-(12-16 % P_2O_5), medium-(17-25 % P_2O_5), and high-grade-(26-35 % P_2O_5) ores [30]. Calcium phosphates, such as fluorapatite ($Ca_3(PO_4)_3 \cdot CaF_2$), are the most common P sources. Since the average P content of P_i ore is 13 %, beneficiation is required to upgrade the quality of the P_i rock and increase the content of apatite (and thus P_i) via removal of sand and clay (15 % to 33 %) [20, 31]. While P_i rock can be used directly for the production of superphosphates and nitric phosphates (both fertilizers) [20], it is primarily processed to produce phosphoric acid, which is the precursor for many of the intermediate and end uses of P_i [10, 20, 32, 33].

The two primary methods for phosphoric acid production are the wet acid digestion process and the direct thermal conversion [11]. In the wet acid digestion process, crude phosphoric acid is produced by reacting sulfuric acid with P_i rock in a wet process facility. The rock is dried, crushed, and mixed with sulfuric acid, forming gypsum (calcium sulfate) as a byproduct. Each ton of P_i processed generates 5 tons of phosphogypsum [19, 34]. Gypsum crystals are precipitated and separated from the acid by filtration. They must be thoroughly washed to recover at least 99 % phosphoric acid. The resulting wet-process acid typically contains 26-30 % P_2O_5 and is often concentrated to 40-55 % P_2O_5 using vacuum evaporators to meet the required standards. Due to its low quality, the produced acid is mainly used for fertilizer applications [11, 20, 35]. Thermic acid production comprises three steps: combustion, hydration, and demisting. Liquid elemental phosphorus is heated in air at 1,650-2,760 °C to form phosphorus pentoxide, which is then hydrated with water or dilute phosphoric acid to produce concentrated phosphoric acid. The demisting step removes acid mist from exhaust gases using high-pressure drop demisters. The final phosphoric acid (75-85 % H_3PO_4) is of high quality and is used in high-grade chemicals as well as non-fertilizer products [20, 35].

In addition to the P_i content, concerns arise from impurities in P_i rock, including non-phosphorus minerals such as heavy metals and radioactive elements. These compounds must be removed to improve quality, ensure health and safety, and protect the environment. Although heavy metals and radioactive elements are primarily contained in phosphogypsum byproducts, some also enter fertilizers [20, 36-38]. Therefore, new European Union (EU) regulations have been lowering the allowable thresholds for contaminating phosphoric acid with heavy metals, even for its use in fertilizers (from 60 to 20 mg/kg cadmium over a decade), to prevent toxic and radioactive buildup in soil, plants, and water [39, 40]. This could ultimately have a significant impact on human food safety [41, 42]. Moreover, mined P_i used in agriculture and industry is often lost to the environment or captured in the ash of burned sludge, demonstrating the linearity of human P_i use [43-46]. Thus, the linear phosphorus economy poses a threat to the UN Sustainable Development Goals (SDGs), such as zero hunger and responsible consumption of natural resources. Clean water and biodiversity in aquatic ecosystems are threatened by eutrophication, an ecological issue caused by excess P from point sources (e.g., sewage outfalls) and nonpoint sources (e.g., agricultural soil leaching) [18, 20, 47]. Together with nitrogen, this leads to an overgrowth of cyanobacteria. The subsequent decomposition of biomass increases organic matter, depletes oxygen (leading to hypoxia), and acidifies the environment by releasing dissolved CO_2. This contributes to the death of aquatic life [10, 48, 49]. Eutrophication results in significant environmental damage and substantial costs, including $2.2 billion annually in the U.S. due to reduced property values [50]. These environmental issues are why P is considered a “Janus-faced” element, despite its importance in both agriculture and industry [29], and why it has been widely recognized as critical to Earth's stability [51]. In 2015, P exceeded its planetary boundary and is now in a “high risk” zone. Hence, current P use is unsustainable and threatens ecosystems and human life [52, 53]. Paradoxically, concerns about “peak phosphorus” and “phosphorus scarcity” are emerging, despite increasing amounts of P leaving the human system [3, 19]. There is an ongoing debate about when global P supplies become limited. Limitation is a matter of supply and demand, with current P reserves being mined at a rate much faster than they are naturally replenished [3, 12, 23, 28, 54]. However, the exact timing is controversial due to uncertainties regarding global P reserves and their quality, though estimates have been as early as around 2030 [19, 55]. The EU declared P_i rock in 2014 and elemental P in 2017 as critical raw materials due to their high economic importance and supply risks [56-58]. This is particularly true given the unequal global distribution of P resources [3, 22]. P_i rock mining is primarily concentrated in a few countries, including Morocco, China, and the USA [59, 60]. Morocco alone holds 75 % of the global P_i rock reserves. This raises geopolitical concerns due to its monopoly on global P_i reserves and its control over reserves in Western Sahara [19, 61]. Regarding the political status of Western

Sahara, the UN Security Council recommended in October 2025 that Western Sahara be placed under Morocco's sole sovereignty while granting it autonomous rights [62]. Due to this political uncertainty and to prevent a P-limited collapse, a transition from a linear to a circular P_i economy is necessary, emphasizing the reuse and recycling of P [43, 63, 64].

1.3 Phosphorous removal strategies

P is essential to life, as it cannot be substituted nor synthesized [15]. As Isaac Asimov put it: "We may be able to substitute nuclear power for coal, and plastics for wood, and yeast for meat, and friendliness for isolation-but for phosphorus, there is neither substitute nor replacement." [65, 66]. A 700 % spike in fertilizer prices in 2007 and the declining rock quality highlight the urgency of P sustainability [3, 67]. However, significant P losses occur through field erosion, leaching, and animal production, especially from non-gastric animals such as pigs, which cannot digest phytate-bound P [3, 19]. Moreover, 30-50 % of mined P is lost before entering the value chain. Hence, interest is growing in recovering P from low-grade mining waste [29, 68]. Additionally, over 80 % of global wastewater is discharged untreated, as households and industries lack sewer connections [29, 69]. This communal wastewater regularly contains contaminants such as pharmaceuticals and heavy metals, in addition to P [70, 71], which pose a significant challenge for P removal. When industrial and domestic wastewater is treated, P is initially removed non-specifically by microbes in the activated sludge. However, this process typically achieves removal efficiencies of only 10-30 % [72, 73]. If these levels do not meet regulatory limits, enhanced targeted P removal can be achieved through chemical treatments such as adsorption and precipitation, or by intensifying P uptake via specific microorganisms [73-75]. While adsorption is limited by the adsorbent capacity [76, 77], chemical precipitation with metal salts, such as ferric chloride and alum, is more effective and widely used in urban wastewater treatment plants (WWTPs) [10, 75]. Precipitation methods can achieve P removal efficiencies of over 90 % [76]. However, most P ends up in activated sludge, which is often incinerated in industrial countries, as the microbial biomass is contaminated with pharmaceuticals and heavy metals. Since not all harmful substances of sewage sludge are destroyed via combustion, the handling of heavy metals and toxic emissions (e.g., mercury, dioxins, furans, acid gases, and NO_x) remains a significant concern, especially regarding environmental risks [77-80]. Moreover, combustion produces ash with poorly available P forms, such as apatite and Fe-whitlockites [81, 82], and is usually landfilled at specialized sites, thereby losing P for reuse [83, 84].

1.4 Phosphorus recovery strategies

At this point, it is essential to differentiate between P removal and recovery. P removal aims to produce P-free waste streams, while P recovery focuses on extracting usable P byproducts from waste streams [10]. In this way, P recovery primarily ensures sustainable P resource management, while also helping to reduce P pollution [3, 19, 44]. P recovery is possible at various points, but only with accessible waste streams. Key sources include wastewater, manure, and slaughter waste [85]. In this regard, new legislation mandates higher P recovery efficiency. Germany's Sewage Sludge Ordinance demands a higher P recovery of 50 % from sludge and 80 % from ash by 2029, if P levels exceed 20 g/kg dry matter [86]. In Sweden, 60 % of P in sewage should be returned to land [19, 87]. Hence, P recovery technologies from wastewater become more critical for achieving true P sustainability [85]. Additionally, sewage sludge represents a significant energy source that can be harnessed to promote sustainable waste management [10].

In contrast to P recovery (supply), P recycling refers to the subsequent reuse of recovered P within relevant value chains (demand) [88]. Thereby, P recycling benefits supply security, fairness to future generations, and support for a circular economy [89]. The following criteria for successful implementation of P recycling technologies were defined: market potential for the end product, strong developer or seller support, compatibility with existing systems, high recovery rates (P, contaminants), low investment and operating costs, minimal waste, societal and political acceptance, and added benefits like lower wastewater treatment costs [85]. Several P recovery strategies have been established, each offering different recovery efficiencies, cost profiles, and compatibility depending on WWTP type and sludge composition [85]. Struvite precipitation (used in processes like AirPrex and ANPHOS) is employed in over 40 plants and performs effectively in Enhanced Biological Phosphorus Removal (EBPR)-type WWTPs with high P_i and ammonia concentrations. Struvite can function as a slow-release fertilizer. This strategy can reduce operating costs for WWTPs by preventing scaling, lowering P and nitrogen return loads, and reducing disposal costs. However, it is unsuitable for plants using chemical precipitation (Fe/Al salts), has low recovery rates, and the struvite may carry residual sludge. This raises concerns about food chain contamination via struvite [85]. CO_2-based extraction (e.g., applied in Extraphos) utilizes pressurized CO_2 and heated water to leach 50-70 % of P_i from sludge. The P_i is precipitated and recovered as dicalcium phosphate (DCP) under atmospheric pressure with high efficiency, moderate operating costs, and low chemical use. DCP can be used in fertilizers, but the process installation is costly and not suited for centralization [85]. Alkaline leaching (e.g., JSA) uses NaOH to leach P from sewage sludge ash and subsequent P_i precipitation with $Ca(OH)_2$. This avoids heavy metal contamination in contrast to acid leaching. This technique recovers 35-40 % of P as calcium hydroxyapatite, which is sold as fertilizer [85]. Phosphoric acid recovery (e.g., TetraPHos)

treats sewage sludge ash with phosphoric acid, purifying it to industrial-grade phosphoric acid. It recovers over 80 % of P in the ash, makes the precipitants from sewage works (Fe, Al) recyclable, and produces gypsum as a byproduct. Phosphoric acid recovery is best suited for iron-rich ashes and less efficient with aluminum-rich ashes due to Al dissolution [85, 90, 91]. Alternatively, ash from combustion can be used as a raw material in conventional P_i fertilizer production with sulfuric acid [92].

1.5 Biological phosphorus removal strategies

In addition to the conventional activated sludge process, various biological processes for enhanced P removal are available. These processes can reduce effluent P levels by 75-93 % [10]. Although biological P removal may be less efficient than chemical methods, it offers several advantages, including reduced chemical use, lower sludge production, and higher quality P recovery [10, 93]. EBPR uses microorganisms that store P_i as polyphosphate (polyP) within their cells. Additionally, extracellular microbial polymers may contribute by binding and precipitating P_i [94, 95]. EBPRs work by cycling wastewater and microbial biomass through anaerobic and aerobic zones (Figure 2).

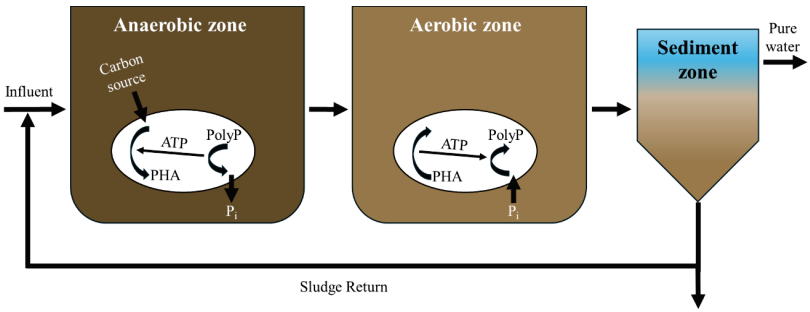


Figure 2: Schematic presentation of Enhanced Biological Phosphorus Removal (EBPR). Wastewater and microbial biomass are cycled through anaerobic and aerobic zones to enrich organisms that accumulate polyP. In the anaerobic zone, polyP is broken down to release P_i, providing energy for carbon uptake and storage as PHA. In the aerobic zone, PHA is degraded to generate ATP for polyP synthesis. Because more P_i is taken up aerobically than is released anaerobically, EBPR results in a net P_i removal from the wastewater. The information is based on [49]. The figure was created via PowerPoint.

In the anaerobic zone, the environment is characterized by an electron acceptor deficiency and a high carbon content. PolyP is degraded to P_i to increase the transmembrane proton gradient, whereas carbon is taken up via a proton-symport pump and stored as polyhydroxyalkanoate (PHA). In the aerobic zone, the environment is rich in electron acceptors but deficient in carbon.

Cells use the stored PHA to generate energy and take up more P_i than they have released, storing it as polyP. This results in net P removal from the wastewater [49, 96-99]. EBPR is implemented by complex microbial communities [100]. The Photo-Enhanced Biological Phosphorus Removal (PEBPR) is a new approach that combines polyP-accumulating organisms (PAO) from the EBPR with algae. It uses light/dark cycles to create aerobic/anaerobic conditions, enabling both PAOs and algae to accumulate polyP and remove P efficiently [101]. Despite these examples, it is assumed that broad systemic changes are required to achieve P sustainability [3]. However, technological advancements still play a crucial role in P sustainability and this comprehensive systematic change. One possibility is the targeted accumulation of polyP by microorganisms from waste streams, with polyP considered a value-added product. The baker's yeast *Saccharomyces cerevisiae* (*S. cerevisiae*) accumulates high amounts of polyP, and the use of waste streams for polyP production has already been successfully demonstrated [102, 103].

1.6 Inorganic polyphosphates: structure, applications, and production

Inorganic polyPs are polymers made of P_i units, range from a few to more than a thousand units, and are linked by energy-rich phosphoanhydride (P-O-P) bonds [104, 105]. They are highly negatively charged biopolymers with a structure like RNA and other polyanions, resulting in similar chemical reactivity [106] (Figure 3).

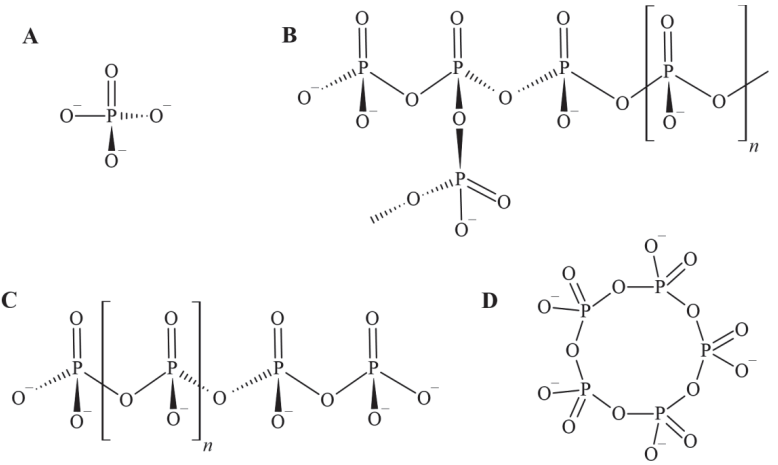


Figure 3: Molecular structure of P_i and polyP.
A) Single phosphate molecule; B) Branched polyP; C) Linear structure of polyP; D) Cyclic polyP. n can range from zero up to more than a thousand repeat units. The information is based on [106, 107, 113-115]. The molecular structures were generated with ChemSketch (Toronto, ON, Canada).

Hence, polyP can effectively chelate metal ions such as Ca^{2+}, Mg^{2+}, and Mn^{2+}. Moreover, it forms complexes with other cellular compounds, such as proteins and nucleic acids [49, 107, 108]. Three structural types of polyPs are defined. These include cyclic condensed phosphates (metaphosphates, $P_nO^{n-}{}_{3n}$), linear polyPs (most studied, found in all organisms, $P_nO^{(n+2)-}{}_{3n+1}$), and branched polyPs (ultraphosphates) [106, 107, 109-111]. PolyPs are widespread across all forms of life, having been identified in archaea, bacteria, algae, fungi, protists, plants, insects, and mammals [104, 105, 108, 112-115]. However, neither the biological function nor the synthesizing or degrading enzymes of cyclic and branched polyPs are known. Recent studies investigated whether these polyP structures occur naturally in biological systems or are instead an analytical artifact [109, 110, 116]. Cyclic polyP (up to six P_i-subunits), such as hexametaphosphate, is commercially available in low purity. The existence of mono- and dimetaphosphates has not been demonstrated in practice and is theoretically unlikely [107]. Mandala et al. (2020) [117] reported the *in vivo* presence of cyclic polyP using non-destructive NMR, suggesting that previously detected cyclic polyP is not solely a purification artifact. These molecules, likely limited to eight P_i-subunits, are reported to bind to proteins like ribonuclease A and nicotinamide adenine dinucleotide (NAD) kinase. Although the biological role remains unclear, cyclic polyPs' role as a progenitive structurization entity in the origin of life has been discussed [118]. Regarding branched polyPs, it was long believed that they could not exist in aqueous environments due to rapid hydrolysis [116]. However, Dürr-Mayer et al. (2021) [110] disproved this hypothesis by measuring the hydrolysis rate of synthesized, branched polyPs. They discovered that ultraphosphate linearizes through the rearrangement of terminal P_i, a process they defined as the phosphate walk. However, the presence of branched polyP in biological systems remains unconfirmed, but it cannot be excluded [64, 107]. The widespread distribution of polyP in living cells is related to its versatile and vital functions. This includes P_i and energy storage, cation sequestration, non-enzymatic post-translational modification, pH buffering, the formation of membrane channels, contribution to cell envelope structure and function, regulation of gene expression and enzyme activities, as well as involvement in stress response, survival, and adaptation to the stationary phase [49, 104, 119-125]. In higher vertebrates, it is also involved in bone tissue development and blood coagulation [126, 127]. These biological functions are connected to key properties of polyP: it is an osmotically neutral P reserve, the phosphoanhydride bonds store energy, and it forms complexes with cations and other cell components [49].

In addition to its cellular functions, polyP is of industrial interest and is used across diverse industries due to its unique physicochemical properties, affordability, non-toxicity, and biodegradability [49]. The physicochemical properties of polyP depend on the chain length and counterions. The cation-complexing ability, phosphoanhydride bonds, bacteriostatic activity, and

hydrophilicity increase with increasing chain length. The buffering capacity, the reactivation of actomyosin, and the acidifying function are more pronounced with short-chain polyPs [128]. The diverse molecular properties and counterions of polyP enable its use in several key application areas. In the food industry, polyP is used in baking powders (as acidifying agents), meat and fish (to improve tenderness and water-holding capacity), processed cheese (as emulsifying salts by binding calcium), and food safety (to control pathogens such as *Bacillus cereus* and *Clostridia*) [129-136]. Moreover, polyPs are legally permitted food additives in Europe (E450-E452). Speculations about the health effects of polyP in foods (e.g., hyperactivity, osteoporosis) have not been confirmed. However, regulatory limits have been established, recommending up to 40 mg P/kg body weight and including food-specific maximum permitted levels ranging from 500 to 20,000 mg/kg (as P_2O_5). 3,000 mg P/person per day is considered a tolerable upper intake level for human health [130]. Notably, despite discussions about health risks associated with polyP, no substitutes for all of its functions in the food industry are available [137, 138]. In addition to the food sector, polyP is used in numerous other fields. Ammonium polyphosphates (APP) are used as P_i fertilizer, particularly in soil applications [139]. Compared to rock P_i and superphosphates, it has a higher water solubility and is more effective [49]. Plants absorb P_i, so polyP must first be broken down. Hence, it does not provide an immediate response under P deficiency, but polyP offers longer-lasting nutrient availability [49, 139, 140]. Moreover, APPs are highly effective, halogen-free inorganic flame retardants. When exposed to high heat, APP combustion produces non-flammable gases, such as water vapor and ammonia, which dilute the concentration of oxygen and other combustible volatiles. At the same time, the decomposition of APP yields a protective intumescent char layer through dehydration and carbonization of the host polymer via phosphoric acid and the capture of released gases. This protective barrier suppresses the release of flammable gases and effectively limits fire propagation [139]. Therefore, APP is widely used to fireproof materials such as paper, wood, and textiles [49]. Another prominent application of polyP is in water treatment due to its effectiveness in sequestering metal ions, preventing mineral scale formation, and dissolving already existing scale deposits. This improves the efficiency and carrying capacity of water distribution systems. Moreover, it provides an anticorrosion effect through the formation of colloid particles. These particles result from the absorption of calcium ions [49].

Industrial polyP is primarily produced chemically by heating phosphoric acid (H_3PO_4), which leads to condensation reactions releasing water and forming diphosphoric acid ($H_2P_2O_7$). At temperatures between 400-800 °C, further condensation forms polyP chains of varying lengths [141]. This chemical polyP synthesis relies on fossil resources, has a significant carbon footprint, and is limited to 2-40 P_i-subunits at large scale [45, 131]. In addition, polyP can be produced

biotechnologically. Biological systems can naturally produce longer polyP chains of more than 1,000 P_i-subunits [142]. In *S. cerevisiae,* polyP usually accounts for about 1.5 % (as P_2O_5) of the cell dry weight (CDW) [143]. Under specific process conditions, *S. cerevisiae* hyperaccumulates polyP, reaching levels higher than those physiologically required [144, 145]. These conditions involve P_i starvation and subsequent P_i feeding [1]. The starvation response in *S. cerevisiae* is an adaptive, energy-efficient, and protective mechanism that enables cells to survive fluctuating environments. This is crucial for microorganisms, since natural P_i availability is rarely constant [146]. Hyperaccumulation replenishes depleted P_i stores, buffers high external P_i levels, facilitates the rapid resumption of growth, and enhances competitiveness [147-154]. It is also speculated that hyperaccumulation prepares *S. cerevisiae* for future P_i scarcity [146, 155]. This resembles microbial bet-hedging strategies [156]. Bet-hedging relies on population heterogeneity, which was demonstrated for polyP accumulation in the cyanobacterium *Synechocystis* sp. PCC 6803, but not in *S. cerevisiae* [157, 158]. Through the hyperaccumulation protocol, baker's yeast can accumulate up to 28 % (w/w) polyP (as KPO_3) in CDW from various P_i-rich sources, including waste streams [1, 103]. Industrial wash waters and biomass from crop-processing have already been applied as a P_i source for polyP accumulation with *S. cerevisiae* [102, 103]. PolyP-rich *S. cerevisiae* can then be used to manufacture either polyP-rich yeast extract or pure bio-polyP [1, 159]. The application potential of polyP-rich yeast extract was demonstrated in meat patty production, where it functioned as both a texture stabilizer and a flavor enhancer. Moreover, it confirmed the effective use of non-fossil, food-grade P_i for polyP production [102, 103]. This can help transition the linear P_i value chain into a circular one, in which spent P_i is made accessible for recycling and reuse while developing a value-added product [45].

1.7 Phosphate homeostasis in *Saccharomyces cerevisiae*

P_i is essential for many cellular functions. Hence, yeasts have evolved a regulatory mechanism to acquire, store, and release this molecule [146, 160, 161]. P_i homeostasis is maintained through a synergistic, multilayered system that ensures a sufficient supply during scarcity and prevents accumulation under conditions of excess [146]. Excess P_i can decrease the free energy provided by P_i-liberating reactions, such as nucleotide hydrolysis. This can ultimately stall the cellular metabolism [146]. The significance of P_i regulation is underscored by the substantial number of the ~6,000 yeast genes involved in P_i-related processes, including 25 genes directly involved in P_i homeostasis [146, 160, 162, 163]. The phosphate-responsive signal transduction (PHO) pathway is responsible for regulating P_i homeostasis through the transcriptional regulation of most genes involved [164]. It is controlled through a P_i-responsive kinase (Pho80p/Pho85p/Pho81p) [165].

The Pho85p cyclin-dependent kinase is involved in various cellular processes, including cell cycle control and amino acid metabolism [166, 167]. It gains target specificity by associating with different cyclins. All P_i homeostasis-related effects are mediated through the interaction with cyclin Pho80p [146] (Figure 4).

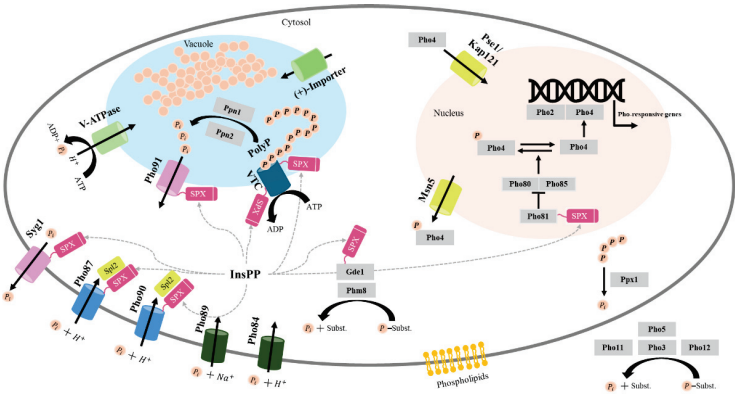


Figure 4: Central metabolic pathway of polyP production in *S. cerevisiae*.
PolyP production and P_i homeostasis are regulated by the PHO pathway. The SPX domains interact with inositol pyrophosphates. Abbreviations: PHO = genes of phosphate signal transduction pathway; P_i = free phosphate; PolyP = polyphosphate; InsPP = inositol pyrophosphates; SPX = Syg1p/Pho81p/XPR1p domain; V-ATPase = vacuolar ATPase; VTC = eukaryotic vacuolar transporter chaperone; Ppn1p = endo- and exopolyphosphatase; Ppn2p = Zn^{2+}-dependent endopolyphosphatase; Kap121p = karyopherin/importin; Ppx1p = exopolyphosphatase; Msn5p = karyopherin; Phm8p = lysophosphatidic acid phosphatase; Spl2p = regulator of low-affinity phosphate transporter; Pse1p = karyopherin/importin; Syg1p = plasma membrane protein; Gde1p = glycerophosphocholine phosphodiesterase. The information is based on [128, 146]. The figure was created via PowerPoint.

The Pho85p/Pho80p kinase is controlled via the cyclin-dependent kinase inhibitor Pho81p, thereby functioning as the primary regulator of the PHO pathway [168]. Pho85p/Pho80p is constitutively associated with Pho81p but inhibits the kinase activity only under P_i limitation (< 0.2 mM P_i). In its active state at high P_i levels (10 mM P_i), the complex catalyzes the hyperphosphorylation of Pho4p [160, 168-170]. Pho4p is the transcription factor that regulates the expression of genes controlled by the PHO pathway. Its hyperphosphorylation impairs Pho4p's interaction with the second necessary transcription factor Pho2p and favors Pho4p's export into the cytosol. This represses the expression of PHO-regulated target genes. Under P_i limitation, the hypophosphorylated form of Pho4p induces transcription of target genes related to P_i homeostasis [165]. The Pho81p gene expression itself is feedback-regulated. On the one hand, the Pho85p/Pho80p cyclin-dependent protein kinase complex post-translationally phosphorylates Pho81p [171]. On the other hand, expression of Pho81p is induced by Pho4p under P_i-limiting conditions [170].

Protein regulation in P_i homeostasis depends on an evolutionarily conserved intracellular phosphate reception and signaling pathway (INPHORS) in which cytosolic P_i levels translate into changes of inositol pyrophosphates (InsPPs). InsPPs are highly phosphorylated molecules that contain one or more pyrophosphate moieties [146, 172]. Their concentration changes in response to cytosolic P_i availability [173, 174] and is communicated to SPX (Syg1p/Pho81p/XPR1p) receptor domains [175-177]. The SPX domains, found in P_i transporters, signaling proteins, and polyP polymerase, provide a basic binding surface for InsPPs through which they modulate protein activity [175, 176, 178]. Depending on the specific target protein, this interaction may either activate or repress the function [179]. Hence, InsPPs play a key role in maintaining P_i homeostasis as messenger molecules [178]. However, further research is necessary to determine whether different isomers serve distinct signaling functions [173, 180, 181]. A recent publication by Chabert et al. (2023) [173] emphasizes the significance of 1,5-InsP8 in P_i homeostasis. At high P_i levels, 1,5-InsP8 accumulates and binds the SPX domain of Pho81p. This weakens the interaction with Pho80p and thereby prevents inhibition of the Pho85p/Pho80p kinase. When P_i is limited, 1,5-InsP8 levels drop, leaving the SPX domain unbound. This activates Pho81p, enabling it to stably bind and inhibit the Pho85p/Pho80p kinase, which ultimately results in the activation of the PHO pathway [173]. Thereby, *S. cerevisiae* can distinguish P_i scarcity from P_i starvation. The shift into P_i starvation is a complex process, during which cells gradually adapt to decreasing P_i levels through distinct, time-separated waves of gene activation [146, 182]. When P_i levels gradually decline, Pho85p kinase activity decreases, which results in a partially dephosphorylated Pho4p transcription factor, thereby inducing a subset of PHO genes (*PHO11*, *PHO12*, *PHO84, PHO86*) and the vacuolar transporter chaperone complex (VTC) genes. This recovers P_i from various extracellular sources and allows cells to store P_i in the form of polyP [146, 160, 182-186]. The Pho4p-dependent gene expression is stabilized for several generations, preventing oscillatory activation and inactivation of the PHO pathway under moderate P_i limitation [146]. When the first wave of genes is insufficient to replenish cytosolic P_i or P_i is completely depleted from the cultivation medium, a more profound decline in cytosolic P_i triggers the second wave of gene inductions via complete Pho4p dephosphorylation [146, 182, 183]. The cells begin to hydrolyze internal polyP stores [144, 145, 187], recuperate P_i from internal substrates (nucleotides, lipids) [160, 188, 189], and activate additional genes for external P_i acquisition (*PHO5*, *PHO89*) [147, 182]. Moreover, metabolites of the citrate cycle increase, oxygen consumption increases, and levels of glycolytic intermediates decline under P_i starvation. Mitochondrial respiration may also be activated as a P_i-efficient alternative to glycolysis for energy production [149]. This all results in a reduced growth rate of *S. cerevisiae* [146].

When cells experience severe P_i starvation, they halt after two additional divisions and enter the quiescent G0 phase [146]. The question of how the cell recognizes the different cytosolic P_i concentrations remains poorly understood. Mild P_i scarcity causes moderate drops in ATP and InsPPs, prompting partial activation of P_i foraging while allowing normal growth. Severe P_i starvation leads to broader metabolic shifts, including changes in 5-aminoimidazole-4-carboxamide ribonucleotide (AICAR), S-adenosylmethionine (SAM), and substantial reductions in ATP and InsPPs, which collectively trigger a complete transcriptional P_i starvation response [149].

1.8 Polyphosphate metabolism in *Saccharomyces cerevisiae*

After *S. cerevisiae* experienced profound P_i starvation, it can hyperaccumulate high levels of polyP under P_i-replete conditions [1, 144, 145]. This polyP is mainly stored in the acidocalcisome-like vacuoles, together with high concentrations of divalent cations (Ca^{2+}, Mn^{2+}, Zn^{2+}) and basic amino acids [143, 190-192]. Besides that, minor polyP amounts are found in mitochondria, the ER, or the nucleus [193-195]. The vacuolar polyP is mainly required to buffer the cytoplasmic P_i concentration to maintain cellular homeostasis when external P_i levels fluctuate [187]. Under P_i starvation, cells mobilize P_i into the cytosol from vacuolar polyP [196, 197]. This allows the organism to maintain a constant cytosolic P_i content [187]. PolyP, in addition to serving as a P_i reservoir, is also involved in cellular osmoregulation. It reduces the osmotic pressure of free P_i and the osmotic activity of amino acids in the vacuole [146, 197]. Moreover, vacuolar polyP contributes to heavy metal detoxification [198] and could function as a substitute for ATP as an energy source [121]. In algae, it has been demonstrated that polyP is involved in the response to alkaline stress [199].

The VTC complex in yeast synthesizes polyP from inorganic P_i [190]. All VTC complexes include Vtc1p and Vtc4p. Vtc1p is a transmembrane protein with three membrane-spanning domains, whereas Vtc4p functions as a Mn^{2+}-dependent catalytically active component responsible for polyP synthesis from nucleotide triphosphates [200, 201]. All subunits of the VTC complex, except for Vtc1p, consist of a hydrophilic central domain and an additional N-terminal SPX domain [202, 203]. The central domains of Vtc2p, Vtc3p, and Vtc5p are assumed to have no catalytic role and are involved only in regulatory functions [204, 205]. Although all VTC complexes consist of Vtc1p and Vtc4p, different isoforms with either Vtc2p or Vtc3p exist [160]. Under P_i-rich conditions, the Vtc1p/2p/4p isoform is primarily found in the ER, while the second isoform (Vtc1p/3p/4p) is associated with the vacuole. When P_i becomes limited, both complexes relocate to the vacuole [204]. The Vtc5p subunit can associate with the VTC complex to increase

its activity, but it is not essential for functionality [205]. The same applies to Vtc2p and Vtc3p. Single deletion of either subunit reduces the cellular polyP content, whereas double deletion completely abolishes polyP production. Vtc1p and Vtc4p are essential for polyP synthesis in *S. cerevisiae* [206]. Besides its function as polyP polymerase, the VTC complex also acts as polyP translocase, as polyP production at the cytosolic membrane and transport into the organelle lumen are coupled [190]. The electrochemical potential across the vacuolar membrane provides the driving force for polyP translocation. This gradient is maintained by the V-type H^+-ATPase. Moreover, the storage of the negative charges of polyP requires compensation in the form of uptake or release of cations or anions [146, 190]. Since polyP strongly impacts cytosolic P_i homeostasis, its accumulation requires extensive control [146]. The VTC polymerase activity is stimulated by diverse InsPPs, with 1,5-InsP8 likely being the key activator of VTC-mediated polyP synthesis [173, 207]. This is in line with the levels of polyP under P_i-rich conditions and under P_i starvation. *S. cerevisiae* synthesizes polyP when cytosolic P_i levels are high, whereas it consumes polyP under low P_i levels due to a switched-off VTC complex [1, 145, 173, 178, 208]. The vacuolar polyP is consumed through degradation by endopolyphosphatases Ppn1p and Ppn2p under P_i-limiting conditions. The P_i is exported back into the cytosol via Pho91p, which is the only P_i transporter not located in the cellular membrane [146, 209]. It has been reported that in the case of Ppn1p, exopolyphosphatase activity is also present [210]. PolyP can be hydrolyzed to P_i and tripolyphosphate by Ppn1p, but the enzyme requires Mn^{2+} or Mg^{2+} for activity and is potentially inhibited by pyrophosphate and ATP [146, 211]. Ppn2p is Zn^{2+} dependent and depicts no exopolyphosphatase activity [196]. Another exopolyphosphatase localized outside of the vacuole is Ppx1p. This enzyme hydrolyzes polyP chains as short as three P_i residues but cannot degrade PP_i and ATP [212, 213]. Since its location does not match the central storage location of polyP in the vacuole, Ppx1p fulfills functions other than those of Ppn1p and Ppn2p. Ppx1p counteracts the toxic accumulation of freely diffusible polyP in the cytosol [160, 190]. Both elevated cytosolic polyP and elevated cytosolic P_i levels are harmful for *S. cerevisiae*. PolyP production allows *S. cerevisiae* to store P_i in a non-toxic form in the vacuole [146]. Four transporters are responsible for taking up P_i in *S. cerevisiae* (Pho84p, Pho87p, Pho89p, and Pho90p). Pho84p and Pho89p are high-affinity transporters with K_m values of 8-40 µM [146, 214, 215]. Pho84p functions as H^+/P_i symporter optimal at acidic pH, whereas Pho89p is a Na^+/P_i symporter and active at alkaline pH [214-218]. Pho87p and Pho90p are low-affinity transporters (K_m: 200-800 µM) that are regulated by SPX domains [146, 209, 219]. Having both low- and high-affinity transporters enables *S. cerevisiae* to detect a P_i decline early and across a broad concentration range. This extends the transition phase and the time for cells to adapt from P_i-replete to P_i-starvation conditions [146, 220].

Despite this connected network of P_i uptake, export, and storage in *S. cerevisiae*, it remains unclear how cells coordinate all the steps of degrading and producing polyP [146, 190].

1.9 Scope and outline of this thesis

The central objective of this thesis is to contribute to the transition of the currently established linear P_i economy into a circular P_i economy through polyP production with *S. cerevisiae*. This offers the possibility of producing a value-added product with unique material characteristics, as well as the potential to reuse and recycle P_i from various waste streams. The thesis provides a foundation for screening strain collections by downscaling the polyP hyperaccumulation protocol of Christ and Blank (2019) [1] and characterizing a new fluorescence dye for polyP detection in yeast extracts. This enables the identification of previously uncharacterized genes that enhance polyP synthesis in *S. cerevisiae* through metabolic engineering or the application of novel baker's yeast strains with improved production characteristics as hosts for polyP production. The media development offers two primary opportunities. On the one hand, it facilitates the recycling of P_i, thereby enhancing the efficiency of polyP production. On the other hand, it provides new approaches to improve our understanding of polyP metabolism in *S. cerevisiae*.

In Chapter 1, the reader is introduced to the background of the contemporary P_i problem, with a particular emphasis on human intervention in the natural P cycle (Chapter 1.1 and 1.2). This leads to the description of industrially established P removal (Chapter 1.3) and recycling strategies (Chapter 1.4). In this context, biological P removal strategies and their mode of operation are presented (Chapter 1.5). Finally, polyP production with *S. cerevisiae* is presented as an alternative contribution to the circular P_i economy, with a special focus on the physicochemical characteristics and applications of polyP (Chapter 1.6), as well as on the mechanisms of P_i homeostasis (Chapter 1.7) and polyP metabolism (Chapter 1.8) in baker's yeast.
Chapter 2 provides an overview of the experimental approaches employed in this thesis to generate the data presented in Chapters 3-7.

In Chapter 3, the fluorescence sensor JC-D7 is presented and characterized for detecting biologically produced polyP in extracts from *S. cerevisiae*. This includes the sensor's ability to differentiate concentrations and chain lengths of chemical polyP standards, as well as its resilience against various abiotic factors and extraction agents. The dye was ultimately utilized to elucidate the varying polyP production levels of multiple *S. cerevisiae* strains, thereby demonstrating its suitability for high-throughput applications.

In Chapter 4, the pipeline for polyP hyperaccumulation and semi-quantitative polyP detection via JC-D7 in a small-scale setting was adapted to the yeast knockout collection, consisting of

4,765 strains with single-gene deletions in non-essential genes. This involved screening with a semi-automated robotic platform at KU Leuven. The objective of the screening was to provide a comprehensive overview of polyP metabolism and to identify new targets for enhancing polyP synthesis in *S. cerevisiae* through metabolic engineering.

In Chapter 5, an industrial *S. cerevisiae* strain collection of 153 strains was evaluated for their capacity to accumulate polyP. The workflow consisted of the downscaled, high-throughput polyP hyperaccumulation protocol with semi-quantitative polyP detection through JC-D7. The purpose of this screening was to compare the polyP accumulation ability of the strains with the established production host *S. cerevisiae* VH2.200. Promising strains were validated via the established hyperaccumulation protocol and the quantitative enzymatic assay for polyP detection from Christ and Blank (2019) [1].

In Chapter 6, the starvation phase of the polyP hyperaccumulation protocol was examined to verify the positive effect of Verduyn trace elements and vitamins on polyP accumulation. The components responsible for the increase in polyP were identified through individual screening of all trace elements and vitamins. The influence of the two responsible components was validated in various *S. cerevisiae* strains, and their metabolic effects were measured via transfer-rate online measurement (TOM) cultivations and superfolder green fluorescent protein (sfGFP) readout.

In Chapter 7, the phospholipid metabolism was examined for its interconnection with polyP metabolism. Consequently, several strains with single-gene mutations in the phospholipid pathway were characterized by their ability to accumulate polyP. During this screening, the medium used in the starvation and feeding phases of the hyperaccumulation protocol was further modified to assess the impact of individual media components on the final polyP production level.

Chapter 8 summarizes the key conclusions of this doctoral thesis and discusses them within a broader context. The chapter begins with a discussion about the linear P_i economy and its impact on the UN Sustainable Development Goals. Subsequently, it explores the potential contributions of polyP production to promote a circular P_i economy. In this context, a comparison is made between the chances of success of polyP-rich yeast extracts and pure bio-polyPs, with a particular focus on their potential for paving the way for the market entry of biotechnological polyP.

Chapter 2

Materials and Methods

Parts of this chapter are published as:

Deitert, A., Fees, J., Mertens, A., Nguyen Van, D., Maares, M., Haase, H., Blank, L. M., and Keil, C. Rapid Fluorescence Assay for Polyphosphate in Yeast Extracts Using JC-D7. *Yeast*, 41, 593-604, 2024, doi: 10.1002/yea.3979.
[Reprinted (adapted) with permission from John Wiley & Sons Ltd. Open Access CC BY-NC-ND 4.0. © The Authors 2024]

Deitert, A., Baier, M., Eerlings, R., Fees, J., Österlein Kück, A., Repin, J., Demling, P., and Blank, L. M. Polyphosphate Accumulation Is Determined by Zinc and Inositol in *Saccharomyces cerevisiae*. *Yeast*, 0, 1–12, 2025, doi: 10.1002/yea.70006.
[Reprinted (adapted) with permission from John Wiley & Sons Ltd. Open Access CC BY-NC-ND 4.0. © The Authors 2025]

Contributions:

The strains listed in the section 2.5.1 and Suppl. Table A10 were constructed by Makarius Baier at the Institute of Applied Microbiology (iAMB), RWTH Aachen University (Aachen, Germany). Makarius Baier is the original author of the section 2.6.1. Duc Nguyen Van and Claudia Keil (TU Berlin, Berlin, Germany) conducted experiments to test the robustness of the JC-D7 signal against abiotic factors and extraction agents (Chapter 3). Claudia Keil is the original author of these sections in the Chapters 2.2 and 3. The Chemische Fabrik Budenheim (Budenheim, Germany) provided chemical polyphosphate standards (section 2.2.1). Lieselotte Vermeersch conducted the high-throughput screening experiments using the microbe handler HiTMan and is the original author of the section 2.3.3. She is affiliated with the VIB Laboratory for Systems Biology (KU Leuven, Leuven, Belgium) and the Laboratory for Genetics and Genomics (KU Leuven, Leuven, Belgium). These sections have been included in this thesis, either in their entirety or partially in an adapted form. This chapter was written by Alexander Deitert and critically reviewed by Philipp Demling and Lars Mathias Blank.

2 Material and Methods

2.1 General Methods

2.1.1 Chemicals

Unless otherwise stated, all chemicals used in this thesis were purchased from Carl Roth GmbH & Co. KG (Karlsruhe, Germany) or Sigma-Aldrich (St. Louis, MO, USA). The JC-D7 dye was purchased from InvivoChem LLC (Libertyville, IL, USA).

2.1.2 Strains and media

This section addresses commonly used strains, whereas strains utilized exclusively within a specific chapter are described in detail in the corresponding Materials and Methods section of the respective chapter. The industrial strains *S. cerevisiae* VH2.200 and *S. cerevisiae* Ethanol Red® were used in this work (hereinafter referred to as VH2.200 and Ethanol Red, respectively). VH2.200 was provided by the VH Berlin e.V. (Research Institute for Baker's Yeast, Berlin, Germany), and Ethanol Red was provided by Leaf (Lesaffre, Marcq-en-Baroeul, France). Moreover, the laboratory strain *S. cerevisiae* CEN.PK113-7D (hereinafter referred to as CEN.PK WT) was utilized.

2.1.3 Cultivation conditions for producing polyP-rich *S. cerevisiae* cells

The hyperaccumulation protocol established by Christ and Blank (2019) [1] was applied to produce polyP-rich yeast cells. In brief, the protocol initially included a *S. cerevisiae* preculture by inoculating 10 ml of synthetic defined (SD-)medium (6.8 g/l yeast nitrogen base without amino acids, 20 g/l glucose, pH 5.4) with single colonies from a yeast extract peptone (YEP) agar plate (30 °C, 200 rpm, 100 ml flask, 24 h). 1 % (v/v) inoculum from the preculture was then used for cell mass production in 50 ml SD-medium (30 °C, 200 rpm, 500 ml flask, 24 h). Subsequently, the cell mass was harvested by centrifugation (5,000 g, 5 min), washed with deionized water, air-dried for 5 min on P_i-free filter paper, and stored at 4 °C (for a maximum of 2 weeks). 2.5 g/l *S. cerevisiae* cell wet weight (CWW) was then cultivated in 50 ml P_i-depleted starvation medium (23.96 g/l glucose, 1.32 g/l $(NH_4)_2SO_4$, 0.99 g/l KCl, 0.58 g/l $CaCl_2 \cdot 2\ H_2O$, 2.02 g/l disodium succinate; trace elements (TE): 15.0 mg/l Na_2EDTA, 4.5 mg/l $ZnSO_4 \cdot 7\ H_2O$, 1.0 mg/l $MnCl_2 \cdot 2\ H_2O$, 0.3 mg/l $CoCl_2 \cdot 6\ H_2O$, 0.3 mg/l $CuSO_4 \cdot 5\ H_2O$, 0.4 mg/l $Na_2MoO_4 \cdot 2\ H_2O$, 0.1 mg/l KI, 4.5 mg/l $CaCl_2 \cdot 2\ H_2O$, 3.0 mg/l $FeSO_4 \cdot 7\ H_2O$, 1 mg/l H_3BO_3; trace vitamins (TV):

0.05 mg/l biotin, 1.0 mg/l nicotinic acid, 1.0 mg/l Ca-D-pantothenate, 0.2 mg/l p-aminobenzoic acid, 1.0 mg/l pyridoxine hydrochloride, 1.0 mg/l thiamine hydrochloride, 25.0 mg/l myo-inositol, pH 5.0) at 30 °C and 200 rpm in a 500 ml flask for 6 h. At the end of each starvation phase, the cells were harvested (5,000 g, 5 min), washed once with deionized water, and dried on P_i-free filter paper (5 min). This was followed by storage of the cells at 4 °C until the start of the feeding phase (17 h). The P_i-starved *S. cerevisiae* cells were then transferred to 10 ml feeding medium (component A (1.11x concentrated): 49.99 g/l glucose, 9.06 g/l KH_2PO_4, pH 6.0; component B (10x concentrated): 40.66 g/l $MgCl_2$; component A and component B were unified in a ratio of 9:1 before inoculation). A maximal concentration of 30 g/l CWW was applied and cultivated (30 °C, 200 rpm, 100 ml flask, 2.5 h). Afterward, P_i-fed *S. cerevisiae* cells were harvested by centrifugation (5,000 g, 5 min), washed twice with deionized water, dried on P_i-free filter paper (5 min), and stored at -20 °C until polyP analysis [221, 222]. Any methods deviating from this protocol are described in the Materials and Methods section of the respective chapter.

2.1.4 Enzymatic polyP analytics

Phenol/chloroform extraction was used to extract polyP from polyP-enriched *S. cerevisiae* [221]. The Phosfinity kit from Aminoverse B.V. (Nutz, the Netherlands) was used according to the supplied protocol to determine the P_i and polyP concentration [222]. PolyP values in this thesis refer to cellular polyP contents (as KPO_3) in percentage of CDW [% (w/w) polyP (as KPO_3)]. These polyP values can be converted to the percentage of P in CDW [% P (w/w)] by applying a factor of 0.26. The average polyP chain length was determined enzymatically using fluorescence-based measurements in black 96-well F-bottom microtiter plates (MTPs), following the protocol of the Phosfinity ChainQuant kit (Aminoverse B.V., Nutz, the Netherlands). Any methods deviating from these protocols are described in the Materials and Methods section of the respective chapter.

2.1.5 JC-D7 fluorescence assays

JC-D7 polyP analytics in the absence of cells were performed according to Angelova et al. (2014) [223], using a 10 mM JC-D7 stock solution prepared in pure dimethyl sulfoxide (DMSO). Subsequently, equal volumes of 50 µM JC-D7 in assay buffer (20 mM HEPES buffer, pH 7.4, containing 1 % (v/v) DMSO) and polyP solution (0-1,000 µg/ml) were combined in a 96-well polystyrene MTP. After 30 min of incubation at 30 °C, fluorescence measurements were conducted at room temperature using a Tecan Infinite M200 Reader (Tecan Austria GmbH, Grödig/Salzburg, Austria; excitation at 390 nm with a bandwidth of 9 nm, emission at 530 nm

with a bandwidth of 20 nm, detector gain 50). The influence of detergents and inorganic metal salts on JC-D7 fluorescence in the presence of polyP was tested by preincubating 50 µl of the polyP chain length mixture (10 µg/ml polyP, section 2.2.1) with 50 µl of 4-fold concentrated detergent or metal salt test solutions (each prediluted in double-distilled water) for 30 min at 30 °C. Subsequently, 100 µl of 50 µM JC-D7 was added, followed by another 30 min incubation at 30 °C before fluorescence measurement. To evaluate the influence of the metal chelator ethylenediaminetetraacetic acid (EDTA), polyP samples pretreated with inorganic metal salts (final concentration 1 mM) were additionally incubated with 1 mM EDTA for 30 min before JC-D7 addition and fluorescence detection. *S. cerevisiae* extracts (preparation according to Christ and Blank (2018) [221]) used in this work were diluted 1:500 in assay buffer. Afterwards, 100 µl of the respective dilution were mixed with 100 µl JC-D7 (20 µM) for 30 min at 30 °C and fluorescence was measured in an Agilent BioTek Synergy Mx (Agilent Technologies, Santa Clara, USA; excitation at 390 nm with a bandwidth of 9 nm, emission at 530 nm with a bandwidth of 9 nm, automatic gain adjustment). Any methods deviating from this protocol are described in the Materials and Methods section of the respective chapter.

2.1.6 Analysis of cultivation broth

Concentrations of sodium acetate, glycerol, glucose, ethanol, and succinate were determined using a high-performance liquid chromatography (HPLC-UV-RI) system (DIONEX UltiMate 3000 consisting of the autosampler WPS-3000 (RS), the column oven TCC-3000 (RS), and the pump module LPG-3400SD, all Thermo Fisher Scientific, Waltham, MA, USA) with an ISERA Metab AAC 300 x 7.8 mm separation column (particle size = 10 µm, ISERA GmbH, Düren, Germany). Non-cultivated medium and cultivation supernatant samples were measured. Samples were diluted 1:2 with deionized water and filtered (Berrytec syringe filters, pore size = 0.22 µm, d = 13 mm, Berrytec GmbH, Harthausen, Germany) before the measurement. The column temperature was set to 40 °C, and the run time of the method was 25 min per sample. For the isocratic method, a mobile phase of 5 mM H_2SO_4 was pumped at a constant flow rate of 0.6 ml/min. The injection volume of the samples was 5 µl. The DIONEX UltiMate 3000 Variable Wavelength Detector (UV) was set to 210 nm. In addition, a refractive index (RI) detector SHODEX RI-101 (Showa Denko Europe GmbH, Munich, Germany) was used. The succinate concentration was determined using the UV detector, and the concentrations of all other substances were determined using the RI detector.

2.1.7 Statistical analysis

The statistical significance of experimental results was calculated by GraphPad Prism software version 8.02 (GraphPad Software Inc., CA, USA) using the tests indicated in the respective figure legends in Chapter 3. One-way ANOVA via the GraphPad Prism software version 13.02 (GraphPad Software Inc., California, USA) was applied to test the experimental results in Chapter 6 for significance (*p < 0.05, **p < 0.01, ***p < 0.001, ****p < 0.0001).

2.2 Material and Methods for Chapter 3

2.2.1 Chemicals

The chemically produced sodium polyPs named Budit 4, 7, 9 were obtained from Budenheim (Budenheim, Germany). Budit 4 has a chain length of 20-25 P_i-subunits, Budit 7 has 10-15 P_i-subunits, and Budit 9 has 4-6 P_i-subunits. Graham's salt (sodium polyphosphate, Emplura, lot 1.06529.1000) was sourced from Sigma-Aldrich Chemie GmbH (Taufkirchen, Germany) and has an average chain length of 22 P_i-subunits, as described by Robinson et al. (2022) [224]. Stock solutions (10 mg/ml) of both Graham's salt and Budit polyPs were prepared by dissolving the respective powders in double-distilled water. A polyP mixture was then prepared by combining equal volumes of Budit 4, Budit 7, and Budit 9 stock solutions, resulting in a final polyP concentration of 10 µg/ml. APPs with chain lengths ranging from 7 to 1472 P_i-subunits were obtained from Budenheim (Budenheim, Germany). Among these, only APP8 dissolved in standard buffer (1 mM MOPS, 0.1 mM EDTA, pH 7) at a concentration of 2 g/l. For the other APPs, 240 mM NaCl was added to facilitate dissolution at the same concentration.

2.2.2 Strains

BY4742 MATα *his3Δ1 leu2Δ0 lys2Δ0 ura3Δ0* (in this chapter referred to as BY4742 WT) was obtained from EUROSCARF (Oberursel, Germany). BY4742 strains with single deletions of YDR452W/*PPN1* (in this chapter referred to as BY4742 *ppn1*Δ) and YFR034C/*PHO4* (in this chapter referred to as BY4742 *pho4*Δ) were selected from the single-gene deletion yeast knockout (YKO) collection (EUROSCARF, Oberursel, Germany).

2.2.3 Media

The media applied in the hyperaccumulation protocol is based on Christ and Blank (2019) [1]. In case of the auxotrophic BY4742 strains, the preculture and starvation media were additionally supplied with the corresponding amino acids [225].

2.3 Material and Methods for Chapter 4

2.3.1 Strains

In addition to the already mentioned strains, BY4741 MATa *his3Δ1 leu2Δ0 met15Δ0 ura3Δ0* (subsequently referred to as BY4741 WT) was used in this chapter. BY4741 WT was obtained from EUROSCARF (Oberursel, Germany). Moreover, the YKO collection (BY4741 background) was used for screening (EUROSCARF, Oberursel, Germany) [226]. This strain collection comprises 4,765 *S. cerevisiae* strains.

2.3.2 Media

The media applied in the hyperaccumulation protocol is based on Christ and Blank (2019) [1]. 0.79 g of CSM powder (MP Biomedicals, Irvine, CA, USA) was added to each liter of SD-medium and starvation medium according to the manufacturer's instructions to compensate for auxotrophies of BY4741.

2.3.3 Microtiter plate cultivation in the HiTMan robotic platform

The hyperaccumulation protocol developed by Christ and Blank (2019) [1] was modified for high-throughput screening. The cell mass was not adjusted to 2.5 g/l CWW before starvation or a maximum of 30 g/l CWW before the feed phase. The YKO collection (BY4741-based) was spotted from -80 °C storage on 2 % yeast peptone agar plates using a Singer Rotor HDA pinning robot (San Francisco, CA, USA), and incubated for 48 h at 30 °C. All strains were inoculated into 150 µl of SD-medium using a Singer Rotor HDA pinning robot and incubated overnight at 30 °C. The following growth, starvation, and feed phases of the polyP screening protocol were performed using a custom-made Perkin Elmer (Revvity) Explorer G3 (Waltham, MA, USA) workstation robotic system, which includes a Janus liquid handler, centrifuge, multimode plate reader, and incubators. Of the preculture, 5 µl were transferred to 145 µl of fresh SD-medium and then incubated overnight at 30 °C. For the starvation phase, cultures were centrifuged for 5 min at 4,500 rpm and washed with 150 µl water. The supernatant was removed, and the plates were stored

at 4 °C overnight. The next day, the cultures were resuspended in 150 µl starvation medium and incubated at 30 °C for 6 h, shaking at 300 rpm. After incubation, cultures were again centrifuged for 5 min at 4,500 rpm and washed with 150 µl water. The supernatant was removed, and the plates were stored at 4 °C overnight. The next day, the cultures were resuspended in 150 µl of feed medium and incubated for 2.5 h at 30 °C with shaking at 300 rpm. After incubation, the optical density at 600 nm (OD_{600}) of a 1:100 diluted sample was measured (Victor Nivo multimode plate reader), cultures were centrifuged for 5 min at 4,500 rpm, and washed twice with 150 µl water. The supernatant was removed, and the culture pellets were stored at -20 °C for 1-2 weeks until the next steps. Pellets were resuspended in 100 µl of lysis buffer (1 % sodium dodecyl sulfate (SDS), 0.2 M lithium acetate), and cells were lysed via sonication in six 30 s sonication cycles with 1 min breaks on ice after every sonication step (S 120 Elmasonic, Singen, Germany), using a custom plate holding device (Suppl. Figure A5). The cell lysis samples were stored at -20 °C until polyP detection. For analysis, the cell lysis samples were thawed and diluted 1:500 with JC-D7 buffer (20 mM HEPES, 1 % (v/v) DMSO, pH 7.4). 100 µl of the 20 µM JC-D7 working solution was pipetted into a black-edged, flat-bottom 96-well plate (Greiner Bio One (Kremsmünster, Austria); cat. no. 655087), and fluorescence was measured (excitation = 405/10 nm; emission = 530/30 nm). Next, 100 µl of the diluted cell lysis samples was added. Subsequently, the plates were incubated for 30 min at 30 °C, after which fluorescence was measured again. This protocol of the JC-D7 fluorescence assay for polyP detection differs slightly from previously mentioned methods [223, 227].

2.3.4 Data analysis

For all polyP measurements, the raw data were normalized to the OD_{600} of each corresponding strain. The OD_{600}-corrected JC-D7 signal was used as an indicator of the polyP content. Subsequently, the polyP levels were expressed relative to the median of all cultures on an individual 96-well plate. Strains with an OD_{600}-corrected JC-D7 signal at least 0.5 times lower or 2.0 times higher than the median were selected for further analysis. The thresholds were chosen due to the feasible number of strains for subsequent experiments and a particular interest in high-producing strains. Mutant strains that failed to grow were excluded from further consideration. The analysis was limited to mutants with an OD_{600} of at least 1.0. Protein-protein interaction networks and functional enrichment of the selected single-gene deletion mutants were analyzed using the STRING database [228]. Edges in the network represent both functional and physical protein associations. Clustering within STRING was performed on the condition that no single gene would be considered its own cluster. This resulted in 20 clusters for further analysis.

2.4 Material and Methods for Chapter 5

2.4.1 Strains

In addition to the strains already mentioned, an industrial strain collection purchased from VH Berlin e.V. (Research Institute for Baker's Yeast, Berlin, Germany) was used in this chapter. The strain collection comprised 153 industrial *S. cerevisiae* strains, including both traditional industrial and modern industrial strains (Suppl. Table A5). The strains are named according to their original nomenclature in the strain collection of the Research Institute for Baker's Yeast (VH-strain collection) for clarity and consistency.

2.4.2 Microtiter plate cultivation

The polyP hyperaccumulation protocol developed by Christ and Blank (2019) [1] was modified to enable high-throughput screening. This includes the omission of the adjustment of cell mass to 2.5 g/l CWW before the starvation phase and to a maximum of 30 g/l CWW before the feeding phase. Screening for strains with the best polyP content was conducted in 0.8 ml (2.2 ml/well, 96-well MTP), whereas screening for the best absolute producers was performed in 2.5 ml (11 ml/well, 24-well MTP). For preculture preparation, SD-medium was inoculated with a single colony from a YEP agar plate and incubated at 30 °C (300 rpm, 24 h). A 1 % (v/v) inoculum was then used to inoculate SD-medium and cultivate it under the same conditions for biomass generation (30 °C, 300 rpm, 24 h). After cultivation, the entire cell mass from each well was harvested by centrifugation (5,000 g, 5 min), washed once with deionized water, and stored at 4 °C for a maximum of 2 weeks. Subsequently, the complete cell mass was transferred to P_i-free starvation medium and incubated at 30 °C and 300 rpm for 6 h. Cells were subsequently harvested (5,000 g, 5 min), washed once with deionized water, and stored at 4 °C until the start of the feeding phase (17 h). P_i-starved cells were then transferred entirely to P_i-rich feeding medium and cultivated at 30 °C and 300 rpm for 2.5 h. The workflow after the feed phase varies depending on the method chosen for polyP analysis, which was performed either via JC-D7 fluorescence assay or enzymatic polyP quantification [221, 222, 227]. The JC-D7 method was used for the broad screening of 153 industrial and control strains. Fluorescence signals obtained from this assay were correlated with the final cell concentrations of the respective strains, which were measured using the Growth Profiler 960 (EnzyScreen, Heemstede, the Netherlands). 300 µl of culture broth from each strain was transferred into 96 half-deepwell MTPs (1.1 ml/well) and incubated for 1 h at 30 °C with shaking at 225 rpm in the Growth Profiler 960. Subsequently, biomass formation was assessed using the 'green value' obtained from image-based well analysis via Growth Profiler Control Software v4_9_0, with readings taken every 30 min for 1 h [229]. The remaining culture

broth with P_i-fed *S. cerevisiae* cells (500 µl) was harvested by centrifugation (5,000 g, 5 min), washed twice with deionized water, and stored at -20 °C until JC-D7 analysis was performed (section 2.4.4). The enzymatic assay for polyP quantification was applied in all other cultivations. In this case, the complete culture broth with P_i-fed *S. cerevisiae* cells was harvested by centrifugation (5,000 g, 5 min), washed twice with deionized water, and dried on P_i-free filter paper (5 min). 25-30 mg of CWW were stored at -20 °C until enzymatic polyP analysis was performed [221, 222].

2.4.3 Shake flask cultivation

Christ and Blank (2019) [1] developed the shake flask-based polyP hyperaccumulation protocol. For this chapter, the protocol was modified to align with the conditions of the MTP-based high-throughput screening format. This includes omitting biomass standardization to 2.5 g/l CWW for the starvation phase and to a maximum of 30 g/l CWW for the feeding phase. The entire cell mass was transferred throughout the hyperaccumulation protocol. The intermediate and focused screening for strains with the highest polyP content was performed in 10 ml culture volumes (in 100 ml flasks), while the secondary and refined screening for strains with the highest absolute polyP production was conducted in 25 ml volumes (in 250 ml flasks). Otherwise, the conditions followed the MTP protocol, except that the shaker speed was set to 200 rpm. Since only the enzymatic assay for polyP quantification was used in this format, the working procedure followed the one previously presented for the MTP format. The five strains showing the highest polyP content in the intermediate screening were also cultivated according to the polyP hyperaccumulation protocol by Christ and Blank (2019) [1]. This protocol follows the cultivation methods described above but includes biomass standardization, variable culture volumes, and intermediate cell mass drying on P_i-free filter paper (5 min).

2.4.4 JC-D7 fluorescence assays

For JC-D7-based polyP analysis, 500 µl of *S. cerevisiae* culture broth was resuspended in 300 µl lysis buffer (1 % SDS, 0.2 M lithium acetate). Cell disruption was performed via sonication (six cycles of 30 s each, followed by a 1 min cooling interval on ice). An in-house device enabled the simultaneous sonication of the entire MTP (Suppl. Figure A5) using the Bandelin Sonorex RK 100 (Bandelin Electronics, Berlin, Germany). JC-D7 staining was performed as described in the Materials and Methods section 2.1.5 [223, 227]. The cell extracts were diluted 1:500 in assay buffer (20 mM HEPES, pH 7.4, 1 % DMSO).

2.4.5 Size determination

Cell concentrations were determined using a Coulter Counter 4 (Beckman Coulter GmbH, Krefeld, Germany), based on particle size distribution (3-18 µm). Samples were diluted in Isoton II solution (Beckman Coulter GmbH, Krefeld, Germany) to stay below 10 % of the instrument's maximum particle concentration. This minimizes the measurement of artifacts. Before the measurement, the samples were adjusted to an OD_{600} of 1.0 with fresh SD-medium and cooled to reduce cell growth. For analysis, 0.1 ml of the diluted sample was mixed with 19.9 ml Isoton II. All measurements were performed in duplicate unless otherwise stated [230].

2.4.6 Ploidy

Ploidy was determined by flow cytometry using the protocol described by Todd et al. (2018) [231]. Actively growing cells from overnight cultures were fixed in ethanol, washed with sodium citrate, and treated with RNase A. Deoxyribonucleic acid (DNA) was stained overnight with propidium iodide, and fluorescence intensity was measured using a FACS Canto II flow cytometer (BD Biosciences, Franklin Lakes, NJ, USA). A total of 20,000 events were recorded per sample. Data analysis was performed using FlowJo™ v10.8 (BD Biosciences, Franklin Lakes, NJ, USA).

2.4.7 BioLector cultivation

The maximal growth rate (μ_{max}) of the best-performing strains of the VH-strain collection was determined in the BioLector I (Beckman Coulter GmbH, Baesweiler, Germany) in 48-well flower plates (M2P-MTP-48-B, Beckman Coulter GmbH, Baesweiler, Germany). Cultivations in the BioLector I were conducted in Verduyn medium with 20 g/l glucose at 30 °C, 1,000 rpm (3 mm throw), and 85 % humidity. A total of 1.2 ml of Verduyn medium was inoculated with *S. cerevisiae* preculture and adjusted to an initial OD_{600} of 0.1. The strains were cultivated in replicates (n = 4) for 24 h. The biomass was monitored every 30 min via backscatter measurements (gain = 60, λ_{ex} = 620 nm, λ_{em} = 620 nm).

2.4.8 Data analysis

Initial screening results of the JC-D7 fluorescence assay (Figure 13) are depicted as normalized fluorescence values (fluorescence/green value ratio). All values were normalized to the control strain VH2.200. This strain was included on each plate.

2.5 Material and Methods for Chapter 6

2.5.1 Strains

In addition to those strains already mentioned, the engineered strain *S. cerevisiae* CEN.PK113-7D pPr$_{Pho5}$-sfGFP was studied. *S. cerevisiae* CEN.PK113-7D pPr$_{Pho5}$-sfGFP was generated by introducing the plasmid pPr$_{Pho5}$-sfGFP into *S. cerevisiae* CEN.PK113-7D (hereinafter referred to as CEN.PK pPr$_{Pho5}$-sfGFP). The gene encoding the fluorescent reporter protein sfGFP was expressed under the control of the *PHO5* promoter to investigate the PHO pathway activation (Suppl. Figure A15) [173].

2.5.2 Modification of trace elements and vitamins in the starvation medium

Verduyn trace elements and vitamins were supplemented to the starvation medium according to Christ and Blank (2019) [1]. The concentrations refer to the mineral salts medium designed by Verduyn et al. (1992) [232]. To investigate the effect of individual trace elements and vitamins on polyP production, *S. cerevisiae* was cultivated in modified versions of the starvation medium. For this, trace element and vitamin solutions containing only a single component were prepared (Suppl. Table A8 and Table A9). To narrow down the specific trace elements influencing polyP accumulation, all trace elements were clustered into three distinct groups (Table 1).

Table 1: Clusters of trace elements applied for screening.
Trace elements were randomly assigned to the respective groups.

Group 1	Group 2	Group 3
Na_2EDTA	$CoCl_2 \cdot 6\ H_2O$	$FeSO_4 \cdot 7\ H_2O$
$ZnSO_4 \cdot 7\ H_2O$	$CuSO_4 \cdot 5\ H_2O$	H_3BO_3
$MnCl_2 \cdot 2\ H_2O$	$Na_2MoO_4 \cdot 2\ H_2O$	$CaCl_2 \cdot 2\ H_2O$
	KI	

In a series of cultivations, one group of trace elements each was omitted. PolyP production with *S. cerevisiae* was then compared to a fully supplemented starvation medium (positive control, PC) and starvation medium without any trace elements (NE_{TE}). Next, if the omission of a specific trace element group led to reduced polyP levels, *S. cerevisiae* was cultivated in a starvation medium lacking each component from the respective group individually. The vitamins were examined by omitting each individually from the starvation medium in a series of cultivations. The results were then compared to the PC and starvation medium without vitamins (NE_{TV}). Finally, polyP hyperaccumulation was performed in a starvation medium containing only the trace

elements and vitamins identified to be beneficial for polyP production. Results were then compared to the PC and starvation medium without trace elements and vitamins (NE_{TE+TV}).

2.5.3 Oxygen and carbon dioxide transfer rates

The TOM device (Adolf Kuhner AG, Birsfelden, Switzerland) was applied to monitor the respiratory activity of *S. cerevisiae* cultures during the starvation phase by non-invasive online determination of the oxygen transfer rate (OTR) and carbon dioxide transfer rate (CTR) in up to eight individual shake flasks. OTR and CTR were calculated according to Anderlei et al. (2004) [233]. Starvation experiments were conducted in 50 ml medium under the conditions mentioned above (30 °C, 200 rpm, 500 ml flask, 6 h). The OTR and CTR measurements were performed in 20-min cycles. These are divided into a 5-min measuring phase, a 1.17-min flushing phase, and a 13.83-min aeration phase.

2.5.4 BioLector cultivation

Starvation experiments with CEN.PK pPr_{Pho5}-sfGFP were performed in the BioLector I (Beckman Coulter GmbH, Baesweiler, Germany) in 48-well flower plates (M2P-MTP-48-B, Beckman Coulter GmbH, Baesweiler, Germany) to monitor GFP expression and growth online. Cultivations in the BioLector I were conducted at 30 °C, 1,200 rpm (3 mm throw), and 85 % humidity. The filling volume in the plates was 1.2 ml. 0.2 mg/l geneticin (G418) was added to all cultivations with CEN.PK pPr_{Pho5}-sfGFP to ensure plasmid retention. All other parameters are based on the above-mentioned conditions of the starvation phase. GFP (gain = 90, λ_{ex} = 488 nm, λ_{em} = 520 nm) and scattered light (gain = 50, λ_{ex} = 620 nm, λ_{em} = 620 nm) were measured with two internal filter modules. The OD-corrected GFP signal was calculated by correlating GFP to the scattered light signal.

2.5.5 Enzymatic polyP analysis

PolyP levels (section 2.1.4) for the initial screening of relevant trace elements and vitamins are expressed relative to the PC. Otherwise, polyP values in this chapter refer to cellular polyP contents (as KPO_3) in percent in CDW [% (w/w) polyP (as KPO_3)].

2.6 Material and Methods for Chapter 7

2.6.1 Strains

In addition to the strains described above, *S. cerevisiae* BY4742 MATα *his3Δ1 leu2Δ0 lys2Δ0 ura3Δ0* (hereafter referred to as BY4742 WT) was obtained from EUROSCARF (Oberursel, Germany). BY4742 strains carrying single deletions in phospholipid metabolism (Suppl. Table A11) were selected from the YKO single-gene *S. cerevisiae* deletion collection (EUROSCARF, Oberursel, Germany). The BY4742 *pah1*Δ strain was not available via the YKO collection. This strain, along with strains carrying mutations in inositol uptake or synthesis (Suppl. Table A10), was generated by Makarius Baier using *S. cerevisiae* CEN.PK113-7D as the parental strain (iAMB, RWTH Aachen University, Aachen, Germany). Gene deletions were performed using a CRISPR/Cas9-based approach. The plasmid pV1382, which encodes Cas9 and a guide RNA scaffold, was used for targeted mutagenesis (kindly provided by Gerald Fink; Addgene plasmid #111436) [234]. Guide RNAs (gRNAs) were designed using the CRISPOR tool [235] to minimize off-target effects and maximize on-target activity. For each gene targeted, approximately 500 bp upstream and 500 bp downstream of the open reading frame (ORF) were amplified by PCR and joined by 30 bp of homologous overlap in a fusion PCR to generate a ~1 kb repair template lacking the ORF. The CRISPR/Cas9 plasmid containing the gene-specific gRNA insert and the corresponding repair template was co-transformed into the *S. cerevisiae* strain CEN.PK113-7D using a standard heat shock transformation protocol. Transformants were selected on YEP medium supplemented with nourseothricin (YEP-Nat). Successful gene deletions were confirmed by PCR using one primer located outside and one within the repair template, followed by Sanger sequencing of the PCR product.

2.6.2 Cultivation procedure

The media composition and polyP hyperaccumulation procedure followed the methods described by Christ and Blank (2019) [1]. Initially, cells were cultivated in SD-medium to obtain biomass. Starvation and feeding phases were conducted in 24-well MTPs using 2.5 ml of the respective medium per well. For the starvation phase, 2.5 g/l CWW was transferred into 15 ml of starvation medium (six wells per replicate). Cultures were incubated at 30 °C and 300 rpm for 6 h. The entire culture volume from each replicate was harvested (5,000 g, 5 min) to obtain sufficient biomass for comparison with the media development study by Christ and Blank (2019) [1] or to account for poor growth of various mutant strains. The cells were washed once with deionized water and stored at 4 °C until the feeding phase (17 h later). For the feeding phase, P_i-starved cells were transferred to feeding medium and incubated at 30 °C and 300 rpm for 2.5 h, using 2.5 ml

per well (one well per replicate). For media characterization, the cell concentration was adjusted to 30 g/l CWW. In case of phospholipid metabolism mutants or strains carrying mutations in inositol uptake/synthesis, the lowest available cell mass in each experiment served as the reference for cell mass adjustment. The complete culture broth containing P_i-fed *S. cerevisiae* cells was harvested (5,000 g, 5 min), washed twice with deionized water, and dried on P_i-free filter paper (5 min). Samples of 25-30 mg CWW were stored at -20 °C until analysis. PolyP was quantified using the enzymatic assay described by Christ and Blank [221, 222] in all cultivations. Only mutants in inositol uptake/synthesis were cultivated in shake flasks according to Christ and Blank (2019) [1] to obtain sufficient biomass for analysis, as some of these strains showed poor growth in MTPs (section 7.3.3).

2.6.3 Media

Depending on the strain, the medium originally developed by Christ and Blank (2019) [1] was modified. Except for the control, all starvation media in this chapter contained only $ZnSO_4$ (2.5 mg/l) and inositol (25 mg/l) instead of the complete set of Verduyn trace elements and vitamins. For media development experiments, only the factors under investigation were varied during the initial screening of the components' effects. Following the initial screening, combined adjustments were made to the media composition of both the starvation and feeding medium. Final comparisons were made using the production medium described by Christ and Blank (2019) [1]. Details on the modified medium components and their concentrations are provided in Figure 26, Figure 27, and Table 5. Unit prices provided by Carl Roth GmbH & Co. KG (Karlsruhe, Germany) or Sigma-Aldrich (St. Louis, MO, USA) were used to calculate the costs of the starvation and feeding medium in the polyP hyperaccumulation protocol (Suppl. Table A12 and Table 5). For phospholipid mutant strains, SD and starvation media were supplemented with amino acids and uracil according to Pronk (2002) [225] due to auxotrophies of BY4742: 0.150 g/l uracil, 0.125 g/l L-histidine, 0.50 g/l L-leucine, and 0.125 g/l L-lysine. The pH was adjusted to 5.4 for the SD-medium and to 5.0 for the starvation medium using HCl or NaOH. The feeding medium was not modified. If the screening involved Mg^{2+}-dependent proteins, the starvation medium was additionally supplemented with 1.9 g/l $MgCl_2$. In the case of the *pah1*Δ knockout and strains carrying mutations in inositol synthesis or uptake, no additional supplementation was necessary, as those mutations were introduced in the CEN.PK113-7D strain. Any deviations from these methods are detailed in the respective results section.

2.6.4 Enzymatic polyP analysis

For media development experiments, absolute polyP values were reported to enable direct comparison with Christ and Blank (2019) [1]. In contrast, polyP values for phospholipid mutants and strains with mutations in inositol synthesis or uptake were expressed relative to their respective WT controls.

Chapter 3

Rapid fluorescence assay for polyphosphate in yeast extracts using JC-D7

Published as:

Deitert, A., Fees, J., Mertens, A., Nguyen Van, D., Maares, M., Haase, H., Blank, L. M., and Keil, C. Rapid Fluorescence Assay for Polyphosphate in Yeast Extracts Using JC-D7. *Yeast*, 41, 593-604, 2024, doi: 10.1002/yea.3979.

[Reprinted (adapted) with permission from John Wiley & Sons Ltd. Open Access CC BY-NC-ND 4.0. © The Authors 2024]

Contributions:

Alexander Deitert, Claudia Keil, and Jana Fees conceived the study. Experiments were performed by Duc Nguyen Van under the supervision of Claudia Keil [236] (TU Berlin, Berlin, Germany), and by Anna Mertens under the supervision of Alexander Deitert and Jana Fees [237] (iAMB, RWTH Aachen University, Aachen, Germany). Duc Nguyen Van and Claudia Keil analyzed abiotic disturbance factors and investigated the JC-D7 response to chemically produced polyPs. Alexander Deitert, Anna Mertens, and Jana Fees analyzed polyP staining using yeast extracts. Alexander Deitert, Claudia Keil, Jana Fees, Maria Maares, Hajo Haase, and Lars Mathias Blank contributed to writing the original published article, which is integrated in this chapter. Claudia Keil is the original author of the following sections of the published article: “JC-D7 Fluorescence Assays”, “JC-D7 Response to Chemically Produced PolyPs”, “Potential Abiotic Disturbance Factors Influencing JC-D7 Measurements”, and the part of the discussion about abiotic disturbance factors. Those sections have been included in this thesis, either in whole or partially in an adapted form for complete comprehension. Alexander Deitert is the original author of the other included sections. Philipp Demling and Lars Mathias Blank critically reviewed the chapter.

3 Rapid fluorescence assay for polyphosphate in yeast extracts using JC-D7

3.1 Abstract

PolyP is a ubiquitous and multifunctional polymer present across all domains of life. In industrial applications, it is valued for its distinctive physicochemical properties, including pH buffering, water retention, and antimicrobial effects. Despite its significance, polyP analysis remains challenging, with ^{31}P NMR still regarded as the gold standard. In this chapter, we present a semi-quantitative and straightforward approach for polyP detection in yeast extracts using the fluorescent dye JC-D7. The fluorescence intensity of JC-D7 was influenced by both polyP concentration and chain length within the tested range (0.5-500 µg/ml), precluding its use for absolute quantification in samples of unknown polymer composition. JC-D7 fluorescence was not affected by inorganic P_i concentrations up to 50 mM. However, several metal ions, most notably Fe^{2+}, Cu^{2+}, Co^{2+}, Zn^{2+}, Pb^{2+}, and Hg^{2+}, substantially reduced fluorescence, likely due to interference with polyP-dye interactions. In contrast, other abiotic factors, such as pH and temperature, showed a minimal impact. Following validation, the JC-D7 assay was employed to evaluate polyP accumulation in yeast strains carrying deletions in genes associated with polyP metabolism. Overall, this method offers a sensitive and robust detection of polyP in yeast extracts, facilitating high-throughput screening for strains with improved polyP biosynthesis. This would ultimately contribute to the development of sustainable P utilization strategies.

3.2 Introduction

Inorganic polyP is the linear polymer of P_i linked by phosphoanhydride bonds and is ubiquitous in all domains of life [104, 105]. The widespread presence of polyP is related to its diverse cellular functions, including P_i and energy storage, sequestration of cations, membrane channel formation, regulation of enzyme activities, control of gene expression, and stress response [49]. Several bacteria, algae, yeast, and fungi can rapidly and selectively hyperaccumulate P_i and store it as polyP, a phenomenon described for more than 70 years [1, 108, 113, 238]. Besides its physiological roles, polyP is of significant interest in numerous industrial applications due to its physicochemical properties [49]. PolyPs are nonflammable, biodegradable, and nontoxic. Therefore, they are used in fertilizers, flame retardants, or as food additives [49, 130]. Some properties are also directly defined by the polyP chain length. For example, the reactivation of actomyosin in meat products is most pronounced with $polyP_2$. Moreover, short-chain polyPs are mildly acidic and can be used as pH-buffering agents. Long-chain polyPs are highly hydrophilic

and bacteriostatic, both of which are beneficial properties in the food industry [49, 239]. Additionally, their cation complexing ability increases with longer chain lengths [240]. Despite the importance of polyP in biology and industry, many research questions regarding polyP, such as the primary signal(s) for polyP hyperaccumulation across the domains of life or the distribution of polyP in different cellular compartments, such as the mitochondrion, the nucleus, and the vacuole, remain unanswered [104, 105, 114]. One of the key challenges is the limited availability of easy-to-use, inexpensive methods for the direct detection and investigation of polyP [241, 242]. Currently, ^{31}P NMR is the analytical gold standard for identifying and quantitatively determining polyP concentrations and molecular weight. However, ^{31}P NMR requires samples with high polyP concentrations, expensive instruments, and has a low throughput [109, 243]. Recently, two enzymatic assays for determining the total polyP content and average chain length were developed [109, 222]. Although these assays enable reliable, high-throughput characterization, they rely on complex enzymatic conversion steps to detect the single monomer or dimer of polyP via colorimetric and fluorometric signals, respectively. Therefore, polyP is not detected in its original molecular structure, and specific enzymes are required. Another option for determining the total polyP content in samples is the use of low-molecular-weight fluorescent probes. For polyP detection, 4′,6-diamidino-2-phenylindole (DAPI) is the most popular fluorescence probe. DAPI/polyP complexes emit yellow-green fluorescence (maximum emission intensity at 550 nm), while DAPI/DNA complexes exhibit their emission maximum in the blue-white part at 475 nm (DAPI excitation at 360 nm) [244]. Despite its high affinity towards polyP, DAPI is known to interact with lipid inclusions [245, 246], nucleotides [247], RNA [247], and inositol phosphates [248]. Moreover, polyPs with a chain length below 15 P_i-subunits cannot be detected via DAPI [249]. Therefore, DAPI staining-based detection is limited by interferences from sample-related materials and its inability to cover the entire range of polyP chain lengths. Angelova et al. (2014) [223] introduced the fluorescent probe JC-D7 to specifically detect polyP *in vitro* and endogenous polyP in mammalian tissue sections. In this study, JC-D7 exhibited high selectivity for polyP and no responsiveness to a wide range of ubiquitous cellular P_i-containing molecules, such as DNA, RNA, ATP, and GTP [223]. Later on, Zhu et al. (2020) [250] applied the dye for the detection of plant polyP [250], and just recently, the sensor has found application as a polyP-dye in environmental algae and bacteria [251]. To our knowledge, JC-D7 has not yet been described for use in polyP detection in microbes used in biotechnology and food technology, including yeasts [45].

Here, we present the transfer of the protocol previously published by Angelova et al. (2014) [223] to extracts of *S. cerevisiae*. Baker's yeast is particularly intriguing for polyP research, given its ability to accumulate up to 28 % (w/w) polyP (as KPO_3) per CDW [1]. The impact of polyP

concentration and chain length differences, as well as polyP ligands such as metal cations and polyP extraction agents, on the fluorescence of JC-D7 was investigated. With the assay in hand, yeast strains carrying gene deletions in (poly)phosphate homeostasis were characterized.

3.3 Results

With the overall goal of developing a simple polyP detection method for assessing bio-polyP in *S. cerevisiae* samples, we investigated the suitability of the fluorescent dye JC-D7 as a sensor. For this purpose, industrial polyP and yeast-derived polyP were analyzed under various conditions using JC-D7.

3.3.1 JC-D7 response to chemically produced polyPs

The relationship between JC-D7 fluorescence intensity and polyP standards of varying concentrations and average chain lengths (ranging from 4 to 1,500 P_i-subunits) was investigated (Figure 5; Suppl. Figure A1 and Figure A2). The experimental conditions are based on those described by Angelova et al. (2014) [223].

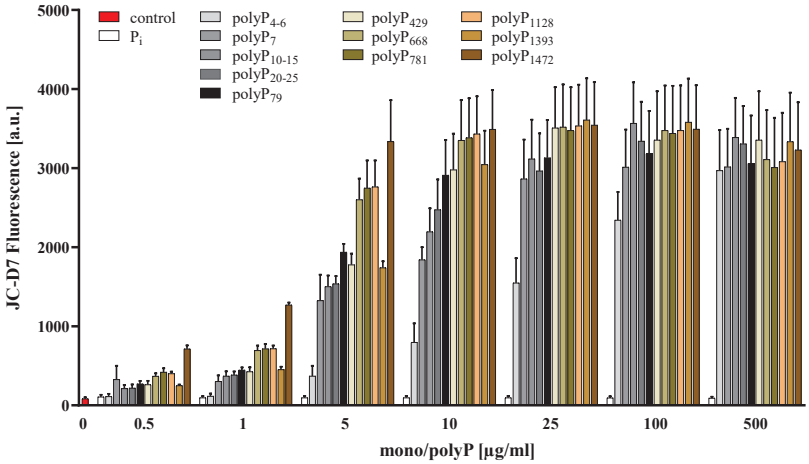


Figure 5: PolyP concentration and chain length dependence of the JC-D7 fluorescence signal.
25 µM solutions of JC-D7 were combined with increasing quantities of P_i or polyP of different chain lengths, followed by fluorescence detection (λ_{ex} = 390 nm, λ_e = 530 nm; Tecan Infinite M200 Reader). Values represent the means ± SEM of three independent experiments. Data associated with this figure were obtained from [236]. The figure was originally designed by Claudia Keil, was previously published [227], and is reprinted with permission from Yeast, published by John Wiley & Sons Ltd.

The JC-D7 fluorescence signal increased with both the concentration and chain length of polyP standards, reaching up to a 40-fold enhancement relative to buffer-only controls. No fluorescence response was detected in the presence of P_i, even at physiologically relevant concentrations of up to 50 mM (data not shown). JC-D7 detected polyPs with average chain lengths ranging from 4 to 1472 P_i-subunits, although signal intensity remained low at the lowest tested concentrations of 0.5 and 1 µg/ml (1.3- to 4.4-fold above control). At concentrations above 10 µg/ml and chain lengths exceeding 79 P_i-subunits, the fluorescence signals were saturated. A two-way ANOVA was conducted to evaluate the effect of polyP concentration and chain length on JC-D7 fluorescence (Suppl. Table A1). It revealed statistically significant impacts of concentration ($F = 151.9$, $p < 0.001$), chain length ($F = 24.7$, $p < 0.001$), and their combination ($F = 2.2$, $p < 0.001$). These interaction effects and fluorescence saturation limit the utility of JC-D7 for accurate quantification in samples with heterogeneous chain length distributions. However, it still provides a robust semi-quantitative method for evaluating polyP.

3.3.2 Potential abiotic disturbance factors influencing JC-D7 measurements

PolyP is an anionic molecule. Hence, it binds and sequesters cations, which may mask its P_i backbone and influence its interaction with the fluorescence dye JC-D7. Thus, various metal salts were tested for their effects on JC-D7 fluorescence (Figure 6; Suppl. Figure A3)

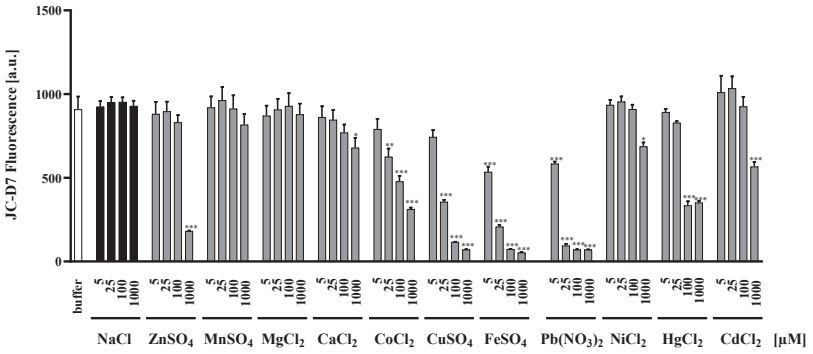


Figure 6: PolyP-mediated JC-D7 fluorescence in the presence of inorganic metal salts.
10 µg/ml of polyP mix was pretreated with either assay buffer or increasing quantities of metal salt solutions for 30 min, followed by detection of JC-D7 fluorescence emission (25 µM JC-D7; λ_{ex} = 390 nm, λ_{em} = 530 nm; Tecan Infinite M200 Reader). Data are presented as means ± SEM of three independent experiments. Significant differences from buffer incubations are marked by asterisks (*$p < 0.05$, **$p < 0.01$, ***$p < 0.001$; One-Way ANOVA with Dunnett's post-hoc Test). Data associated with this figure were obtained from [236]. The figure was originally designed by Claudia Keil, was previously published [227], and is reprinted with permission from Yeast, published by John Wiley & Sons Ltd.

It was observed that various metal ions strongly affected polyP-mediated JC-D7 fluorescence, significantly reducing the signal intensity. Among them, certain metals (Co, Cu, Fe, Pb) appeared to exhibit a stronger inhibitory effect than other tested inorganic ions. This effect of inorganic metal ions on polyP-induced JC-D7 fluorescence was further investigated using the metal chelator EDTA (Figure 7).

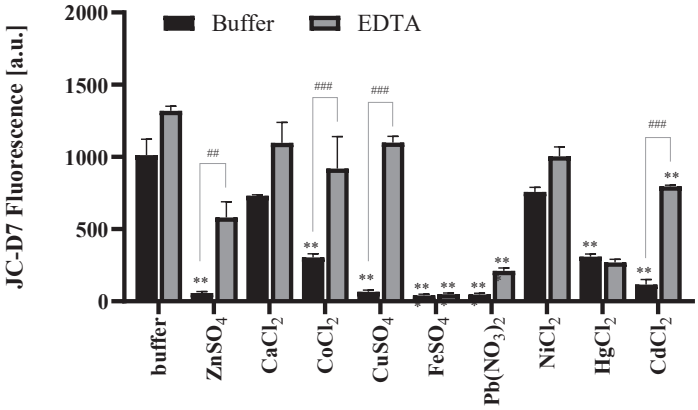


Figure 7: The effect of EDTA on metal salt quenching of polyP JC-D7 fluorescence.
10 µg/ml of polyP mix was pretreated with 1 mM metal salt solutions, followed by buffer- or 1 mM EDTA-posttreatment and fluorescence detection with 25 µM JC-D7 (λ_{ex} = 390 nm, λ_{em} = 530 nm; Tecan Infinite M200 Reader). Data are presented as means ± SEM of three independent experiments. Significant differences from buffer incubations (**p < 0.01, ***p < 0.001; Two-Way ANOVA/Tukey post-hoc test) or metal salt treatment ($^{\#\#}$p < 0.01; $^{\#\#\#}$p < 0.001; Two-Way ANOVA/Tukey post-hoc test) are indicated. Data associated with this figure were obtained from [236]. The figure was originally designed by Claudia Keil, was previously published [227], and is reprinted with permission from Yeast, published by John Wiley & Sons Ltd.

The previously observed quenching of the JC-D7 fluorescence signal was reduced for some metal-containing solutions after pre-treatment with EDTA. This was most pronounced for Zn, Co, Cu, and Cd. However, in some cases, EDTA treatment had little or no impact on the metal-induced quenching. This demonstrates the importance of considering macro- and microminerals when using JC-D7 to assess polyP in yeast samples. Components from extraction buffers must be evaluated for their potential impact on the interaction of JC-D7 and polyP when working with cell extracts. Therefore, the effect of common polyP extraction agents was assessed [221]. A 30-min pretreatment of the polyP mix with NaCl, LiCl, Triton X-100, SDS, Nonidet P-40 (NP-40), and Pluronic F-127 only resulted in a reduction in the JC-D7 fluorescence signal (25 µM) for SDS concentrations ≥ 0.1 %. All other agents revealed no significant impact at the tested concentrations (Figure 8).

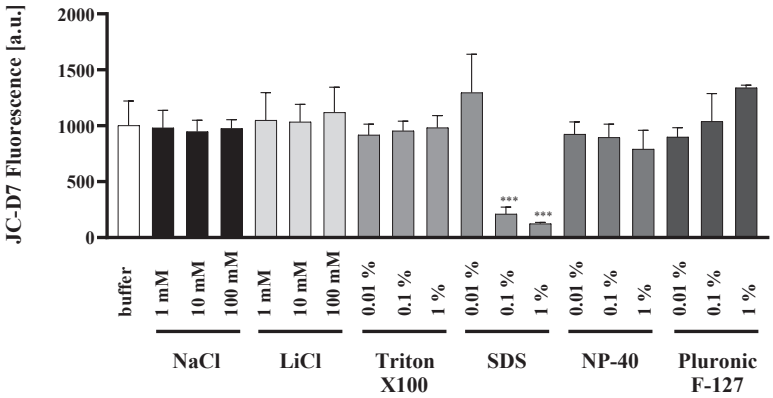


Figure 8: Effect of common polyP extraction agents on polyP JC-D7 fluorescence.
10 µg/ml of a polyP mix was pretreated with either assay buffer or increasing quantities of yeast polyP extraction agents for 30 min, followed by fluorescence detection with 25 µM JC-D7 (λ_{ex} = 390 nm, λ_{em} = 530 nm; Tecan Infinite M200 Reader). Data are presented as means ± SEM of three independent experiments. Significant differences from buffer incubations are marked by asterisks (***p < 0.001; One-Way ANOVA with Dunnett's post-hoc Test). Data associated with this figure were obtained from [236]. The figure was originally designed by Claudia Keil, was previously published [227], and is reprinted with permission from Yeast, published by John Wiley & Sons Ltd.

3.3.3 Validation of polyP detection with JC-D7 in polyP-rich *S. cerevisiae* extract

Even under various experimental conditions, JC-D7 could not be loaded into intact yeast cells for direct measurement of intracellular polyP (data not shown). Instead, the JC-D7 reaction with extracts from polyP-enriched *S. cerevisiae* VH2.200 cells ($VH2.200_{fed}$) was compared with those of $polyP_{20-25}$ (Budit 4), $polyP_{10-15}$ (Budit 7), $polyP_{4-6}$ (Budit 9) (either at 2.5 or 5.0 µg/ml) standards (Suppl. Figure A4). JC-D7 fluorescence analysis at 530 nm, as depicted by Angelova et al. (2014) [223], is also applicable for polyP detection in yeast extracts. PolyP Budit spectra match yeast extract spectra, suggesting that no other sample-related components interfere with JC-D7 fluorescence detection. The spectra also demonstrate an increase in signal intensity with both chain length and the concentration of the respective Budit standard (2.5 µg/ml vs. 5.0 µg/ml). However, this increase is not proportional, as observed previously (Figure 5). It is possible to analyze yeast samples with both reduced polyP concentrations or chain lengths, resulting in a low fluorescent signal intensity using JC-D7, because the intensity of the lowest Budit spectra ($polyP_{4-6}$) is 2.8-fold higher compared to the control (buffer). Thus, JC-D7 is suitable for semi-quantitative assessment of chemically produced polyP as well as bio-polyP in *S. cerevisiae* extract, even at low concentrations.

A series of measurement parameters, including temperature, pH value, and incubation time, were tested to optimize the JC-D7 fluorescence staining protocol (Figure 9). These parameters have previously been demonstrated to be critical for fluorescence measurements [252]. Therefore, extracts of the industrial yeast VH2.200 and the laboratory strain CEN.PK WT were either applied after P_i starvation or P_i feeding. Considering the temperature during the JC-D7 treatment period, no differences in the relative fluorescence intensity were observed between 24 °C and 30 °C (Figure 9A).

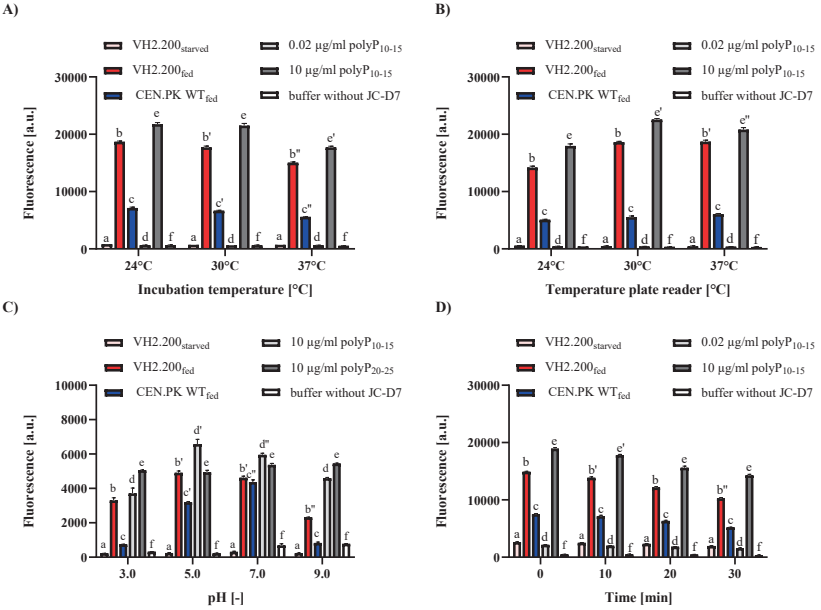


Figure 9: Optimization of JC-D7 application on yeast extracts.
PolyP standards as well as extracts from P_i-starved or P_i-fed yeasts were treated with 10 µM JC-D7 followed by fluorescence detection (λ_{ex} = 390 nm, λ_{em} = 530 nm; Agilent BioTek Synergy Mx). The impact of the (A) incubation temperature during JC-D7 staining; (B) temperature of the plate reader during readout; (C) pH of the JC-D7 staining buffer, and (D) duration of incubation (all time points mixing via pipetting) after adding JC-D7 dye was analyzed. Data are presented as means ± SEM of three independent experiments. (A-D) The effect of the different parameters in the respective panels was analyzed with one-way ANOVA/ Tukey's multiple comparison test ($p < 0.05$). Significant differences within one panel are indicated by not sharing the same letters. $VH2.200_{starved}$ (a); $VH2.200_{fed}$ (b, b`, b``); $CEN.PK\ WT_{fed}$ (c, c``); 0.02 µg/ml $polyP_{10-15}$ (d, d`, d``); 10 µg/ml $polyP_{10-15}$ (e, e`, e``); 10 µg/ml $polyP_{20-25}$ (e); Buffer without JC-D7 (f). Data associated with this figure were obtained from [237]. The figure was originally designed by Claudia Keil, was previously published [227], and is reprinted with permission from Yeast, published by John Wiley & Sons Ltd.

However, a labeling temperature of 37 °C led to a minor decrease in fluorescence. Consequently, 30 °C was used for further JC-D7 incubations. Besides that, the effect of temperature variations inside the plate reader during fluorescence measurement was investigated

(24 °C, 30 °C, and 37 °C) (Figure 9B). In general, the relative fluorescence intensity readout was highest at 30 °C. However, here only differences with *S. cerevisiae* VH2.200 extract, and polyP$_{10\text{-}15}$ (Budit 7) were detected (Figure 9B). Next, the influence of the pH value on the fluorescence intensity of JC-D7 was investigated (Figure 9C). Yeast extracts and chemical polyP standards were diluted in buffers with pH values ranging from 3.0 to 9.0. A fluorescence signal was measurable regardless of the pH value of the test solution. Though the JC-D7 signal decreased for samples containing cell extract at the pH values of 3.0 and 9.0. Therefore, solutions with these two pH values should be avoided to prevent a substantial drop in the fluorescence signal. In our setup, the pH value was kept around 7.4 by HEPES buffer. Moreover, the incubation time after JC-D7 addition was examined (Figure 9D). Samples were mixed, and the JC-D7 signals were determined immediately (t = 0 min) and at various time intervals. Incubation times of 10 min resulted in fluorescence intensities approximately comparable to those measured directly. However, after 20 min incubation, the fluorescence values of cell extract samples and chemically produced polyP standards slightly decreased and continued to decline after 30 min incubation. The cause of the signal decline after 20 min remains ambiguous and necessitates further investigation. Based on these findings, it is advisable to conduct measurements on JC-D7-treated samples promptly, or within a 20 min timeframe, to mitigate potential signal reduction. As the JC-D7 evaluation methodology demonstrates stability under various test conditions, it can be utilized for evaluating a broad spectrum of chemical polyP samples, polyP-containing yeast cell extracts, and likely also extracts prepared from other prokaryotic and eukaryotic cells or tissues.

Finally, the suitability of JC-D7 for evaluating yeast samples with different polyP concentrations was assessed. Therefore, extracts of yeast strains with varying polyP accumulation capabilities were treated with JC-D7 (Figure 10A), and the results were compared to those of the established enzymatic assay for total polyP quantification, which utilizes *S. cerevisiae* exopolyphosphatase scPpx1p and inorganic pyrophosphatase scIpp1p (Figure 10B) [222]. In the enzymatic assay, VH2.200$_{fed}$ exhibited a polyP content of 26.8 % (w/w) polyP (as KPO_3), whereas CEN.PK WT$_{fed}$ produced 4.3 % (w/w) polyP (as KPO_3), and BY4742 WT$_{fed}$ produced 7.5 % (w/w) polyP (as KPO_3). However, by deleting the endo- and exopolyphosphatase Ppn1p [253], BY4742 *ppn1*Δ increased the polyP production up to 10.3 % (w/w) polyP (as KPO_3) (Figure 10B) [254, 255]. In BY4742 *pho4*Δ, in which the transcriptional activator Pho4p [256] was deleted, the polyP content was markedly lower (2.9 % (w/w) polyP (as KPO_3)). Under P_i limitation, Pho4p activates transcription of PHO-responsive genes together with Pho2p, leading to the expression of Pho regulon genes, including P_i transporters, phosphatases, and vacuolar storage regulators. These genes play a crucial role in the P_i import process and in maintaining intracellular P_i levels [160, 169, 215]. Applying JC-D7 to these *S. cerevisiae* extracts, the fluorescence data (Figure 10A)

matched the trend of the enzymatic polyP data. The strain-related differences in polyP levels were depicted via fluorescence measurement (Figure 10A). Therefore, one can assess and categorize the polyP production of various yeast strains based on the JC-D7 fluorescent signal.

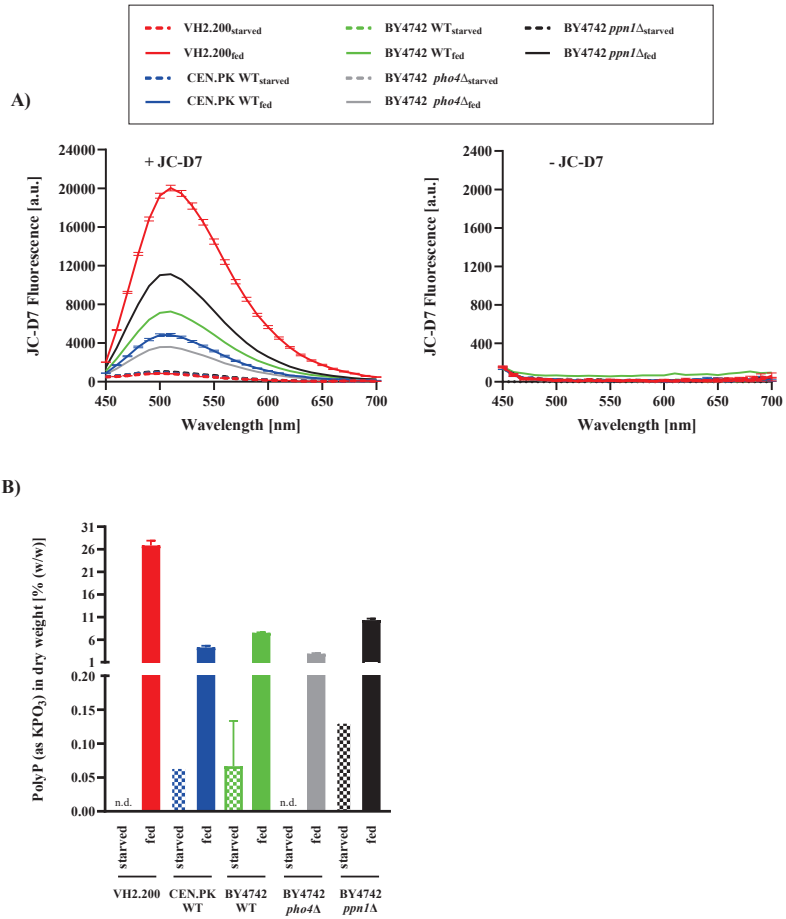


Figure 10: Comparison of JC-D7 fluorescence measurements and enzymatic analysis of polyP in yeast extracts.
(A) Extracts from P_i-starved or P_i-fed yeasts were treated either with 10 µM JC-D7 or buffer (30 °C, 30 min), followed by detection of fluorescence emission spectra (λ_{em} = 450-700 nm). (B) The same extracts were analyzed for their polyP content by enzymatic assays. Values represent the means ± SEM of three independent experiments. Data associated with this figure were obtained from [237]. The figure was originally designed by Claudia Keil, was previously published [227], and is reprinted with permission from Yeast, published by John Wiley & Sons Ltd.

3.4 Discussion

In our work, the protocol for polyP detection published by Angelova et al. (2014) [223] was applied to *S. cerevisiae* extract samples. After validating the capability of JC-D7 for detecting chemically synthesized polyPs with varying chain lengths, we examined the influence of potential interfering abiotic factors and parameters originating from yeast pre-treatment or yeast extract preparation procedure (metal cations, extraction agents, pH, and temperature). Finally, JC-D7 was tested as a polyP fluorescence dye on various yeast cell extracts, including two *S. cerevisiae* strains from the YKO collection that contained single gene deletions in polyP metabolism.

PolyP was detected across various concentrations and chain lengths via JC-D7, with inorganic P_i concentrations up to 50 mM not interfering with the fluorescence measurements. These findings are consistent with those reported by Angelova et al. (2014) [223]. As cellular P_i levels in yeast usually range between 10-75 mM [153, 257], polyP detection with JC-D7 should not be affected by P_i from yeast samples. Angelova et al. (2014) [223] reported a 5- to 15-fold increase in JC-D7 fluorescence with 10 µg/ml polyP of 15, 60, or 120 P_i-subunits and saturation at 50 µg/ml for $polyP_{60}$. In this study, a stronger fluorescence response was observed within the same concentration and chain length range, as saturation was reached at 10 µg/ml for polyP molecules containing 79 or more P_i-subunits. Consistent with Angelova et al. (2014) [223], longer polyP chains resulted in stronger JC-D7 fluorescence responses. This study reported a minimum detection limit of 0.5 µg/ml polyP with JC-D7, which is considerably higher than the detection limit demonstrated by Angelova et al. (2014) [223] (2 µg/ml). Our statistical analysis confirmed that both polyP concentration and chain length, as well as their combination, significantly influence the JC-D7 fluorescence signal. This is highly relevant given the pronounced polydispersity of polyP in biological samples [242, 255, 258, 259], which presents a challenge for accurate quantification [109, 222]. Although JC-D7's application is limited to semi-quantitative analysis, it is suitable for evaluating polyP in biological samples. Christ et al. (2019) [109] developed two sequential enzymatic assays for the quantitative determination of total polyP concentration using P_i standards (20-200 µM P_i) and the average polyP chain length employing $polyP_2$ standards (1-10 µM). In this study, JC-D7 fluorescence signals aligned well with enzymatic assay results across various *S. cerevisiae* extracts, which confirmed the consistency between these two analytical methods. However, JC-D7 does not allow quantitative evaluation due to the combined effects of polyP concentration and chain length on the fluorescence signal. The lowest Budit 7 concentration tested with JC-D7 (0.5 µg/ml) corresponds to 4.0 µM P_i in the enzymatic total polyP assay [109] (see Suppl. Information 1), indicating a slightly higher sensitivity of the JC-D7 assay compared to the enzymatic assay. Hence, the choice between these polyP detection methods should depend on the sample quantity and the specific research objective.

DAPI is another fluorescence dye used to detect polyP, exhibiting emission at 525 nm upon binding [242, 244]. In contrast to JC-D7, DAPI lacks specificity for polyP [223]. DAPI is commonly used to detect DNA, as it displays an emission maximum of 450-475 nm when bound to double-stranded DNA [244, 260, 261]. Therefore, when analyzing biological samples/extracts that may contain DNA and other nucleic acids, regarding their polyP content, JC-D7 can be advantageous due to its specificity. Moreover, DAPI only detects polyP chains longer than 15 P_i-subunits and shows minimal or no response to short-chain polyPs (3-5 P_i-subunits) at concentrations between 0.5 and 3 µM P_i [244, 249]. Similarly, short-chain polyPs are neither effectively detected via the PPK, PPX, and TBO-based quantification methods described by Ohtomo et al. (2008) [262], nor by the affinity polyP labeling technique using a recombinant polyP-binding domain introduced by Saito et al. (2005) [263]. Unlike JC-D7, DAPI fluorescence intensity revealed no variation when exposed to polyP standards ranging from 15 to 130 P_i-subunits at concentrations of 1.5-3 µM P_i [249]. Aschar-Sobbi et al. (2008) [244] observed faster fluorescence kinetics in DAPI-polyP binding for polyP with an average chain length of 130 P_i-subunits compared to 15 P_i-subunits. This difference in rate was proposed as a potential indicator for the polyP chain length. However, this principle was only demonstrated for these two specific chain lengths at a concentration of 0.5 µg/ml [244]. Similar to JC-D7, DAPI fluorescence induced by polyP likely involves multiple independently contributing factors, which complicate accurate quantification. Further, Aschar-Sobbi et al. (2008) [244] demonstrated an approximately linear correlation between the DAPI fluorescence signal and polyP in the range of 25-200 ng/ml for $polyP_{75}$. At a concentration of 1.5 µg/ml a saturation in signal intensity is reached [244]. Therefore, DAPI offers higher sensitivity but reaches saturation at lower polyP levels compared to JC-D7. The sensitivity of JC-D7 remains well-suited for the intended application with yeast extracts, as enzymatic quantification via the total polyP assay revealed polyP levels of approximately 2 mM P_i in low-producing and up to approximately 45 mM P_i in high-producing strains [222]. Moreover, the studies by Aschar-Sobbi et al. (2008) [244] and Diaz and Ingall (2010) [249] reported reduced DAPI fluorescence in the presence of ≥ 10 mM calcium or salinity levels of 150 mM for polyP chains of ~15 P_i-subunits, respectively. In this study, 100 mM NaCl, LiCl, $MgSO_4$, or $CaCl_2$ did not affect the JC-D7 fluorescence signal. Angelova et al. (2014) [223] only reported a reduction in JC-D7's polyP response in the presence of 150 mM KCl. Similarly, Yang et al. [25] demonstrated a negative influence of NaCl concentrations exceeding 100 mM on JC-D7 fluorescence.

Notably, Christ and Blank (2018) [221] observed a diminishing effect on polyP detection at NaCl concentrations of 5 mM during extraction, potentially due to decreased extraction efficiency and/or direct inhibition of polyP detection using the enzymatic assay. Although the precise cause

of the inhibition was not clarified, the link between polyP extraction and detection should be considered. Among the detergents tested, only SDS at concentrations greater than 0.1 % (v/v) affected the polyP-induced JC-D7 fluorescence. An adverse effect of SDS was also noted during optimization of analytical polyP extraction by Christ and Blank (2018) [221]. When adding 2.8 % (v/v) SDS to the lysis buffers for polyP extraction, polyP quantification was completely inhibited. SDS breaks ionic bond interactions, hydrophobic interactions, as well as hydrogen bonds when interacting with proteins [49]. This might have led to denaturation and thus inactivation of the enzymes applied for polyP quantification by Christ and Blank (2018) [222]. The detergent may also have impaired the interaction between JC-D7 and polyPs. Future studies will require an in-depth analysis to determine the mechanism by which JC-D7 interacts with polyP, providing more insight into its favorability for polyP detection compared to other detection methods.

The JC-D7 measurement and enzymatic polyP quantitation in yeast extracts showed similar patterns in this study. The above-average polyP accumulation capacity of *S. cerevisiae* VH2.200 [1, 103] was demonstrated by both methods. Moreover, yeast mutants previously identified to hypo- (gene deletion mutant of transcriptional activator YFR034C/*PHO4*) or hyperaccumulate (gene deletion mutant of polyphosphatase YDR452W/*PPN1*) polyP [160, 255, 264] in the enzymatic quantification could be verified with the JC-D7 fluorescence assay. In the future, the JC-D7 fluorescence assay might be used for high-throughput screening of various engineered and natural yeast strains. As a result of these findings, yeasts with more efficient biotechnological polyP production reusing P_i-containing wastewater or side streams can be identified [64, 103]. PolyP is a polyelectrolyte and forms complexes with metal cations through interaction with its negatively charged P_i groups. Metal-polyP complexes play a crucial role in metal sequestration and detoxification in both prokaryotic and eukaryotic microorganisms [112, 265, 266]. It was reported that polyP binds monovalent (Na^+, Ag^+), divalent (Ca^{2+}, Mn^{2+}, Sr^{2+}, Zn^{2+}, Co^{2+}, Ni^{2+}, Cu^{2+}), and trivalent (Fe^{3+}, Al^{3+}, Eu^{3+}) cations [267-269], exhibiting dissociation constants in the micromolar to nanomolar range [240]. This aligns well with the P_i/element ratio and concentrations found in yeast [270, 271]. The complex formation itself is influenced by the polyP chain length and the metal ion's coordination environment [240, 267, 269]. Our study also demonstrated quenching of the JC-D7 signal after treatment with metal salts, particularly $FeSO_4$, $CuSO_4$, $CoCl_2$, $ZnSO_4$, $Pb(NO_3)_2$, and $HgCl_2$. This may result from metal-induced conformational changes in polyP [267, 269, 272], which potentially interfere with JC-D7's binding. According to Yan et al. (2023) [273], Zn^{2+} destabilizes the P-O-P bond in polyP and promotes hydrolysis by inducing conformational changes through chelation. This effect appears negligible in this study, as the addition of the metal chelator EDTA was sufficient to restore JC-D7 fluorescence in the presence of Zn^{2+}. Moreover, membrane-permeable chelators such as Tris(2-pyridylmethyl)amine (TPA) or

N,N,N′,N′-tetrakis(2-pyridylmethyl)ethylenediamine (TPEN) could be employed to mitigate metal-induced quenching during JC-D7-based polyP detection in Zn^{2+}-rich yeast samples [274]. In addition to Zn^{2+}, these chelators effectively bind other divalent metal ions, including Cd^{2+}, Co^{2+}, Ni^{2+}, and Cu^{2+} [275]. Thus, they are considered promising tools for preventing metal-induced quenching of the JC-D7 signal and improving assay performance.

3.5 Conclusion

This chapter presents the first application of JC-D7 for detecting biologically produced polyP in *S. cerevisiae* extracts. The JC-D7 assay demonstrated robustness against various abiotic factors and common extraction agents. Hence, JC-D7 is established as an additional, reliable tool for polyP detection in baker's yeast. Due to its high sensitivity and semi-quantitative nature, JC-D7's primary application is envisioned in high-throughput screening workflows as a pre-screening stage. In the following chapters, the JC-D7 fluorescence assay is used to rapidly classify *S. cerevisiae* strains originating from a genome-wide library of mutants with single-gene deletions of non-essential genes and an industrial strain collection based on their polyP production capacity. Thereby, JC-D7 provides a valuable tool for further investigation of yeast polyP accumulation and for advancing the development of bio-based polyP production.

Chapter 4

Screening of the Yeast Knockout collection to identify new engineering targets in polyphosphate metabolism

Contributions:

Alexander Deitert conceived the study, analyzed the data, prepared figures, and wrote this chapter. Lieselotte Vermeersch conducted all experiments using the microbe-handling robot (HiTMan) at KU Leuven (Leuven, Belgium). Roy Eerlings, Lennart Brans, and Anna Mertens contributed to pre-experiments and preparations essential for the execution and planning of the study (iAMB, RWTH Aachen University, Aachen, Germany). This chapter was critically reviewed by Philipp Demling and Lars Mathias Blank.

4 Screening of the Yeast Knockout collection to identify new engineering targets in polyphosphate metabolism

4.1 Abstract

PolyP is of interest from both biological and industrial perspectives. From a biological perspective, it is relevant because of its universal distribution and its involvement in various cellular functions. Owing to its unique physicochemical properties, polyP is used in a wide range of industrial applications. Although chemical polyP synthesis is well-established, biotechnological polyP synthesis offers several advantages, particularly in terms of sustainability and the potential to generate novel polymers with unique properties. *S. cerevisiae* is an interesting polyP-producing organism as an established host organism in both industry and research. However, despite decades of research, the mechanisms underlying polyP hyperaccumulation in baker's yeast remain poorly understood. In this chapter, the established polyP hyperaccumulation protocol for *S. cerevisiae* was integrated together with the JC-D7 fluorescence assay. A high-throughput workflow using a robotic platform was developed to identify previously unknown mutations affecting polyP metabolism from the YKO collection. This screening identified 171 potential targets for metabolic engineering to enhance polyP production in *S. cerevisiae*. Many of these genes have not previously been associated with polyP metabolism. Overall, this chapter demonstrates the feasibility of high-throughput screening for polyP hyperaccumulation in *S. cerevisiae*. Thereby, it contributes to elucidating the genetic regulation of polyP metabolism and its interconnections with other metabolic pathways. These findings can accelerate the development of biotechnological polyP production, thereby supporting sustainable P use and the transition away from a linear P economy.

4.2 Introduction

PolyP is a linear polymer made of P_i linked by energy-rich phosphoanhydride bonds [104, 105]. It is essential for various biological functions and is used in different industrial domains, including agriculture, water treatment, food, and pharmaceuticals [1, 49]. It acts as a soluble cation exchanger, is highly hydrophilic, buffers pH, exhibits bacteriostatic effects, is biodegradable, and has no toxic properties. The prevalent method for synthesizing industrial polyP is chemical condensation, carried out at 800 °C [276]. Since chemical synthesis is accompanied by certain disadvantages, including its CO_2 footprint and limitations in the polyP chain lengths it covers, alternative synthesis routes are being explored [1, 45, 131]. One alternative is the biotechnological production of polyP. Significant advancements have been made in this field with *S. cerevisiae*. A

hyperaccumulation protocol was developed that produced the highest reported polyP content of 28 % (w/w) polyP (as KPO_3) in *S. cerevisiae* [1]. This was also successfully transferred to P_i-rich waste streams [103].

In addition, considerable progress has been made in elucidating polyP metabolism, its regulation, and its connection with other cellular metabolic pathways [146]. A variety of studies have contributed to this understanding, including the systematic analysis of polyP concentrations in mutants of non-essential yeast genes in the YKO strain collection by Freimoser et al. (2006) [152]. This study was the first to isolate and quantify polyP in an entire mutant cell collection, as previously, only single mutant strains had been analyzed. Consequently, Freimoser et al. (2006) [152] established the foundation for a multitude of polyP research projects in yeast and other microorganisms [1, 108, 113, 238, 277, 278]. His study identified 255 knockout mutant strains with altered polyP levels. Most of the affected genes encode proteins involved in cytoplasmic functions, vacuole processes, or in transport and transcription. Hence, it was demonstrated that polyP connects various cellular pathways, including energy, carbohydrate, and P_i metabolism. Although many previously unknown genes were identified, uncertainties remain regarding polyP metabolism, also because Freimoser et al. (2006) [152] primarily identified strains with reduced polyP levels. In this regard, advancements in polyP analytics and polyP hyperaccumulation [109, 221, 222] have the potential to complement their results. Christ and Blank (2019) [1] developed a polyP hyperaccumulation protocol, which led to substantially increased polyP levels compared to previous studies and defined critical cultivation parameters for polyP accumulation. This, together with improved polyP extraction, yields 24-fold more polyP compared to Freimoser et al. (2006) [152]. As a result, it should become possible to more precisely detect differences in polyP accumulation between individual strains, due to the elevated overall polyP levels. Besides that, the enzymatic quantification methods developed by Christ and Blank (2018) [221, 222] cover all polyP chain lengths [109, 222, 242]. In contrast, Freimoser et al. (2006) [152] employed selective polyP extraction and quantification methods, only detecting polyP larger than 60 P_i-subunits. Although the enzymatic assay offers the opportunity to provide a more comprehensive overview of polyP metabolism in *S. cerevisiae* strain collections through a straightforward assessment of titer and chain length, it is not applicable for high-throughput screenings due to relatively high costs, stringent sample preparation requirements, and operational challenges. In this regard, the fluorescent dye JC-D7 provides a semi-quantitative alternative for polyP detection in yeast extracts, making it suitable for high-throughput screenings due to its simplicity, speed, affordability, robustness, and sensitivity as demonstrated in Chapter 3.

In this chapter, an adapted version of the protocol developed by Christ and Blank (2019) [1] was employed for high-throughput screening. The adapted protocol was combined with the JC-D7

fluorescence-based polyP detection to screen the YKO collection, marking the first small-scale application of these methodologies. Consequently, this approach should facilitate the identification of novel candidates that yield interesting phenotypes (i.e., reduced/elevated polyP content, growth-inhibiting). Based on these phenotypes, this study aims to gain a comprehensive understanding of polyP metabolism in *S. cerevisiae*, characterize the function of single genes, and identify previously unknown contributors within this complex, widely interconnected network. Thereby, new potential targets for the metabolic engineering of currently established production hosts should be identified to enhance the titer of biotechnological polyP production in *S. cerevisiae*.

4.3 Results

With the overall goal of identifying previously unknown genes involved in polyP metabolism and developing a more thorough understanding of the regulatory mechanisms behind P_i homeostasis in *S. cerevisiae,* a comprehensive set of 4,765 single-gene deletions in the YKO strain collection was screened for their effect on polyP synthesis via a high-throughput polyP hyperaccumulation and analysis workflow.

4.3.1 Identification of promising mutations for polyP synthesis

Control strains were first subjected to the downscaled, modified hyperaccumulation and subsequent quantification protocol to evaluate the suitability of this approach for high-throughput screening of polyP synthesis. The results of this pre-experiment confirmed the applicability of the workflow, including the cultivation strategy, polyP extraction, and polyP quantification (Suppl. Figure A6). However, previous shake-flask cultivations resulted in higher overall polyP signals (data not shown). The discrepancy between these cultivations is attributed to the cell mass adjustment in the original protocol [1], the reduced cultivation volume, uneven mixing in the robotic handling platform, and adjustments in the media composition. Nonetheless, the results of the pre-experiment support the transfer of the methodology to the high-throughput screening of the YKO collection. Here, only 1.1 % of the 4,765 strains showed no growth, providing additional validation of the assay's operational functionality. To determine polyP hyper- or hypoaccumulation of strains in this screening, the OD_{600}-corrected JC-D7 signal was used. 497 strains with a 1.5-fold improved OD_{600}-corrected JC-D7 signal compared to the median of all strains in the respective MTP were found. A preliminary examination suggested that some genes were identified that have a direct connection to polyP metabolism, thus representing plausible hits. These included *vma21*Δ, *pho91*Δ, and *pho80*Δ. Notably, the identification of Pho80p as a crucial

regulatory element in the polyP metabolism of *S. cerevisiae* is particularly relevant. Nevertheless, this number of strains (497) exceeds the limit for efficient screening and subsequent polyP analysis, which is performed via the quantitative enzyme assay [222]. Thus, it was crucial to reduce the number of strains by implementing more stringent selection criteria.

Only strains with a relative 2.0-fold higher OD_{600}-corrected JC-D7 signal compared to the median were now selected for further analysis. As a result, the total number of strains exhibiting elevated polyP contents was reduced to 157. Promising genes for further investigation included *vps74*Δ, *pho91*Δ, and *fbp1*Δ. Notably, several strains exhibited strongly elevated polyP levels, displaying OD_{600}-corrected JC-D7 signals of up to 46.0-fold above the median of the respective MTP. For instance, mutations affecting the mitochondrial V-ATPases, such as *vma11*Δ and *vma22*Δ, exhibited OD_{600}-corrected JC-D7 signals that were 6.0-fold and 14.0-fold higher than the median, respectively. These values are implausibly high and concern genes with known adverse effects on polyP production [152, 279]. The elevated signals likely resulted from analytical artifacts, as they coincided with substantially reduced OD_{600} values, indicating poor growth of the respective strains. To address this, a minimum OD_{600} threshold of 1.0 was introduced as an additional selection criterion, serving as a prerequisite for sufficient growth. This criterion is also relevant for the transfer of the respective mutations into biotechnological polyP production hosts, where sufficient growth is essential for industrial applications. This additional selection criterion reduced the total number of strains exhibiting polyP hyperaccumulation properties to 103 (Suppl. Figure A8 and Table A3). Additionally, 70 strains with hypoaccumulation properties were identified by applying an OD_{600}-corrected JC-D7 signal threshold of 0.5 relative to the median. This number was further reduced to 68 after applying the growth restriction criteria and included several known or noteworthy candidates, such as *vtc4*Δ, *mdm31*Δ, and *mrpl6*Δ (Suppl. Figure A7 and Table A2). A protein interaction network was generated via STRING, displaying functional and/or physical interactions between hypo- (red) and hyperaccumulating (blue) strains identified in this screening (Figure 11 and Suppl. Figure A9). Although many proteins lack direct connections, those included in the network interact more frequently than expected for a random set of proteins of comparable size and connectivity derived from the genome [228]. This suggests that these proteins are, at least in part, functionally or biologically interconnected. A functional enrichment analysis of the 171 selected mutants was conducted via STRING to provide a comprehensive overview of the pathways potentially involved in polyP synthesis in *S. cerevisiae* (Figure 12 and Suppl. Table A4). The functional enrichment shows statistically overrepresented biological pathways, processes, or functions. In this screening, 2.7 % of the yeast genome has been identified as contributing to the regulation of P_i/polyP levels. Thereby, the identified genes span a

broad range of cellular processes, particularly those related to mitochondrial translation, arginine and proline metabolism, maintenance, and nucleosome organization (Suppl. Table A4).

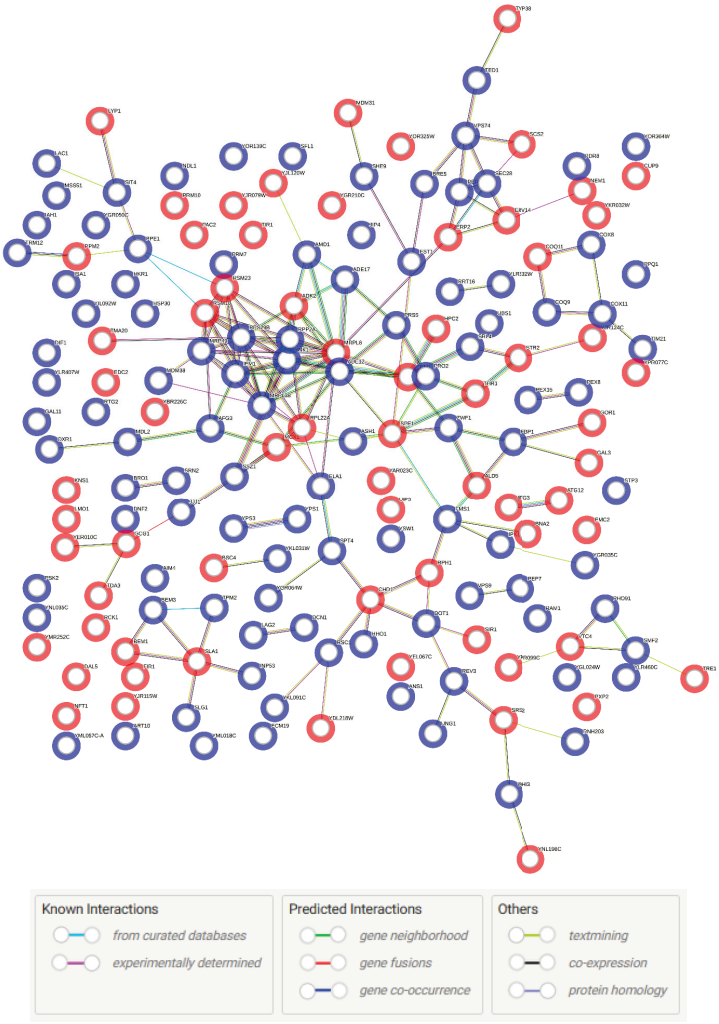


Figure 11: Protein interaction network of hypo- and hyperaccumulating deletions in the YKO collection.
Strains with an OD_{600}-corrected JC-D7 signal of 0.5x (red) and 2.0x (blue) were selected. The respective values were compared with the median of all cultures in an individual 96-well MTP (n = 1). The cultivation was performed according to the Chapter 2.3. This network was generated via STRING [228].

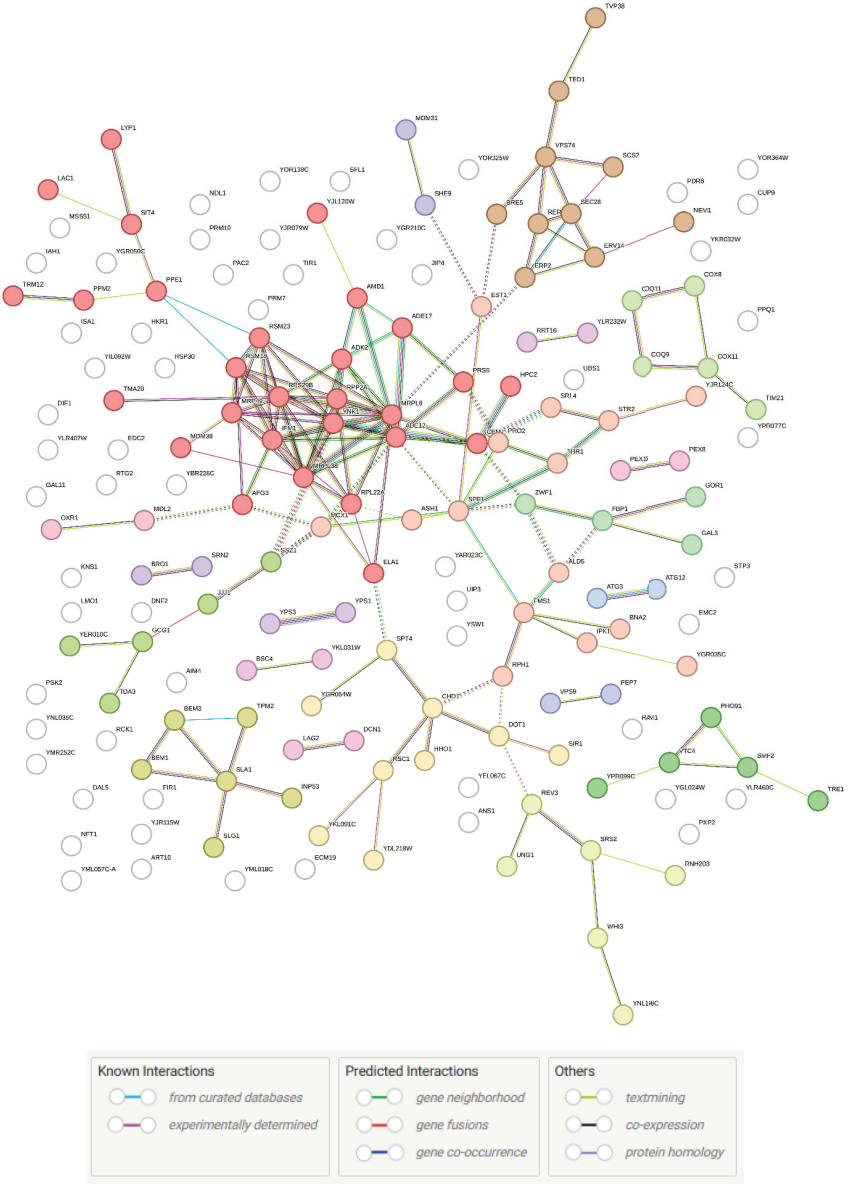


Figure 12: Protein interaction network including functional clustering of hypo- and hyperaccumulating deletions in the YKO collection.
Strains with an OD_{600}-corrected JC-D7 signal of 0.5x and 2.0x were selected. The respective values were compared with the median of all cultures in an individual 96-well MTP (n = 1). The cultivation was performed according to the Chapter 2.3. This network was generated via STRING [228].

Table 2 lists the genes that were identified by Freimoser et al. (2006) [152] and in this screening. The dataset from this study included strains with no growth or growth below the OD_{600} threshold of 1.0, as those strains were identified in the screening by Freimoser et al. (2006) [152] and only strains with no growth were excluded in their screening.

Table 2: Gene deletions identified in this screening and by Freimoser et al. (2006) [152].
Genes are categorized based on their growth status and whether the mutations exhibited hypo- or hyperaccumulating properties in this study. Strains showing no growth (O) or insufficient growth ($OD_{600} \leq 1.0$) according to the screening criteria (I), strains exhibiting the same polyP accumulation properties between the screenings (X), and strains showing varying polyP accumulation properties (Y). Comparison is based on final time point (24 h) of the third screening round by Freimoser et al. (2006) [152].

Freimoser et al. (2006) [152]	PolyP hypoaccumulation (this study)	PolyP hyperaccumulation (this study)	Insufficient growth (this study)
YBR217W	Y		
YCR028C-A		Y	I
YCR047C		X	I
YCR081W*		Y	I
YDL090C		X	
YHR025W	X		
YHR026W		Y	I
YHR060W		Y	I
YJL012C	X		
YLR226W*		Y	I
YNL198C	X		
YNL268W	X		
YOR140W		Y	
YPL234C		Y	I
YPL271W		X	I
YPR099C	X		
YPL129W**			O
YDR114C**			O
YDR127W			O
YEL031W			O
YOR241W**			O
YLR447C			O
YNL025C*			O
YLR240W			O
YLR396C			O
YPL268W			O

*Gene knockouts displaying polyP hyperaccumulation in just one of the intermediate time points (2 h, 4 h, 8 h) in the third screening round conducted by Freimoser et al. (2006) [152].
**Gene knockouts displaying polyP hyperaccumulation in the study by Freimoser et al. (2006) [152] at the final time point (24 h) of the third screening round, but insufficient growth in this study.

A total of 26 overlapping genes were identified. The comparison of polyP accumulation properties is based on the final time point (24 h) of the third screening round, as reported by Freimoser et al. (2006) [152]. Most of the strains identified in their study exhibited reduced polyP levels, with elevated levels observed only at specific time points during the screening. After excluding strains with no growth (O), the overlap between the two screenings decreased to 16 genes. Among these, eight genes (X) exhibited the same polyP phenotype as reported by Freimoser et al. (2006) [152] and eight genes (Y) showed opposite trends. These genes, particularly those showing the same trend in both screenings and exhibiting sufficient growth, represent the most interesting candidates for further investigation. This includes, for example, *atp15*Δ, a subunit of the F_1F_0-ATP synthase complex, and *vtc4*Δ, the Mn^{2+}-dependent catalytically active component in the VTC complex [152, 280]. The essential function of Vtc4p in polyP synthesis in *S. cerevisiae* was confirmed in a previous study [206], whereas the effect of Atp15p on polyP metabolism has not yet been elucidated. However, a potential effect could arise from the interconnection between polyP metabolism and energy metabolism in *S. cerevisiae* [146, 152]. This, however, requires further investigation.

4.4 Discussion

Large strain libraries necessitate high-throughput screening to efficiently evaluate individual variants. This involves automation and miniaturization, which was accomplished in this study using a high-throughput cultivation system integrated into a liquid-handling robotic platform [281, 282]. The study by Freimoser et al. (2006) [152] predominantly identified strains exhibiting polyP hypoaccumulation, which is attributed to their workflow with low polyP levels, selective polyP extraction, and targeted quantification methods [128]. At the same time, their protocol does not induce maximal polyP production in *S. cerevisiae*. In this study, 40 % of the identified strains with altered polyP characteristics were hypo-, and 60 % were hyperaccumulating. However, the selection criteria for identifying hyperaccumulating strains are more stringent than those for hypoaccumulation. When applying symmetrical thresholds, referring to an OD_{600}-corrected JC-D7 signal of ≤ 0.5× or ≥ 1.5× the median, 87 % of the strains hyperaccumulated polyP. Therefore, it can be assumed that this study and that of Freimoser et al. (2006) [152] identified different subsets of strains, as evidenced by the low percentage of overlap.

The predominance of polyP hyperaccumulating strains in this screening may be attributed to several underlying factors. Notably, *S. cerevisiae* BY4741 WT exhibited relatively low polyP levels under the applied screening conditions, making it more challenging to identify strains with reduced polyP levels. This is illustrated by the difference in the JC-D7 fluorescence signal ratio

between BY4741 WT and VH2.200 in this screening and in the results presented in Chapter 3, which were 0.04 and 0.34, respectively. The ratios between CEN.PK WT and VH2.200 were also slightly reduced, although not as pronounced as in the previous example, with values of 0.15 in this screening and 0.23 in the screening described in Chapter 3. CEN.PK WT usually produces polyP levels similar to those of BY4741 WT in the established polyP hyperaccumulation protocol (Chapter 3). The reduced polyP production is likely the result of the specific workflow employed, which includes the use of a liquid-handling robotic platform, small-scale cultivation, and a nutrient-rich medium that differs from the conditions typically used in polyP hyperaccumulation protocols [1]. This nutrient-rich medium had to be applied, despite previous studies demonstrating its negative impact on polyP production (data not shown), as BY4741 harbors several auxotrophies. Biomass formation is also thought to have had a direct effect on the final signal strength in this study, as the protocol lacks steps for cell mass standardization, whose influence was previously demonstrated [128]. Another contributing factor is the JC-D7 fluorescent dye. Fluorescence signals are inherently sensitive to ambient conditions, and in this screening, JC-D7 appears to exhibit a comparatively elevated baseline signal [227]. This may limit the detection of strains with reduced polyP contents and is likely intensified by low absolute amounts of polyP produced in 200 µl culture volume. Moreover, although the influence of various abiotic and biotic factors on JC-D7's signal intensity has been evaluated, additional factors specific to the specialized screening methods described in this chapter may also contribute [223, 227]. As a result, the number of strains with reduced polyP levels is likely underestimated, given that several mutant strains reported to exhibit polyP hypoaccumulation were not detected in this screening [146, 152, 160].

The current screening identified numerous novel genes as candidate targets for metabolic engineering due to substantially elevated or reduced polyP levels, including *atp15*Δ, *vtc4*Δ, *vps74*Δ, *pho91*Δ, *fbp1*Δ, *mdm31*Δ, and *mrpl6*Δ. These genes are directly linked to P_i homeostasis, vacuolar function, and energy metabolism. However, data on strains that hyperaccumulate or hypoaccumulate polyP are limited in the literature. Furthermore, the polyP synthesis network is highly redundant, allowing the loss of a single gene and its function to be compensated for by other genes or gene copies in polyploid strains, thereby complicating the generation of clear phenotypes [140]. To date, only a limited number of gene deletions have resulted in a substantial increase in polyP accumulation, including *pho80*Δ, *pho85*Δ, and *ppn1*Δ [209, 283, 284]. Conversely, mutant strains with impaired V-ATPase or VTC complex function, as well as knockouts of genes within the PHO pathway, have been shown to accumulate less polyP under P_i-rich conditions [160, 176, 285, 286]. This includes *vtc1*Δ, *vtc4*Δ, *pho81*Δ, *pho84*Δ, *pho4*Δ, *pho2*Δ, and *vma4*Δ [146, 160, 202, 283, 285]. Some of these strains exhibited compromised growth [160] and/or displayed polyP levels that deviated by less than 0.5-fold below or 1.5-fold above those of the respective WT-strain

in literature. Additionally, the literature contains discrepancies regarding the impact of specific gene deletions on polyP production in *S. cerevisiae.* For example*,* some studies have suggested a negative regulatory role for *pho80*Δ, while others have proposed a positive one [160, 278, 284, 286, 287]. However, none of these studies employed the polyP hyperaccumulation and subsequent quantification protocol presented by Christ and Blank (2019) [1], resulting in substantially reduced polyP production, selective polyP extraction, and imprecise polyP quantification. This could have ultimately led to the signal being within the noise level, thereby preventing clear discrimination of signal differences. Contrarily, this study identified several genes that are potentially associated with P_i metabolism and homeostasis when subjected to the hyperaccumulation protocol. Freimoser et al. (2006) [152] demonstrated that polyP synthesis is intricately linked to multiple metabolic pathways, indicating that functionally important mutations may be broadly distributed throughout the *S. cerevisiae* genome. In this context, the present study identified 171 novel candidate genes. However, the link between polyP metabolism and statistically overrepresented processes, such as mitochondrial translation or amino acid metabolism, requires further investigation. When interpreting the results, it is crucial to consider the single-iteration nature of this screening. Due to the large number of strains, associated costs (e.g., JC-D7 dye, robotic platform), and the significant experimental workload (e.g., medium exchange, polyP extraction), the screening was conducted without replicates. As a result, it is not possible to distinguish whether observed effects are due to actual biological differences or experimental variability.

4.5 Conclusion

This chapter presents the first genome-wide, high-throughput application of the JC-D7 fluorescence dye combined with the *S. cerevisiae* polyP hyperaccumulation protocol and a robotic handling platform to detect differences in biologically produced polyP levels. While the effects of identified gene deletions require confirmation through follow-up studies, 171 potential targets have been revealed for metabolic engineering aimed at enhancing polyP production in *S. cerevisiae*. Notably, many of these genes have not previously been linked to polyP metabolism. High-level polyP production is essential for scaling biotechnological polyP production with *S. cerevisiae* to industrial scales and achieving efficient recycling of inorganic P_i from waste streams. This would ultimately support the shift from a linear P_i economy toward a sustainable circular model. Following this initial successful demonstration of JC-D7 in a high-throughput setting, it was subsequently applied in the next chapter to screen an industrial collection of 153 strains for their polyP accumulation properties.

Chapter 5

Screening of an industrial *Saccharomyces cerevisiae* library to identify polyphosphate hyperaccumulating strains

Contributions:

Alexander Deitert conceived the study, conducted all cultivation experiments, analyzed the data, prepared the figures, and wrote this chapter. Anna Mertens (cultivation, size determination) and Lennart Brans (cultivation, size determination) performed experimental work under the supervision of Alexander Deitert (iAMB, RWTH Aachen University, Aachen, Germany). The maximal growth rate of the best-performing VH-collection strains was determined by Angelina Henk (iAMB, RWTH Aachen University) under the supervision of Alexander Deitert, Philipp Demling, and Tobias Karmainski [288]. Dominik Engels from the Chair of Biochemical Engineering (AVT.BioVT) at RWTH Aachen University assisted in handling the Coulter Counter (Multisizer X) and its data analysis (Suppl. Table A6). The ploidy analysis was conducted with support from the Flow Cytometry Facility, a core facility of the Interdisciplinary Center for Clinical Research (IZKF) within the Faculty of Medicine at RWTH Aachen University. Karla Stein from the iAMB (RWTH Aachen University) assisted with the experimental preparation for the ploidy determination and data analysis. The chapter was critically reviewed by Philipp Demling and Lars Mathias Blank.

5 Screening of an industrial *Saccharomyces cerevisiae* library to identify polyphosphate hyperaccumulating strains

5.1 Abstract

Biotechnological polyP production with *S. cerevisiae* is a promising alternative to the currently established chemical production process. Although the hyperaccumulation protocol yields a production of 28 % (w/w) polyP (as KPO_3), adaptations in the cultivation strategy or transfers to the bioreactor have not markedly improved yields or chain lengths. Metabolic engineering could overcome these limitations, but the utilization of products derived from genetically modified organisms (GMOs) is extensively controlled and strictly regulated. Therefore, this chapter investigated the polyP-accumulating potential of 153 industrial non-GMO *S. cerevisiae* strains and characterized their production in terms of polyP content, polyP productivity, and average polyP chain length. This study identified strains exhibiting the highest polyP content and highest average polyP chain length reported for baker's yeast, surpassing the previous benchmark organism *S. cerevisiae* VH2.200. The correlation between polyP accumulation and cell size was not confirmed. However, characterization of promising strains in terms of ploidy suggests a link between polyploidy and elevated polyP accumulation. The identification of strains with improved polyP production capabilities offers the potential to advance biotechnological polyP production with *S. cerevisiae* by yielding polyP with unique material characteristics and providing new hosts for metabolic as well as reaction engineering. This can ultimately contribute to more sustainable P management and the development of more economical bio-polyP synthesis.

5.2 Introduction

PolyP is a linear polymer consisting of P_i connected by high-energy phosphoanhydride bonds, with chain lengths ranging from as few as two to more than 1,000 P_i-subunits [142]. It is conserved across all domains of life and plays a crucial role in numerous cellular processes [49, 121, 152]. In addition to its biological significance, polyP has considerable industrial and commercial value due to its versatile physicochemical properties [49, 128]. These properties enable applications in a wide range of products, including food additives, water treatment reagents, and slow-release P_i fertilizers for agriculture. P_i fertilizers are especially essential for productive crop cultivation, making agriculture one of the largest consumers of P_i resources [3, 19]. Currently, industrial polyP is produced via chemical synthesis, in which purified orthophosphates undergo a condensation

reaction to form polyP chains [276]. Due to the harsh conditions during purification and synthesis, only short-chain polyP (< 40 P_i-subunits) is commercially produced on a large scale. However, P_i resources are becoming increasingly scarce, as P_i rock is a non-renewable resource [3, 61]. Consequently, the reuse and recycling of spent P_i are critical [43]. The yeast *S. cerevisiae* can selectively accumulate P_i and polymerize it into polyP [1, 144, 145]. Additionally, biological systems can produce high-molecular-weight polyP, which would offer new, distinct features compared to short-chain polyP [49, 128, 142]. For biotechnological applications and as a host for polyP production, *S. cerevisiae* is of special interest. Its biotechnological value is based on several advantageous traits, including its strong fermentative capacity and its resilience to environmental stresses such as high osmolarity and low pH [289]. Additionally, *S. cerevisiae* is classified as Generally Recognized As Safe (GRAS), is relatively easy to cultivate, and decades of industrial knowledge exist in terms of bioprocess development with baker's yeast [290-293]. Christ and Blank (2019) [1] developed a small-scale hyperaccumulation strategy that enabled *S. cerevisiae* to achieve the highest reported content of 28 % (w/w) polyP (as KPO_3) to date. The robustness of this approach was demonstrated in studies by Fees et al. (2022) [103], in which industrial waste streams and plant residues were successfully introduced as alternative P_i feedstocks. However, the average polyP chain lengths in *S. cerevisiae* typically range from 20 to 30 P_i-subunits [128, 158]. During downstream processing (DSP) of bio-polyP or polyP-enriched yeast extract, these chain lengths are further reduced by the purification conditions [103, 128]. As a result, the achievable chain lengths do not yet provide an advantage over chemically synthesized polyP. However, preliminary findings reveal substantial strain-dependent variation in both polyP accumulation and average chain length, emphasizing the critical role of strain selection and optimization [1, 158].

In this chapter, the previously developed polyP hyperaccumulation protocol for high-throughput screening was adapted to a library of industrial *S. cerevisiae* strains to identify those capable of accumulating long-chain polyP at high titers with improved production properties compared to the established host *S. cerevisiae* VH2.200. It was anticipated that the background from diverse industrial processes and associated genetic modifications would result in a broad range of polyP production levels. The screening yielded numerous strains with beneficial polyP production characteristics. Notably, this study reported the highest polyP content as well as the highest average polyP chain length in baker's yeast. These strains can ultimately serve as promising hosts for targeted metabolic engineering and polyP production in laboratory- and pilot-scale bioreactors.

5.3 Results

With the overall goal of identifying *S. cerevisiae* strains for the accumulation of long-chain polyP at high titers, a library of 153 previously uncharacterized industrial strains was screened for improved polyP accumulation properties in terms of polyP content, absolute polyP production, and average chain length compared to the currently best-performing polyP production host, *S. cerevisiae* VH2.200.

5.3.1 Identifying strains with the highest polyP content

Initially, the industrial strain collection was cultivated in triplicate in the high-throughput polyP hyperaccumulation protocol. The polyP levels were semi-quantitatively determined using the assay based on the JC-D7 fluorescence dye, as established in Chapter 3 and tested in Chapter 4. The screening included control strains producing low (CEN.PK WT) and high (VH2.200) polyP levels but did not involve a robotic handling platform. The results are depicted as normalized fluorescence values (fluorescence/green value ratio) in Figure 13. The values were normalized to the measurements of the control strain VH2.200.

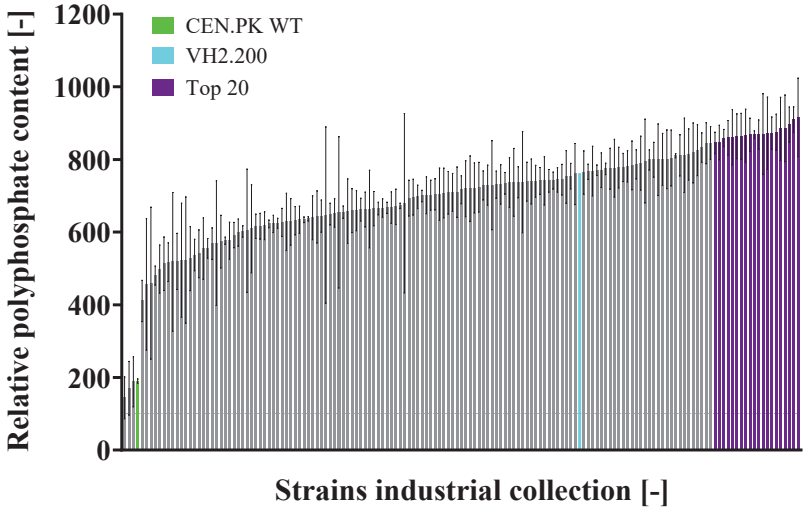


Figure 13: PolyP screening of the VH-strain collection in the non-adapted protocol for highest relative polyP signal.
Strains were cultivated in triplicate in the non-adapted protocol in MTPs. PolyP levels were measured via JC-D7. The fluorescence values were correlated with the cell density using the green value signal from the Growth Profiler and subsequently normalized to VH2.200. CEN.PK WT is shown in green, VH2.200 in cyan, and the 20 best-performing strains in purple. The results are represented as the mean of three replicates ± SEM.

66 % of the industrial strains exhibited lower polyP contents than VH2.200, while 33 % showed higher production. This demonstrated considerable variability within the strain collection. CEN.PK WT displayed the fourth-lowest polyP level overall. The polyP values of both CEN.PK WT and VH2.200 align with previously reported values determined via JC-D7 in Chapter 3 [227]. This consistency confirms the reliability of the assay. In this broad screening, VH2.102 was the strain yielding the highest normalized fluorescence signal on average. It outperformed VH2.200 by 20 % and exceeded the value of the laboratory reference strain CEN.PK WT by 380 %. However, the polyP quantification revealed relatively high variability compared to other methods [221, 222]. This variability is related to the JC-D7 dye and the cultivation procedure. Factors such as polyP chain length, absolute polyP levels, and external conditions influence the fluorescence signal [227]. Additionally, the analysis software of Growth Profiler 960 quantifies the cell density through images, which can be influenced by the cell shape [294]. Potential sources of error and variability are also introduced by the multiple-step process of cultivation and polyP quantification. However, as demonstrated in the previous chapters, the normalized fluorescence value correlates with polyP content and thus served here as an initial semi-quantitative estimate of polyP contents across the strain collection. Based on these results, the Top 20 strains were selected for the intermediate screening, comprising twelve baker's yeast strains, six dry baker's yeast strains, and two distiller's yeast strains (Suppl. Table A5). Additional information on the selected strains was not provided. In the second screening round, polyP was extracted using the phenol-chloroform method and quantified enzymatically, following the protocol by Christ and Blank (2018) [221, 222] to confirm the results. The enzymatic assay is quantitatively accurate but not suited for high-throughput screening. The enzymatic assay for polyP detection and increased culture volumes substantially reduced the standard error of the mean. The trends observed in the broad screening were mainly confirmed for the best-performing strains (Figure 14).

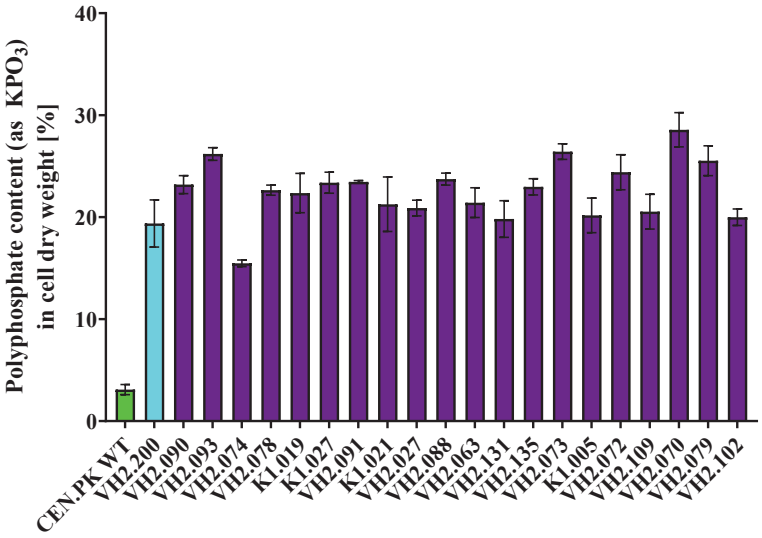


Figure 14: PolyP screening of the Top 20 strains of the VH-strain collection for the best relative producer in the non-adapted protocol.
Strains were cultivated in triplicate in the non-adapted protocol in MTPs. PolyP levels were measured via enzymatic total polyP assay. CEN.PK WT is depicted in green and VH2.200 in cyan. PolyP content (as KPO_3) per CDW [% (w/w)]. The results are represented as the mean of three replicates ± SEM. The strains are sorted based on their performance in the broad JC-D7 screening (Figure 13).

Most strains that previously exhibited higher polyP contents than VH2.200 maintained this trend, except for strain VH2.074, which exhibited lower polyP levels in both the MTP screening and a subsequent shake flask cultivation (data not shown). While the exact cause was not determined, it may be linked to the variability of the initial JC-D7 screening. As a result, strain VH2.074 was excluded from further analysis. Moreover, the polyP content ratios of the Top 20 strains relative to VH2.200 were slightly different from those in the broad screening, likely due to differences in the detection method. In the intermediate screening, VH2.200 produced 21.6 % (w/w) polyP (as KPO_3). The best-performing strain, VH2.070, achieved a polyP level of 28.6 % (w/w) polyP (as KPO_3), representing a 32.4 % increase compared to VH2.200. The polyP levels observed for VH2.200 and CEN.PK WT were lower than the maximum values reported in previous studies [1, 158], potentially due to modifications in the hyperaccumulation protocol used in this screening, which deviates from the original method by Christ and Blank (2019) [1]. This concerns the cultivation volume and the cell mass standardization between the cultivation steps of the protocol. To maintain comparability with the broad screening, the cell mass was not adjusted to 2.5 g/l CWW before P_i starvation, nor to a maximum of 30 g/l CWW before P_i feeding. The cell mass was not adjusted in the broad screening due to practical reasons. Differences in oxygen

supply in MTPs compared to shake flaks should not have affected final polyP levels [295], since previous studies with VH2.200 revealed no impact of oxygen levels on polyP hyperaccumulation [1]. The Top 5 strains were selected for the focused screening (Figure 15).

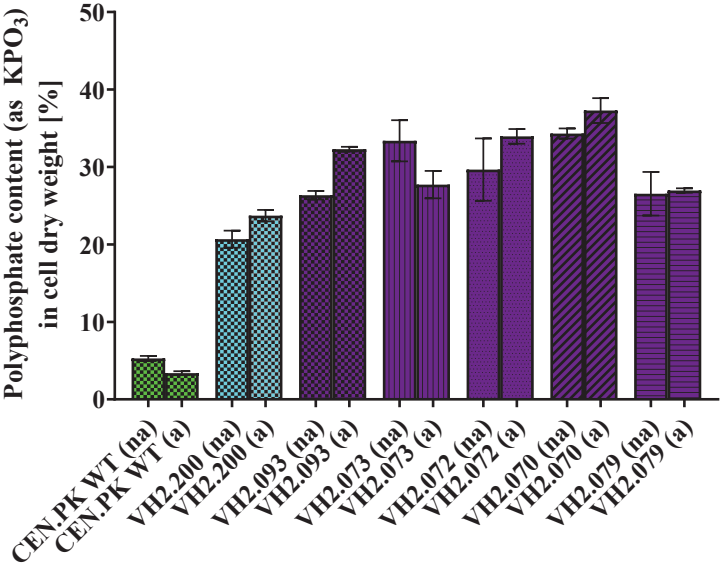


Figure 15: PolyP screening of the Top 5 strains of the VH-strain collection for the best relative producer in the adapted and non-adapted protocol.
Strains were cultivated in triplicate in both protocols in shake flasks. PolyP levels were measured via an enzymatic total polyP assay. CEN.PK WT is depicted in green and VH2.200 in cyan. PolyP content (as KPO_3) per CDW [% (w/w)]. Cultivation without (na) and with cell mass standardization (a) according to Christ and Blank (2019) [1]. The results are represented as the mean of three replicates ± SEM. The strains are sorted based on their performance in the broad JC-D7 screening (Figure 13).

The selected strains included one distiller's yeast (VH2.070) and four dry baker's yeasts (VH2.072, VH2.073, VH2.079, VH2.093). PolyP hyperaccumulation with these strains was evaluated in shake flasks in two different cultivation conditions. One condition followed the hyperaccumulation protocol described by Christ and Blank (2019) [1], with cell mass standardization before P_i starvation and feeding. The other procedure omitted this adaptation to mimic the conditions of screening rounds 1 and 2. This is illustrated in Figure 15, where (a) refers to the protocol including cell mass standardization, and (na) refers to the protocol without cell mass standardization. This focused screening round aimed to validate previous results using the original shake flask protocol and to assess the influence of cell mass standardization on these strains. As shown in Figure 15, all industrial strains except VH2.073 exhibited increased polyP content after standardizing the cell mass. This confirms previous findings for VH2.200 [128]. The effect of cell mass standardization may be attributed to key resources being shared among fewer

cells and to higher cell densities in previous screening rounds. High-cell-density yeast bioprocesses face challenges such as limited oxygen transfer capacity, restricted mass transfer rates, and glycolytic oscillations [296-299]. All Top 5 strains outperformed VH2.200 in polyP content in both conditions. Notably, strain VH2.070 achieved 37.3 % (w/w) polyP (as KPO_3) in the cell-standardized protocol, the highest reported content to date [1]. This surpasses the previous best value by 33 %.

Since polyP in *S. cerevisiae* is primarily stored in the vacuole, it was hypothesized that polyP production capacity might be directly proportional to cell size, suggesting a steric effect. The sizes of the Top 5 strains, controls (VH2.200 and CEN.PK WT), and low polyP strains (VH2.017 and VH2.129) were measured using the Multisizer X (Suppl. Table A6). The average diameter of *S. cerevisiae* cells, ranging from 5 to 10 µm as reported in literature, aligns well with the measurements in this chapter [300-302]. The only exception was CEN.PK WT, which had an average cell diameter of 4.77 µm. Among the two low producers, one is smaller than VH2.200, while the other matches VH2.200's size. Notably, the high-producing strain VH2.072 is also smaller than VH2.200. Thus, the cell size does not correlate with the final polyP content. Ploidy analysis (Suppl. Figure A11) suggests multiple genome or chromosome copies in all the Top 5 strains. In some cases, the exact ploidy could not be assessed by flow cytometry, likely due to chromosomal copy number variation (CCNV) or chromosomal rearrangements [290]. Strains with enhanced polyP production may possess additional copies of genes involved in polyP synthesis, such as those from the PHO pathway [146]. However, this hypothesis was not explored in the present study and requires further investigation.

5.3.2 Identifying strains with the highest absolute polyP production

Besides the polyP content, absolute polyP production can be a crucial strain-specific trait for industrial production. Lower polyP contents per cell can be compensated for by increased biomass production. Therefore, the 20 strains with the highest absolute JC-D7 fluorescence signal were selected from the broad screening of 153 strains to identify the best absolute polyP producer (Suppl. Figure A10). These 20 strains comprised ten baker's yeast strains, nine dry baker's yeast strains, and one strain for which no further information is available. They were cultivated in MTPs using the non-adapted protocol to preserve variations in growth and total biomass production (Suppl. Table A5). Figure 16A and Figure 16B depict the polyP content and absolute polyP production achieved in this cultivation.

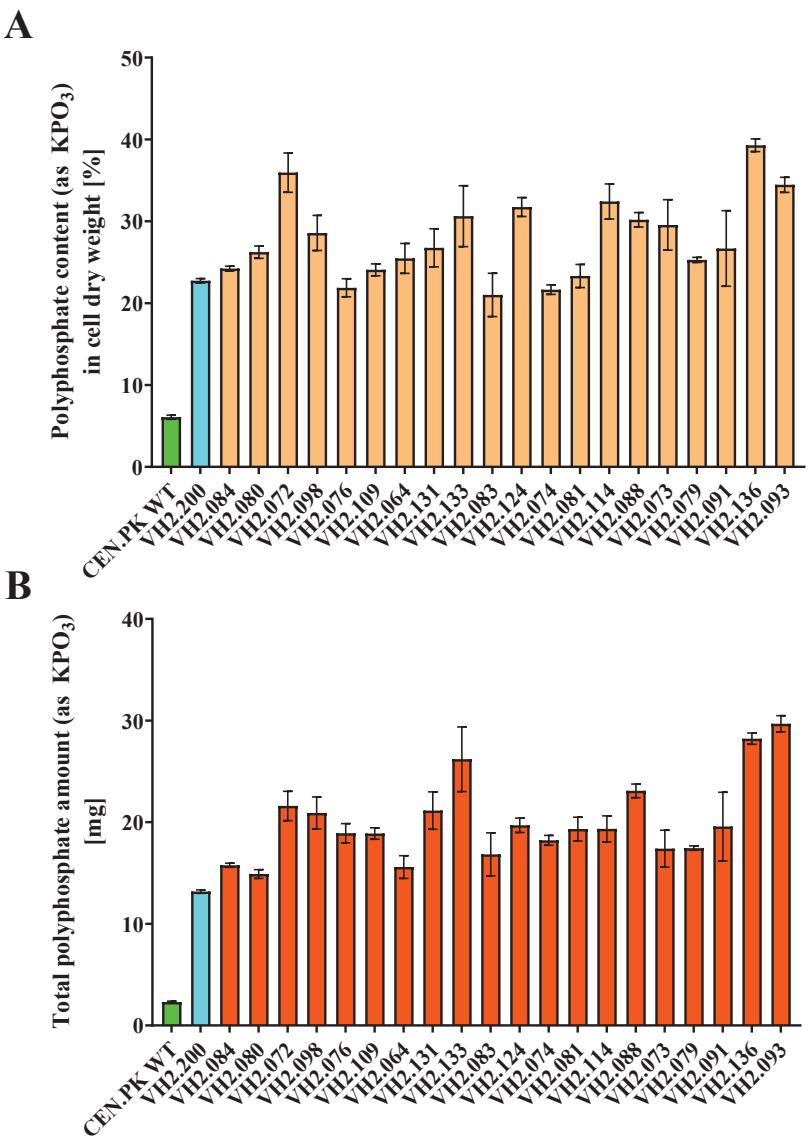


Figure 16: PolyP screening of the Top 20 strains of the VH-strain collection for the best absolute producer in the non-adapted protocol.
Strains were cultivated in duplicate in the non-adapted protocol in MTPs. PolyP levels were measured via the enzymatic total polyP assay. CEN.PK WT is depicted in green and VH2.200 in cyan. (A) PolyP content (as KPO_3) mass per CDW [% (w/w)]; (B) Total polyP amount (as KPO_3) produced per strain [mg]. The results are represented as the mean of two replicates ± SEM. The strains are sorted based on their performance in the broad JC-D7 screening (Suppl. Figure A10).

The polyP content varied among the selected strains, with some exhibiting levels comparable to those of VH2.200, while others produced substantially higher amounts. VH2.200 reached a content of 22.7 % (w/w) polyP (as KPO_3). The highest polyP content was observed in strain VH2.136 with 39.3 % (w/w) polyP (as KPO_3). However, the polyP content served only as an indicator of the absolute amount of polyP produced. When considering the total cell mass (Figure 16B), it was demonstrated that all tested strains exhibited increased total polyP production compared to VH2.200. This finding confirms the reliability of the broad screening. VH2.200 produced 13.2 mg of polyP by the end of the cultivation. The highest polyP producer, VH2.093, exhibited a 2.25-fold increase by producing 29.7 mg polyP. The other strains selected for secondary screening of the best absolute polyP producer also revealed substantial increases of 2.14-fold (VH2.136), 1.99-fold (VH2.133), 1.75-fold (VH2.088), and 1.64-fold (VH2.072) in polyP production compared to VH2.200. Two of these strains (VH2.072 and VH2.093) were also identified in the screening for the highest polyP content. This is particularly advantageous from a bioprocessing perspective, as their combination of high polyP content per CDW and elevated absolute polyP production simplifies DSP and improves process efficiency. However, VH2.136 with a content of 39.3 % (w/w) polyP (as KPO_3) was not identified in the previous screening procedure, in which it ranked 67th (Suppl. Table A7). This might be explained by the assay's variability and the JC-D7 dye's dependence on both polyP content and chain length. Nonetheless, the findings confirm the suitability of JC-D7 for high-throughput screening, as strains selected based on JC-D7 fluorescence were validated in follow-up screenings for both polyP content and total production.

The Top 5 best producers were subsequently evaluated using the non-adapted protocol in shake flasks for refined screening (Figure 17). Here, the polyP contents of these strains generally align with the results from the Top 20 secondary screening (Figure 16). Only strain VH2.072 showed a reduced polyP content of 24.0 % (w/w) polyP (as KPO_3) compared to 27.6 % (w/w) polyP (as KPO_3) in VH2.200. In the previous secondary screening, VH2.072 exhibited a polyP content of 35.9 % (w/w) polyP (as KPO_3) and VH2.200 of 22.7 % (w/w) polyP (as KPO_3). However, the biological duplicates of VH2.072 displayed considerable variation, with polyP values of 17.0 % and 31.0 % (w/w) polyP (as KPO_3). This points to potential inconsistencies in strain performance. The cause of this variation remains unclear, but it may be linked to differences between individual colonies. Due to this variability and lower biomass yield compared to VH2.200, VH2.072 exhibited reduced total polyP production. A subsequent cultivation of VH2.072 confirmed these findings (data not shown). Nevertheless, this outcome highlights the robustness of the screening procedure and its workflow. The cell sizes of these high-producing strains were also measured using Multisizer X and compared to VH2.200 (Suppl. Table A6). The

results further support the conclusion that cell size is not correlated with elevated polyP content. Notably, strain VH2.136 exhibited one of the highest measured polyP contents of 41.5 % (w/w) polyP (as KPO_3). However, the size is substantially smaller compared to other strains.

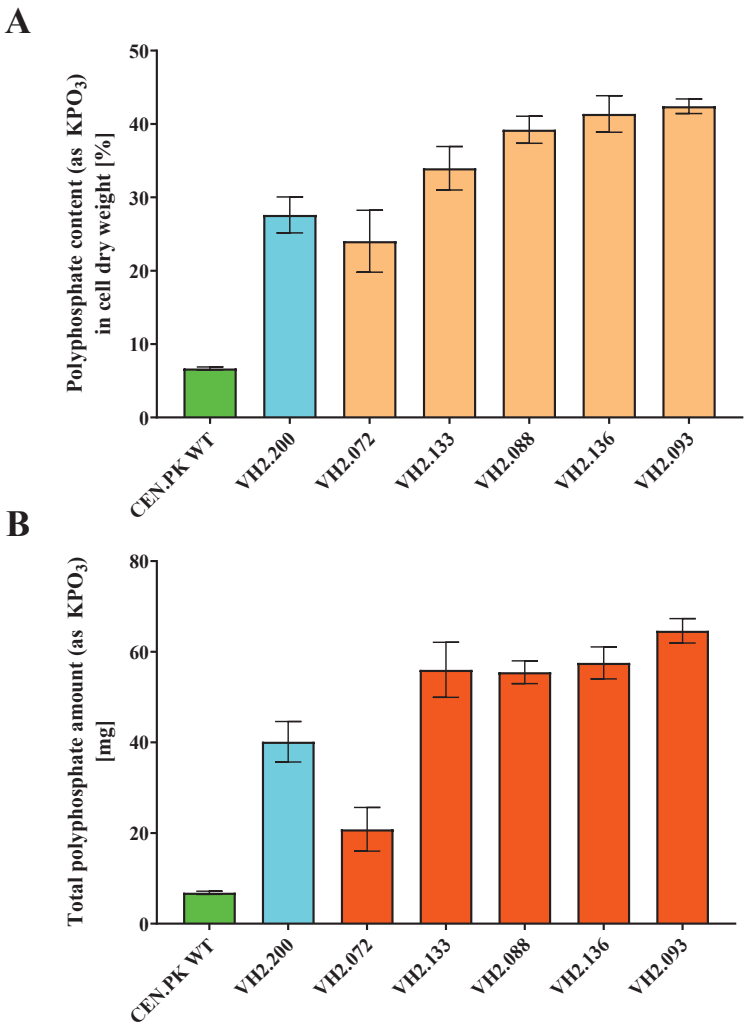


Figure 17: PolyP screening of the Top 5 strains of the VH-strain collection for the best absolute producer in the non-adapted protocol.
Strains were cultivated in duplicate in the non-adapted protocol in shake flasks. PolyP levels were measured via the enzymatic total polyP assay for two technical replicates of each duplicate. CEN.PK WT is depicted in green and VH2.200 in cyan. (A) PolyP content (as KPO_3) mass per CDW [% (w/w)]; (B) Total polyP amount (as KPO_3) produced per strain [mg]. The results are represented as the mean of four replicates ± SEM. The strains are sorted based on their performance in the broad JC-D7 screening (Suppl. Figure A10).

5.3.3 Chain length and growth rate of best-producing strains

The Top 5 strains from both the polyP content and absolute polyP screenings were analyzed for their polyP chain length (Table 3).

Table 3: Average polyP chain length and maximal growth rate (μ_{max}) of the best-performing VH-collection strains.
This includes industrial strains from the Top 5 in both screenings for polyP content and absolute polyP production. The average chain length results are represented as the mean of at least two replicates ± SEM. For the maximal growth rates, strains were cultivated in Verduyn medium with 20 g/l glucose. The strains were grown using the BioLector at 30 °C with an initial OD_{600} of 0.1 and a shaking speed of 1,000 rpm. The growth rates (1/h) were calculated from the logarithmic phase of the growth curves. The mean of four replicates was applied [288].

Strain	Average chain length [P_i-subunits]	Maximal growth rate [1/h]
VH2.200	36.5 ± 2.5	0.33
VH2.070	28.0 ± 1.6	0.23
VH2.072	53.5 ± 3.0	0.26
VH2.073	35.3 ± 7.7	0.19
VH2.079	33.4 ± 8.3	0.27
VH2.088	42.9 ± 5.6	0.18
VH2.093	51.2 ± 9.9	0.30
VH2.133	34.5 ± 3.8	0.21
VH2.136	65.7 ± 7.6	0.29

The chain length is a key factor influencing the applicability of bio-polyPs. Hence, differences in average chain length among the strains are an essential criterion for selecting a potential new host organism for production. VH2.200 exhibited an average polyP chain length of 36.5 P_i-subunits, which is consistent with previous findings [1]. Some strains produce substantially longer chains than VH2.200, with lengths of 51.2 P_i-subunits (VH2.093), 53.5 P_i-subunits (VH2.072), and 65.7 P_i-subunits (VH2.136). This provides new opportunities for tailor-made bio-polyP production suited to specific applications, especially since all these strains exhibit higher polyP levels and/or elevated absolute production. Additionally, this is advantageous compared to the chemical industry, which is limited to 40 P_i-subunits at an industrial scale.

The maximal growth rate (μ_{max}) of each identified strain was determined to evaluate their suitability for high-cell-density fed-batch bioreactor cultivations according to established industrial standards (Table 3). Hence, media can be tailored to strain-specific needs, preventing overfeeding and ethanol production. Avoiding ethanol is crucial to maximizing biomass yield, minimizing byproducts, and maintaining consistent process conditions. Literature reports a respirofermentative threshold of 0.38 1/h in glucose-limited chemostat cultivations. Above this

dilution rate, alcoholic fermentation occurred alongside respiration [303]. This value is strain-dependent, as other studies cite thresholds as low as 0.28 1/h [304]. The respirofermentative threshold, as a physiological limitation, in conjunction with physical constraints on heat and oxygen transfer in industrial-scale bioreactors, determines the achievable specific growth rate under industrial fed-batch conditions. The specific growth rate usually corresponds to 60 % of the respirofermentative threshold observed in glucose-limited chemostat cultivations. Hence, a growth rate of 0.18 1/h is typically set for *S. cerevisiae* strains in industrial fed-batch settings [305]. The μ_{max} determined under batch conditions in the BioLector I is considered to be close to the respirofermentative threshold observed in glucose-limited chemostats. These results reveal strain-specific differences in growth rates, with the current host strain, VH2.200, achieving a μ_{max} of 0.33 1/h. The lowest μ_{max} was recorded for strain VH2.088 at 0.18 1/h. Although the μ_{max} values of the most promising strains are close to those of VH2.200, they demonstrate that, with specific growth rates of around 60 % of the respirofermentative threshold, some strains would perform well below the industrial standard for fed-batch cultivations, such as VH2.088 [305]. Therefore, the industrial suitability of these strains needs to be evaluated in bioreactor cultivations to determine whether potential deficits in growth rate can be compensated by substantially increased polyP production.

5.4 Discussion

Despite recent advancements in *S. cerevisiae* polyP hyperaccumulation [128, 158], significant optimization potential remains. This includes improving production with existing strains by applying process-guided strain engineering as well as harnessing the vast natural and industrial diversity of *S. cerevisiae* strains for superior polyP production traits [289]. Academic model strains, such as *S. cerevisiae* CEN.PK and *S. cerevisiae* BY4741 exhibit low levels of polyP accumulation. Nevertheless, their haploid nature and well-characterized genetics have made them the primary hosts for metabolic engineering aimed at elucidating the mechanisms of polyP metabolism in yeast [146, 149, 173, 306]. Christ and Blank (2019) [1] highlighted the strain-dependent variability in polyP accumulation by comparing diverse *S. cerevisiae* strains, including supermarket baker's yeast, brewer's yeast, *S. cerevisiae* CEN.PK WT, and *S. cerevisiae* VH2.200 [1]. Back then, VH2.200 was identified as a promising host for polyP production, as it accumulates 28 % (w/w) polyP (as KPO_3). This represented the highest reported content at that time [1]. However, since VH2.200 was selected from a relatively small group of test strains, it was assumed that broader screening could identify even better-accumulating *S. cerevisiae* strains [307, 308]. The present study investigated a collection of 153 industrial baker's yeasts to explore their polyP

production capabilities. Many industrial *S. cerevisiae* strains have been selectively bred or adapted to exhibit specific phenotypic traits, such as reduced side product formation, enhanced ethanol yield (e.g., distiller's yeast), or optimized CO_2 production for leavening (e.g., baker's yeast) [290, 309-311]. Consequently, the VH-strain collection included both modern and older industrial strains applied for different purposes. The older strains were likely subject to less intensive breeding and selection pressures, preserving a broader natural phenotypic and genotypic diversity [290, 311]. Several strains with elevated polyP content, total polyP production, and average polyP chain length were identified. The initial broad screening employed the polyP-specific fluorescent dye JC-D7, thereby highlighting its suitability for high-throughput screenings, as discussed in Chapter 4. JC-D7 proved effective for prescreening the VH-strain collection, despite certain limitations [227], as its results were confirmed by the quantitative enzymatic polyP assay [221, 222]. Although JC-D7 likely led to the exclusion of some promising strains due to increased assay variability, there is no alternative for high-throughput applications. Enzymatic polyP quantification is not suitable due to its high costs, complex handling, and stringent requirements for sample preparation and sample purity [221, 222]. Moreover, employing independent polyP detection methods increases the confidence in the polyP production capabilities of the respective strains [227, 242]. Consequently, this chapter reports the highest documented polyP content to date, at 42.4 % (w/w) polyP (as KPO_3), in VH2.093 [1]. Unfortunately, no additional information is available on this dry baker's yeast. Additionally, several other strains exhibited elevated polyP levels and/or enhanced absolute polyP production compared with VH2.200, confirming the hypothesis that better-performing strains can be discovered through screening approaches. Applying strains with high polyP production capacity offers several advantages, including increased product yields, improved P_i recovery from waste or industrial streams, and new host organisms for metabolic engineering [1, 158]. The introduction of beneficial genetic mutations may further enhance polyP content or chain length in these strains [146]. In this chapter, some strains exhibited polyP chain lengths exceeding both the chemically maximal accessible length of 40 P_i-subunits and that of VH2.200 [1, 131]. The enzymatic assay yields results consistent with those obtained via ^{31}P NMR, the analytical gold standard for determining the concentrations and molecular weight of polyP [109, 242]. Discrepancies with chain lengths reported via polyacrylamide gel electrophoresis are related to these methods' limitations, as it does not accurately resolve short polyP chains [109, 159, 312]. Although the average polyP chain lengths observed in this chapter are significantly shorter than the maximum of more than 1,000 P_i-subunits reported in biological systems [142], polyP production in *S. cerevisiae* offers access to a novel biopolymer with uniquely adjustable physicochemical properties. Thus, a novel biobased compound with diverse applications in materials science could be introduced into the industrial

sector. Despite these promising developments, this study was unable to definitively determine the underlying mechanisms responsible for the enhanced polyP production capabilities, both in terms of content and chain length. Although polyP is primarily stored in the vacuole of *S. cerevisiae* [146], the cell size and elevated polyP storage capacity did not correlate. Next, ploidy and/or the number of specific chromosomes were thought to influence the polyP production levels. The high-producing strains of the initial screening (Figure 15) exhibited higher ploidy levels than the haploid strain CEN.PK and the diploid strain Ethanol Red. Moreover, their profile differed from that of the current production host, VH2.200. However, accurate ploidy classification of these strains remained challenging, as only haploid and diploid reference organisms were available for calibration. Based on its flow cytometry profile, VH2.200 is presumed to be tetraploid. The higher ploidy in VH2.200 relative to the CEN.PK WT may lead to increased polyP production by increasing the copy number of genes involved in the PHO pathway and polyP accumulation. Several studies demonstrate that variations in the copy number of individual genes or genomic loci can influence phenotypes in *S. cerevisiae* [146, 308, 313, 314]. Evolutionary engineering studies have also associated CCNV with beneficial traits, including improved product tolerance, inhibitor tolerance, and sugar fermentation kinetics [308]. This study did not investigate whether such effects apply specifically to PHO pathway genes and did not test low-producing strains for comparison. However, the strain collection comprised industrial *S. cerevisiae* strains that have been selectively bred and adapted for specific applications, such as baking. Notably, *S. cerevisiae* strains employed in the baking and brewing industries are typically polyploid [289]. A comprehensive analysis of 330 bakery strains revealed that 67 % of commercial bakery strains and 35 % of those isolated from natural sourdoughs are tetraploid. Most of these strains are autotetraploid, originating from hybridization events between distinct diploid *S. cerevisiae* strains [310]. The application of *S. cerevisiae* to specific, controlled fermentation environments has driven adaptation through human selection. This resulted in polyploidy, aneuploidy, heterozygosity, chromosomal rearrangements, transcriptional network rewiring, genome decay, copy-number variations, and the accumulation of nonsense mutations in non-essential or undesired genes [290, 311, 315-318]. While flow cytometry does not allow for the resolution of specific chromosomal copy number variations or segmental gene duplications, it can detect deviations in overall DNA content [308]. Alternative methods for assessing the chromosomal copy number include contour-clamped homogeneous electric field (CHEF) electrophoresis, quantitative real-time PCR (qPCR), array comparative genomic hybridization (aCGH), and next-generation sequencing (NGS) [308]. NGS and qPCR represent particularly promising approaches for assessing copy number variation. However, qPCR may face limitations in distinguishing between whole chromosome copy number changes and specific chromosomal region duplications (i.e.,

segmental aneuploidy). NGS requires high sequencing coverage for accurate estimation of the copy number by correlating the sequence's read depth with the relative abundance of its copy number across the entire genome [308, 319]. The collection strains display polyploid characteristics, but their profiles partially deviate from those of the reference strains and VH2.200. Therefore, further genetic characterization of the identified strains is required once the final polyP production strain has been selected for bioreactor cultivation.

Fed-batch cultivations enable pure respiratory growth of *S. cerevisiae* under aerobic conditions by maintaining glucose concentrations below a critical threshold. Hence, overflow metabolism can be prevented [303, 320-322]. This Crabtree effect directs most of the carbon source toward ethanol production, resulting in low yields of other target metabolites and the accumulation of byproducts [323]. A specific growth rate of 0.18 1/h for *S. cerevisiae* in the exponential-feed phase of industrial fed-batch cultivations considers the constraints imposed by the respirofermentative threshold and reactor properties (oxygen and heat transfer) [304, 305, 321]. The specific growth rate of several promising strains from the VH-collection is lower than that of currently established *S. cerevisiae* strains [305]. Therefore, the suitability of the promising strains for industrial polyP accumulation through fed-batch bioreactor cultivations requires further investigation. However, their polyP accumulation properties position these yeasts as promising candidates to support the transition toward a circular and sustainable P_i bioeconomy.

5.5 Conclusion

This chapter confirms the robustness of the JC-D7 fluorescence assay for polyP detection, as demonstrated in Chapters 3 and 4, proving that it can be successfully applied to an industrial strain collection using a modified protocol without a robotic handling platform. Several strains exhibited superior polyP production characteristics compared to the current production host, VH2.200, including higher polyP content, increased absolute polyP production, and longer average polyP chain lengths. These findings advance the development of more efficient polyP hyperaccumulation strategies by introducing novel host strains for metabolic engineering, enhanced P_i recovery, and high-cell-density fed-batch cultivations in stirred-tank bioreactors. As a result, this work contributes to increasing the technology readiness level of the process, which is an essential prerequisite for industrial evaluation and the transition of the technology to large-scale production.

Chapter 6

Influence of trace elements and vitamins on polyphosphate hyperaccumulation in *Saccharomyces cerevisiae*

Published as:

Deitert, A., Baier, M., Eerlings, R., Fees, J., Österlein Kück, A., Repin, J., Demling, P., and Blank, L. M. Polyphosphate Accumulation Is Determined by Zinc and Inositol in *Saccharomyces cerevisiae*. *Yeast*, 0, 1–12, 2025, doi: 10.1002/yea.70006.

[Reprinted (adapted) with permission from John Wiley & Sons Ltd. Open Access CC BY-NC-ND 4.0. © The Authors 2025]

Contributions:

Alexander Deitert conceived the study, conducted all cultivation experiments, analyzed the data, prepared the figures, and wrote this chapter. Ailín Österlein Kück (cultivations) [324] and Julia Repin (cultivations) [325] performed experiments and prepared figures under the supervision of Alexander Deitert (iAMB, RWTH Aachen University, Aachen, Germany). Plasmids and strains were designed, constructed, and characterized by Makarius Baier at iAMB (RWTH Aachen University). Jana Fees at iAMB (RWTH Aachen University) supported the strain engineering of this study. Philipp Demling, Roy Eerlings, and Lars Mathias Blank critically reviewed the chapter.

6 Influence of trace elements and vitamins on polyphosphate hyperaccumulation in *Saccharomyces cerevisiae*

6.1 Abstract

PolyP is an intriguing polymer with diverse biological and industrial applications. Chemical polyP production is energy-intensive and limited in chain length at large-scale production. Alternatively, biological production offers a sustainable solution. Recent research endeavors highlighted *S. cerevisiae* as a promising organism for polyP hyperaccumulation, achieving up to 28 % (w/w) polyP (as KPO_3). P_i starvation and P_i feeding are essential for this hyperaccumulation phenotype. Prior research has demonstrated that trace elements and vitamins increase polyP production in *S. cerevisiae* when added to the cultivation medium during P_i starvation. However, the role of trace elements and vitamins in enhancing polyP accumulation remained unclear. This chapter identified inositol and zinc to drive polyP accumulation across various laboratory and industrial *S. cerevisiae* strains. Moreover, these components influence the energy metabolism of yeasts. Our findings suggest that zinc boosts the PHO pathway during P_i starvation. The influence of inositol on polyP hyperaccumulation remains elusive, as it does not directly affect the PHO pathway. These findings contribute to the ever-growing understanding of polyP metabolism in *S. cerevisiae* and provide additional targets for optimizing biological polyP production.

6.2 Introduction

Inorganic polyP is the linear polymer of P_i connected by phosphoanhydride bonds and consisting of two to more than 1,000 P_i-subunits [104, 142]. PolyP plays a central role in various cellular processes, including energy- and P_i storage, cellular stress response, and membrane transport [107]. In humans and animals, it is also involved in biomineralization and blood coagulation [49, 326]. Its unique and diverse physicochemical properties, partially dependent on the chain length, deem polyP of interest for industrial purposes [49, 131]. Biodegradability, non-flammability, and non-toxicity are properties independent of the polyP chain length, making it suitable for use in fertilizers, flame retardants, and food additives [45, 49]. Other properties, including pH-buffering capacity, are more pronounced in short-chain polyPs. Additionally, $polyP_2$ and $polyP_3$ play a unique role in enhancing the water-holding capacity of meat after rigor mortis [239]. Properties such as cation-complexing ability and bacteriostatic activity are more pronounced in long-chain polyPs, which are of interest to the food industry [49, 130, 135]. PolyP is produced chemically from phosphoric acid (obtained from P_i rock) by a condensation reaction

at high temperatures [276]. Besides being highly energy-intensive and based on fossil resources, production is limited to manufacturable polyP chain lengths of 2-40 P_i-subunits at large scale [131]. Projected environmental benefits, including less energy consumption at benign process conditions and the potential to recycle different P_i sources, promoted the search for alternative, biological polyP production processes. It has been known since the 1960s that organisms, such as algae and yeast, selectively take up P_i and polymerize it intracellularly into polyP under certain conditions [145, 238]. This cellular process is referred to as polyP hyperaccumulation. PolyP hyperaccumulation has been primarily studied from a genetic and physiological perspective in microbes [146, 190]. Despite polyP's industrial relevance, few attempts have been made to produce polyP-rich biomass or pure biotechnologically synthesized (bio-)polyP [1, 159].

Previous studies have demonstrated that *S. cerevisiae* can be an efficient and robust host for polyP production. Moreover, *S. cerevisiae* is considered safe (GRAS), it is easy to cultivate, and yeast extract production is industrially established [289, 291, 327]. Christ and Blank (2019) [1] reported a cultivation strategy for polyP hyperaccumulation involving P_i starvation and subsequent P_i feeding, in which baker's yeast produces up to 28 % (w/w) polyP (as KPO_3) per CDW. The robustness of the strategy was demonstrated using industrial waste streams or plant residues as P_i sources for polyP production [102, 103]. Prior research highlighted that trace elements and vitamins drastically increase polyP production in *S. cerevisiae* when added to the cultivation medium during the starvation phase of the hyperaccumulation protocol [1]. However, the observed effects were not pinpointed to individual components of the cultivation medium.

In this chapter, the individual trace elements and vitamins in the cultivation medium that are responsible for elevated polyP production in the hyperaccumulation protocol were identified. After identification, the effects of the components were confirmed in industrial and laboratory yeast strains. Additionally, initial attempts were made to determine their mode of action in polyP metabolism. Thereby, this work improves the understanding of polyP hyperaccumulation in *S. cerevisiae* and lays a foundation for identifying the mechanisms involved in polyP accumulation.

6.3 Results

With the overall goal of characterizing polyP production by *S. cerevisiae* in our previously published polyP hyperaccumulation protocol, the role of individual trace elements and vitamins during the starvation phase was investigated, thereby aiming to reduce the amount of required nutrients and save resources.

6.3.1 Systematic screening for beneficial trace elements in polyP hyperaccumulation

The sub-groups of the original trace element composition (Table 1) were systematically omitted in a series of cultivations with VH2.200 to narrow down the trace elements in the starvation phase responsible for elevated polyP production (Figure 18A).

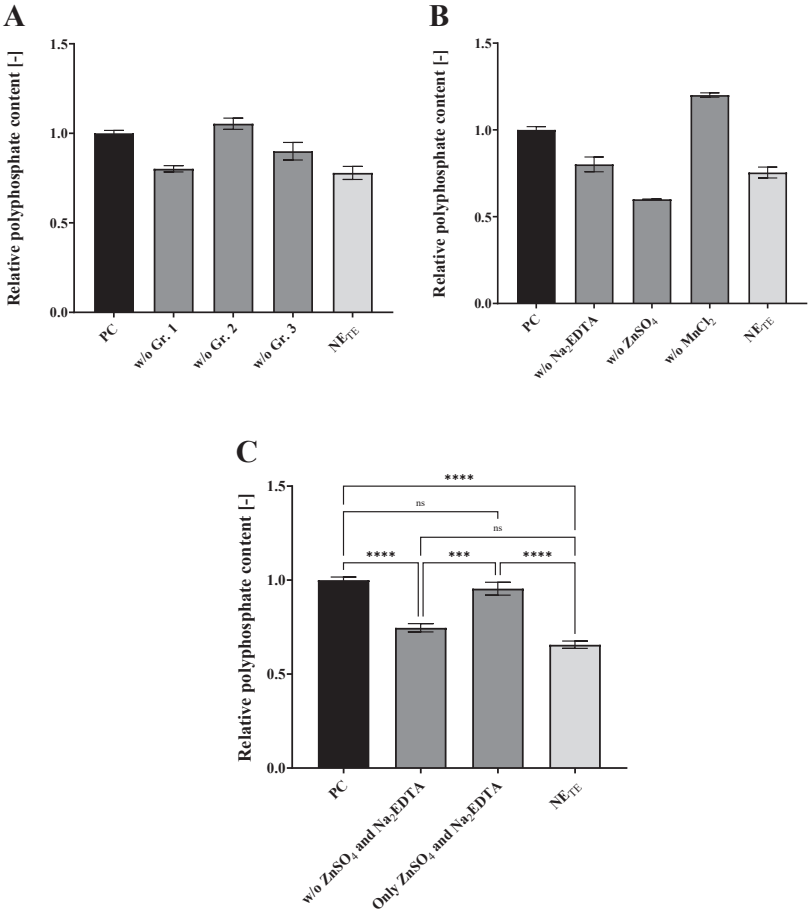


Figure 18: Influence of trace elements on polyP hyperaccumulation of VH2.200.
Cultivation in starvation medium with different combinations of trace elements. PC (all trace elements) and NE_{TE} (w/o any trace elements). (A) Omission of groups of trace elements. PC, w/o Group 1 (Na_2EDTA, $ZnSO_4$, and $MnCl_2$), w/o Group 2 ($CoCl_2$, $CuSO_4$, Na_2MoO_4, and KI), w/o Group 3 ($FeSO_4$, H_3BO_3, and $CaCl_2$), and NE_{TE} (n = 2); (B) Individual omission of trace elements of Group 1. PC, w/o Na_2EDTA, w/o $ZnSO_4$, w/o $MnCl_2$, and NE_{TE} (n = 2); (C) Combined effect of added Na_2EDTA and $ZnSO_4$. PC (n = 6), w/o Na_2EDTA and $ZnSO_4$ (n = 4), only with Na_2EDTA and $ZnSO_4$ (n = 4), and NE_{TE} (n = 6). Data are presented as means ± SEM. Significant differences marked by asterisks (*p < 0.05, **p < 0.01, ***p < 0.001, ****p < 0.0001; One-way ANOVA). Data associated with this figure were obtained from [324]. The figure was previously published [329] and is reprinted with permission from Yeast, published by John Wiley & Sons Ltd.

If the omission of a specific trace element group reduced polyP levels compared to fully supplemented medium, VH2.200 was further cultivated in media lacking each individual component of that group. The omission of Group 1 led to a relative polyP content of 0.80 ± 0.02, of Group 2 to 1.05 ± 0.04, and of Group 3 to 0.90 ± 0.07 compared to the fully supplemented positive control (PC). The omission of all trace elements (NE_{TE}) resulted in a relative polyP content of 0.78 ± 0.05. As only the omission of Group 1 led to a significant decrease in polyP content, the contribution of the individual trace elements of Group 1 to polyP hyperaccumulation was further examined. Although the omission of Group 3 showed a non-significant 10 % decrease in polyP content compared to the PC (1.00 ± 0.02), the individual examination of Group 3 components did not influence polyP hyperaccumulation (Suppl. Figure A12). The cultivations lacking individual components of Group 1 (Figure 18B) resulted in a relative polyP content of 0.60 ± 0 and 0.80 ± 0.06 without (w/o) $ZnSO_4$ and Na_2EDTA, respectively. On the contrary, cultivations without $MnCl_2$ resulted in a relative polyP content of 1.20 ± 0.02. The omission of all trace elements (NE_{TE}) resulted in a relative polyP content of 0.75 ± 0.04, confirming the results from the first series of cultivations. Therefore, $ZnSO_4$ and Na_2EDTA were selected as beneficial trace elements for polyP production. As the final adjusted starvation medium is designed to contain only relevant trace elements, $MnCl_2$ is omitted. The observed positive impact of its absence on polyP production is thereby covered. Thus, the effect of the absence of $MnCl_2$ was not investigated further. The role of Na_2EDTA and $ZnSO_4$ was verified by adding only these two components or all other trace elements except Na_2EDTA and $ZnSO_4$ (Figure 18C). Adding only Na_2EDTA and $ZnSO_4$ resulted in a relative polyP content of 0.95 ± 0.03, representing no significant difference from the PC. NE_{TE} resulted in a lower relative polyP content of 0.66 ± 0.02 compared to these approaches ($p < 0.0001$). Similarly, when adding all trace elements in the starvation except for Na_2EDTA and $ZnSO_4$, the relative polyP content was reduced (0.75 ± 0.02). Hence, the relative content of the PC was significantly higher ($p < 0.0001$), but no significant difference to the NE_{TE} is detectable for this approach. This confirmed the impact of Na_2EDTA and $ZnSO_4$ on polyP hyperaccumulation, while all other trace elements added in the original protocol can be omitted.

6.3.2 Systematic screening for beneficial vitamins in polyP hyperaccumulation

The vitamin mixture, containing besides bona fide vitamins compounds such as inositol, was individually omitted to determine the components in the starvation phase responsible for elevated polyP production (Figure 19A). The relative polyP content of modified media without nicotinic acid (1.04 ± 0.03), without p-aminobenzoic acid (1.07 ± 0.03), without biotin (1.12 ± 0.12), without pyridoxine HCl (1.06 ± 0.02), without calcium pantothenate (1.00 ± 0.08), and without thiamine HCl (1.00 ± 0.02) revealed no substantial difference compared to the PC and were not considered for further analysis. In contrast, the modified medium without inositol exhibited a relative polyP level of 0.75 ± 0. This was comparable to the level of 0.82 ± 0.02 when omitting all vitamins (NE_{TV}). As a result, inositol was identified as the only beneficial compound in the vitamin mixture for polyP production.

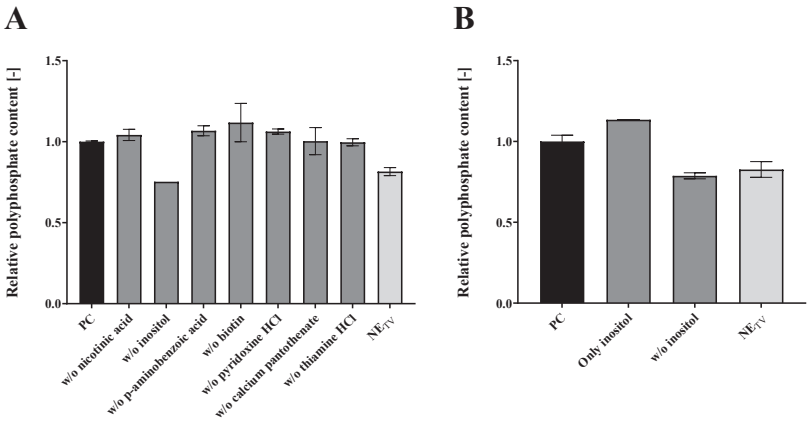


Figure 19: Influence of individual vitamins on polyP hyperaccumulation of VH2.200.
Cultivation in starvation medium with different combinations of vitamins. PC (all vitamins) and NE_{TV} (w/o any vitamins). (A) w/o nicotinic acid, w/o inositol, w/o p-aminobenzoic acid, w/o biotin, w/o pyridoxine hydrochloride, w/o calcium pantothenate, and w/o thiamine hydrochloride; (B) Only with and w/o inositol. All cultivations were performed in duplicates (n = 2). Data are presented as means ± SEM. Data associated with this figure were obtained from [324]. The figure was previously published [329] and is reprinted with permission from Yeast, published by John Wiley & Sons Ltd.

Hyperaccumulation with a cultivation step in modified starvation medium containing only inositol and a second medium containing all vitamins except inositol confirmed its impact on polyP accumulation (Figure 19B). The medium with inositol exhibited a relative polyP content of 1.13 ± 0. Just omitting inositol resulted in a relative content of 0.79 ± 0.03. This is similar to NE_{TV} (0.83 ± 0.07). These results confirm the impact of inositol on polyP accumulation, while all other vitamins added in the original protocol can be neglected.

6.3.3 Investigating the combined effect of zinc and inositol on polyP hyperaccumulation in *S. cerevisiae* VH2.200

The identified positive impact of zinc and inositol on polyP hyperaccumulation was combined and tested for synergetic effects (Figure 20).

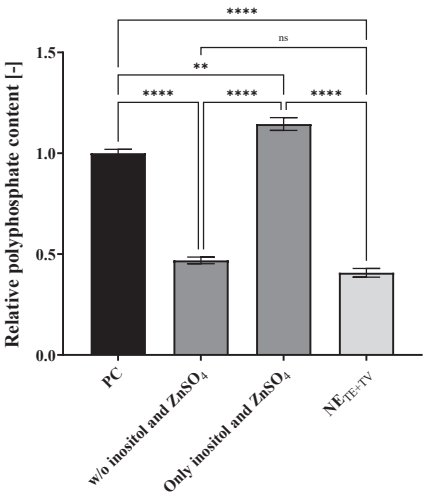


Figure 20: Influence of zinc and inositol on polyP hyperaccumulation of VH2.200.
Cultivation in a modified starvation medium. PC (all vitamins + trace elements, n = 6), w/o inositol and $ZnSO_4$ (n = 4), only with inositol and $ZnSO_4$ (n = 4), and NE_{TE+TV} (w/o any trace elements and vitamins, n = 6). Data are presented as means ± SEM. Significant differences marked by asterisks (*$p < 0.05$, **$p < 0.01$, ***$p < 0.001$, ****$p < 0.0001$; One-Way ANOVA). Data associated with this figure were obtained from [324]. The figure was previously published [329] and is reprinted with permission from Yeast, published by John Wiley & Sons Ltd.

Modified medium containing only inositol and $ZnSO_4$ resulted in a relative polyP content of 1.14 ± 0.03, even demonstrating a significant increase compared to the PC ($p < 0.01$). The relative polyP value of the NE_{TE+TV} (0.41 ± 0.02) was significantly lower than that of the modified medium ($p < 0.0001$). The addition of all other trace elements and vitamins except for inositol and $ZnSO_4$ resulted in a significantly lower relative polyP content (0.47 ± 0.02) compared to the PC (1.00 ± 0.02; $p < 0.0001$). A non-significant difference compared to the NE_{TE+TV} was also demonstrated. Inositol and $ZnSO_4$ independently contributed approximately 34 % to the final polyP level (Suppl. Figure A13). Therefore, both inositol and $ZnSO_4$ are beneficial for polyP accumulation. If only the two out of all trace elements and vitamins are present during starvation, high polyP levels can be reached. The final modified medium contained inositol and $ZnSO_4$ but no Na_2EDTA since Na_2EDTA functions as a chelator [328]. Therefore, by omitting the chelator from the starvation medium, the ions of the starvation medium are more accessible to *S. cerevisiae*,

further saving resources. Moreover, the number of poorly soluble ions and the total number of ions have been drastically reduced in the experiments shown here compared to the original medium composition. The results of Figure 20 confirm that omitting Na_2EDTA from the starvation medium has no negative impact, since even a higher polyP content relative to the PC can be obtained with only inositol and $ZnSO_4$. These results confirm the individual influence of zinc and inositol on reaching high polyP contents with VH2.200. Still, additional yeast strains must be tested to make a more general statement about the impact of zinc and inositol on polyP metabolism.

6.3.4 Validating the effect of zinc and inositol across diverse yeast strains

The combination of various inositol and zinc concentrations in the starvation medium was applied to demonstrate its impact on polyP production for commonly used laboratory (CEN.PK WT) and industrial (VH2.200 and Ethanol Red) *S. cerevisiae* strains (Figure 21). The concentration range was based on previous data by Christ and Blank (2019) [1] as well as preliminary analysis with *S. cerevisiae* VH2.200 (data not shown).

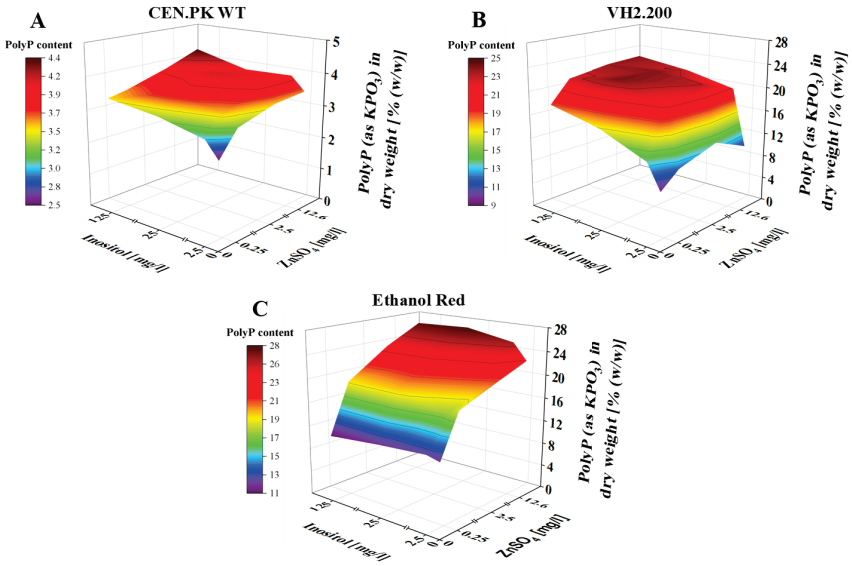


Figure 21: 3D-surface diagrams for the effect of inositol and zinc on polyP hyperaccumulation of diverse yeast strains.
PolyP levels with varying inositol (0, 2.5, 25, 125 mg/l) and $ZnSO_4$ (0, 0.25, 2.5, 12.6 mg/l) concentrations. (A) *S. cerevisiae* CEN.PK WT; (B) VH2.200; (C) Ethanol Red. The colors of the spanned surface indicate the final polyP content as depicted in the legend: *S. cerevisiae* CEN.PK WT (0-4.4 % (w/w), VH2.200 (0-25 % (w/w)) and Ethanol Red (0-28 % (w/w)). Data are presented as means (n = 3). Data associated with this figure were obtained from [325]. The figure was previously published [329] and is reprinted with permission from Yeast, published by John Wiley & Sons Ltd.

The data demonstrate independent increases in polyP levels with zinc and inositol, as well as strain-specific concentration responses. In the case of VH2.200 and CEN.PK WT, a slight increase in concentration of either substance already substantially elevated the final polyP content. A further increase had relatively small effects. The increase in polyP from minimal (0 mg/l inositol, 0 mg/l $ZnSO_4$) to optimal concentration level was 2.4-fold (25 mg/l inositol, 0.25 mg/l $ZnSO_4$) and 2.0-fold (125 mg/l inositol, 12.6 mg/l $ZnSO_4$) for VH2.200 and CEN.PK WT, respectively. Interestingly, the polyP content in Ethanol Red is not strongly influenced by the inositol level but more by the zinc concentration. The polyP content of Ethanol Red increased 2.3-fold from minimal to optimal concentration (25 mg/l inositol, 12.6 mg/l $ZnSO_4$). Hence, in cultivations with Ethanol Red, inositol can be omitted from the starvation medium to reduce medium costs further. Nevertheless, optimal zinc and inositol concentrations are crucial to achieve maximal polyP production and must be adapted to each yeast strain. TOM cultivations were performed to measure the respiratory activity of yeast strains during starvation in order to investigate the influence of zinc and inositol on cells besides polyP production. This confirmed the metabolic effect of zinc and inositol on the yeast strains in the starvation phase (Figure 22).

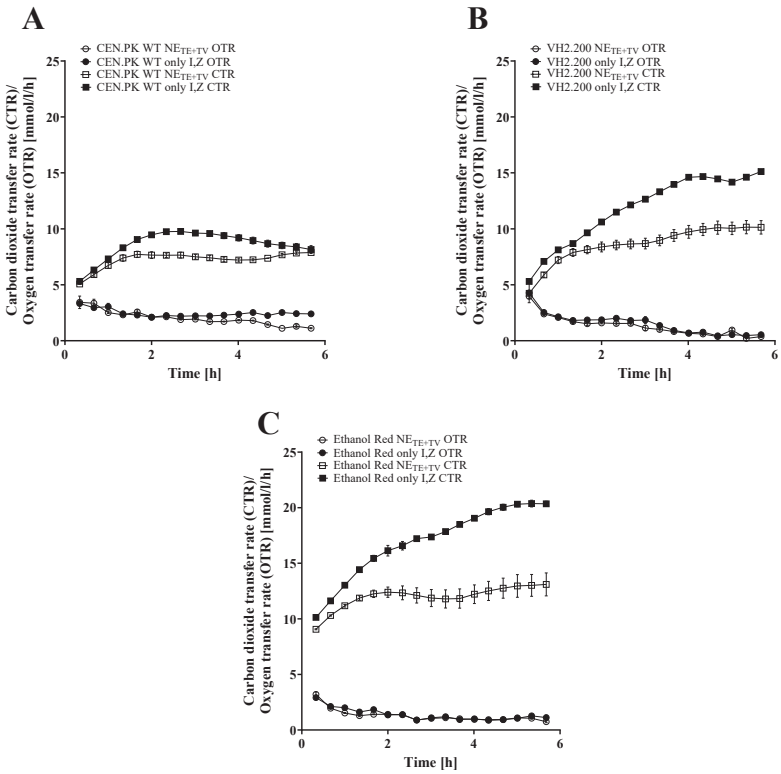


Figure 22: TOM cultivation with various yeast strains in starvation medium without or only with inositol and zinc.
OTR and CTR for cultivations in starvation medium w/o any trace elements and vitamins (NE$_{TE+TV}$) or only with inositol and $ZnSO_4$. (A) *S. cerevisiae* CEN.PK WT (125 mg/l inositol, 12.6 mg/l $ZnSO_4$); (B) VH2.200 (25 mg/l inositol, 2.5 mg/l $ZnSO_4$); (C) Ethanol Red (25 mg/l inositol, 12.6 mg/l $ZnSO_4$). All cultivations were performed in duplicates (n = 2). Data are presented as means ± SEM. Data associated with this figure were obtained from [325]. The figure was previously published [329] and is reprinted with permission from Yeast, published by John Wiley & Sons Ltd.

The OTR remained unaffected by these additions, but the CTR was increased in all approaches with zinc and inositol. The CTR increased particularly strongly in cultivations with VH2.200 and Ethanol Red. The increased CTR signals in cultivations with inositol and zinc compared to cultivations without inositol and zinc (NE$_{TE+TV}$) correlated with elevated biomass production, ethanol production, and glucose consumption (Table 4), all indicating increased fermentative activity.

Table 4: Metabolic impact of inositol and zinc on *S. cerevisiae* during P_i starvation.
The table was previously published [329] and is reprinted with permission from Yeast, published by John Wiley & Sons Ltd.

		Glucose uptake rate [g/l/h]	Ethanol production rate [g/l/h]	Biomass increase [g/l/h]
VH2.200	NE_{TE+TV}	0.94	0.30	0.06
	Only inositol and zinc	1.46	0.53	0.28
CEN.PK WT	NE_{TE+TV}	0.93	0.28	0.07
	Only inositol and zinc	1.12	0.34	0.19
Ethanol Red	NE_{TE+TV}	1.22	0.43	0.23
	Only inositol and zinc	1.55	0.56	0.34

Moreover, the final polyP content was substantially lower in cultivations without zinc and inositol (Suppl. Figure A14). Altogether, these measurements confirm the influence of zinc and inositol on polyP hyperaccumulation and the energy metabolism of diverse yeast strains. However, the mode of action of these two components remains unknown.

6.3.5 Assessing the role of zinc and inositol in PHO pathway activation under P_i starvation conditions

The plasmid (pPr_{Pho5}-sfGFP) was constructed similarly to the published plasmid of Chabert et al. (2023) [173] and applied to determine the mechanism of action of inositol and zinc in polyP synthesis/polyP signaling (Suppl. Figure A15). The plasmid contains sfGFP, whose expression is controlled by the *PHO5* promoter that is regulated by the PHO pathway. The PHO genes ensure P_i homeostasis, specifically at P_i starvation conditions [146]. Thus, the starvation status of the cells can be monitored during cultivation using GFP as a proxy. The non-altered CEN.PK WT strain and CEN.PK pPr_{Pho5}-sfGFP were cultivated in starvation medium without trace elements and vitamins, only with inositol and zinc, as well as in P_i-rich feeding medium (Figure 23A). No increase in the OD-corrected GFP signal for CEN.PK WT and CEN.PK pPr_{Pho5}-sfGFP in the P_i-rich medium was observed, validating the introduction of the plasmid to detect PHO pathway activation. In the absence of P_i, the *PHO5* promoter is induced by the PHO pathway. This is confirmed by a rising OD-corrected GFP signal in experiments with CEN.PK pPr_{Pho5}-sfGFP. Regarding the medium composition, the signal increase was stronger in the medium containing only zinc and inositol than in the medium without trace elements and vitamins.

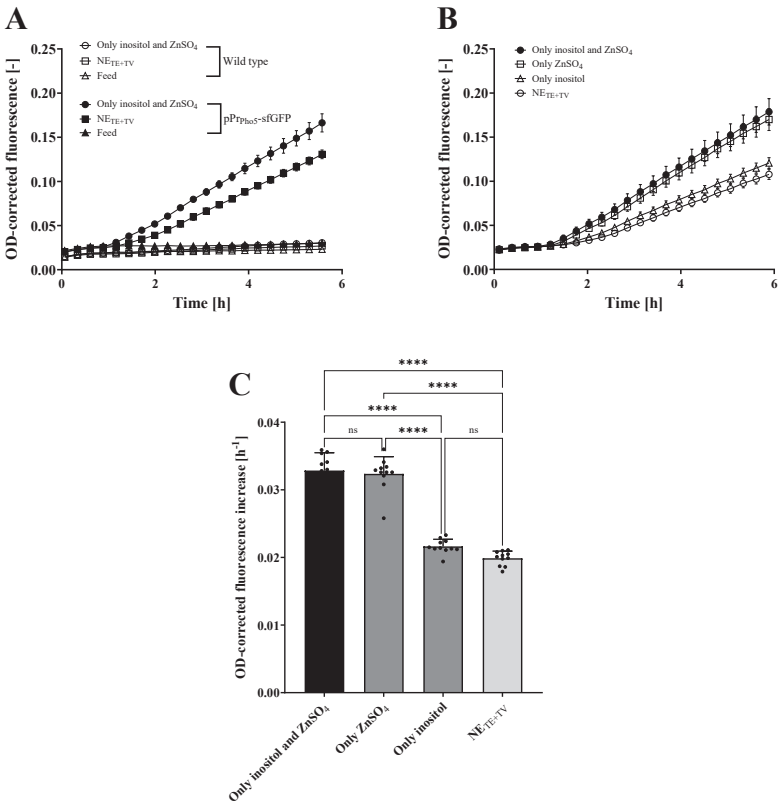


Figure 23: PHO pathway activation by *S. cerevisiae* in the starvation phase of the polyP hyperaccumulation protocol.
Assaying PHO pathway activation through live GFP readout during cultivation at different conditions. (A) OD-corrected fluorescence for CEN.PK WT (n = 7) and CEN.PK pPr$_{Pho5}$-sfGFP (n = 8), starvation medium w/o any trace elements and vitamins (NE$_{TE+TV}$), only with inositol and $ZnSO_4$, as well as P_i-rich feeding medium; (B) OD-corrected fluorescence for CEN.PK pPr$_{Pho5}$-sfGFP (n = 11), starvation medium only with inositol and $ZnSO_4$, only with $ZnSO_4$, only with inositol, and w/o any trace elements and vitamins (NE$_{TE+TV}$); (C) Calculation of rates for OD-corrected GFP increase between 3-6 h of (B). GFP (gain = 90, λ_{ex} = 488 nm, λ_{em} = 520 nm), biomass (gain = 50, λ_{ex} = 620 nm, λ_{em} = 620 nm). Data are presented as means ± SD. Significant differences marked by asterisks (*p < 0.05, **p < 0.01, ***p < 0.001, ****p < 0.0001; One-Way ANOVA). Data associated with this figure were obtained from [325]. The figure was previously published [329] and is reprinted with permission from Yeast, published by John Wiley & Sons Ltd.

The enhanced PHO pathway activation suggests an influence of either inositol, zinc, or both on the starvation response. Parallel flask cultivations confirmed polyP hyperaccumulation in CEN.PK WT and CEN.PK pPr$_{Pho5}$-sfGFP (Suppl. Figure A16). Another cultivation containing only inositol or only zinc was performed to determine their individual contribution to PHO pathway activation (Figure 23B-C). This demonstrated that zinc is responsible for enhanced PHO

pathway activation, as indicated by a non-significant difference in the rate of OD-corrected GFP increase compared with the approach using zinc and inositol. The approach with inositol resulted in a non-significant difference compared to the approach without trace elements and vitamins. Therefore, it can be concluded that zinc plays a significant role in activating the PHO pathway under P_i starvation, thereby contributing to enhanced subsequent polyP accumulation. The presence of extracellular inositol does not improve the starvation response via the PHO pathway.

6.4 Discussion

Prior research highlighted the addition of both trace elements and vitamins to the starvation medium to substantially increase polyP titers [1]. Here, previously published methods of media characterization were adapted to elucidate the beneficial components from either mixture, highlighting zinc and inositol as the major regulators (Figure 21) [330, 331]. Attributing the positive effect on polyP accumulation to inositol and zinc offers a wide range of opportunities for further optimization, including a deeper understanding of the polyP hyperaccumulation process, targeted process and enzyme engineering on inositol- and zinc-utilization, strain-specific media adaptation, and reduction of process cost by minimizing trace element and vitamin usage in cultivations. Numerous cellular mechanisms are influenced by inositol and zinc, as both compounds play essential roles in the general homeostasis of *S. cerevisiae*. Zinc is required for the structural stability of proteins [332], utilized among others as a cofactor in transcription factors and alcohol dehydrogenases [333-335], or as a signaling molecule [336]. These vital roles underline the involvement of zinc in a multitude of cellular processes, including gene transcription [337], phospholipid metabolism [338], and stress response [339]. 8.8 % of the yeast genome is assumed to encode zinc-binding proteins [340]. Therefore, it is challenging to pinpoint the exact genetic element or cellular mechanism responsible for the observed increase in polyP. A genome-wide association study identified 108 single-gene deletion mutants associated with zinc stress (6 mM), including *PHO85*, *PHO87, PHO90, VTC2, VTC4*, *VTC5, VMA5*, and *VMA16* [341]. Although the maximal zinc concentration in our hyperaccumulation method (0.08 mM) is distant from the concentrations tested by Zhao et al. (2020) [341], a metabolic connection between zinc and polyP is still apparent. This is supported by other studies that report an influence of zinc on the activity of the endopolyphosphatase Ppn2p as well as on the activity and accumulation of the alkaline phosphatase Pho8p [207, 342]. (Poly)phosphatases are essential for mobilizing P_i and thereby contribute to P_i homeostasis [146, 343]. Although the connection to polyP hyperaccumulation remains uncharacterized, the PHO pathway plays a critical role. By using the *PHO5*-regulated sensor for tracking PHO pathway activation during starvation, a strong response

to zinc addition was observed. These results suggest that zinc plays a direct role in P_i homeostasis and the starvation response. As a cofactor of transcription factors, it might stimulate the expression of PHO genes or influence the activity of proteins in the PHO pathway as a critical catalytic factor. As the promoter output of *PHO5* is further downstream in the pathway, a large variety of additional regulations might influence the signal output [173]. Therefore, the exact mode of action and whether zinc acts directly or indirectly on one of the enzymes in the PHO pathway remains unclear and has not been investigated in this study.

Recently, the role of inositol in the PHO pathway was elucidated by modulation with InsPPs, ATP, and polyP at both metabolic and signaling levels. On the one hand, this modulation plays a role in cellular P_i homeostasis, but on the other hand, it is also influenced by cellular P_i homeostasis itself [180]. The abundance of InsPPs changes depending on the cytosolic P_i level and thereby acts in conjunction with SPX domains to perform a coordinated P_i signaling response in *S. cerevisiae*. SPX domains are primarily found in proteins involved in P_i transport, P_i storage, and polyP synthesis [175, 178]. However, pinpointing the exact role of InsPPs in P_i signaling was hindered in the past due to analytical limitations, resulting in contradicting statements [173, 207]. The study by Chabert et al. (2023) [173] emphasized the role of 1,5-InsP8 in signaling cytosolic P_i levels, correlating P_i scarcity with the absence of 1,5-InsP8 in *S. cerevisiae*. Our sensory system noted no increased starvation response via inositol addition. Hence, inositol may influence the starvation response independently of the PHO pathway by modulating phospholipid synthesis, transcription regulation, physiological stress response, energy metabolism, or autophagy [179, 338, 344, 345]. The influence of inositol is limited exclusively to the starvation phase, as addition to the feed does not lead to increased polyP accumulation. When cultivating our strains under P_i starvation in TOM cultivations, increased fermentative activity was observed, which might be associated with InsPPs. Besides its role in P_i homeostasis, InsPPs function as metabolic signaling molecules, indicating cellular energy availability [146, 346, 347]. This sensing affects the carbon flux distribution, most prominently between fermentation and respiration. In this context, the enzymes controlling the reaction between InsP6 and 5-InsP7 are of relevance. Qin et al. (2023) [348] reported an inositol pyrophosphatase encoded by *OCA5* that dephosphorylates 5-InsP7 to InsP6. Deletion of *OCA5* increased respiration and repressed fermentation. Szijgyarto et al. (2011) [346] reported that deletion of *KCS1*, which catalyzes the reaction from InsP6 to 5-InsP7, results in activation of glycolysis and repression of respiration. In both cases, the glucose uptake and ethanol production rates were affected [346, 348]. Although cultivations in this chapter were performed under P_i-starvation conditions and without mutations of enzymes interacting with 5-InsP7 and InsP6, increases in ethanol production and glucose uptake were observed. The added value of inositol during P_i scarcity might result from its role in maintaining P_i distribution between ATP, InsPP,

and polyP. ATP is required by *S. cerevisiae,* but more respiration is impossible since fermentation occurs under the applied conditions due to the Crabtree effect [322]. Therefore, more carbon (glucose) is taken up by *S. cerevisiae* and converted to ethanol. In approaches with inositol, more ethanol is produced, which can lead to changes in P_i homeostasis through changes in energy homeostasis. Elevated ATP levels in these approaches can then lead to increased polyP production during P_i repletion or result in a stronger starvation response. It is striking that the polyP content in Ethanol Red does not change with varying inositol concentrations in the starvation phase compared to other tested strains (Figure 21). Ethanol Red produces high ethanol yields and maintains high cell viability under these conditions [349, 350]. Previous publications reported that elevated ethanol concentrations and tolerance in yeast strains are related to high levels of phosphatidylinositol in the cellular membrane with inositol supplementation [351, 352]. Ethanol tolerance and insensitivity to inositol supplementation in the starvation phase in Ethanol Red might hence be related to naturally high inositol production. This trait could result from domestication [290].

In summary, zinc has a positive effect via the direct activation of the PHO pathway during P_i starvation, while the role of inositol in enhanced polyP hyperaccumulation remains elusive. Since those two components are sufficient to enhance polyP hyperaccumulation, and even small concentrations trigger a boost in production, the starvation medium can be simplified by omitting unnecessary trace elements and vitamins. In addition to the obvious ecological and economic advantages of conserving resources, reduced usage of components can simplify product purification and, especially in this case, wastewater treatment, which is in turn beneficial for the environmental footprint of the process.

6.5 Conclusion

Identifying zinc and inositol to enhance polyP hyperaccumulation opens new avenues for studying P_i starvation in *S. cerevisiae*. The production of (bio-)polyP is gaining increasing industrial attention as a potential replacement for energy-intensive processes based on fossil resources. There is a strong incentive to turn the yeast-based approach into a profitable process. Applying our findings in combination with approaches in metabolic engineering and bioprocess development can support this cause. This chapter contributes to an improved understanding of polyP accumulation and more efficient polyP production, thereby facilitating an envisioned circular P_i economy.

Chapter 7

Characterizing the starvation and feed phase in the hyperaccumulation protocol for polyphosphate production

Contributions:

Alexander Deitert conceived the study, conducted all cultivation experiments, analyzed the data, prepared the figures, and wrote the chapter. The strains listed in Suppl. Table A10 were constructed by Makarius Baier at the iAMB (RWTH Aachen University, Aachen Germany). Alina Electra Maas performed cultivation experiments and prepared figures under the supervision of Alexander Deitert [353] (iAMB, RWTH Aachen University). Philipp Demling and Lars Mathias Blank critically reviewed this chapter.

7 Characterizing the starvation and feed phase in the hyperaccumulation protocol for polyphosphate production

7.1 Abstract

S. cerevisiae is a promising production host for the biotechnological production of polyP. Although polyP hyperaccumulation with baker's yeast has been established since the 1960s and further refined recently, the nutritional requirements for efficient polyP hyperaccumulation remain poorly defined. Therefore, biotechnological polyP production suffers from process inefficiencies, high nutrient consumption, and both ecological as well as economic drawbacks. In this chapter, a rational strategy for defining the minimal media requirements during the P_i starvation and feeding phases of the polyP hyperaccumulation protocol was presented. The minimal medium concentrations enable the specification of requirements for P_i-waste streams used as substrates and efficient polyP production by reducing byproduct formation and DSP complexity. In this context, the specific function of inositol during P_i starvation was investigated using phospholipid mutant strains, as well as mutants lacking inositol transporters or the ability to synthesize inositol *de novo*. These findings advance our understanding of the physiological basis and key mechanisms underlying polyP hyperaccumulation in *S. cerevisiae.* This can ultimately support the introduction of polyP with broad industrial applications.

7.2 Introduction

The baker's yeast *S. cerevisiae* can selectively accumulate P_i and convert it into polyP [1, 146]. Microbial polyP production represents a promising alternative to established chemical synthesis, which is currently limited to short-chain polymers (< 40 P_i residues) on an industrial scale. In contrast, polyP chains of several hundred P_i-subunits were identified in microbial systems [142]. Due to its versatile physicochemical properties, polyP is of considerable industrial interest [49, 104]. This includes applications in the food industry, agriculture, environmental protection, and medicine [49]. The potential of *S. cerevisiae* to accumulate high levels of polyP was demonstrated in the 1960s by Langen and Liss (1958) [144]. This, along with the studies of Christ and Blank (2019) [1], revealed that baker's yeast most effectively accumulates polyP through a sequence of P_i starvation and subsequent P_i feeding, termed polyP hyperaccumulation [1, 144]. PolyP from *S. cerevisiae* can be used in its pure form (bio-polyP) or as polyP-rich yeast extract [45]. The potential bio-polyP applications are diverse, including pharmaceutical and technical uses, whereas

polyP-rich yeast extract would primarily be suited as a food additive [45, 128]. This adds the unique physicochemical properties of polyP to conventional yeast extract [45]. However, the current hyperaccumulation protocol faces several challenges, including integrating waste streams as sources of P_i. PolyP hyperaccumulation with *S. cerevisiae* is typically carried out in decoupled process steps. Its efficiency is reduced by limited biomass formation due to the Crabtree effect and elevated levels of undesired byproducts [323, 354, 355]. In addition, substantial quantities of glucose and P_i are not converted by *S. cerevisiae* and are consequently discarded as waste [1]. P_i-rich waste streams are typically characterized by fluctuating P_i concentrations, the presence of heavy metal contaminants, and variable levels of other elements such as magnesium, iron, and sulfate [70, 71, 103]. Microorganisms are capable of selectively taking up P_i while leaving heavy metals behind [356]. This enables the production of polyP that is free from contamination [103]. Nonetheless, minimizing the number and concentration of required components in the polyP hyperaccumulation process is crucial for identifying the essential nutritional demands of *S. cerevisiae* for efficient polyP synthesis. This facilitates the development of a more sustainable and effective biotechnological polyP production process [128, 158]. Recent studies have demonstrated that zinc and inositol positively affect final polyP levels during the P_i starvation phase of the hyperaccumulation protocol [329]. Consequently, the number of components in the chemically defined minimal medium of the starvation phase is substantially reduced [1, 329], as other trace elements and vitamins are no longer included. Specifically, the addition of zinc to the starvation medium triggered an enhanced starvation response in *S. cerevisiae* [329]. While the mode of action of inositol in the polyP hyperaccumulation protocol remains unclear, previous studies suggested a link between inositol, zinc, P_i, and polyP via the phospholipid metabolism in *S. cerevisiae* [338, 357-359]. Phospholipids are involved in lipid metabolism, membrane transport, membrane integrity, and signal transduction [338]. They are amphipathic molecules, consisting of a hydrophobic tail group and a hydrophilic head group. The head group contains P along with other polar groups [338]. This P accounts for approximately 4 % (w/w) of phospholipids, and phospholipids contribute 5-10 % (w/w) of total cellular biomass [6, 8]. A link between phospholipid and polyP metabolism has not yet been systematically explored.

This chapter presents a rational strategy for defining the minimal media requirements of *S. cerevisiae* in the starvation and feed phase of the polyP hyperaccumulation protocol, enabling efficient biotechnological polyP production with reduced nutrient input. Supplementing only zinc and inositol as beneficial components of the trace element and vitamin solution, while redefining other minimal medium requirements for effective polyP production, improves the economic and ecological profile of the hyperaccumulation process by minimizing byproduct formation, reducing nutrient concentrations in the waste stream, and simplifying DSP. To elucidate the role of inositol

in polyP metabolism, its mode of action during the P_i starvation phase was investigated using phospholipid mutant strains as well as strains lacking inositol transporters and/or *de novo* inositol synthesis. Overall, this work advances our understanding of polyP hyperaccumulation in *S. cerevisiae* by defining its minimal medium requirements and shedding light on the role of inositol in the process.

7.3 Results

With the overall goal of defining the minimal requirements of *S. cerevisiae* for effective polyP accumulation and elucidating the role of inositol in polyP hyperaccumulation, the influence of individual medium components in both starvation and feed media was assessed, and mutants in phospholipid and inositol metabolism were examined for their ability to accumulate polyP.

7.3.1 Defining minimal medium requirements for effective polyP hyperaccumulation

On the one hand, identifying zinc and inositol as key elements for polyP hyperaccumulation simplifies the composition of the starvation medium, as demonstrated in Chapter 6. On the other hand, it may affect the nutritional requirements of *S. cerevisiae* compared to those described in the protocol developed by Christ and Blank (2019) [1]. HPLC analysis revealed that a substantial amount of glucose in the starvation and feed media is either converted to ethanol due to the Crabtree effect or remains in the medium [1, 329]. This is a disadvantage for the economic and ecological viability of polyP production with *S. cerevisiae*. Therefore, the influence of all medium components, except trace elements and vitamins, was evaluated in both starvation and feed media in this chapter by varying their concentrations. The experiments were carried out with a starvation medium that, instead of containing all Verduyn trace elements and vitamins, contained only zinc and inositol. The concentrations tested by Christ and Blank (2019) [1] served as a foundation for further research. Initially, the concentrations of glucose, KCl, $CaCl_2$, and succinate in the starvation medium were individually tested for their impact. The concentration of $(NH_4)_2SO_4$ was examined after the initial tests to differentiate its effect from that of succinate. $(NH_4)_2SO_4$ not only serves as a nitrogen source and supports maximal growth during P_i starvation, a prerequisite for maximal polyP accumulation, but also influences the pH of the cultivation broth [360]. In this way, it partially covers the role of succinate, which functions solely as a pH buffer and is not metabolized by *S. cerevisiae* [1]. The pH values of both the starvation and feed media play a crucial role in polyP accumulation with *S. cerevisiae* [1]. Figure 24 presents the results of varying the concentrations of glucose, KCl, $CaCl_2$, and succinate individually.

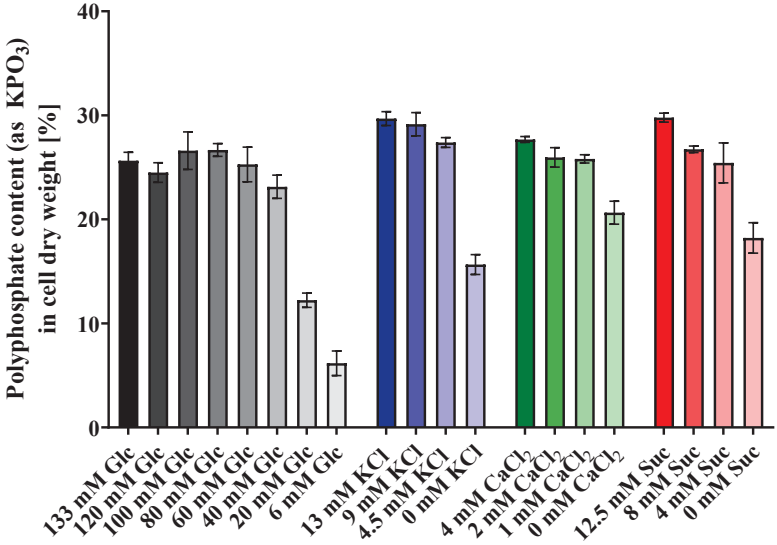


Figure 24: Evaluating the impact of glucose, KCl, $CaCl_2$, and succinate in the starvation medium on polyP production with VH2.200.
Cultivation and medium preparation according to sections 2.1.2 and 2.1.3. The medium components were individually varied, while all other concentrations were based on those reported by Christ and Blank (2019) [1]. The glucose level (6-133 mM), KCl (0-13 mM), $CaCl_2$ (0-4 mM), and succinate level (0-12.5 mM) were varied. The feeding medium was prepared according to Christ and Blank (2019) [1]. Cultivation was performed in MTPs to generate enough cell mass for enzymatic polyP quantification. The results represent the mean of two replicates ± SEM (n = 2).

This trial was intended as a preliminary assessment of how individual medium components affect polyP production. The findings indicate that glucose concentrations above 80 mM do not have a positive effect on polyP accumulation. At 40 mM and 60 mM glucose, the final polyP titer shows minimal variation. The most pronounced reduction in polyP accumulation occurs when the glucose concentration is set below 20 mM, which also corresponds to a decrease in final cell mass after the starvation phase (data not shown). For KCl and $CaCl_2$, polyP levels remain stable until these components are completely omitted from the medium. Several previous studies have suggested a link between KCl, $CaCl_2$, P_i homeostasis, and polyP production [146, 361, 362]. Therefore, small amounts of KCl and $CaCl_2$ are necessary for optimal polyP production. Reducing succinate slightly lowers polyP levels, with the most substantial drop observed when the concentration is decreased from 4 to 0 mM. In addition to optimizing the starvation medium, the concentrations of glucose and P_i in the feed medium were also evaluated (Figure 25). P_i and glucose levels were based on Christ and Blank (2019) [1]. The results show stable polyP levels across a glucose range of 100-250 mM and P_i concentrations between 25-40 mM.

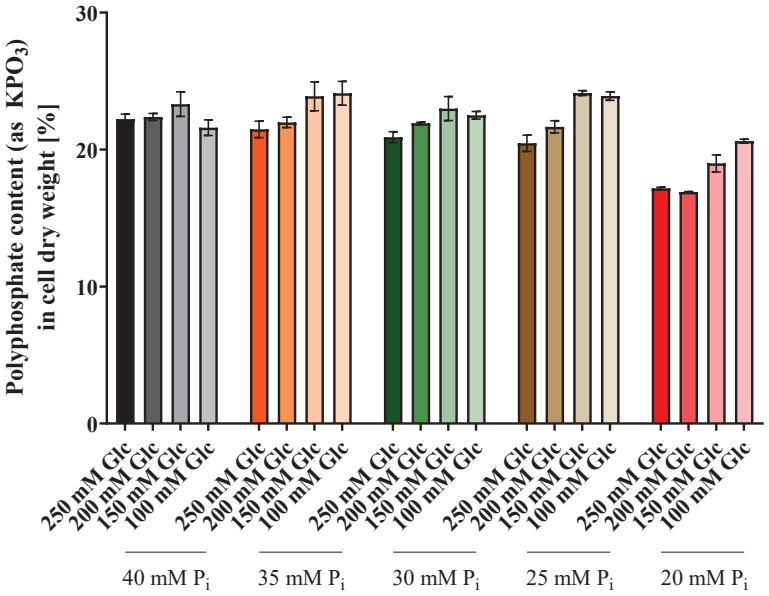


Figure 25: Evaluating the impact of glucose and phosphate in the feed medium on polyP production with VH2.200.
Cultivation and medium preparation according to sections 2.1.2 and 2.1.3. The medium components were individually varied, while all other concentrations were based on those reported by Christ and Blank (2019) [1]. The glucose (100-250 mM) and P_i concentration (20-40 mM) were varied. The starvation medium was prepared according to Christ and Blank (2019) [1]. MTPs were used to obtain sufficient cell mass for enzymatic polyP quantification. The results represent the mean of two replicates ± SEM (n = 2).

However, glucose concentrations of 100 mM and 150 mM appear to perform best in all conditions. This effect may be related to a combination of factors, such as lower osmotic pressure, reduced glucose available for ethanol production, and yet sufficient glucose to generate adequate energy. Furthermore, a reduction in P_i levels below 25 mM resulted in a substantial decline in polyP accumulation. Both glucose and P_i are essential for polyP production. Glucose provides energy, while P_i serves as the monomer for polyP synthesis [146]. In these experiments, the original $MgCl_2$ concentration was kept at the level reported by Christ and Blank (2019) [1] to isolate the impact of P_i, as magnesium acts as a counterion for polyP [363-365]. Notably, the hyperaccumulation experiments focused on varying individual media components, while all others were kept at their original concentrations. Therefore, the combined effect of all component adjustments must be considered for a comprehensive evaluation. The findings from Figure 24 and Figure 25 were combined to formulate optimized starvation and feed media with minimal effective nutrient concentrations (Figure 26 and Table 5).

Table 5: Composition of all starvation and feed media used to define the minimal nutritional requirements of VH2.200 for polyP hyperaccumulation.
The different combinations of starvation and feed media were numbered M1–M8.

	M1	M2	M3	M4	M5	M6	M7.1-3	M8.1-4
Starvation (mM)								
Glucose	80	80	60	60	80	60	133	80
$(NH_4)_2SO_4$	10	10	10	10	10	10	10	2.5
KCl	4.5	4.5	4.5	4.5	4.5	4.5	13.3	4.5
$CaCl_2$	1	1	1	1	1	1	4	1
Na_2succinate	8	8	4	4	8	4	12.5	4
P_i-Feed (mM)								
Glucose	100	100	100	100	160	160	250	100
KH_2PO_4	30	25	30	25	25	25	60	25
$MgCl_2$	20	20	20	20	20	20	15(1), 10 (2), 5 (3)	20 (1) 15 (2), 10 (3), 5 (4)

All reduced media formulations were directly compared to the original medium developed by Christ and Blank (2019) [1]. Their starvation medium was supplemented with the complete set of trace elements and vitamins, whereas the adapted starvation medium contained only inositol and zinc. Due to its impact on final polyP levels in the pre-tests, two glucose concentrations (60 and 80 mM) were selected for the starvation medium, and two P_i concentrations (25 and 30 mM) for the feed medium (Figure 26). The glucose concentration in the feed medium was set at 100 mM. To ensure comparability, the cell mass in all cultivations was adjusted to 2.5 g/l CWW prior to the starvation phase and to 30 g/l CWW prior to the feed phase, as described by Christ and Blank (2019) [1]. Metabolite uptake rates were calculated by subtracting the final concentration of a metabolite from its initial concentration. The result was divided by the cultivation time and the culture's final OD_{600} value. Metabolite production rates were calculated in the same way, except that the initial concentration was subtracted from the final concentration. The cultivations revealed reduced polyP levels in the adapted media compared to the original formulation (Figure 26A). However, this decrease of 13.5-17.4 % was moderate compared to the reduction in medium components in the modified starvation and feed media. Although *S. cerevisiae* cells efficiently took up P_i across all tested feed formulations, it was not fully depleted under any condition after 2.5 h (Figure 26B).

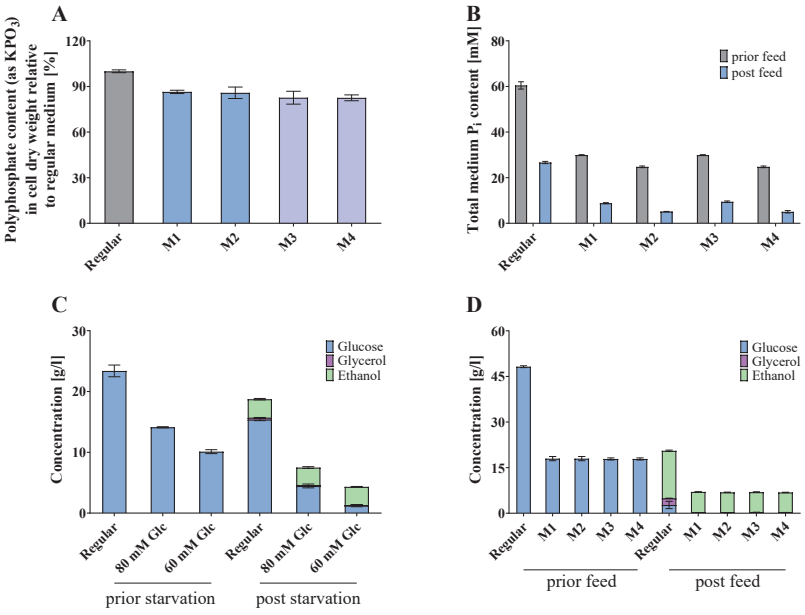


Figure 26: Evaluating the impact of completely reduced starvation and feed media on polyP production with VH2.200.
Cultivation and medium preparation according to sections 2.1.2 and 2.1.3. The medium components were individually varied and compared to the original starvation and feeding medium developed by Christ and Blank (2019) [1]. The regular starvation medium (133 mM glucose, 10 mM $(NH_4)_2SO_4$, 13.3 mM KCl, 4 mM $CaCl_2$, and 12.5 mM Na_2succinate, supplemented with Verduyn vitamins and trace elements) was compared to the media with 60 or 80 mM glucose (60/80 mM glucose, 10 mM $(NH_4)_2SO_4$, 4.5 mM KCl, 1 mM $CaCl_2$, and 4 mM (for 60 mM glucose) or 8 mM (for 80 mM glucose) Na_2succinate). Both minimal media were supplemented with inositol (25 mg/l) and zinc (2.5 mg/l). Additionally, three feeding media were investigated: the regular medium (250 mM glucose, 60 mM P_i) and two media with reduced P_i concentrations (25 or 30 mM) and glucose concentrations (both 100 mM). M1 = 80 mM glucose, 30 mM P_i, M2 = 80 mM glucose, 25 mM P_i, M3 = 60 mM glucose, 30 mM P_i, M4 = 60 mM glucose, 25 mM P_i. (A) PolyP content at the end of the hyperaccumulation protocol; (B) P_i content in cultivation broth at the end of the hyperaccumulation protocol; (C) Results of HPLC analysis before and after the starvation phase of the hyperaccumulation protocol; (D) Results of HPLC analysis before and after the feeding phase of the hyperaccumulation protocol. The data are shown in a stacked format. Cultivations were performed in MTPs to generate enough cell mass for enzymatic polyP quantification. The results represent the mean of two replicates ± SEM (n = 2). Data associated with this figure were obtained from [353].

While only 56 % of total P_i was consumed in regular medium, 68–80 % was taken up by *S. cerevisiae* in the minimal media. A lower initial P_i concentration of 25 mM (M2, M4) compared to 30 mM (M1, M3) had only a minor impact on polyP accumulation but resulted in less residual P_i at the end of cultivation. The cellular P_i uptake rate in regular medium was considerably higher at 0.64 mM_{Pi}/h, compared to 0.41-0.45 mM_{Pi}/h in modified feed media. The higher P_i uptake rate in regular medium is partly related to increased polyP levels. Besides that, P_i might also have been

diverted into metabolites besides polyP, which were not investigated in this cultivation. Metabolite concentrations before and after the starvation phase are shown in Figure 26C. In the regular medium, approximately 34 % of the initial glucose was consumed, while depletion increased to 68 % and 88 % at glucose concentrations of 80 mM and 60 mM, respectively. The glucose uptake rate was around 0.33 g/l/h in all tested media, since more glucose remained unused in the regular medium. The ethanol production profiles were similar across all P_i starvation media, with concentrations of ~3.0 g/l and production rates of ~0.12 g/l/h. Final glycerol concentrations were highest in the regular medium (~0.3 g/l) and lowest in the modified starvation media (~0.11 g/l). After the P_i feeding phase, metabolite levels revealed apparent differences between the media (Figure 26D). In the regular feed medium, glucose levels decreased from 48.21 g/l to 2.71 g/l, while ethanol reached a final concentration of 15.64 g/l. This corresponds to glucose uptake and ethanol production rates of 0.86 g/l/h and 0.29 g/l/h, respectively. In media M1-M4, the glucose was completely consumed, and final ethanol levels of ~6.68 g/l were detected. This results in substantially lower glucose uptake rates of ~0.38 g/l/h and ethanol production rates of 0.14 g/l/h compared to the feed medium by Christ and Blank (2019) [1]. Glycerol accumulation was highest in the regular medium (~2.2 g/l) but remained below 0.3 g/l in all modified media (M1-M4). Hence, the modified media substantially decreased residual glucose and byproducts compared to the control at the cost of slightly reduced final polyP levels. This revised medium represents a substantial simplification of the original formulation by Christ and Blank (2019) [1], which facilitates the formulation of minimal media requirements for polyP accumulation in *S. cerevisiae*. Moreover, media expenses were reduced from €3.11 to €1.36 per liter (a 56 % decrease), with reduced impact on final polyP accumulation (Suppl. Table A13).

Since HPLC analysis revealed no residual glucose and lower ethanol levels in the modified feed media compared to the original formulation by Christ and Blank (2019) [1], a follow-up cultivation was conducted. In this setup, the difference in the final ethanol concentration (in carbon molar terms) between regular and modified media was used to adjust the initial glucose concentration equimolarly. Under the conditions of the hyperaccumulation protocol, *S. cerevisiae* primarily ferments glucose to ethanol, generating the ATP for energy and polyP formation [1, 146, 159, 321]. Hence, the regular feed medium containing 250 mM glucose was compared to modified feed media with 100 mM and 160 mM glucose (Table 5 and Suppl. Figure A17). In all cases, the initial P_i concentration was set to 25 mM. Apart from these adjustments, the overall media composition remained unchanged. The polyP content in the modified media ranged from approximately 82.5 % to 96.1 % of the levels observed in the regular medium (Suppl. Figure A17), which is slightly higher than in previous cultivations. However, this increase is not related to elevated initial glucose levels in the feed medium, as these had no positive effect on P_i

consumption nor the efficiency of polyP accumulation. The higher relative polyP content of M2 and M4 compared to Figure 26 is most likely attributable to batch-to-batch variation. However, additional side products were produced in M5 and M6 compared to M2 and M4 during the feed phase due to increased initial glucose levels. Finally, the $(NH_4)_2SO_4$ concentration in the starvation medium and the $MgCl_2$ concentration in the feed medium were re-evaluated. Christ and Blank (2019) [1] demonstrated that a certain amount of $(NH_4)_2SO_4$ is required for achieving an entirely starved *S. cerevisiae* culture. The results showed that reducing $(NH_4)_2SO_4$ concentration to 2.5 mM did not negatively affect final polyP levels (Suppl. Figure A18). PolyP accumulation, in fact, was slightly elevated. In the final media adaptation, $MgCl_2$ levels in the feeding medium were varied as the last remaining parameter (Figure 27).

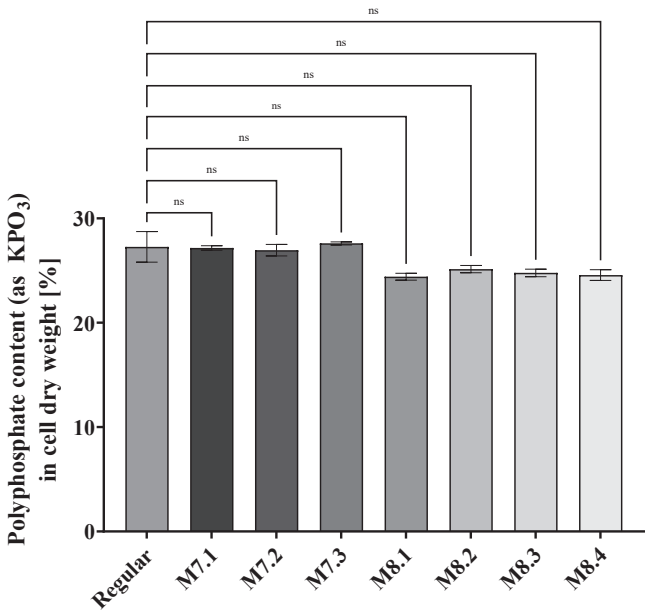


Figure 27: Evaluating the impact of reduced $MgCl_2$ concentrations in the feeding medium on polyP production with VH2.200.
Cultivation and medium preparation according to the sections 2.1.2 and 2.1.3. The medium components were individually varied and compared to the original starvation and feeding medium developed by Christ and Blank (2019) [1]. Starvation media were prepared with reduced concentrations (80 mM glucose, 2.5 mM $(NH_4)_2SO_4$, 4.5 mM KCl, 1 mM $CaCl_2$, and 4 mM Na_2succinate). The minimal media were supplemented with inositol (25 mg/l) and zinc (2.5 mg/l). For comparison reasons, the feeding medium of Christ and Blank (2019) [1] was varied in $MgCl_2$ content: 15 mM (M7.1), 10 mM (M7.2), and 5 mM (M7.3). Additionally, feeding media were investigated with 100 mM glucose, 25 mM P_i, and varying $MgCl_2$ concentrations of 20 mM (M8.1), 15 mM (M8.2), 10 mM (M8.3), 5 mM (M8.1) were applied. Cultivations were performed in MTPs to generate enough cell mass for enzymatic polyP quantification. The results represent the mean of two replicates ± SEM (n = 2). Significant differences marked by asterisks (*p < 0.05, **p < 0.01, ***p < 0.001, ****p < 0.0001; One-Way ANOVA).

80 mM glucose and 4 mM succinate were chosen for the starvation medium. The reduced succinate level of 4 mM compared to 8 mM in previous cultivations with 80 mM glucose was intentionally chosen, as lower ammonium consumption may reduce the need for buffering. Additionally, this could improve nutrient efficiency for polyP production. Figure 27 illustrates the effect of varying $MgCl_2$ concentrations (5-20 mM) on final polyP levels. No significant impact on polyP accumulation was observed for most treatments. While lower concentrations were not examined in this study, previous work by Christ and Blank (2019) [1] highlighted the essential role of Mg^{2+} in supporting polyP synthesis. The reduction of required $(NH_4)_2SO_4$ and $MgCl_2$ levels, without further impacting the final polyP level, resulted in a decrease in medium costs from 1.59 €/l to 1.36 €/l (Suppl. Table A12 and Table A13). This represents a 56 % reduction compared to the original medium by Christ and Blank (2019) [1]. A holistic optimization of individual media components could likely restore polyP levels to those achieved with the original medium. However, this chapter aimed to identify the minimal concentrations of components required for efficient polyP production. Beyond the clear ecological and economic advantages of reduced resource use, simplified media formulations improve DSP and overall sustainability. The results confirm that *S. cerevisiae* remains robust across a range of media fluctuations, provided essential thresholds are met. This is a crucial insight for future work utilizing different P_i-rich waste streams as substrates. In summary, the number and concentration of media components were substantially reduced, with only minor effects on polyP production in a high-producing strain. Therefore, this chapter extends previous optimization efforts focused on trace elements and vitamins. The beneficial role of inositol was reaffirmed, though its role in polyP hyperaccumulation remains unclear. To explore this further, several *S. cerevisiae* BY4742 strains with deletions in genes involved in phospholipid metabolism, inositol transport, and *de novo* inositol synthesis were investigated.

7.3.2 Influence of inositol and zinc on phospholipid metabolism

Figure 28A-B shows the polyP levels of strains from the YKO collection with mutations in the phospholipid metabolism. The media are based on the original protocol by Christ and Blank (2019) [1], except that only zinc and inositol were added, rather than the complete Verduyn trace elements and vitamins in the starvation medium. In the cultivation of Figure 28A, $MgCl_2$ was included in the starvation medium due to the Mg^{2+}-dependence of the *PHM8* encoded lysophosphatidic acid (LPA) phosphatase. In the absence of Mg^{2+}, it would not have been possible to distinguish whether any observed effect was due to the respective knockout or to non-functional LPA.

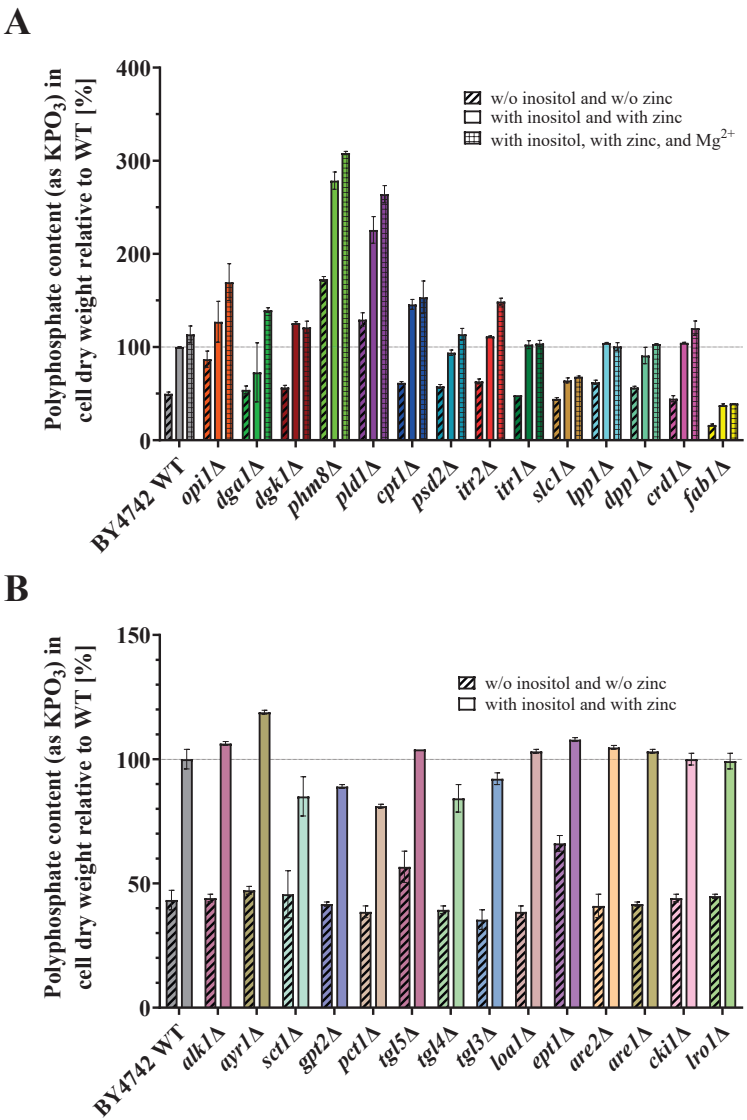


Figure 28: Investigating the effect of phospholipid metabolism-associated genes on polyP accumulation in BY4742 deletion mutants.
BY4742 WT and corresponding mutants were cultivated following the standard operating procedure for generating polyP-rich cells (sections 2.1.2 and 2.1.3). The starvation medium was supplemented with amino acids to account for strain-specific auxotrophies [225]. (A) Starvation medium w/o zinc and inositol, with zinc (2.5 mg/l) and inositol (25 mg/l) or with zinc, inositol, and $MgCl_2$ (1.9 g/l); (B) Starvation medium w/o zinc and inositol or with zinc (2.5 mg/l) and inositol (25 mg/l). PolyP production was evaluated relative to BY4742 WT. The results represent the mean of two replicates ± SEM (n = 2). Data associated with this figure were partially obtained from [325, 353].

Notably, the addition of $MgCl_2$ boosted polyP production independent of LPA expression. The effect of Mg^{2+} was also confirmed for CEN.PK WT but not for VH2.200 (data not shown). The reason is unclear but may relate to strain-specific differences, as CEN.PK and BY4742 naturally have lower polyP levels than VH2.200. Adding inositol and zinc boosted polyP accumulation across all tested strains. Notably, *phm8*Δ and *pld1*Δ showed elevated polyP levels, whereas *fab1*Δ showed very low levels. Strains such as *opi1*Δ and *cpt1*Δ exhibited slightly higher polyP levels than BY4742 WT. Since the effect of $MgCl_2$ on polyP production in BY4742 was independent of LPA expression (Figure 28A), 15 additional mutations were tested for their polyP expression level only supplemented with zinc and inositol (Figure 28B). Most strains revealed no improvement in polyP accumulation and had slightly lower levels than BY4742 WT. 13 additional BY4742 mutants were screened only under inositol and zinc supplementation to identify varying polyP production patterns (Suppl. Figure A19). All strains produced polyP levels comparable to the BY4742 WT, except for *gpd1*Δ and *vip1*Δ, which showed notable differences. The *gpd1*Δ knockout resulted in substantially elevated polyP levels, whereas *vip1*Δ exhibited a marked reduction in polyP production. Overall, the screening of 42 BY4742 single-gene mutants showed no clear link between phospholipid metabolism and polyP synthesis, leaving zinc and inositol's exact roles unclear. The *pah1*Δ knockout strain was also studied, which was not available via the YKO collection, but was constructed with CEN.PK WT as the parental strain. *PAH1* encodes a Mg^{2+}-dependent phosphatidate phosphatase [366]. This enzyme converts phosphatidate (PA) to diacylglycerol (DAG) and plays roles in phospholipid biosynthesis, membrane growth, and vacuolar homeostasis [366]. Additionally, PA is a key intermediate in phospholipid synthesis (PLS) and regulates the transcription of PLS genes [367]. Due to this Mg^{2+} dependency of Pah1p, one cultivation was supplemented with $MgCl_2$. Otherwise, the BY4742 WT would exhibit the same phenotype as the *pah1*Δ knockout strain, making it impossible to identify any deviating effect. Under non-supplemented conditions, CEN.PK WT and *pah1*Δ showed similar polyP levels. Surprisingly, the increase in polyP was more pronounced in CEN.PK WT than in the *pah1*Δ knockout strain with zinc and inositol supplementation (Figure 29).

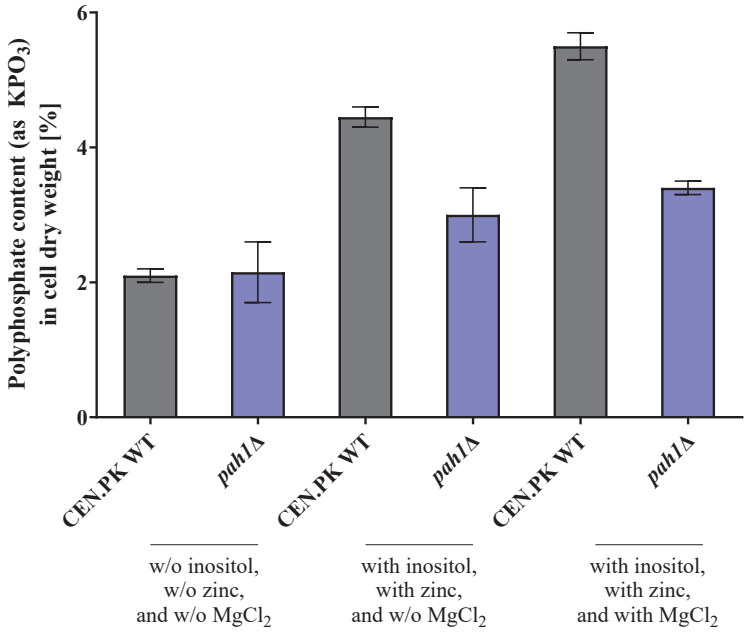


Figure 29: PolyP accumulation in CEN.PK WT and CEN.PK *pah1*Δ under various supplemented starvation media.
CEN.PK *pah1*Δ and CEN.PK WT were cultivated according to the standard operating procedure for generating polyP-rich cells (sections 2.1.2 and 2.1.3). The starvation medium was either not supplemented or contained zinc (2.5 mg/l), inositol (25 mg/l), and/or $MgCl_2$ (1.9 g/l). Error bars indicate the standard error across two biological replicates. Data associated with this figure were obtained from [353].

Since *PAH1* encodes a Mg^{2+}-dependent phosphatidate phosphatase, similar polyP levels were expected. This difference may result from residual cellular Mg^{2+} levels, partial substitution of Mg^{2+} function by Zn^{2+}, or partial activity of Pah1p in the absence of Mg^{2+}. However, since the literature reports neither a substitutive effect of Zn^{2+} nor significant Pah1p activity in the absence of Mg^{2+}, residual cellular Mg^{2+} levels are considered the most likely explanation. Mg^{2+} addition led to elevated polyP levels in this cultivation, independent of *PAH1* expression. Overall, these results suggest a potential, however limited, role of Pah1p in polyP synthesis. However, since no deviating polyP accumulation pattern was observed in *pah1*Δ nor any other phospholipid knockout strain, the effect of external zinc and inositol supplementation could not be pinpointed via mutations in phospholipid metabolism. Since *S. cerevisiae* can synthesize inositol *de novo*, the impact of external inositol was further investigated using strains with mutations in inositol synthesis and uptake.

7.3.3 Influence of inositol transport and production on polyP synthesis

Figure 30 shows data from single biological replicates, illustrating polyP accumulation in CEN.PK WT and knockout mutants with deleted genes involved in inositol synthesis/uptake, grown with or without inositol.

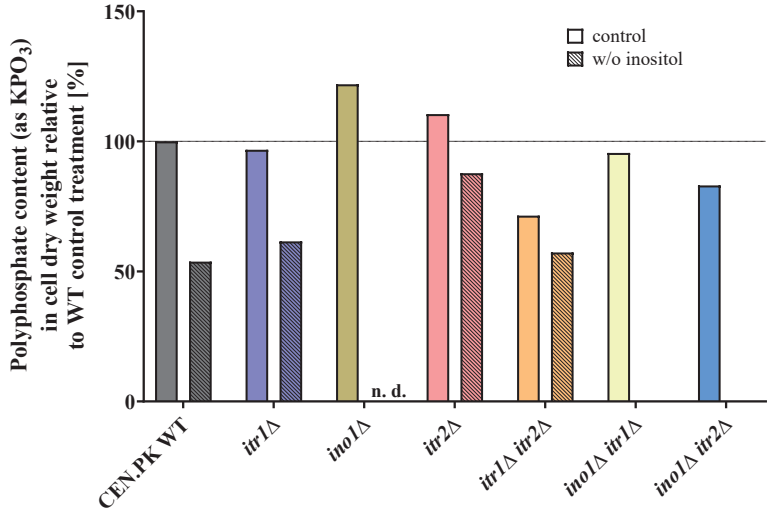


Figure 30: Investigating the effect of inositol metabolism-associated genes on polyP accumulation in CEN.PK deletion mutants.
CEN.PK WT and corresponding mutants were cultivated following the standard operating procedure for generating polyP-rich cells (sections 2.1.2 and 2.1.3). The control was supplemented with both zinc (2.5 mg/l) and inositol (25 mg/l), whereas the inositol-deficient medium contained only zinc (2.5 mg/l). All strains with mutations in inositol *de novo* synthesis, the uptake, or their combination. Data from a single biological replicate is presented. Missing bars indicate insufficient cell growth under inositol depletion. "n. d." denotes non-detectable polyP levels, despite successful cultivation in the indicated medium. Data associated with this figure were obtained from [353].

All strains accumulated polyP under control conditions, establishing a baseline for comparison with inositol-deficient conditions. Under control conditions, polyP levels in the tested mutants varied by up to ± 29 % relative to CEN.PK WT. While CEN.PK *ino1*Δ showed a slight increase, the double mutant CEN.PK *itr1*Δ*itr2*Δ exhibited the most substantial reduction, accumulating only ~71.4 % of the WT polyP level. In CEN.PK *ino1*Δ, polyP was not detectable in the absence of inositol. Moreover, some strains did not reach an adequate cell mass for polyP hyperaccumulation analysis without inositol supplementation. To overcome this, selected mutants were cultivated at higher volumes to ensure enough biomass (Suppl. Figure A20). The CEN.PK *itr1*Δ*itr2*Δ mutant showed similar polyP levels compared to CEN.PK WT without inositol. Interestingly, polyP levels increase with inositol supplementation even though inositol should not enter the cell due to the

deletion of *ITR1* and *ITR2* (Suppl. Figure A20). The reason for this observation remains unknown. Concluding, these results confirm that extracellular inositol is taken up by *S. cerevisiae* and directly affects polyP accumulation. Additionally, the severe growth reduction in *ino1*Δ strains under inositol-free conditions highlights the importance of inositol for overall cellular fitness.

7.4 Discussion

This chapter investigated the influence of all medium components of the starvation and feed medium developed by Christ and Blank (2019) [1] on polyP accumulation with *S. cerevisiae* VH2.200. According to the results of Chapter 6, a medium reduced in Verduyn trace elements and Verduyn vitamins was used as the starting point for further medium evaluation [329]. Growing yeast in media containing only essential supplements at optimal concentrations is economically and ecologically advantageous, while also simplifying media preparation and product purification [331, 368-370]. In commercial biotechnology processes, DSP accounts for 20-40 % of the total production costs of bulk fermentation products [371, 372]. However, the primary costs for biotechnological bulk products are associated with upstream processing (USP) [372]. For example, the fermentation medium often accounts for over 50 % of the total costs in beverage production [373]. Therefore, a well-balanced and optimized medium is crucial for maximizing yeast performance, minimizing byproduct formation, and ensuring that DSP remains cost-effective and straightforward [373-375]. Otherwise, chemical synthesis may offer a more competitive alternative. This includes C-sources, as well as major, minor, and trace nutrients [373]. In this chapter, all components in the starvation and feed medium could be substantially lowered without notably affecting the final polyP levels (Figure 26 and Figure 27). Lower glucose levels led to decreased ethanol formation via the Crabtree effect [323]. This improves the target product yield and minimizes byproducts (Figure 26). Moreover, it can potentially reduce the USP and DSP costs of polyP production. The cultivation procedure and medium were based on Christ and Blank (2019) [1]. Still, this chapter expanded the scope by testing intermediate concentrations, increasing the number of replicates, and considering additional parameters beyond the final polyP content [1]. PolyP content, resource inputs, and byproduct formation were evaluated during media optimization. Through optimization, the media cost was reduced by 56 % while maintaining comparable polyP levels. Figure 27 and Table 5 highlight the substantial reduction in component concentrations compared to Christ and Blank (2019) [1], as well as the reduced impact on final polyP levels [1]. Beyond cost efficiency and easier purification, this approach supports the use of industrial waste streams or plant residues as P_i sources, as fewer additional nutrients are required [103]. This would support the transition from a linear P_i economy to a circular model [45, 64].

Hence, this chapter demonstrates the robustness of *S. cerevisiae's* polyP production, even at fluctuating media concentrations, if the essential components are present at minimal levels. Inositol and zinc are two of those critical factors [329]. Here, the impact of inositol on polyP synthesis was further examined. Although inositol, zinc, and P_i are involved in phospholipid metabolism in *S. cerevisiae* [338, 359], no general correlation with polyP accumulation or inositol-related effects was detected. Inositol and zinc have a contradictory effect on the phospholipid metabolism in *S. cerevisiae* [338]. Inositol addition or zinc deficiency promotes phosphatidylinositol synthesis and reduces PA levels, while inositol depletion or zinc supplementation increases PA accumulation. These conditions do not account for the impact of P_i starvation in combination with inositol and zinc supplementation. Nevertheless, the phospholipid mutant strains (Figure 28) confirmed the previously reported positive effect of zinc and inositol on polyP hyperaccumulation [329]. However, some mutants emerged as promising candidates for further investigation to improve polyP production. Deletions in *phm8*Δ and *pld1*Δ increased total polyP levels, whereas *fab1*Δ and *vip1*Δ decreased them. Phm8p functions as nucleotidase and LPA phosphatase [189, 376]. Under low P_i conditions, it primarily acts as LPA phosphatase, converting LPA to monoacylglycerol (MAG) while releasing P_i to attenuate P_i starvation [358, 359]. LPA and MAG are crucial intermediates in the metabolism of membrane phospholipids and triacylglycerol [359, 377]. The role of *PHM8* in the P_i starvation response is highlighted due to its upregulation via the transcription factor Pho4p under these conditions [146, 182, 358, 378]. Pho4p is the key transcription factor within the P_i-responsive PHO regulon [164, 379] and regulates a broad set of genes involved in P_i homeostasis [160, 185, 215, 380]. While Phm8p degrades LPA to MAG, LPA can also be acylated via *SLC1*- and *ALE1*-encoded lysoPA/lysophospholipid acyltransferases to form PA, a precursor for all glycerophospholipids in yeasts [338, 359, 381-384]. MAG itself serves as a precursor for the synthesis of diacylglycerol and triacylglycerol [359, 385]. The role of *PHM8* in P_i recycling is well established, as *phm8*Δ mutants cannot survive extended P_i starvation [146]. However, the mechanism by which *phm8*Δ enhances polyP synthesis remains unclear. It may be related to impaired recycling of P_i from intracellular sources, such as nucleoside monophosphates and LPA, which could potentially lead to stronger P_i starvation signaling and increased polyP accumulation [146, 189, 358]. Another deletion that positively impacted polyP synthesis was *pld1*Δ. *PLD1* encodes a phosphatidylcholine-specific phospholipase D, which hydrolyzes phosphatidylcholine (PHC) into PA and choline [367]. Choline can be incorporated into PHC via the CDP-choline branch of the Kennedy pathway, while PA serves as a precursor for other phospholipids [338, 386]. Although the Kennedy pathway and CDP-DAG pathway are both used to produce PHC, the CDP-DAG pathway is the main route for its synthesis in the absence of external choline [386]. Depending on the synthesis pathway, PHC serves different physiological

roles [387, 388]. When PHC turnover is reduced, altered PA levels could affect phospholipid metabolism, given PA's central role as a signaling lipid and metabolic intermediate [389]. This chapter did not determine whether the distinct physiological roles of PHC or altered PA levels influence polyP accumulation. However, phospholipids represent a primary cellular P_i reservoir [390]. In plants and some fungi, PHC turnover is crucial for replacing phospholipids with non-P lipids during P_i starvation [390, 391]. However, *S. cerevisiae* lacks the *BTA1* homolog for this pathway, and no significant changes in major phospholipids, including PHC and PA, have been observed under P_i-limiting conditions [376, 391]. Hence, the *BTA1* gene could represent another target for enhanced polyP production in *S. cerevisiae* via metabolic engineering. However, the effect of *pld1*Δ on polyP synthesis in *S. cerevisiae* remains unclear. The *fab1*Δ mutant showed substantially lower polyP levels than BY4742 WT. Fab1p is a vacuolar membrane kinase that produces phosphatidylinositol (3,5)P_2 and is crucial for vacuole function and morphology in yeasts [392, 393]. Freimoser et al. (2006) [152] also discovered that *FAB1* is important for maintaining regular polyP levels in their systematic screening. Since polyP is synthesized via the VTC complex in the vacuolar membrane, significant changes in vacuole function or morphology can negatively influence polyP production. The other interesting strain showing reduced polyP titers was *vip1*Δ. Vip1p is a bifunctional inositol pyrophosphate kinase and phosphatase and generates 1-InsP7 and 1,5-InsP8 from InsP6 and 5-InsP7 through its kinase domain [394, 395]. Hence, Vip1p may link lower cytosolic P_i levels to reduced concentrations of 1,5-InsP8 and 1-InsP7, thereby triggering a stronger P_i starvation response and ultimately leading to higher cellular polyP levels. InsPPs are vital since they act on the SPX domains of proteins involved in P_i homeostasis [146]. Some other studies report no significant quantitative difference in polyP levels in *vip1*Δ strains [264, 396]. However, these studies did not apply P_i starvation conditions, as described in this chapter, and may therefore observe a different influence. The *gpd1*Δ strain was not analyzed further, as it displayed elevated polyP levels compared to BY4742 WT in only one out of three replicates, for reasons that remain unclear. Since mutations with a positive effect on polyP synthesis were linked to PA, a *pah1*Δ mutant was generated. PAH1p encodes an Mg^{2+}-dependent PA phosphatase that converts PA into DAG [338, 366]. The *pah1*Δ mutant accumulates PA, leading to the upregulation of phospholipid biosynthetic genes, a decrease in triacylglycerol (TAG) content, and increased membrane biogenesis [338, 397-400]. Under starvation conditions lacking zinc and inositol, *pah1*Δ accumulated polyP at levels comparable to those of the CEN.PK WT. However, when zinc and inositol were supplemented, the mutant exhibited a reduced increase in polyP accumulation (Figure 29). The addition of inositol and/or zinc may reduce cellular fitness or divert key resources (e.g., ATP and inositol) toward enhanced phospholipid synthesis under these conditions [401, 402], thereby limiting their availability for polyP production. However, the mechanism linking

phospholipid metabolism to polyP synthesis remains unclear. The reported effect of *pah1*Δ on vacuolar fusion is unlikely to account for the observed phenotype [403], as a similar impairment would be expected under non-supplemented conditions. Interestingly, this chapter confirms that external inositol enhances polyP synthesis, even though *S. cerevisiae* is inherently capable of inositol biosynthesis [404, 405]. It can substitute for and compensate for endogenous inositol production, as evidenced by the restoration of polyP accumulation to WT levels. In all mutants, polyP levels were higher than under inositol-free conditions [329]. Moreover, this chapter highlights the critical role of *INO1* under conditions lacking exogenous inositol, as *INO1* deletion mutants are unable to synthesize inositol endogenously [406-409]. Consequently, this mutant fails to accumulate polyP and exhibits severe growth defects in the absence of inositol supplementation. Moreover, inositol depletion has been shown to impair glucose uptake, decrease the specific growth rate (due to the prolongation of the G2 phase), reduce cell viability, and increase lipid accumulation [357, 368]. The observed reduction in polyP production is likely due to myo-inositol's role as a precursor for InsPP [347]. InsPPs regulate polyP accumulation and are crucial for overall P_i homeostasis [146, 173, 177, 178]. Previous studies identified two distinct myo-inositol transporters in *S. cerevisiae*, *ITR1* and *ITR2*, with Itr1p acting as the primary transporter and Itr2p as a minor one in minimal medium [410]. Deletion of either transporter had no negative impact on polyP accumulation, as levels remained comparable to those in the CEN.PK WT strain. This chapter confirmed the functional independence of the two transporters, as reflected in their distinct regulatory patterns. Itr1p is repressed by inositol and choline via Opi1p, whereas derepression is mediated by Ino2p and Ino4p [406, 411, 412]. Itr2p is constitutively expressed [412], contributing to a robust regulatory system that safeguards inositol-dependent processes such as polyP synthesis. Surprisingly, the *itr1*Δ*itr2*Δ double mutant exhibited increased polyP accumulation when supplemented with inositol compared to inositol-free conditions. As both inositol transporters were deleted, similar polyP levels were expected under both conditions. This unexpected result suggests that additional cellular uptake mechanisms can partially compensate for the loss of the two transporters. Non-specific transporters, such as hexose transporters, may display low or indirect affinity for inositol and facilitate residual uptake, particularly when overexpressed or in the absence of competition. This hypothesis is supported by the structural similarity between glucose and inositol [413]. The affinity and specificity of these alternative transport systems for inositol would be much lower than those of Itr1p and Itr2p. The K_m values of Itr1p and Itr2p are approximately 100 µM and 140 µM, respectively [414]. Another possibility is that transporters involved in inositol metabolism, such as Git1p, contribute to inositol uptake. Git1p transports glycerophosphoinositol, which is released from membrane turnover, back into the cell when extracellular inositol becomes scarce. The imported molecule can then serve as an

inositol source for *S. cerevisiae* [415]. The affinity of these auxiliary systems may be too low to play a noticeable role and to support cellular growth when Itr1p and/or Itr2p are present. Therefore, it might remain masked under normal conditions. Nonetheless, no evidence exists that such mechanisms operate in baker's yeast to support polyP production.

This chapter demonstrates that the starvation and feed media used in the *S. cerevisiae* polyP hyperaccumulation protocol can be further optimized without substantially affecting final polyP yields. Reducing the concentration of medium components not only saves resources but also increases the economic and environmental viability of biotechnological polyP production. Moreover, the mode of action of inositol in polyP hyperaccumulation was investigated. Although no overarching effect on phospholipid metabolism was observed, several promising mutations were identified. Mutations affecting endogenous inositol biosynthesis and uptake confirmed that exogenous inositol has a positive influence on polyP accumulation.

7.5 Conclusion

In conclusion, this chapter lays the groundwork for further optimization of biotechnological production of bio-polyP or polyP-rich yeast extract, improving both the ecological and economic footprint. Overall, these results support the transition towards a circular P_i bioeconomy, as they enable a more precise definition of the requirements for utilizing P_i-rich waste streams. By elucidating the role of inositol during the P_i starvation phase and identifying previously unknown regulatory targets, this work also provides new insights into investigating polyP metabolism in *S. cerevisiae*. Combined with ongoing developments in metabolic engineering and reaction engineering, these insights may lead to a competitive alternative to fossil-based chemical polyP production and provide an incentive to establish *S. cerevisiae*-based polyP production as a commercially viable option.

Chapter 8

General Discussion

Contributions:

This chapter was written by Alexander Deitert and critically reviewed by Philipp Demling and Lars Mathias Blank.

8 General Discussion

8.1 The role of polyP in achieving the UN Sustainable Development Goals

The SDGs provide a unified plan for global peace and prosperity for people and the planet. In this plan, all nations are encouraged to work together in an international partnership to create a better present and future [416]. The global challenges underscore the need for sustainable resource management and form the basis for numerous research initiatives and the concept of circular (bio)economy. This thesis aimed to contribute to the development of a sustainable P_i economy by leveraging *S. cerevisiae's* ability to accumulate P_i from potential waste streams as polyP. In a recent publication, Walsh et al. (2023) [43] highlighted that the currently prevailing linear P_i economy has an impact on several SDGs (Figure 31), including: (1) No poverty; (2) Zero hunger; (3) Good health and well-being; (6) Clean water and sanitation; (8) Decent work and economic growth; (9) Industry, innovation, and infrastructure; (11) Sustainable cities and communities, (12) Responsible consumption and production; (14) Life below water; (15) Life on land; (17) Partnerships for the goals.



Figure 31: 17 UN Sustainable Development Goals adopted by all United Nations Members.
The SDGs emphasize the interdependence of the environmental, social, and economic dimensions of sustainable development. This figure is adapted from United Nations Sustainable Development Goals (https://www.un.org/sustainabledevelopment). The content of this publication has not been approved by the United Nations and does not reflect the views of the United Nations or its officials or Member States.

The urgency of transitioning to a more sustainable P_i economy is underscored by the planetary boundaries concept, developed by Rockström et al. (2009) [50], and "The Helsinki Declaration". In "The Helsinki Declaration", 500 scientists and researchers request policymakers to promote a

circular P_i economy [417, 418]. Moreover, on July 23, 2025, the International Court of Justice issued an advisory opinion on the obligations of states regarding climate change. The Court confirmed that a clean, healthy, and sustainable environment constitutes a human right and that climate change is a universal and severe threat to humanity. Consequently, states are obligated under international law to prevent significant environmental damage [419]. While this advisory opinion is specifically related to climate change, analogous arguments can be identified in the context of the current linear P_i economy.

The following section discusses how this work and polyP/P_i biotechnology can contribute to achieving specific SDGs. The relevance of P_i for several SDGs was introduced in Chapter 1.2 of this thesis. Therefore, aspects only marginally addressed in Chapter 1.2, such as the environmental impact of P_i mining, its economic significance for mining countries, and the socio-economic implications, are further detailed in this chapter. P_i mining is associated with various environmental impacts, including changes in land use, habitat destruction, dust emissions, water pollution, and interference with aquifer systems [420-422]. Additionally, P_i mining significantly contributes to biodiversity loss and the destruction of ecosystems essential to human survival [423]. This effect is intensified by low P_i fertilizer efficiencies and inefficient P_i utilization. Studies have suggested that approximately 70 % of P_i fertilizer is not absorbed by crops [21]. Unused P_i from fertilizer either accumulates as inaccessible legacy P in soils or is lost to the environment [43]. Therefore, soils cultivated for decades should, in theory, contain sufficient P to support plant growth for years [64]. However, most of this P is unavailable to crops as it is tightly bound to counterions, such as iron. This limits the diffusion and uptake of P [64, 424]. Moreover, 95 % of P is lost throughout the value chain, from mining and agriculture to human consumption [425]. The severity of the situation can be demonstrated with the example of the Baltic Sea. Even if the nutrient reduction targets outlined in the Baltic Sea Action Plan are achieved, the marine basins will require until the year 2200 to recover from eutrophication [426].

Due to rising global fertilizer demand, disruption of marine and terrestrial nutrient cycles is expected to intensify further [3, 18, 43]. In addition, exploitable P_i reserves, defined as accessible and economically viable, are being gradually depleted [23, 25, 43]. As a result, the quality of the remaining P_i rock is declining, as concentrations of undesirable components such as minerals and heavy metals are increasing [19]. Contaminants such as cadmium are considered hazardous due to their toxicity, tendency to accumulate in soils, availability to crops, and potential for leaching [427-430]. Hence, P extraction is becoming increasingly energy-intensive, costly, and generates more waste [19, 25]. Since approximately 80 % of the heavy metals present in P_i ore are transferred into phosphoric acid, regulatory measures have been implemented [431]. EU legislation introduced stricter limits on heavy metal contamination in phosphoric acid and fertilizer products to mitigate

associated environmental and health risks [45, 432]. However, no cost-effective technologies are currently available for the efficient removal of heavy metals from P_i rock [431]. Additionally, the physical accessibility of remaining P_i reserves is becoming increasingly challenging. This is demonstrated by projects such as the offshore P_i mining development in Namibia, which involves seabed extraction [25]. Seabed mining is controversial due to its potentially severe environmental impacts on the largely unexplored deep-sea ecosystem. This includes threats to pelagic and benthopelagic fauna, noise and light pollution, and sediment plume generation [433, 434].

In addition to its environmental impact, P_i is of significant economic importance. This primarily relates to the final applications of P_i and applications along the value chain, but P_i mining itself is also of substantial economic relevance for many countries. P_i and P_i rock exports constitute a significant share of total exports in Togo (8.8 %), Jordan (4.3 %), and Morocco (2.8 %) [435]. Additionally, P_i mining has significant economic impacts, as it creates jobs, generates export revenue, and supports macroeconomic stability [435-437]. This highlights the complex and interconnected nature of the current P_i economy and the need to consider the P_i issue from multiple perspectives. This includes the ecological and economic impacts on mining regions, as well as the political and ethical dimensions of the P_i economy.

Several countries with significant P_i reserves are affected by political instability, corruption, and resource exploitation [438]. A challenging situation arises in this context due to Western Sahara's P_i reserves [439]. According to the UN, Western Sahara is classified as a non-self-governing territory [440]. However, the UN Security Council's Resolution 2797 of October 2025, which recommends that Western Sahara be placed under Moroccan sovereignty while granting it autonomous rights, is a potential turning point in reviving UN-mediated negotiations and advancing a political solution [62]. Morocco controls approximately 75 % of the region west of the sand berm, where significant P_i reserves are located [441, 442]. This raises legal and ethical concerns regarding the extraction of resources, such as P, in a disputed territory. Currently, the UN and EU share the position that "where resource exploitation activities are conducted in non-self-governing territories for the benefit of the people of those territories, on their behalf or in consultation with their representatives, they are considered as legal" [443, 444]. This position leaves room for interpretation and misuse, particularly given the limited global distribution of P_i rock reserves. Current estimates suggest that approximately 74×10^9 tons of accessible P_i rock exist globally. Morocco holds the largest share of approximately 68 %, followed by China (5 %), Egypt (4 %), and Tunisia (3 %) [445]. Consequently, global P_i rock reserves are geographically concentrated and controlled by a few countries and corporations. This creates a dependency for many nations and regions, which must rely on imports of P_i fertilizers or raw P_i rock for domestic fertilizer production [61]. For example, the EU possesses limited P_i reserves, with only Finland

holding significant reserves (1.4 % of global reserves) [43, 446]. This dependency is considered a strategic concern by the EU, prompting it to classify P_i as a critical raw material in 2014 [56]. A potential reserve in Norway might change this situation, though [447]. The anticipated future shortage of P_i reserves is expected to intensify geopolitical leverage, destabilize commodity supply chains, and increase costs due to limited competition in an increasingly monopolized market [43, 61, 422, 448-450]. China is the world's largest producer and consumer of P_i rock [451, 452]. It extracted approximately 110×10^6 tons of P_i rock in 2024, followed by Morocco (30×10^6 tons) and the United States (20×10^6 tons) [445]. This P_i was primarily used to produce P_i fertilizer, which enabled China to feed 21 % of the world's population with only 7 % of the global arable land [452-454]. Since China does not possess the largest reserves [451, 452], Chinese studies recommend that China regulates its domestic production capacity, limits extraction rates, and invests in the development of foreign P_i resources to secure a long-term supply [452]. These demands follow previous activities related to managing resource scarcity in monopolized markets. China, as the leading producer and exporter of rare earth elements, implemented export controls on this critical resource. These restrictions have led to fear of global shortages and price surges, highlighting the risks associated with essential resources in monopolized markets [455-457]. Given China's dominant role in both the production and processing of rare earths, this scenario underscores the potential for similar dynamics in the global P_i market. An example from 2022 demonstrates that P_i supply chains are already unstable, even in the absence of acute shortages. Rising coal prices in China triggered electricity rationing, which in turn forced several fertilizer plants to reduce production. In response, China imposed export quotas on fertilizers, particularly P_i fertilizers. This was explained as a necessity to protect the domestic supply and ensure food security. These implemented export quotas significantly reduced global P_i availability, underscoring the vulnerability of the internationalized P_i market [458].

All this highlights the far-reaching influence of P on the SDGs. Several studies emphasize that achieving these SDGs by 2030 is highly challenging with current strategies in place, particularly when balancing economic development, environmental protection, and social equity [459, 460]. According to Walsh et al. (2023) [43], addressing these challenges requires bold actions. PolyP production with *S. cerevisiae* aims to contribute to a circular P_i economy by reducing reliance on P_i mining and promoting more sustainable P_i use. This can be achieved by recycling P_i from waste streams and generating value-added products, such as polyP-rich yeast extract or purified bio-polyP. Using P_i from alternative sources is a promising strategy to lower the environmental footprint of P_i use and reduce overall P_i input [45]. This would also promote the cascade use of already mined P_i, in which this P_i is used as long as possible before disposal [64]. Previous studies have demonstrated that *S. cerevisiae* can hyperaccumulate P_i from diverse waste streams and

convert it into polyP [102, 103]. P_i was extracted from plant-based waste streams, where it predominantly occurs as phytate. However, phytate-bound P_i is largely inaccessible to most organisms due to its poor bioavailability and strong chelating properties, especially for divalent cations [461-463]. When phytate-rich plant products are used as feed for monogastric animals, the undigested P_i is excreted in the manure. This contributes to overfertilization and P runoff, which exacerbate environmental P_i depletion [464]. Phytate-bound P_i is valorized by producing polyP-rich yeast extract, which can subsequently be applied in the production of food, for example of meat patties. The organic and premium food segments are promising entry points for *S. cerevisiae*-derived polyP, as they offer higher margins and attract sustainability-minded consumers.[45, 128]. PolyP-rich yeast extract demonstrated functional properties similar to or superior to those of conventional stabilizers and flavor enhancers [102]. At the same time, the process yielded P-depleted plant biomass, suitable for use in livestock feed. Phytate-rich press cake is typically treated with phytase enzymes to release bioavailable P_i before being applied as animal feed [465]. However, the approach by Herrmann et al. (2023) [102] demonstrated not only the recycling but also the upcycling potential of biotechnologically produced polyP from *S. cerevisiae*. This is particularly relevant for the valorization of waste streams, such as sewage sludge [45, 466]. Around 90–95 % of P from wastewater is typically retained in sewage sludge through biological and/or chemical precipitation [83]. In Germany, most sewage sludge is currently incinerated. Approximately half undergoes mono-incineration, primarily in stationary fluidized-bed reactors, while the other half is disposed of through co-incineration, especially in coal-fired power plants and cement kilns. The amendments to the German Sewage Sludge Ordinance will most likely limit co-incineration as a disposal option, as P recovery from sludge in waste incineration plants and cement kilns is not feasible due to low P concentrations or the lack of available recovery technologies. Sewage sludge ashes from mono-incineration and co-incineration are currently mainly backfilled or landfilled, which hinders effective P recovery [83, 84].

Only a small portion of P_i is recovered directly from sewage sludge, mainly as an agricultural fertilizer, because contamination with pharmaceuticals and heavy metals renders it unsuitable for food-grade use [70, 71, 84]. *S. cerevisiae* is robust towards varying P_i concentrations, various P_i sources, fluctuating composition of other ions, and heavy metals [103]. No toxic elements such as cadmium or lead were detected in bio-polyP, and only P_i was taken up from wash waters by *S. cerevisiae* [103, 467]. Purifying P_i from contaminants, such as heavy metals, and producing polyP opens new possibilities for its applications. On average, 75 % and 70 % of the P_i from plant extracts and wash waters were recycled with *S. cerevisiae*, respectively [103]. While the removal of P_i from wastewater is becoming increasingly efficient, reuse and recovery efforts still fall short [64], especially because recycled P_i must be economically competitive with conventionally

produced products derived from non-renewable P_i rock. Historically, P_i rock prices have fluctuated between $70 and $200 per ton, with a temporary spike to $450 per ton in 2008. Since the onset of the Russian-Ukrainian war, prices have risen, reflecting growing concerns about supply security and geopolitical instability [468-470]. This highlights the complex interplay between the P_i economy, global geopolitical developments, market speculation, and political factors [43, 470]. The currently established workflow for biotechnological polyP production with *S. cerevisiae* requires further technological development and optimization to meet industrial standards for the economically viable recycling of P_i and the production of bio-polyP or polyP-rich yeast extract [45]. In contrast to the two primary products of current P_i recycling strategies (struvite, phosphoric acid), polyP production with *S. cerevisiae* is promising and offers broad applicability beyond agriculture [471]. This includes its use as a flame retardant, food additive, or in industrial processes [49, 85, 128]. Moreover, polyP can target high-value niche applications, such as enzymatic cascade reactions, where it offers distinct advantages for energy storage over traditional molecules, including ATP, with greater stability, lower cost, and ease of handling [64, 472].

The conventional chemical polyP industry relies on purified P_i sources and energy-intensive processes, in which polyP is produced through the thermal condensation of phosphoric acid at high temperatures. These conditions require substantial fossil energy input [45, 276]. This makes the process vulnerable to soaring gas prices and energy market volatility, as seen during the 2022 energy crisis triggered by the Russian-Ukrainian war [64, 473]. PolyP production with *S. cerevisiae* would offer a bio-based alternative. For such bioprocesses to compete with established chemical methods, they must provide clear advantages, either in cost-effectiveness or in superior product functionality. Sustainability alone is insufficient as a driver for market entry [474]. Currently, large-scale chemical polyP synthesis is limited to chain lengths of up to 40 P_i-subunits. Developing a bioprocess that produces long-chain polyPs would enable access to novel polymers with unique material properties, opening new possibilities in materials science. The current market price of P_i fertilizers is an order of magnitude lower than that of polyP [45], highlighting the use of polyP in technological applications. This price gap between polyP and P_i fertilizers, along with the higher cost of producing an intracellular microbial product compared to the chemical industry, underscores the need for effective DSP [45, 475]. However, the currently employed DSP significantly reduces polyP chain lengths [1]. Hence, DSP must be further optimized, with particular emphasis on developing a sequence of operations that satisfies both economic and ecological requirements to advance biotechnological polyP production with *S. cerevisiae* to an industrial scale. In addition, the use of renewable and low-cost raw materials in USP is essential for the industrial implementation of polyP hyperaccumulation in *S. cerevisiae*. The use of glucose as a carbon source is generally not economically viable. Instead, molasses is

commonly employed as a cost-effective alternative. Molasses is a byproduct of sugar production and is used in various biotechnological applications, including the production of yeast, citric acid, and bioethanol [476-479]. It is rich in fermentable sugars and nutrients, including minerals, vitamins, and trace elements [476]. Although some scientists argue that molasses should not be considered a true byproduct because of the intensive crop cultivation, this perspective is not widely accepted in the broader scientific discourse [479].

Previous studies with *S. cerevisiae* have not achieved polyP contents or chain lengths that surpass those obtained through chemical synthesis. To overcome these limitations, metabolic engineering of *S. cerevisiae* is a promising approach. Targeted modifications could enhance intracellular polyP accumulation, increase average chain length, and improve selective P_i uptake [45]. Such advancements would be crucial for developing a competitive biotechnological alternative to current chemical production methods. However, current legislation in the EU restricts the use of GMOs in several sectors, particularly in food production [480-482]. This regulatory constraint would limit the use of polyP-rich yeast extract derived from genetically modified *S. cerevisiae*, permitting only the use of pure bio-polyP.

This thesis identified multiple candidate strains with naturally enhanced polyP content and increased chain length by screening a diverse library of 153 industrial *S. cerevisiae* strains. These strains provide a valuable foundation for developing and implementing new, non-GMO production strains with improved polyP biosynthesis (see Chapter 5). Moreover, they could serve as new hosts for metabolic engineering in countries and applications where the use of GMOs is less restricted. The initial characterization of these strains, including their growth behavior and maximal growth rate, confirmed their potential for industrial applications. Given their industrial origin, these strains are also expected to exhibit resilience to various stressors commonly encountered in large-scale bioprocesses [289, 290]. Moreover, this thesis contributed to characterizing the starvation and feed phases of the polyP hyperaccumulation protocol, resulting in an adapted medium composition that reduces resource consumption and lowers waste product accumulation. These adaptations define threshold levels of essential nutrients in waste streams or bioreactor cultivations required to achieve high-titer polyP accumulation with *S. cerevisiae*. This enhances the productivity and overall yield of the polyP production process. Although industrial implementation has not yet been achieved, this thesis contributes to laying the groundwork towards meeting the required standards.

However, biotechnological polyP production remains only one part in the broader effort to establish a sustainable, circular P_i economy. Relying solely on technological advancements is unlikely to fully resolve the challenges associated with achieving P_i sustainability [3, 43]. The transition to a circular P_i economy requires fundamental, system-level transformations across existing economic, social, ecological, and legal frameworks [3, 43]. This includes adapting the

civil infrastructure (nutrient recovery facilities) and the legal framework (GMO classification), but it also requires addressing societal attitudes, including dietary preferences and prevailing perceptions regarding the use of human excreta as fertilizers [3, 43]. Meat consumption contributes significantly to P mining, accounting for approximately 72 % of the global average P footprint, which describes the average annual mined P required to produce *per capita* food consumption [483]. Moreover, there is a widespread public aversion to the use of P_i-rich organic materials, such as human excreta, as nutrient sources in food production due to safety concerns. At the same time, regulatory barriers limit their agricultural applications [417]. Thus, this P_i source is often regarded as a pollutant despite its significant recycling potential. Globally, only a small proportion of households were connected to centralized sewerage systems in 2013, resulting in approximately 85 % of P_i in human waste not being recycled [29, 484]. Even in developed countries like France, only 50 % of the excreted P_i is returned to agricultural use. Increasing this ratio can contribute to P_i autarky and reduced environmental degradation [485]. However, Cordell et al. (2009) [19] demonstrated that even if all human excreta were returned to agricultural soils, it would only satisfy approximately 20 % of the current fertilizer demand. Moreover, updated legislation in some countries, along with legal incentives or mandates to enhance P recovery efficiency, could promote innovative measures such as biotechnological P_i recycling and reuse [3, 64, 486]. This can also be achieved by subsidizing the recycling of critical resources or by developing new P_i recycling techniques, thereby making recycled P_i financially competitive. The costs currently prevent a large-scale establishment of these technologies [450, 487]. Additionally, a resource tax that falls with the resource becoming increasingly scarce could be implemented. This way, resources should be extracted more slowly without losing the economic incentive for companies [450].

As exemplified by the food shortage in Sri Lanka following an abrupt ban on synthetic P fertilizers, a transition to a circular P economy can succeed only if environmental, social, and economic alternatives are in place [43, 487]. Although widespread P scarcity has not yet been reached, it is not a matter of if, but when. By critically reassessing the current linear P economy and significantly increasing P recycling rates, it is possible to establish a sustainable and resilient P value chain [45, 450].

8.2 Industrial application of polyP-rich yeast extract or pure bio-polyP

S. cerevisiae can support a circular P economy through the production of pure bio-polyP, polyP-rich yeast extract, or yeast containing polyP. Although bio-polyP has potential for diverse industrial applications due to its physicochemical properties, polyP-rich yeast extract may

represent the most suitable candidate for initial market introduction of polyP products derived from *S. cerevisiae* [128]. An important consideration is the legal status of pure bio-polyP and the polyP-rich yeast extract. Added polyPs are classified as food additives under the codes E450 (diphosphates), E451 (triphosphates), and E452 (polyphosphates) [130]. Their use is strictly regulated, and they must be declared on the ingredient list. In contrast, yeast extract is considered a natural food ingredient rather than a single-component flavor enhancer [488]. Hence, no E-number is assigned, allowing it to be used in food applications without special labeling requirements.

Yeast extract is defined as the water-soluble extract obtained from yeasts, such as baker's yeast or brewer's yeast, following cell membrane disruption [327]. It offers a broad flavor profile, often described as meaty, umami, and salty. The primary flavoring components in yeast extract are nucleotides, amino acids, and peptides [327, 489, 490]. Only nucleotides, hydrolyzed proteins, and monosodium glutamate are more relevant natural food-flavoring ingredients in the food industry [327]. Regarding the use of pure bio-polyP from *S. cerevisiae*, no distinction is made between polyPs produced chemically and those produced biotechnologically in the regulation of food additives [491]. Therefore, the addition of bio-polyPs necessitates explicit labeling on food products. Additionally, the safety of biotechnologically produced polyP for human and animal consumption must be confirmed for both food and feed applications [491]. This process may involve additional time-consuming and expensive inspection procedures by regulatory food authorities [128, 327]. Naturally enriched polyP in yeast extract (e.g., through fermentation) can be regarded as a process-related property. Therefore, if no synthetic polyP additives are used, labeling as food additive may not be required. However, the polyP hyperaccumulation process results in a significant increase in P_i/polyP levels in yeast extract. Conventionally produced yeast extract contains almost no polyP [1]. Hence, polyP-rich yeast extract would probably still need to be labeled as "natural yeast extract with increased phosphate content" or "natural yeast extract (rich in phosphates)". This is appealing to consumers who prefer foods with fewer E-numbers. Chemical polyP is not primarily used in food applications for nutritional or flavor purposes, but rather to perform various technological functions, such as water retention or texture enhancement [45, 49]. For the regulatory classification of polyP-rich yeast extract, the key question is how the purpose of increasing the yeast's natural polyP content through bioprocess development is interpreted. If regulatory authorities regard the technological function as predominant, the polyP in the yeast extracts may be considered a food additive, which would require appropriate classification and labeling [488, 491]. No legally binding classification has yet been established. However, this may be crucial to the economic future of this product. Regardless of whether polyPs are incorporated into a food product as part of another approved food additive or a non-additive

ingredient (such as yeast extract), the maximum permitted levels for polyPs in food applications remain applicable [491]. This is especially relevant, since the European Food Safety Authority (EFSA) has established an acceptable daily intake (ADI) of 40 mg P per kilogram of body weight per day for healthy adults. This limit accounts for the intake of naturally occurring P_i in food or added as a food additive [130]. However, the ADI does not apply to individuals with moderate-to-severe renal impairment, since excess P_i is usually excreted by the kidneys [130]. P_i has low acute oral toxicity and shows no genotoxic or carcinogenic effects. Moreover, developmental toxicity studies report no adverse outcomes. Toxicity from high P_i doses is limited to kidney calcification and tubular nephropathy, while epidemiological data show no consistent link to cardiovascular events [130, 492]. The ADI of 40 mg P/kg body weight/day is well below levels causing clinical effects. Given the health risks for people with impaired kidney function (~10 % of the population) and the potential for ADI exceedance in infants and children, transparent labeling, e.g., "natural yeast extract with increased phosphate content", is recommended [130, 492, 493]. Concealing P_i content in yeast extract could mislead consumers.

However, using polyP from *S. cerevisiae* demands further advancements in DSP and significant investment to develop a scalable, sequential purification process [45, 128]. Current methods for producing polyP-rich yeast extract and pure bio-polyP are harsh, such as evaporation at 80 °C, which can reduce the polyP chain length [1]. This is demonstrated by a decrease in the average polyP chain length from yeast extract paste (10.8 P_i-subunits) to yeast extract powder (3.1 P_i-subunits). Bio-polyP currently has an average chain length of around 20 P_i-subunits, comparable to chemically produced Budit 4 [1, 102, 128]. However, bio-polyP must compete directly with chemically produced polyP, which remains more cost-effective at equivalent chain lengths. Although polyP-rich yeast extracts have shorter chain lengths than pure bio-polyP, the presence of polyP introduces new properties to the yeast extract. Short-chain polyP is also in demand by the industry, for example, as a meat preservative [239]. Moreover, the average chain length does not reflect the full distribution, which includes both shorter and longer polyP chains [102]. Nevertheless, strains with enhanced polyP accumulation and longer chain lengths are particularly interesting for the production of polyP-rich yeast extract and pure bio-polyP. The ability to produce longer polyP chains than the typical chemical limit of 40 P_i-subunits, as demonstrated to be possible by selected industrial strains (Chapter 5), could offer a competitive advantage for market entry of bio-polyP. Another advantage of polyP-rich yeast extract is the possibility to produce it from non-fossil, food-grade P_i recovered from side streams. This yeast extract has been successfully applied in food processing and performs comparably to conventional stabilizers and taste enhancers [103]. The required process can be easily adopted by yeast extract manufacturers with minimal investment, as existing downstream workflows and market

knowledge are already in place [45, 289, 327]. Moreover, variations in cell disruption methods (mechanical, autolysis, organic solvents, etc.), process conditions, and yeast strains enable customization of the yeast extract for specific applications [327].

Yeast extract has gained global significance due to its unique nutritional and biochemical properties, as well as the readily available raw materials. Industrial production mainly uses brewer's and baker's yeast as raw materials [327]. For every 1,000 tons of beer produced, 15-20 tons of raw yeast material are generated [327, 494]. However, brewer's yeasts are typically recycled between batches and undergo strong industry-specific selection for traits such as stress tolerance (e.g., ethanol resistance and nutrient starvation) and efficient sugar utilization. Consequently, these yeasts often exhibit genome degradation, aneuploidy, and loss of a functional sexual cycle [290]. It remains to be tested whether these yeasts can be applied in the polyP hyperaccumulation protocol. This thesis confirmed that industrial yeast can generally be used in the hyperaccumulation protocol without major adaptations (see Chapter 5). Although a higher price can be justified for polyP-rich yeast extract due to added properties via polyP, it should be noted that most yeast extract is still used in low-value applications, such as animal feed or as a growth medium in microbial fermentations [327, 495-497]. The application of yeast extracts as animal feed is related to their balanced nutritional profile, which contains high levels of proteins, vitamin B, and polysaccharides (glucan, mannan, chitin) [327, 497-499]. Moreover, yeast extract functions as both an immunomodulator and a protein supplement in animal feed. It shows promise as a replacement for spray-dried animal plasma (SDAP), which poses potential biosecurity risks and is costly [500, 501]. Positive immune responses have been documented in poultry and various fish species [502, 503].

Although limited, the applications of yeast extract in high-value sectors, such as medicine and cosmetics, are progressing [327]. In cosmetics, yeast extract with its rich nutritional profile can be used for skin moisturization, wound healing, and cell renewal [504-506]. Moreover, yeast extract has antioxidant properties [504]. Hence, yeast extract is used in sun protection and exfoliants, often in combination with other active ingredients [327, 504]. Additionally, yeast extract and its bioactive peptides show potential in the medical and healthcare sectors due to their antioxidant and antibacterial properties [507, 508]. Yeast β-glucan is valued for its health benefits and has been used in the pharmaceutical industry as an immune enhancer with antiviral, antibacterial, and adjuvant properties. Due to increasing interest in β-glucans, the focus has shifted to *S. cerevisiae* as a production host. This relates to economic advantages over cereals or fungi [509]. Other applications, such as soil conditioning and plant growth regulation [510], highlight the broad versatility of yeast extract and its relevance across various fields. However, the application of yeast extracts also has some disadvantages. This includes their high nucleic acid content, typically 6-

15 %, which is significantly higher than in meat products [490]. High purine consumption from nucleic acids can elevate blood uric acid levels and increase the risk of hyperuricemia and gout [490, 511-513]. The FAO/WHO/UNICEF Protein Advisory Group recommends that the additional intake of dietary nucleic acids from single-cell protein-rich novel foods should not exceed 2 grams per day [514]. Approaches for reducing or removing nucleic acids are available but require further development and research by yeast extract manufacturers [513, 515]. Additionally, some consumers complain about the bitter taste component of yeast extract [516]. This taste profile is characteristic of waste brewer's yeast and is commonly associated with beer brewing, particularly with the bitter compounds derived from hops [517, 518]. Similarly, the odor of yeast extract can be repellent and undesirable to some consumers [519].

However, yeast extract is a nutritious, high-quality natural ingredient, classified as GRAS, and widely used in various food applications [45, 490, 520, 521]. As wealth and living standards improve, consumer demand for safe, flavorful, and nutritious food continues to rise, which is expected to drive the growth in the global yeast market [327]. This creates an opportunity to introduce polyP-rich yeast extract to the market, a product that retains the qualities of conventional yeast extract while offering additional, previously unavailable properties. Hence, it opens new possibilities for yeast extract manufacturers and the broader industrial sector. Even if production processes are not yet fully optimized, polyP-rich yeast extract could serve as a gateway for biotechnologically produced polyP from *S. cerevisiae*, helping to establish its role in a circular P_i economy.

8.3 Concluding remarks and outlook

This thesis contributes to the adaptation of the polyP hyperaccumulation process using *S. cerevisiae* for industrial applications, thereby promoting more sustainable P management. Moreover, it aims to elucidate the mechanisms underlying polyP accumulation in baker's yeast to enable efficient metabolic engineering, identify new production strains with enhanced polyP content and chain length, and define minimal media requirements to enable high-level polyP accumulation from P_i-rich waste streams. Media development revealed that zinc and inositol have a positive effect on final polyP levels. Zinc enhanced the starvation response in *S. cerevisiae*, while the mode of action of inositol remained unclear, presenting new opportunities for reaction and strain engineering. High-throughput screening of the VH Research Institute's industrial strain collection identified several candidates with improved polyP production properties. These strains were preliminarily characterized for their growth rate and ploidy. The analysis of minimal medium

requirements enabled a substantial reduction of all medium components, which is crucial for using waste streams and enhancing the economic efficiency of polyP hyperaccumulation in *S. cerevisiae.*

Although the results of this thesis are promising for (pre-)industrial applications, several challenges lie ahead before commercialization can be enabled. Regarding inositol and zinc as beneficial factors for polyP accumulation, further research is needed to pinpoint their role during the starvation phase of *S. cerevisiae*. Transcriptomic analyses should be conducted during both starvation and feeding phases to assess the yeast's response in media with and without zinc, inositol, or their combination. The promising strains from the VH-collection require additional characterization regarding genome rearrangements, ploidy, and carbon utilization. Sequencing their genomes will enable the introduction of beneficial mutations via genome engineering to further enhance polyP production. Due to the polyploid nature of the strains, the CRISPR/Cas9 method currently used for targeted genome engineering must be adapted. Additionally, the minimal media composition needs further optimization to achieve maximum polyP production with promising strains when integrating waste streams into the hyperaccumulation protocol. Several P_i-rich waste streams could be incorporated into the polyP hyperaccumulation protocol. This includes waste from activated nucleotide sugar and human milk oligosaccharide production [522], cleaning-in-place wastewater [103], municipal wastewater sludge [19], and slaughterhouse waste [523]. However, in addition to P_i content and availability, other critical factors must be assessed to determine a waste stream's suitability for industrial-scale applications. These include the volume of waste stream supply, its classification as food-grade or non-food-grade, fluctuations in nutrient composition, and the presence of inhibitory compounds, heavy metals, or pharmaceutical residues. Furthermore, it is critical to investigate whether the waste stream affects the purity and safety of the resulting bio-polyP or polyP-rich yeast extract [45, 524]. Utilizing a consistent, food-grade waste stream would significantly enhance the economic and ecological aspects of polyP hyperaccumulation with *S. cerevisiae*. In this context, it is crucial to clearly define the target markets for polyP-rich yeast extract and pure bio-polyP.

Broadening polyP's use across industries could demonstrate its functional potential. One potential approach is to explore polyP in enzyme cascades for ATP regeneration while recycling P_i-rich waste streams via the hyperaccumulation protocol [64]. PolyP-rich yeast or pure bio-polyP are also promising as slow-release P_i fertilizers for agriculture [49, 525]. Given yeast's metal tolerance, it could extract P_i from municipal wastewater under strict regulations, and the resulting polyP-rich biomass can be applied as fertilizer [45, 356]. The cosmetics industry offers additional market opportunities for biotechnological polyP. Various phosphoric acid derivatives and salts are used as buffering agents, chelating agents, and pH adjusters [526]. For the successful market entry of biotechnological polyP, the focus should be on high-margin applications or leveraging

S. cerevisiae's potential to extract P_i from waste streams. Depending on the target application of polyP-rich products, combining both processes is ideal but challenging.

A significant hindrance for industrial applications is the tripartite batch protocol. Despite being scalable [1], this workflow is inefficient due to low biomass yield, high byproduct formation, poor control, biomass loss, and long setup times [303-305, 322]. Hence, a large-scale one-pot fed-batch cultivation, which is standard in the yeast industry, must be established. This requires detailed characterization of the production strain's stoichiometry for key elements in biomass and polyP synthesis. Knowledge from process-guided strain engineering should be applied to strains with enhanced polyP production properties, such as higher titer and longer chain length, to increase the polyP content in *S. cerevisiae* biomass. It is essential to note that in the EU, products derived from GMOs are legally prohibited in specific applications [45, 481, 482]. Beyond regulatory restrictions, public acceptance of GMOs remains low due to concerns about potential health and environmental risks [527]. The legalization of GMOs remains a contentious issue that is discussed from scientific, ethical, and societal perspectives. A provisional agreement by the European Parliament and the EU Council addresses a regulation for plants developed with new genomic techniques. This includes methods such as CRISPR/Cas9, which can induce changes that could also arise naturally or via conventional breeding [528]. The agreement will need to be ratified by the Council and Parliament before formal adoption. However, it has already drawn criticism from consumer protection organizations and agricultural associations. Besides that, alternative approaches exist to improve yeast polyP production without the use of GMOs. These approaches include inducing beneficial mutations through chemical or physical mutagenesis, classical yeast crossbreeding, or adaptive laboratory evolution [529-532]. These methods avoid legal and public acceptance hurdles [482, 533]. In addition to the regulatory status of the production organism, the DSP of bio-polyP must be critically assessed. Current methods often lack scalability, are economically or environmentally unsustainable, or degrade polyP chain length, limiting their industrial viability [43, 128, 158]. Therefore, a scalable, stepwise purification strategy must be developed. Given the early stage of bio-polyP production and the availability of various production routes and substrates, conducting a life-cycle assessment (LCA) and a techno-economic analysis (TEA) is essential to guide sustainable and cost-effective process development. The LCA examines all in- and outputs, as well as environmental impacts of a product system across its entire life cycle, from raw material extraction and production to distribution, use, and end-of-life (recycling or disposal) [534-536]. Hence, alternative synthesis routes are compared, and ecologically inefficient options are identified. Conducting an LCA is complex and data-intensive, requiring detailed information on material and energy flows, as well as substance-specific data. These data are often limited or difficult to obtain [536, 537]. A TEA evaluates the technical and

economic viability of a process [538]. It identifies critical process parameters affecting profitability, compares the financial impacts of varying process conditions, and highlights opportunities for technological optimization [538, 539]. For polyP production with *S. cerevisiae*, LCA and TEA enable assessment of the economic and environmental advantages of using different P_i-rich waste streams and producing different end products (pure bio-polyP, polyP-rich yeast extract, and polyP-rich yeast). The results of this thesis highlight baker's yeast as an essential contributor to the shift from linear to circular P management. P must ultimately be recognized and treated as the vital element it truly is. This is essential to prevent a P-limited collapse and sustain food security on Earth for future generations [3, 502]. Humanity has no alternative [3].

Appendix

A.1 Appendix for Chapter 3

Table A1: Two-way ANOVA table of the experiment on the polyP-responsibility of the fluorescent dye JC-D7.
The data shown in Figure 5 were statistically analyzed using a two-way ANOVA/Tukey post-hoc test; Significance level $\alpha = 0.05$. Data associated with this table were obtained from [236]. This table was originally designed by Claudia Keil, was previously published [227], and is reprinted with permission from Yeast, published by John Wiley & Sons Ltd.

	SumSq	Df	Mean Sq	F value	p-value
polyP chain length	138745129	11	12613194	24.7	$p < 0.001$
polyP quantity	543731468	7	77675924	151.9	$p < 0.001$
interaction	88003303	77	1142900	2.2	$p < 0.001$
residual	147278613	288	511384		

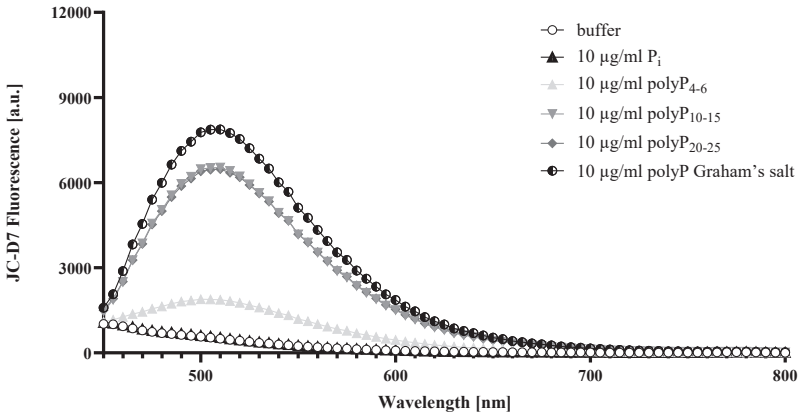


Figure A1: Fluorescence spectra of mono/polyP-treated JC-D7.
25 µM solutions of JC-D7 were treated with assay buffer or 10 µg/ml P_i or polyP solutions for 30 min followed by detection of JC-D7 fluorescence emission spectra ($\lambda_{ex} = 390$ nm). The values are the mean of three replicates. Data associated with this figure were obtained from [236]. The figure was originally designed by Claudia Keil, was previously published [227], and is reprinted with permission from Yeast, published by John Wiley & Sons Ltd.

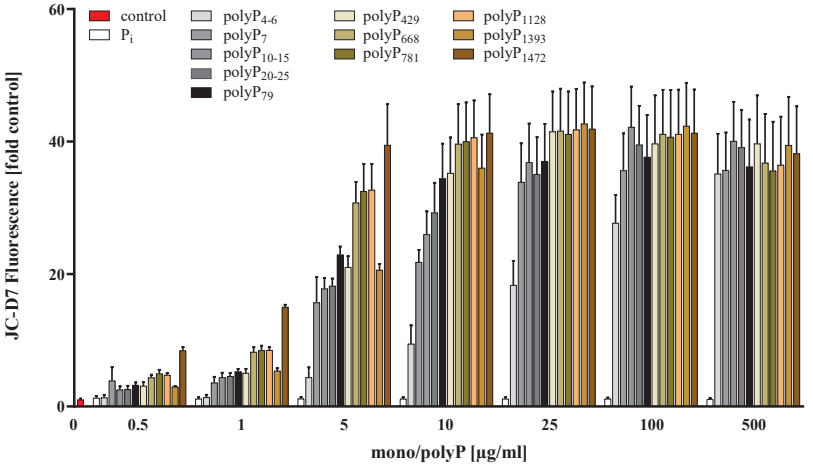


Figure A2: Normalized fluorescence intensity data of mono/polyP-treated JC-D7.
The diagram was generated from the data shown in Figure 5. The fluorescence intensity of JC-D7 in the presence of P_i or polyPs was compared with that of the dye in assay buffer (control). The values are the mean of three replicates. Data associated with this figure were obtained from [236]. The figure was originally designed by Claudia Keil, was previously published [227], and is reprinted with permission from Yeast, published by John Wiley & Sons Ltd.

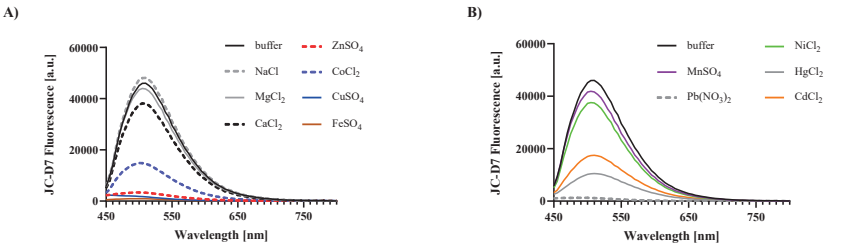


Figure A3: Fluorescence spectra of JC-D7 pretreated with polyP and inorganic metal salts.
10 µg/ml of polyP mix was pretreated with either assay buffer or metal salt solutions for 30 min, followed by detection of JC-D7 fluorescence emission spectra (25 µM JC-D7; λ_{ex} = 390 nm; λ_{em} = 450-700 nm). The values are the mean of three replicates. Data associated with this figure were obtained from [236]. This figure was originally designed by Claudia Keil and was previously published [227], and is reprinted with permission from Yeast, published by John Wiley & Sons Ltd.

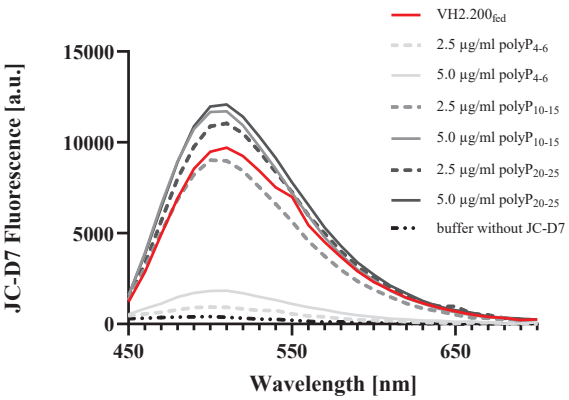


Figure A4: Application of the fluorescent dye JC-D7 to extracts of VH2.200.
PolyP standards and extracts from polyP-rich VH2.200 yeast cells ($VH2.200_{fed}$) were treated with 10 µM JC-D7 (temperature = 30 °C, time = 30 min) followed by detection of fluorescence emission spectra (λ_{ex} = 390 nm; λ_{em} = 450-700 nm; Agilent BioTek Synergy Mx). The values are the mean of two replicates. Data associated with this figure were obtained from [237]. This figure was originally designed by Claudia Keil, was previously published [227], and is reprinted with permission from Yeast, published by John Wiley & Sons Ltd.

Suppl. Information 1. Total polyP content in P_i units according to the methodology described by Christ and Blank (2018) [222] for the Budit 7 standard at a concentration of 0.5 µg/ml.

Lowest measured concentration of Budit 7 in JC-D7 assay = $0.5 \frac{\mu g}{ml}$

Concentration Budit 7 stock solution in total polyP assay (Christ and Blank (2018) [222]) = $1.2 \frac{mg}{ml}$

Total polyP of Budit 7 stock solution in total polyP assay (Christ and Blank (2018) [222]) = 9605 µM P_i

$$\text{Budit 7 concentration factor} \frac{\text{stock solution assay (Christ and Blank (2018)[222])}}{\text{lowest measured concentration JC-D7}} = \frac{1200 \frac{\mu g}{ml}}{0.5 \frac{\mu g}{ml}} = 2400$$

$$\text{Conversion of lowest measured Budit 7 concentration in JC-D7 assay into } P_i = \frac{9605\ \mu M\ P_i}{2400} = 4.0\ \mu M\ P_i$$

A.2 Appendix for Chapter 4

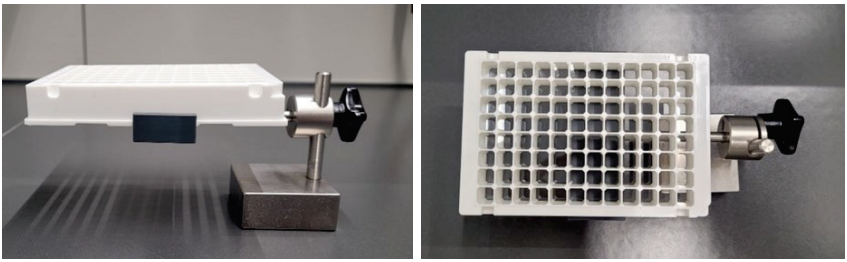


Figure A5: Holding device for sonication of 96-well MTPs applied for screening of the YKO collection and VH-strain collection.
This device was manufactured by the RWTH mechanical workshop (RWTH Aachen University, Aachen, Germany).

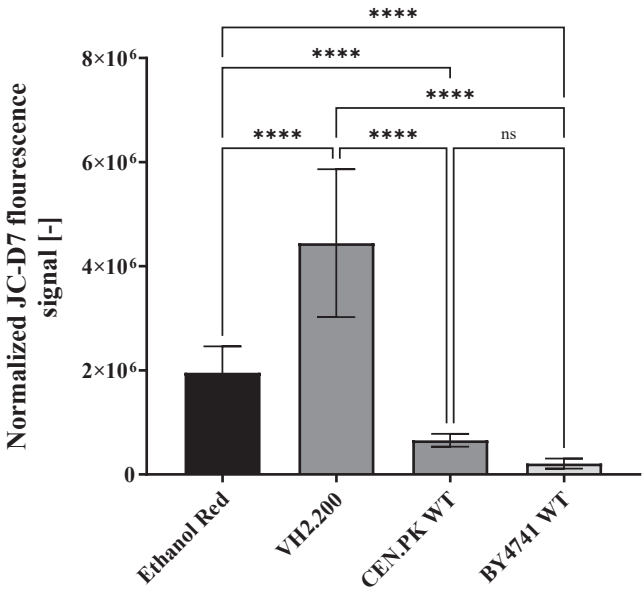


Figure A6: PolyP screening of yeast control strains Ethanol Red, VH2.200, CEN.PK WT and BY4741 WT in the non-adapted protocol via JC-D7.
Strains were cultivated according to the YKO hyperaccumulation protocol, and polyP was measured using JC-D7. The results are normalized to the OD_{600} value of the respective strain and represent the mean of twenty-two replicates + SD. Significant differences marked by asterisks (*p < 0.05, **p < 0.01, ***p < 0.001, ****p < 0.0001; One-Way ANOVA).

Table A2: Hypoaccumulating deletions with an OD_{600}-corrected JC-D7 signal of 0.5x in the YKO collection.

Strains were cultivated according to the YKO hyperaccumulation protocol, and polyP was measured using JC-D7. The results were analyzed according to Chapter 2.3 and compared to the median across all cultures in a single 96-well MTP. The data represent the result of a single measurement.

Number	Strain	Number	Strain	Number	Strain	Number	Strain
1	YAL007C	**21**	YNL198C	**41**	YGL129C	**61**	YKR088C
2	YAR023C	**22**	YKR032W	**42**	YGL158W	**62**	YKR101W
3	YAR027W	**23**	YGR210C	**43**	YER120W	**63**	YKR103W
4	YLL019C	**24**	YPR077C	**44**	YER163C	**64**	YJR124C
5	YLR061W	**25**	YPR099C	**45**	YER164W	**65**	YDL218W
6	YMR252C	**26**	YJL120W	**46**	YER169W	**66**	YDR009W
7	YNL269W	**27**	YJL108C	**47**	YER170W	**67**	YOR325W
8	YNL268W	**28**	YJL092W	**48**	YJL012C	**68**	YNR007C
9	YPL177C	**29**	YHR004C	**49**	YER032W		
10	YPL176C	**30**	YHR009C	**50**	YER035W		
11	YBR200W	**31**	YHR025W	**51**	YER050C		
12	YBR215W	**32**	YHR194W	**52**	YER061C		
13	YBR217W	**33**	YLL007C	**53**	YER073W		
14	YBR226C	**34**	YNL274C	**54**	YHR147C		
15	YBR227C	**35**	YOL141W	**55**	YKL184W		
16	YEL067C	**36**	YJR078W	**56**	YLR290C		
17	YER007C-A	**37**	YJR079W	**57**	YBL007C		
18	YER007W	**38**	YJR088C	**58**	YGL054C		
19	YER010C	**39**	YJR111C	**59**	YJR130C		
20	YER011W	**40**	YJR115W	**60**	YJR152W		

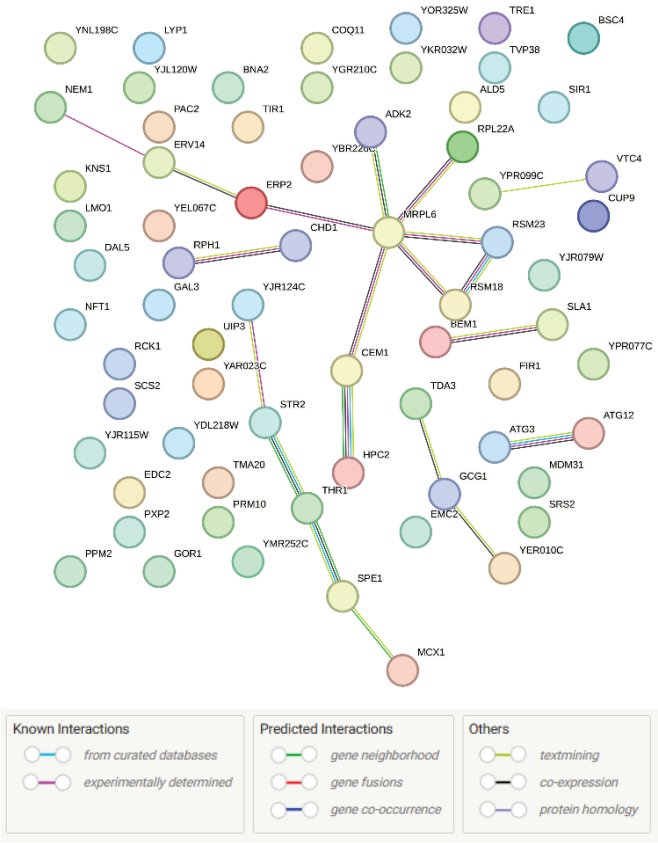


Figure A7: Protein interaction network of hypoaccumulating deletions with an OD_{600}-corrected JC-D7 signal of 0.5x in the YKO collection.
Strains were cultivated according to the YKO hyperaccumulation protocol, and polyP was measured using JC-D7. The results were analyzed according to Chapter 2.3 and compared to the median across all cultures in a single 96-well MTP. The data represent the result of a single measurement. This network was generated via STRING [228].

Table A3: Hyperaccumulating deletions with an OD_{600}-corrected JC-D7 signal of 2.0x in the YKO collection.

Strains were cultivated according to the YKO hyperaccumulation protocol, and polyP was measured using JC-D7. The results were analyzed according to Chapter 2.3 and compared to the median across all cultures in a single 96-well MTP. The data represent the result of a single measurement.

Number	Strain	Number	Strain	Number	Strain	Number	Strain
1	YLR119W	**27**	YDR372C	**53**	YOR126C	**79**	YHR064C
2	YLR120C	**28**	YDR393W	**54**	YOR139C	**80**	YPL132W
3	YLR121C	**29**	YDR420W	**55**	YOR140W	**81**	YML097C
4	YML058C-A	**30**	YER017C	**56**	YLR375W	**82**	YMR120C
5	YML035C	**31**	YHR050W	**57**	YLR377C	**83**	YLR437C
6	YML018C	**32**	YHR075C	**58**	YLR390W	**84**	YLR460C
7	YML005W	**33**	YHR126C	**59**	YLR392C	**85**	YML021C
8	YMR020W	**34**	YCL001W	**60**	YLR395C	**86**	YNR051C
9	YOR008C	**35**	YCR021C	**61**	YLR407W	**87**	YNL035C
10	YOR323C	**36**	YLR128W	**62**	YLR232W	**88**	YNR013C
11	YOL023W	**37**	YLR154C	**63**	YLR233C	**89**	YIL138C
12	YOL025W	**38**	YLR201C	**64**	YLR254C	**90**	YNL105W
13	YOL027C	**39**	YLR203C	**65**	YLR266C	**91**	YGR050C
14	YOL039W	**40**	YKL008C	**66**	YGL252C	**92**	YGR063C
15	YOL044W	**41**	YKL031W	**67**	YPL084W	**93**	YBR148W
16	YOL045W	**42**	YKL067W	**68**	YPL033C	**94**	YBR165W
17	YOL051W	**43**	YKL091C	**69**	YGL024W	**95**	YDL038C
18	YOL061W	**44**	YKL167C	**70**	YNL241C	**96**	YDL061C
19	YPL270W	**45**	YKL170W	**71**	YNL230C	**97**	YDL090C
20	YPL196W	**46**	YKL185W	**72**	YNL227C	**98**	YDR440W
21	YPL179W	**47**	YGR033C	**73**	YNL197C	**99**	YDR475C
22	YPL167C	**48**	YGR035C	**74**	YDR315C	**100**	YDL047W
23	YPL127C	**49**	YGR056W	**75**	YDR323C	**101**	YOR364W
24	YPL115C	**50**	YGR064W	**76**	YIL039W	**102**	YLL027W
25	YBR194W	**51**	YGR077C	**77**	YIL076W	**103**	YNL220W
26	YDR093W	**52**	YOR109W	**78**	YIL092W		

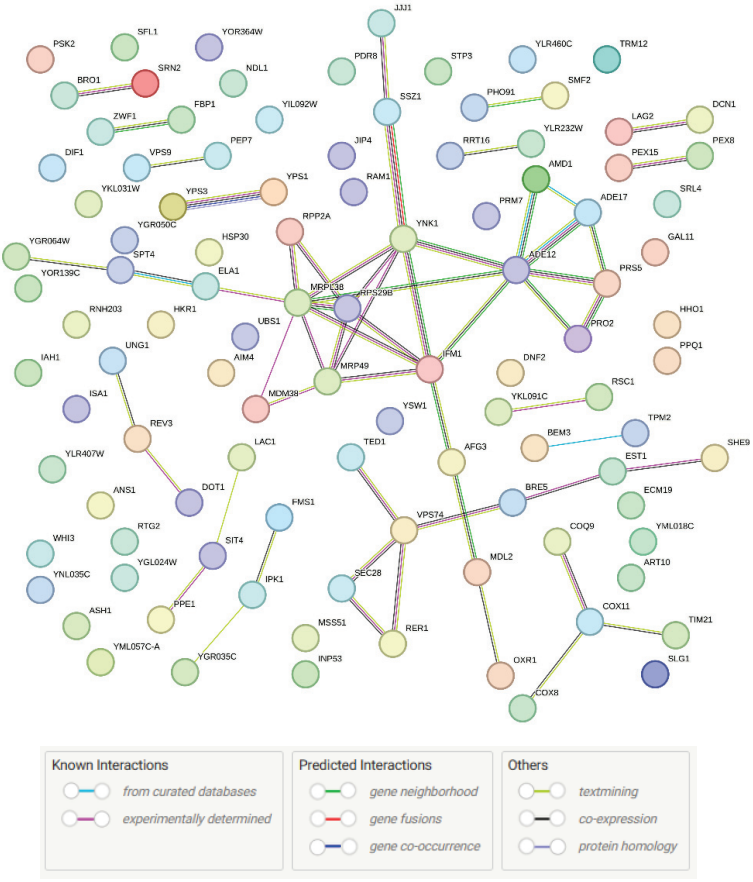


Figure A8: Protein interaction network of hyperaccumulating deletions with an OD_{600}-corrected JC-D7 signal of 2.0x in the YKO collection.
Strains were cultivated according to the YKO hyperaccumulation protocol, and polyP was measured using JC-D7. The results were analyzed according to Chapter 2.3 and compared to the median across all cultures in a single 96-well MTP. The data represent the result of a single measurement. This network was generated via STRING [228].

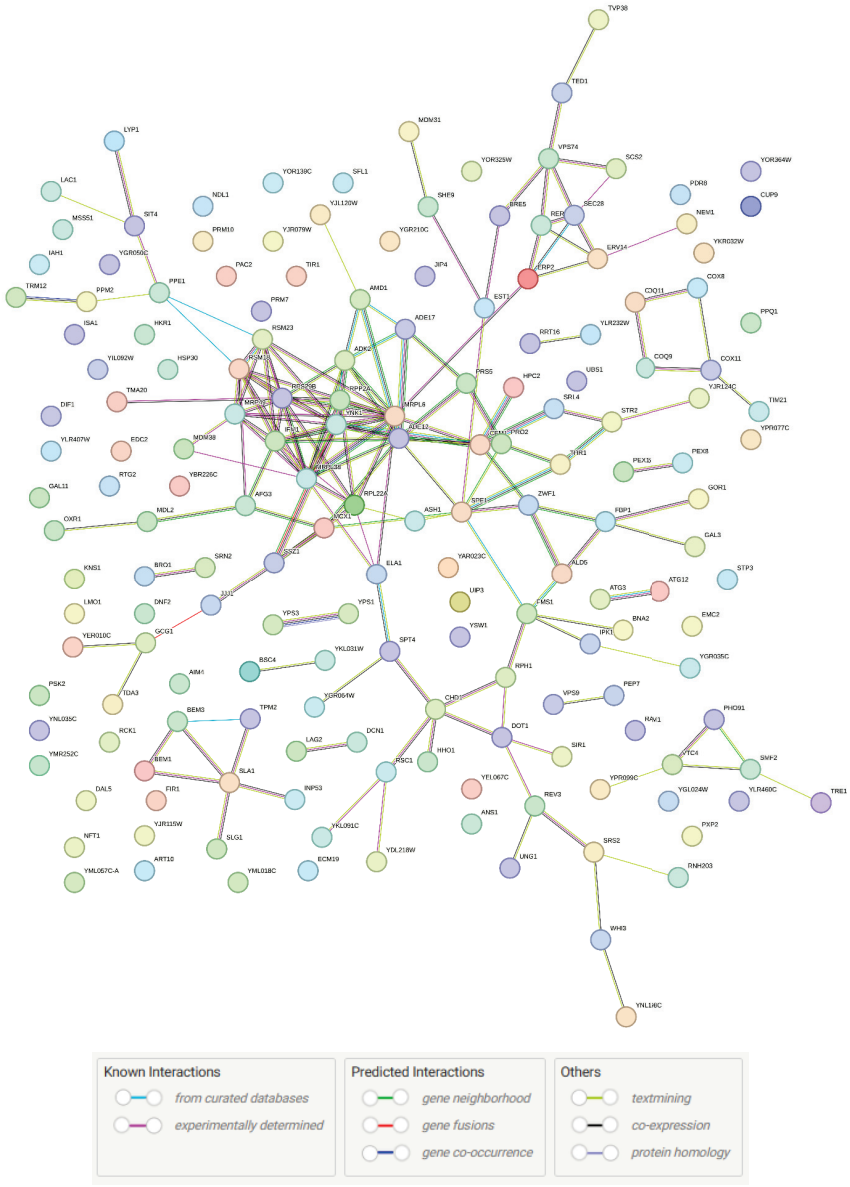


Figure A9: Protein interaction network of hypo- and hyperaccumulating deletions with an OD_{600}-corrected JC-D7 signal of 0.5x and 2.0x in the YKO collection.
Strains were cultivated according to the YKO hyperaccumulation protocol, and polyP was measured using JC-D7. The results were analyzed according to Chapter 2.3 and compared to the median across all cultures in a single 96-well MTP. The data represent the result of a single measurement. This network was generated via STRING [228].

Table A4: Functional clustering of hypo- and hyperaccumulating deletions with an OD_{600}-corrected JC-D7 signal of 0.5x and 2.0x in the YKO collection.
Strains were cultivated according to the YKO hyperaccumulation protocol, and polyP was measured using JC-D7. The results were analyzed according to Chapter 2.3 and compared to the median across all cultures in a single 96-well MTP. The data represent the result of a single measurement. This network was generated via STRING [228].

Clusters

color	cluster Id	gene count	description
	Cluster 1	28	Mitochondrial translation
	Cluster 2	15	Arginine and proline metabolism
	Cluster 3	10	Maintenance of location
	Cluster 4	9	Nucleosome organization
	Cluster 5	6	+ RHOV GTPase cycle
	Cluster 6	6	DNA repair
	Cluster 7	5	GCG1, JJJ1, SSZ1, TDA3, YER010C
	Cluster 8	5	ubiquinone-6 biosynthesis
	Cluster 9	5	PHO91, SMF2, TRE1, VTC4, YPR099C
	Cluster 10	4	Carbohydrate metabolism
	Cluster 11	2	+ Autophagy - other
	Cluster 12	2	+ Vacuole inheritance
	Cluster 13	2	Phosphatidylglycerol metabolism, and Yeast mitochondrial distribution and morpho...
	Cluster 14	2	ATP export
	Cluster 15	2	+ Aspartyl protease
	Cluster 16	2	Uncharacterized
	Cluster 17	2	BSC4, YKL031W
	Cluster 18	2	+ Regulation of ubiquitin-protein transferase activity
	Cluster 19	2	Peroxisome biogenesis
	Cluster 20	2	MDL2, OXR1

A.3 Appendix for Chapter 5

Table A5: Background information on the best-producing strains identified in the screening of the VH-strain collection.

Strain	Information	Strain	Information
VH2.102	Baker's yeast (1985)	**VH2.093**	Dry baker's yeast (1984)
VH2.079	Dry baker's yeast (1981)	**VH2.136**	Dry baker's yeast (-)
VH2.070	Distiller's yeast for sugarcane juice (1981)	**VH2.091**	Baker's yeast (1984)
VH2.109	Baker's yeast – strain also used for dry yeast (1985)	**VH2.073**	Dry baker's yeast (1980)
K1.005	Baker's yeast (1951)	**VH2.088**	Baker's yeast (1988)
VH2.072	Dry baker's yeast (1980)	**VH2.114**	Baker's yeast (1985)
K1.027	Baker's yeast (1962)	**VH2.081**	Baker's yeast (1982)
VH2.135	Baker's yeast (1988)	**VH2.124**	Baker's yeast (1987)
VH2.088	Baker's yeast (1988)	**VH2.133**	Dry baker's yeast (-)
VH2.073	Dry baker's yeast (1980)	**VH2.083**	Dry baker's yeast (-)
VH2.027	Distiller's yeast (1974)	**VH2.074**	No information (1980)
K1.021	Baker's yeast (1960)	**VH2.131**	Baker's yeast (1987)
K1.019	Baker's yeast (1958)	**VH2.064**	Osmotolerant baker's yeast (1980)
VH2.063	Dry baker's yeast (1980)	**VH2.109**	1985 Baker's yeast – strain also used for dry yeast (1985)
VH2.131	Baker's yeast (1987)	**VH2.076**	Baker's yeast (1981)
VH2.091	Baker's yeast (1984)	**VH2.098**	Dry baker's yeast (1984)
VH2.074	Baker's yeast (1980)	**VH2.080**	Baker's yeast (possibly osmotolerant (1981))
VH2.078	Baker's yeast (1981)	**VH2.084**	Dry baker's yeast (1982)
VH2.090	Dry baker's yeast (1983)		

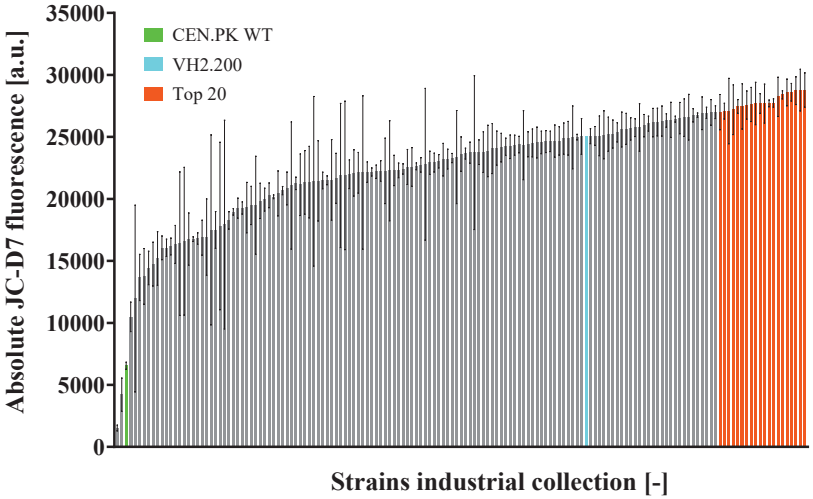


Figure A10: PolyP screening of the complete VH-strain collection in the non-adapted protocol for highest absolute polyP signal.
Strains were cultivated in triplicate in the non-adapted protocol in MTPs. PolyP levels were measured via JC-D7. CEN.PK WT depicted in green and VH2.200 in cyan. The results are represented as the mean of three replicates ± SEM. The results originate from the broad JC-D7 screening (Chapter 2.4).

Table A6: Cell size of best-producing strains in the VH-strain collection.
Cell size and cell number were measured via the Coulter Counter (Multisizer X) at the Chair of Biochemical Engineering (AVT.BioVT, RWTH Aachen University, Aachen, Germany).

Strain	Replicates	Cell size [µm]
VH2.200	7	6.56 ± 0.16
VH2.070	4	7.35 ± 0.15
VH2.072	4	6.54 ± 0.08
VH2.073	4	7.14 ± 0.19
VH2.079	4	5.97 ± 0.13
VH2.088	3	6.01 ± 0.09
VH2.093	2	6.87 ± 0.08
VH2.133	2	6.07 ± 0.07
VH2.136	2	4.60 ± 0.02
VH2.017	2	6.82 ± 0.07
VH2.129	2	5.53 ± 0.11
CEN.PK WT	2	4.77 ± 0.06

Table A7: Ranking the Top 20 highest absolute polyP-producing strains of the VH-strain collection in terms of their relative polyP production level.

Strain	Rank absolute polyP production	Rank relative polyP content
VH2.084	20	25
VH2.080	19	56
VH2.072	18	5
VH2.098	17	75
VH2.076	16	38
VH2.109	15	4
VH2.064	14	35
VH2.131	13	9
VH2.074	12	18
VH2.083	11	70
VH2.133	10	77
VH2.124	9	32
VH2.081	8	21
VH2.114	7	48
VH2.088	6	11
VH2.073	5	7
VH2.079	4	2
VH2.091	3	14
VH2.136	2	67
VH2.093	1	19

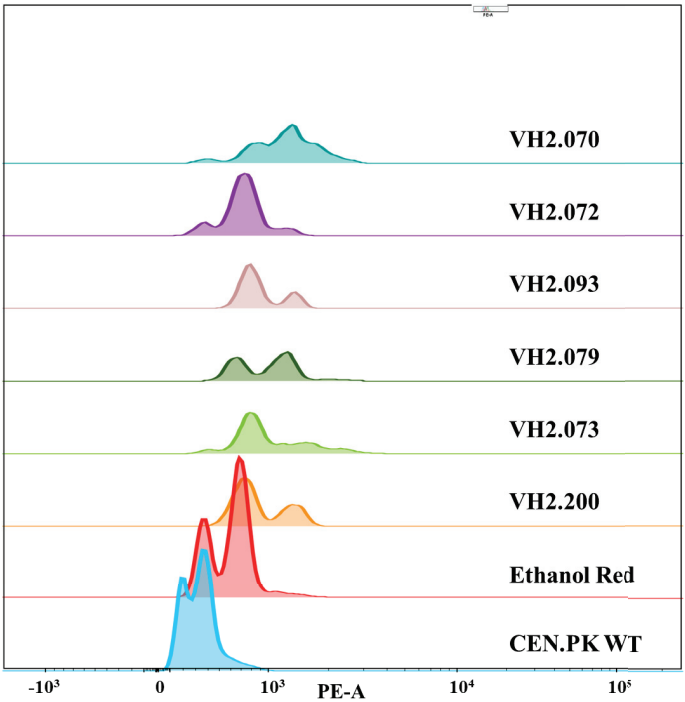


Figure A11: Analysis of yeast ploidy of the Top 5 highest relative polyP producing strains in the VH-strain collection using flow cytometry.
The ploidy was determined using the method described by Todd et al. [231]. The flow cytometry results were analyzed using FlowJo™ v10.8 Software (BD Biosciences, Franklin Lakes, NJ, USA).

A.4 Appendix for Chapter 6

Table A8: Concentration of vitamin stock solutions.
The table was previously published [329] and is reprinted with permission from Yeast, published by John Wiley & Sons Ltd.

Vitamin	Medium concentration [g/l]	Stock concentration [g/l]	Factor medium/ stock concentration	pH value
Biotin	$5.0 \cdot 10^{-5}$	0.2	4000	6.5
Nicotinic acid	$1.0 \cdot 10^{-3}$	1.0	1000	6.5
Calcium pantothenate	$1.0 \cdot 10^{-3}$	1.0	1000	6.5
p-Aminobenzoic acid	$2.0 \cdot 10^{-4}$	0.4	2000	6.5
Pyridoxine HCl	$1.0 \cdot 10^{-3}$	1.0	1000	6.5
Thiamine HCl	$1.0 \cdot 10^{-3}$	1.0	1000	6.5
myo-Inositol	$2.5 \cdot 10^{-2}$	25.0	1000	6.5

Table A9: Concentration of trace element stock solutions.
The table was previously published [329] and is reprinted with permission from Yeast, published by John Wiley & Sons Ltd.

Trace elements	Medium concentration [g/l]	Stock concentration [g/l]	Factor medium/ stock concentration	pH value
Na_2EDTA	$1.5 \cdot 10^{-2}$	1.50	100	4.0
$ZnSO_4 \cdot 7\ H_2O$	$4.5 \cdot 10^{-3}$	0.45	100	4.0
$MnCl_2 \cdot 2\ H_2O$	$1.0 \cdot 10^{-3}$	1.00	1000	4.0
$CoCl_2 \cdot 6\ H_2O$	$0.3 \cdot 10^{-3}$	0.30	1000	4.0
$CuSO_4 \cdot 5\ H_2O$	$0.3 \cdot 10^{-3}$	0.30	1000	4.0
$Na_2MoO_4 \cdot 2\ H_2O$	$0.4 \cdot 10^{-3}$	0.40	1000	4.0
KI	$0.1 \cdot 10^{-3}$	0.20	2000	4.0
$CaCl_2 \cdot 2\ H_2O$	$4.5 \cdot 10^{-3}$	0.45	100	4.0
$FeSO_4 \cdot 7\ H_2O$	$3.0 \cdot 10^{-3}$	0.30	100	4.0
H_3BO_3	$1.0 \cdot 10^{-3}$	0.20	200	4.0

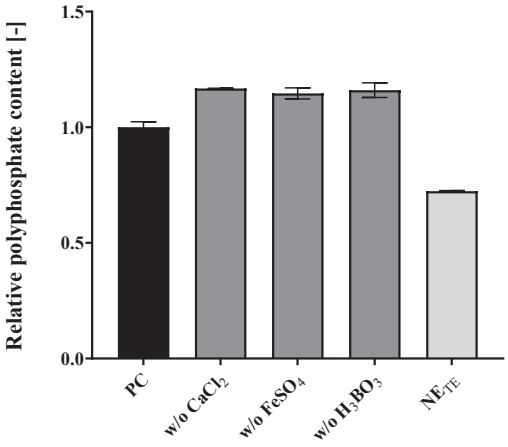


Figure A12: Influence of individual trace elements of Group 3 on polyP hyperaccumulation of VH2.200.
PC (all trace elements), w/o $CaCl_2$, w/o $FeSO_4$, w/o H_3BO_3, and NE_{TE} (w/o any trace elements). All cultivations were performed in duplicates (n = 2). Data are presented as means ± SEM. Data associated with this figure were obtained from [324]. Previously published [329], the figure is reprinted with permission from Yeast, John Wiley & Sons Ltd.

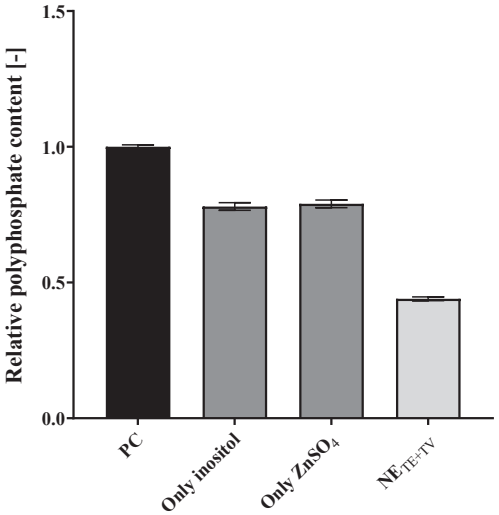


Figure A13: Effect of inositol and zinc on polyP hyperaccumulation of VH2.200.
PC (all vitamins + trace elements), only with inositol, only with $ZnSO_4$, and NE_{TE+TV} (w/o any trace elements and vitamins). All cultivations were performed in duplicate (n = 2). Data are presented as means ± SEM. Data associated with this figure were obtained from [324]. Previously published [329], the figure is reprinted with permission from Yeast, John Wiley & Sons Ltd.

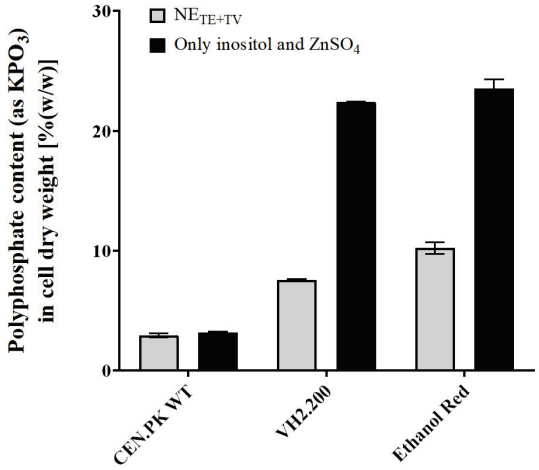


Figure A14: PolyP content of various yeast strains after TOM cultivation in starvation medium w/o any trace elements and vitamins (NE_{TE+TV}) or only with inositol and $ZnSO_4$.
S. cerevisiae CEN.PK WT (125 mg/l inositol, 12.6 mg/l $ZnSO_4$), VH2.200 (25 mg/l inositol, 2.5 mg/l $ZnSO_4$), and Ethanol Red (25 mg/l inositol, 12.6 mg/l $ZnSO_4$). All cultivations were performed in duplicates (n = 2). Values are presented as means ± SEM. Data associated with this figure were obtained from [325]. Previously published [329], the figure is reprinted with permission from Yeast, John Wiley & Sons Ltd.

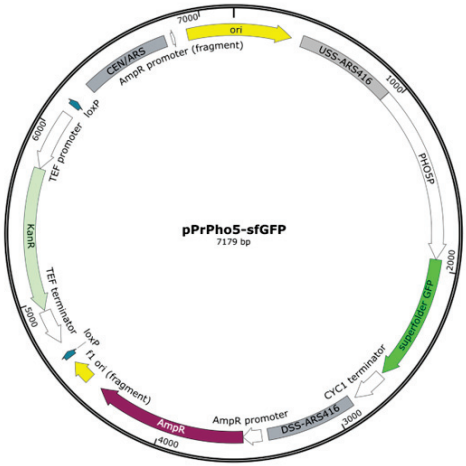


Figure A15: Plasmid map of pPr_{Pho5}-sfGFP to assay PHO pathway activation.
Centromeric plasmid carrying G418 resistance in CEN.PK113-7D. Previously published [329], the figure is reprinted with permission from Yeast, John Wiley & Sons Ltd.

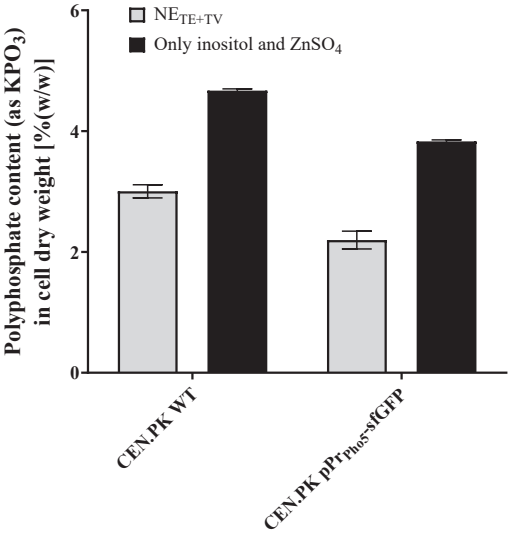


Figure A16: PolyP content of CEN.PK WT and CEN.PK pPr_{Pho5}-sfGFP after BioLector cultivation. Starvation medium w/o any trace elements and vitamins (NE_{TE+TV}) or only with inositol and $ZnSO_4$. All cultivations were performed in duplicates (n = 2). Data are presented as means ± SEM. Data associated with this figure were obtained from [325]. Previously published [329], the figure is reprinted with permission from Yeast, John Wiley & Sons Ltd.

A.5 Appendix for Chapter 7

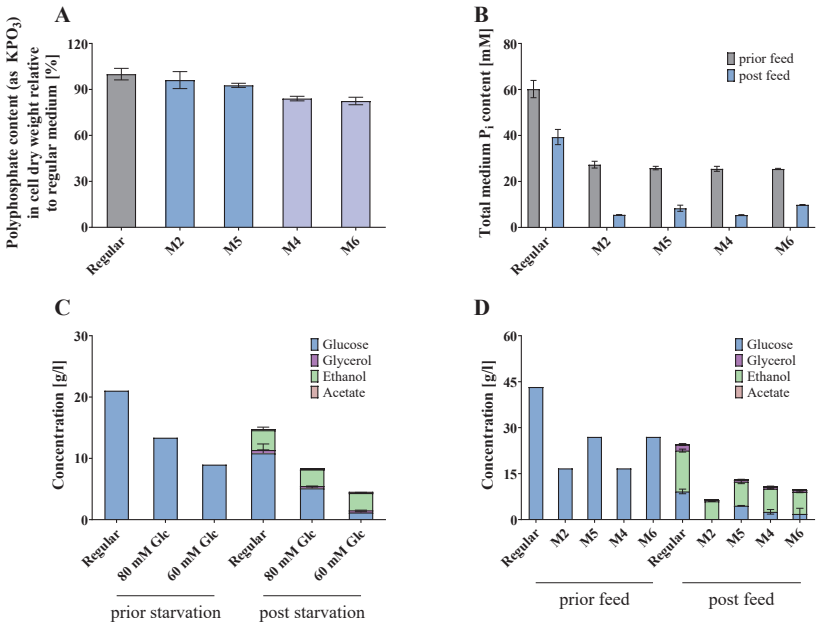


Figure A17: Evaluation of the impact of reduced starvation media and adapted glucose levels in the feed medium on polyP production with VH2.200.
Cultivation and medium preparation according to sections 2.1.2 and 2.1.3. The medium components were individually varied and compared to the original starvation and feed medium developed by Christ and Blank (2019) [1]. The regular medium (133 mM glucose, 10 mM $(NH_4)_2SO_4$, 13.3 mM KCl, 4 mM $CaCl_2$, and 12.5 mM Na_2succinate, supplemented with Verduyn vitamins and trace elements) was compared to the modified starvation media M2/M5 (80 mM glucose, 10 mM $(NH_4)_2SO_4$, 4.5 mM KCl, 1 mM $CaCl_2$, and 8 mM Na_2succinate) and M4/M6 (60 mM instead of 80 mM glucose). Modified minimal media were supplemented with inositol (25 mg/l) and zinc (2.5 mg/l). Additionally, three different media were investigated during the feeding process. The regular feed medium (250 mM glucose, 60 mM P_i) was compared to the feeding media with 25 mM P_i and 100 mM glucose (M2/M4) or 160 mM glucose (M5/M6). (A) PolyP content at the end of the hyperaccumulation protocol; (B) P_i content in cultivation broth at the end of the hyperaccumulation protocol; (C) Results of HPLC analysis before and after the starvation phase of the hyperaccumulation protocol; (D) Results of HPLC analysis before and after the feeding phase of the hyperaccumulation protocol. The data are shown in a stacked format. Cultivations were performed in MTPs to generate enough cell mass for enzymatic polyP quantification. The results represent the mean of two replicates ± SEM (n = 2). Data associated with this figure were obtained from [353].

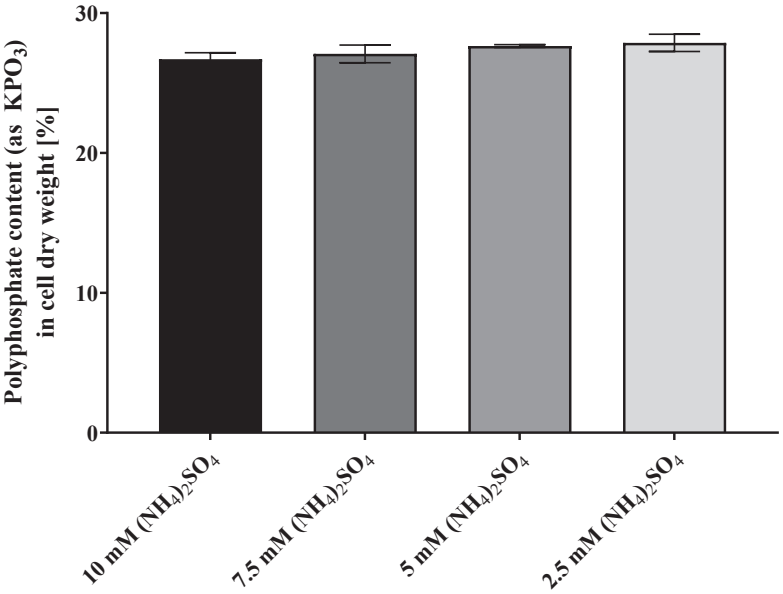


Figure A18: Evaluating the impact of $(NH_4)_2SO_4$ in the starvation medium on polyP production with VH2.200.

Cultivation and medium preparation according to sections 2.1.2 and 2.1.3. The ammonium concentration was individually varied, while all other concentrations were based on those reported by Christ and Blank (2019) [1]. The feed medium was prepared according to Christ and Blank (2019) [1]. Cultivation was performed in MTPs to generate enough cell mass for enzymatic polyP quantification. The results represent the mean of two replicates ± SEM (n = 2).

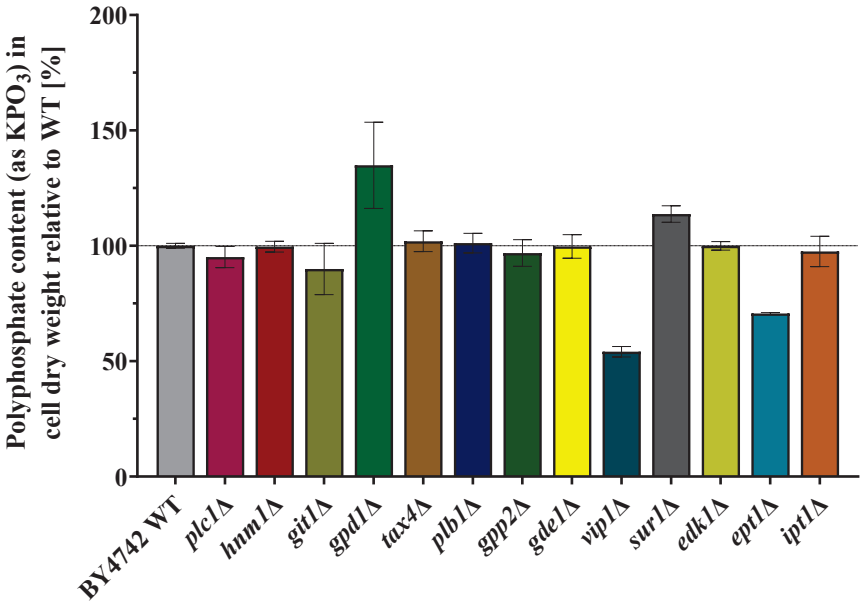


Figure A19: Investigating the effect of additional phospholipid metabolism-associated genes on polyP accumulation in BY4742 deletion mutants.
BY4742 WT and corresponding mutants were cultivated following the standard operating procedure for generating polyP-rich cells (sections 2.1.2 and 2.1.3). The starvation medium was supplemented with zinc (2.5 mg/l), inositol (25 mg/l), and amino acids [225] instead of the full set of TE and TV. PolyP production was evaluated relative to BY4742 WT. Error bars represent the SEM from three (*hnm1*Δ, *git1*Δ, *plb1*Δ, *gpp2*Δ, *sur1*Δ, and *ept1*Δ) or five (BY4742 WT, *plc1*Δ, *gpd1*Δ, *tax4*Δ, *gde1*Δ, *vip1*Δ, and *ipt1*Δ) biological replicates. Data associated with this figure were obtained from [353].

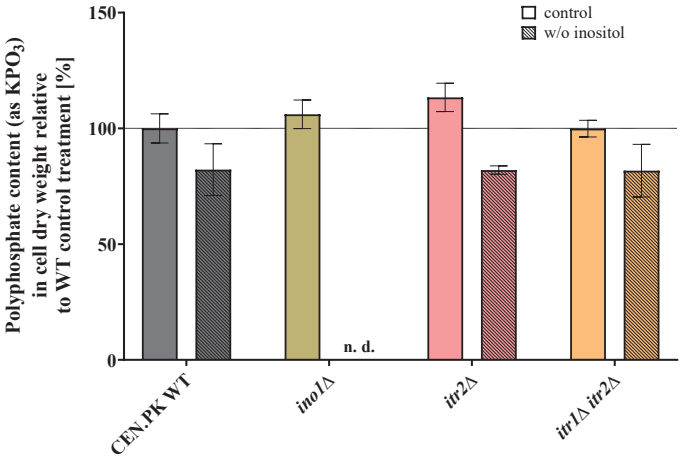


Figure A20: Investigating the effect of *ino1*Δ, *itr2*Δ, and *itr1*Δ*itr2*Δ on polyP accumulation in CEN.PK deletion mutants.
CEN.PK WT and corresponding mutants were cultivated following the standard operating procedure for generating polyP-rich cells (sections 2.1.2 and 2.1.3). The control was supplemented with both zinc (2.5 mg/l) and inositol (25 mg/l), whereas the w/o inositol medium contained only zinc (2.5 mg/l). CEN.PK *ino1*Δ, *itr2*Δ, and *itr1*Δ*itr2*Δ were evaluated for the influence of inositol. Data from two biological replicates is displayed, with error bars representing standard error. "n.d." denotes non-detectable polyP levels, despite successful cultivation in the indicated medium. The results represent the mean of two replicates ± SEM (n = 2). Data associated with this figure were obtained from [353].

Table A10: *S. cerevisiae* strains used to test the influence of inositol on polyP production.

Strains	Genotype	Origin	Abbreviation
CEN.PK113-7D	WT (MATa)	Peter Kötter; Goethe Universität Frankfurt, Germany	CEN.PK WT
CEN.PK113-7D	*pah1*Δ	Makarius Baier; RWTH Aachen University, Germany	*pah1*Δ
CEN.PK113-7D	*itr1*Δ	Makarius Baier; RWTH Aachen University, Germany	*itr1*Δ
CEN.PK113-7D	*ino1*Δ	Makarius Baier; RWTH Aachen University, Germany	*ino1*Δ
CEN.PK113-7D	*itr2*Δ	Makarius Baier; RWTH Aachen University, Germany	*itr2*Δ
CEN.PK113-7D	*itr1*Δ *itr2*Δ	Makarius Baier; RWTH Aachen University, Germany	*itr1*Δ *itr2*Δ
CEN.PK113-7D	*ino1*Δ *itr1*Δ	Makarius Baier; RWTH Aachen University, Germany	*ino1*Δ *itr1*Δ
CEN.PK113-7D	*ino1*Δ *itr2*Δ	Makarius Baier; RWTH Aachen University, Germany	*ino1*Δ *itr2*Δ

Table A11: *S. cerevisiae* strains employed in the phospholipid screening experiments.

Strain	Genotype	Origin	Abbreviation
BY4742	WT (MATα *his3*Δ1 *leu2*Δ0 *lys2*Δ *ura3*Δ0)	EUROSCARF; Oberursel, Germany	BY4272 WT
BY4742	knockout YGR157W/*CHO2*	EUROSCARF; Oberursel, Germany	*cho2*Δ
BY4742	knockout YNL130C/*CPT1*	EUROSCARF; Oberursel, Germany	*cpt1*Δ
BY4742	knockout YDL142C/*CRD1*	EUROSCARF; Oberursel, Germany	*crd1*Δ
BY4742	knockout YOR245C/*DGA1*	EUROSCARF; Oberursel, Germany	*dga1*Δ
BY4742	knockout YOR311C/*DGK1*	EUROSCARF; Oberursel, Germany	*dgk1*Δ
BY4742	knockout YDR284C/*DPP1*	EUROSCARF; Oberursel, Germany	*dpp1*Δ
BY4742	knockout YFR019W/*FAB1*	EUROSCARF; Oberursel, Germany	*fab1*Δ
BY4742	knockout YDR497C/*ITR1*	EUROSCARF; Oberursel, Germany	*itr1*Δ
BY4742	knockout YOL103W/*ITR2*	EUROSCARF; Oberursel, Germany	*itr2*Δ
BY4742	knockout YDR503C/*LPP1*	EUROSCARF; Oberursel, Germany	*lpp1*Δ
BY4742	knockout YHL020C/*OPI1*	EUROSCARF; Oberursel, Germany	*opi1*Δ
BY4742	knockout YJR073C/*OPI3*	EUROSCARF; Oberursel, Germany	*opi3*Δ
BY4742	knockout YER037W/*PHM8*	EUROSCARF; Oberursel, Germany	*phm8*Δ
BY4742	knockout YKR031C/*PLD1*	EUROSCARF; Oberursel, Germany	*pld1*Δ
BY4742	knockout YGR170W/*PSD2*	EUROSCARF; Oberursel, Germany	*psd2*Δ
BY4742	knockout YGL224C/*SDT1*	EUROSCARF; Oberursel, Germany	*sdt1*Δ
BY4742	knockout YDL052C/*SLC1*	EUROSCARF; Oberursel, Germany	*slc1*Δ
BY4742	knockout YGL021W/*ALK1*	EUROSCARF; Oberursel, Germany	*alk1*Δ

Strain	Genotype	Origin	Abbreviation
BY4742	knockout YIL124W/*AYR1*	EUROSCARF; Oberursel, Germany	*ayr1*Δ
BY4742	knockout YBL011W/*SCT1*	EUROSCARF; Oberursel, Germany	*sct1*Δ
BY4742	knockout YKR067W/*GPT2*	EUROSCARF; Oberursel, Germany	*gpt2*Δ
BY4742	knockout YGR202C/*PCT1*	EUROSCARF; Oberursel, Germany	*pct1*Δ
BY4742	knockout YOR081C/*TGL5*	EUROSCARF; Oberursel, Germany	*tgl5*Δ
BY4742	knockout YKR089C/*TGL4*	EUROSCARF; Oberursel, Germany	*tgl4*Δ
BY4742	knockout YMR313C/*TGL3*	EUROSCARF; Oberursel, Germany	*tgl3*Δ
BY4742	knockout YPR139C/*LOA1*	EUROSCARF; Oberursel, Germany	*loa1*Δ
BY4742	Knockout YHR123W/*EPT1*	EUROSCARF; Oberursel, Germany	*ept1*Δ
BY4742	knockout YLR133W/*CKI1*	EUROSCARF; Oberursel, Germany	*cki1*Δ
BY4742	knockout YNR019W/*ARE2*	EUROSCARF; Oberursel, Germany	*are2*Δ
BY4742	knockout YCR048W/*ARE1*	EUROSCARF; Oberursel, Germany	*are1*Δ
BY4742	knockout YNR008W/*LRO1*	EUROSCARF; Oberursel, Germany	*lro1*Δ
BY4742	knockout YPL268W/*PLC1*	EUROSCARF; Oberursel, Germany	*plc1*Δ
BY4742	knockout YGL077C/*HNM1*	EUROSCARF; Oberursel, Germany	*hnm1*Δ
BY4742	knockout YCR098C/*GIT1*	EUROSCARF; Oberursel, Germany	*git1*Δ
BY4742	knockout YDL022W/*GPD1*	EUROSCARF; Oberursel, Germany	*gpd1*Δ
BY4742	knockout YJL083W/*TAX4*	EUROSCARF; Oberursel, Germany	*tax4*Δ
BY4742	knockout YMR008C/*PLB1*	EUROSCARF; Oberursel, Germany	*plb1*Δ
BY4742	knockout YER062C/*GPP2*	EUROSCARF; Oberursel, Germany	*gpp2*Δ

Strain	Genotype	Origin	Abbreviation
BY4742	knockout YPL110C/*GDE1*	EUROSCARF; Oberursel, Germany	*gde1*Δ
BY4742	knockout YLR410W/*VIP1*	EUROSCARF; Oberursel, Germany	*vip1*Δ
BY4742	knockout YPL057C/*SUR1*	EUROSCARF; Oberursel, Germany	*sur1*Δ
BY4742	knockout YDR147W/*EKI1*	EUROSCARF; Oberursel, Germany	*eki1*Δ
BY4742	knockout YHR123W/*EPT1*	EUROSCARF; Oberursel, Germany	*ept1*Δ
BY4742	knockout YDR072C/*IPT1*	EUROSCARF; Oberursel, Germany	*ipt1*Δ
BY4742	knockout YDL047W/*SIT4*	EUROSCARF; Oberursel, Germany	*sit4*Δ
BY4742	knockout YDR127W/*ARO1*	EUROSCARF; Oberursel, Germany	*aro1*Δ
BY4742	knockout YEL060C/*PRB1*	EUROSCARF; Oberursel, Germany	*prb1*Δ
BY4742	knockout YKR042W/*UTH1*	EUROSCARF; Oberursel, Germany	*uth1*Δ
BY4742	knockout YPL154C/*PEP4*	EUROSCARF; Oberursel, Germany	*pep4*Δ
BY4742	knockout YBR296C/*PHO89*	EUROSCARF; Oberursel, Germany	*pho89*Δ
BY4742	knockout YOL084W/*PHM7*	EUROSCARF; Oberursel, Germany	*phm7*Δ

Table A12: Cost of raw materials applied in the starvation and feeding phase of the polyP hyperaccumulation protocol.
Unit prices were provided by Carl Roth GmbH & Co. KG (Karlsruhe, Germany) or Sigma-Aldrich (St. Louis, MO, USA). The respective websites were accessed on March 10, 2025.

	Price [€]	Amount [kg]	Price per kg [€/kg]
Starvation medium			
Glucose · H_2O	26.5	1	26.5
$(NH_4)_2SO_4$	32.9	1	32.9
KCl	36.9	1	36.9
$CaCl_2$ · 2 H_2O	38.9	0.5	77.8
Na_2succinate	96.2	0.5	192.4
Biotin	95.5	0.001	95500
Calcium pantothenate	179	0.25	716
Nicotinic acid	44.9	0.1	449
myo-Inositol	215	0.1	2150
Thiamine HCl	27.5	0.025	1100
Pyridoxine HCl	62.9	0.1	629
p-Aminobenzoic acid	119	1	119
Na_2EDTA · 2 H_20	57.9	0.25	231.6
$ZnSO_4$ · 7 H_2O	21.5	0.5	43
$MnCl_2$ · 2 H_2O	16	0.1	160
$CoCl_2$ · 6 H_2O	219	0.25	876
$CuSO_4$ · 5 H_2O	34.9	1	34.9
Na_2MoO_4 · 2 H_2O	23.9	0.1	239
$CaCl_2$ · 2 H_2O	31.9	1	31.9
$FeSO_4$ · 7 H_2O	40.9	0.5	81.8
H_3BO_3	58.9	1	58.9
KI	38.5	0.1	385
Feeding medium			
Glucose · H_2O	26.5	1	26.5
KH_2PO_4	25.5	0.5	51
$MgCl_2$ · 6 H_2O	24.5	1	24.5

Table A13: Cost assessment of starvation and feeding media used in the polyP hyperaccumulation protocol.

Medium	Price [€/l]	Price reduction compared to Christ and Blank (2019) [1][%]
Regular	3.11	-
M1	1.62	47.8
M2	1.59	49.0
M3	1.39	55.2
M4	1.36	56.3
M8.4	1.36	56.4

References

References

[1] Christ, J. J. and Blank, L. M. *Saccharomyces cerevisiae* containing 28% polyphosphate and production of a polyphosphate-rich yeast extract thereof. *FEMS Yeast Research*, 19, 1-13, 2019, *doi*:10.1093/femsyr/foz011.

[2] Westheimer, F. H. Why nature chose phosphates. *Science*, 235, 1173-1178, 1987, *doi*:10.1126/science.2434996.

[3] Elser, J. J. Phosphorus: a limiting nutrient for humanity? *Current Opinion in Biotechnology*, 23, 833-838, 2012, *doi*:10.1016/j.copbio.2012.03.001.

[4] Blank, L. M. The cell and P: from cellular function to biotechnological application. *Current Opinion in Biotechnology*, 23, 846-851, 2012, *doi*:10.1016/j.copbio.2012.08.002.

[5] Scholz, R. W., Ulrich, A. E., Eilittä, M., and Roy, A. Sustainable use of phosphorus: a finite resource. *Science of the Total Environment*, 461-462, 799-803, 2013, *doi*:10.1016/j.scitotenv.2013.05.043.

[6] Sterner, R. and Elser, J. J. *Ecological Stoichiometry: The Biology of Elements From Molecules to The Biosphere*. 2002, (Princeton University Press).

[7] Elser, J. J., Dobberfuhl, D. R., MacKay, N. A., and Schampel, J. H. Organism Size, Life History, and N:P Stoichiometry: Toward a unified view of cellular and ecosystem processes. *BioScience*, 46, 674-684, 1996, *doi*:10.2307/1312897 %J BioScience.

[8] Elser, J. J. *et al.* Biological Stoichiometry from Genes to Ecosystems. *Ecology Letters*, 3, 540-550, 2000, *doi*:10.1111/j.1461-0248.2000.00185.x.

[9] Gillooly, J. F. *et al.* The metabolic basis of whole-organism RNA and phosphorus content. *Proc Natl Acad Sci U S A*, 102, 11923-11927, 2005, *doi*:10.1073/pnas.0504756102.

[10] Daneshgar, S., Callegari, A., Capodaglio, A. G., and Vaccari, D. The Potential Phosphorus Crisis: Resource Conservation and Possible Escape Technologies: A Review. *Resources*, 7, 37, 2018, *doi*:10.3390/resources7020037.

[11] Kovacs, T. *et al.* in *Naturally Occurring Radioactive Materials in Construction.* From raw materials to NORM by-products (ed Wouter Schroeyers), 135-182, 2017, *doi*:10.1016/B978-0-08-102009-8.00006-2. (Woodhead Publishing).

[12] Filippelli, G. M. The Global Phosphorus Cycle: Past, Present, and Future. *Elements*, 4, 89-95, 2008, *doi*:10.2113/GSELEMENTS.4.2.89 %J Elements.

[13] Filippelli, G. M. Phosphate rock formation and marine phosphorus geochemistry: The deep time perspective. *Chemosphere*, 84, 759-766, 2011, *doi*:10.1016/j.chemosphere.2011.02.019.

[14] Pierrou, U. The global phosphorus cycle. *Ecol. Bull.*, 22, pp.75-88, 1976.

[15] Ashley, K., Cordell, D., and Mavinic, D. A brief history of phosphorus: From the philosopher's stone to nutrient recovery and reuse. *Chemosphere*, 84, 737-746, 2011, *doi*:10.1016/j.chemosphere.2011.03.001.

[16] Liebig, J. Die organische Chemie in ihrer Anwendung auf Agricultur und Physiologie (Organic chemistry in its applications to agriculture and physiology). *Friedrich Vieweg und Sohn Publ. Co*, 1840.

[17] van der Ploeg, R. R., Böhm, W., and Kirkham, M. B. On the Origin of the Theory of Mineral Nutrition of Plants and the Law of the Minimum. *Soil Science Society of America Journal*, 63, 1055-1062, 1999, *doi*:10.2136/sssaj1999.6351055x.

[18] Carpenter, S. R. and Bennett, E. M. Reconsideration of the planetary boundary for phosphorus. *Environmental Research Letters*, 6, 014009, 2011, *doi*:10.1088/1748-9326/6/1/014009.

[19] Cordell, D., Drangert, J.-O., and White, S. The story of phosphorus: Global food security and food for thought. *Global Environmental Change*, 19, 292-305, 2009, *doi*:10.1016/j.gloenvcha.2008.10.009.

[20] Villalba, G., Liu, Y., Schroder, H., and Ayres, R. U. Global Phosphorus Flows in the Industrial Economy From a Production Perspective. *Journal of Industrial Ecology*, 12, 557-569, 2008, *doi*:10.1111/j.1530-9290.2008.00050.x.

[21] Brownlie, W. J. *et al.* Global actions for a sustainable phosphorus future. *Nat Food*, 2, 71-74, 2021, *doi*:10.1038/s43016-021-00232-w.

[22] Ros, M. B. H. *et al.* Towards optimal use of phosphorus fertiliser. *Scientific Reports*, 10, 17804, 2020, *doi*:10.1038/s41598-020-74736-z.

[23] Reijnders, L. Phosphorus resources, their depletion and conservation, a review. *Resources, Conservation and Recycling*, 93, 32-49, 2014, *doi*:10.1016/j.resconrec.2014.09.006.

[24] Falkowski, P. *et al.* The Global Carbon Cycle: A Test of Our Knowledge of Earth as a System. *Science*, 290, 291-296, 2000, *doi*:10.1126/science.290.5490.291.

[25] Cordell, D. and White, S. Life's Bottleneck: Sustaining the World's Phosphorus for a Food Secure Future *Annual Review of Environment and Resources* 39, 161-188, 2014, *doi*:10.1146/annurev-environ-010213-113300.

[26] Anlauf, A. An extractive bioeconomy? Phosphate mining, fertilizer commodity chains, and alternative technologies. *Sustainability Science*, 18, 633-644, 2023, *doi*:10.1007/s11625-022-01234-8.

[27] Sattari, S. Z., Bouwman, A. F., Martinez Rodríguez, R., Beusen, A. H., and van Ittersum, M. K. Negative global phosphorus budgets challenge sustainable intensification of grasslands. *Nat Commun*, 7, 10696, 2016, *doi*:10.1038/ncomms10696.

[28] Mogollón, J., Beusen, A., Grinsven, H., Westhoek, H., and Bouwman, A. Future agricultural phosphorus demand according to the shared socioeconomic pathways. *Global Environmental Change*, 50, 149-163, 2018, *doi*:10.1016/j.gloenvcha.2018.03.007.

[29] Scholz, R. W. Foreword: Phosphorus Recycling — Mending a Broken Biogeochemical Cycle. *Phosphorus Recovery and Recycling*, 2019, *doi*:10.1007/978-981-10-8031-9.

[30] Ryszko, U., Rusek, P., and Kołodyńska, D. Quality of Phosphate Rocks from Various Deposits Used in Wet Phosphoric Acid and P-Fertilizer Production. *Materials*, 16, 793, 2023.

[31] Van Kauwenbergh, S. J. World Phosphate Rock Reserves and Resources Technical Bulletin IFDC-T-75. *IFDC Publications*, 2010.

[32] Bertau, M. *et al.* The Future of Phosphoric Acid Production –Why We Have to Leave Trodden Paths. *ChemSusChem*, 18, e202401155, 2025, *doi*:10.1002/cssc.202401155.

[33] Koppelaar, R. H. E. M. and Weikard, H. P. Assessing phosphate rock depletion and phosphorus recycling options. *Global Environmental Change*, 23, 1454-1466, 2013, *doi*:10.1016/j.gloenvcha.2013.09.002.

[34] Tayibi, H., Choura, M., López, F. A., Alguacil, F. J., and López-Delgado, A. Environmental impact and management of phosphogypsum. *Journal of Environmental Management*, 90, 2377-2386, 2009, *doi*:10.1016/j.jenvman.2009.03.007.

[35] U.S. Environmental Protection Agency. BACKGROUND REPORT AP-42 SECTION 5.11 PHOSPHORIC ACID. 1995, [Online]. Available: https://www3.epa.gov/ttnchie1/ap42/ch08/bgdocs/b08s09.pdf.

[36] Bahsaine, K., Mekhzoum, M. E. M., Benzeid, H., Qaiss, A., and Bouhfid, R. Recent Progress in Heavy Metals Extraction From Phosphoric Acid: A Short Review. *Journal of Industrial and Engineering Chemistry*, 115, 2022, *doi*:10.1016/j.jiec.2022.08.029.

[37] Favaro, D. and Mazzilli, B. Natural radioactivity in phosphate rock, phosphogypsum and phosphate fertilizers in Brazil. *Journal of Radioanalytical and Nuclear Chemistry*, 264, 445-448, 2005, *doi*:10.1007/s10967-005-0735-4.

[38] Kratz, S. and Schnug, E. in *Uranium in the Environment: Mining Impact and Consequences.* Rock phosphates and P fertilizers as sources of U contamination in agricultural soils (eds Broder J. Merkel & Andrea Hasche-Berger), 57-67, 2006, *doi*:10.1007/3-540-28367-6_5 (Springer Berlin Heidelberg).

[39] Srivastava, V. *et al.* Agroecological Responses of Heavy Metal Pollution with Special Emphasis on Soil Health and Plant Performances. *Frontiers in Environmental Science*, Volume 5 - 2017, 2017, *doi*:10.3389/fenvs.2017.00064.

[40] The European Parliament and the Council of the European Union. Fertilising products standards - Regulation (EU) 2019/1009. 2019, [Online]. Available: https://eur-lex.europa.eu/eli/reg/2019/1009/oj.

[41] Suciu, N., Devivo, R., Rizzati, N., and Capri, E. Cd content in phosphate fertilizer: Which potential risk for the environment and human health? *Current Opinion in Environmental Science & Health*, 30, 100392, 2022, *doi*:10.1016/j.coesh.2022.100392.

[42] Knox, A. S., Kaplan, D. I., and Paller, M. H. Phosphate sources and their suitability for remediation of contaminated soils. *Science of the Total Environment*, 357, 271-279, 2006, *doi*:10.1016/j.scitotenv.2005.07.014.

[43] Walsh, M., Schenk, G., and Schmidt, S. Realising the circular phosphorus economy delivers for sustainable development goals. *npj Sustainable Agriculture*, 1, 2, 2023, *doi*:10.1038/s44264-023-00002-0.

[44] Childers, D. L., Corman, J., Edwards, M., and Elser, J. J. Sustainability Challenges of Phosphorus and Food: Solutions from Closing the Human Phosphorus Cycle. *BioScience*, 61, 117-124, 2011, *doi*:10.1525/bio.2011.61.2.6 %J BioScience.

[45] Demling, P., Baier, M., Deitert, A., Fees, J., and Blank, L. M. Biotechnological polyphosphate as an opportunity to contribute to the circularization of the phosphate economy. *Current Opinion in Biotechnology*, 87, 103107, 2024, *doi*:10.1016/j.copbio.2024.103107.

[46] Lin, H., Wang, Y., and Dong, Y. A review of methods, influencing factors and mechanisms for phosphorus recovery from sewage and sludge from municipal wastewater treatment plants. *Journal of Environmental Chemical Engineering*, 12, 111657, 2024, *doi*:10.1016/j.jece.2023.111657.

[47] Jatko, J. T. *et al.* Differentiating between point and non-point source nutrient loadings of wastewater in an agriculturally impacted area using a hybrid statistical model. *Science of the Total Environment*, 912, 169553, 2024, *doi*:10.1016/j.scitotenv.2023.169553.

[48] Diaz, R. J. and Rosenberg, R. Spreading dead zones and consequences for marine ecosystems. *Science*, 321, 926-929, 2008, *doi*:10.1126/science.1156401.

[49] Kulakovskaya, T. V., Vagabov, V. M., and Kulaev, I. S. Inorganic polyphosphate in industry, agriculture and medicine: Modern state and outlook. *Process Biochemistry*, 47, 1-10, 2012, *doi*:10.1016/j.procbio.2011.10.028.

[50] Dodds, W. K. *et al.* Eutrophication of U.S. Freshwaters: Analysis of Potential Economic Damages. *Environmental Science & Technology*, 43, 12-19, 2009, *doi*:10.1021/es801217q.

[51] Rockström, J. *et al.* A safe operating space for humanity. *Nature*, 461, 472-475, 2009, *doi*:10.1038/461472a.

[52] Filippelli, G. M. Balancing the Global Distribution of Phosphorus With a View Toward Sustainability and Equity. *Global Biogeochemical Cycles*, 32, 904-908, 2018, *doi*:10.1029/2018GB005923.

[53] Richardson, K. *et al.* Earth beyond six of nine planetary boundaries. *Science Advances*, 9, eadh2458, 2023, *doi*:10.1126/sciadv.adh2458.

[54] Wellmer, F. W. and Scholz, R. W. Peak minerals: What can we learn from the history of mineral economics and the cases of gold and phosphorus? *Mineral Economics*, 30, 73-93, 2017, *doi*:10.1007/s13563-016-0094-3.

[55] Scholz, R. W. and Wellmer, F.-W. Approaching a dynamic view on the availability of mineral resources: What we may learn from the case of phosphorus? *Global Environmental Change*, 23, 11-27, 2013, *doi*:10.1016/j.gloenvcha.2012.10.013.

[56] Directorate-General for Internal Market, Industry, Entrepreneurship and SMEs (European Commission). Study on the critical raw materials for the EU 2023 – Final report. Grohol, M. and Veeh, C., *Publications Office of the European Union*, 2023, *doi:*10.2873/725585.

[57] European Commission. 20 critical raw materials - major challenge for EU industry. *Press release*, 2014, [Online]. Available: https://ec.europa.eu/commission/presscorner/detail/en/ip_14_599.
[58] European Commission. Report on Critical Raw Materials and the Circular Economy. 2018, [Online]. Available: https://ec.europa.eu/docsroom/documents/27327.
[59] U.S. Geological Survey. Phosphate rock statistics and information. Jasinski, S. M., 2021, [Online]. Available: https://pubs.usgs.gov/periodicals/mcs2021/mcs2021-phosphate.pdf.
[60] U.S Geological Survey. Mineral Commodity Summaries 2023 - PHOSPHATE ROCK. Jasinski, S. M., 2023, [Online]. Available: https://pubs.usgs.gov/periodicals/mcs2023/mcs2023-phosphate.pdf
[61] Elser, J. and Bennett, E. Phosphorus cycle: A broken biogeochemical cycle. *Nature*, 478, 29-31, 2011, *doi*:10.1038/478029a.
[62] United Nations Security Council. Resolution 2797 (2025). 2025, [Online]. Available: https://docs.un.org/en/s/res/2797(2025).
[63] Zhu, F., Cakmak, E. K., and Cetecioglu, Z. Phosphorus recovery for circular Economy: Application potential of feasible resources and engineering processes in Europe. *Chemical Engineering Journal*, 454, 140153, 2023, *doi*:10.1016/j.cej.2022.140153.
[64] Blank, L. M. (Poly)phosphate biotechnology: Envisaged contributions to a sustainable P future. *Microbial Biotechnology*, 16, 1616-1622, 2023, *doi*:10.1111/1751-7915.14250.
[65] Lougheed, T. Phosphorus paradox: scarcity and overabundance of a key nutrient. *Environmental Health Perspectives*, 119, A208-213, 2011, *doi*:10.1289/ehp.119-a208.
[66] Asimov, I. *Asimov on Chemistry* 1974, *ISB-Number*:9780385040051, (NY: Doubleday).
[67] Pradel, M. and Aissani, L. Environmental impacts of phosphorus recovery from a "product" Life Cycle Assessment perspective: Allocating burdens of wastewater treatment in the production of sludge-based phosphate fertilizers. *Science of the Total Environment*, 656, 55-69, 2019, *doi*:10.1016/j.scitotenv.2018.11.356.
[68] Scholz, R. W. and Wellmer, F.-W. Losses and use efficiencies along the phosphorus cycle. Part 1: Dilemmata and losses in the mines and other nodes of the supply chain. *Resources, Conservation and Recycling*, 105, 216-234, 2015, *doi*:10.1016/j.resconrec.2015.09.020.
[69] Environment and Natural Resources Department. Wastewater as a resource. *European Investment Bank*, 2022, [Online]. Available: https://www.eib.org/files/publications/wastewater_as_a_resource_en.pdf.
[70] Kowalik, R., Gawdzik, J., Bąk-Patyna, P., Ramiączek, P., and Jurišević, N. Risk Analysis of Heavy Metals Migration from Sewage Sludge of Wastewater Treatment Plants. *International Journal of Environmental Research and Public Health*, 19, 11829, 2022, *doi*:10.3390/ijerph191811829.
[71] Fijalkowski, K., Rorat, A., Grobelak, A., and Kacprzak, M. J. The presence of contaminations in sewage sludge - The current situation. *Journal of Environmental Management*, 203, 1126-1136, 2017, *doi*:10.1016/j.jenvman.2017.05.068.
[72] Fernandes, J., Ramísio, P. J., and Puga, H. A Comprehensive Review on Various Phases of Wastewater Technologies: Trends and Future Perspectives. 5, 2633-2661, 2024, *doi*:10.3390/eng5040138.
[73] Hreiz, R., Latifi, M. A., and Roche, N. Optimal design and operation of activated sludge processes: State-of-the-art. *Chemical Engineering Journal*, 281, 900-920, 2015, *doi*:10.1016/j.cej.2015.06.125.
[74] Zahed, M. A. *et al.* Phosphorus removal and recovery: state of the science and challenges. *Environmental Science and Pollution Research*, 29, 58561-58589, 2022, *doi*:10.1007/s11356-022-21637-5.
[75] Xu, H., Wei, S., Li, G., and Guo, B. Advanced removal of phosphorus from urban sewage using chemical precipitation by Fe-Al composite coagulants. *Scientific Reports*, 14, 4918, 2024, *doi*:10.1038/s41598-024-55713-2.

[76] Yang, L., Zhou, H., and Moccia, R. Membrane Filtration Coupled with Chemical Precipitation to Treat Recirculating Aquaculture System Effluents. *Journal of Environmental Quality*, 35, 2419-2424, 2006, *doi*:10.2134/jeq2005.0480.

[77] Hamda, A. S., Abo, L. D., Daba, B. J., and Debela, A. B. Transforming sludge to energy: A sustainable strategy for resource recovery and environmental protection. *Cleaner Waste Systems*, 11, 100298, 2025, *doi*:10.1016/j.clwas.2025.100298.

[78] Werther, J. and Ogada, T. Sewage sludge combustion. *Progress in Energy and Combustion Science*, 25, 55-116, 1999, *doi*:10.1016/S0360-1285(98)00020-3.

[79] Zaharioiu, A. M. *et al.* Opportunities regarding the use of technologies of energy recovery from sewage sludge. *Springer Nature Applied Sciences*, 3, 775, 2021, *doi*:10.1007/s42452-021-04758-3.

[80] Shao, J. *et al.* Emission Characteristics of Heavy Metals and Organic Pollutants from the Combustion of Sewage Sludge in a Fluidized Bed Combustor. *Energy & Fuels*, 22, 2278-2283, 2008, *doi*:10.1021/ef800002y.

[81] Häggström, G. *et al.* Single Pellet Combustion of Sewage Sludge and Agricultural Residues with a Focus on Phosphorus. *Energy & Fuels*, 35, 10009-10022, 2021, *doi*:10.1021/acs.energyfuels.1c00882.

[82] Tan, Z. and Lagerkvist, A. Phosphorus recovery from the biomass ash: A review. *Renewable and Sustainable Energy Reviews*, 15, 3588-3602, 2011, *doi*:10.1016/j.rser.2011.05.016.

[83] Mayer, N. and Kaltschmitt, M. Closing the phosphorus cycle: Current P balance and future prospects in Germany. *Journal of Cleaner Production*, 347, 131272, 2022, *doi*:10.1016/j.jclepro.2022.131272.

[84] Schnell, M., Horst, T., and Quicker, P. Thermal treatment of sewage sludge in Germany: A review. *Journal of Environmental Management*, 263, 110367, 2020, *doi*:10.1016/j.jenvman.2020.110367.

[85] Schipper, W. in *Phosphorus Recovery and Recycling.* Success Factors for Implementing Phosphorus Recycling Technologies (eds H. Ohtake & Satoshi Tsuneda), 101-130, 2019, *doi*:10.1007/978-981-10-8031-9_6 (Springer Nature Singapore Pte Ltd).

[86] German Federal Ministry for the Environment, Nature Conservation, Nuclear Safety and Consumer Protection (BMUV). Sewage Sludge Ordinance. 2017, [Online]. Available: https://www.gesetze-im-internet.de/abfkl_rv_2017/BJNR346510017.html.

[87] Hultman, B., Levlin, E., Plaza, E., and Stark, K. Phosphorus recovery from sludge in Sweden-possibilities to meet proposed goals in an efficient, sustainable and economical way. *Integration and optimisation of urban sanitation systems, Proceedings of a Polish-Swedish Seminar, Gdansk*, 23, 2003.

[88] Kabbe, C. in *Phosphorus Recovery and Recycling.* Circular Economy: Bridging the Gap Between Phosphorus Recovery and Recycling (eds Hisao Ohtake & Satoshi Tsuneda), 45-57, 2019, *doi*:10.1007/978-981-10-8031-9_3 (Springer Singapore).

[89] Scholz, R. W. and Wellmer, F.-W. Although there is no Physical Short-Term Scarcity of Phosphorus, its Resource Efficiency Should be Improved. *Journal of Industrial Ecology*, 23, 313-318, 2019, *doi*:10.1111/jiec.12750.

[90] Rak, A. and Lebek, M. Clean technology for P-recycling to phosphoric acid: Remondis TetraPhos®. *European Sustainable Phosphorus Platform*, 2016.

[91] Ploteau, M.-E., Althoff, A., Nafo, I., and Teichgräber, B. Technical report of the Phos4You partnership on processes to recover phosphorus from wastewater. 2021, *doi*:10.17185/duepublico/74788.

[92] Franz, M. Phosphate fertilizer from sewage sludge ash (SSA). *Waste Management*, 28, 1809-1818, 2008, *doi*:10.1016/j.wasman.2007.08.011.

[93] Roy, S. *et al.* Wastewater biorefineries: exploring biological phosphorus removal and integrated recovery solutions. *Current Opinion in Biotechnology*, 92, 103266, 2025, *doi*:10.1016/j.copbio.2025.103266.

[94] Cloete, T. E. and Oosthuizen, D. J. The role of extracellular exopolymers in the removal of phosphorus from activated sludge. *Water Research*, 35, 3595-3598, 2001, *doi*:10.1016/s0043-1354(01)00093-8.

[95] Gebremariam, S. Y., Beutel, M. W., Christian, D., and Hess, T. F. Research advances and challenges in the microbiology of enhanced biological phosphorus removal-a critical review. *Water Environment Research*, 83, 195-219, 2011, *doi*:10.2175/106143010x12780288628534.

[96] Blackall, L. L., Crocetti, G. R., Saunders, A. M., and Bond, P. L. A review and update of the microbiology of enhanced biological phosphorus removal in wastewater treatment plants. *Antonie van Leeuwenhoek*, 81, 681-691, 2002, *doi*:10.1023/A:1020538429009.

[97] Hirota, R., Kuroda, A., Kato, J., and Ohtake, H. Bacterial phosphate metabolism and its application to phosphorus recovery and industrial bioprocesses. *Journal of Bioscience and Bioengineering*, 109, 423-432, 2010, *doi*:10.1016/j.jbiosc.2009.10.018.

[98] Kortstee, G. J., Appeldoorn, K. J., Bonting, C. F., van Niel, E. W., and van Veen, H. W. Biology of polyphosphate-accumulating bacteria involved in enhanced biological phosphorus removal. *FEMS Microbiology Reviews*, 15, 137-153, 1994, *doi*:10.1111/j.1574-6976.1994.tb00131.x.

[99] Kortstee, G. J., Appeldoorn, K. J., Bonting, C. F., van Niel, E. W., and van Veen, H. W. Recent developments in the biochemistry and ecology of enhanced biological phosphorus removal. *Biochemistry (Mosc)*, 65, 332-340, 2000.

[100] Nielsen, P. H., Saunders, A. M., Hansen, A. A., Larsen, P., and Nielsen, J. L. Microbial communities involved in enhanced biological phosphorus removal from wastewater--a model system in environmental biotechnology. *Current Opinion in Biotechnology*, 23, 452-459, 2012, *doi*:10.1016/j.copbio.2011.11.027.

[101] Plouviez, M. and Brown, N. Polyphosphate accumulation in microalgae and cyanobacteria: recent advances and opportunities for phosphorus upcycling. *Current Opinion in Biotechnology*, 90, 103207, 2024, *doi*:10.1016/j.copbio.2024.103207.

[102] Herrmann, K. R. *et al.* Biotechnological production of food-grade polyphosphate from deoiled seeds and bran. *EFB Bioeconomy Journal*, 3, 100048-100048, 2023, *doi*:10.1016/j.bioeco.2023.100048.

[103] Fees, J., Christ, J. J., Willbold, S., and Blank, L. M. Biotechnological production of polyphosphate from industrial wash water. *Biotechnology and Bioengineering*, 2022, *doi*:10.1002/bit.28274.

[104] Rao, N. N., Gómez-García, M. R., and Kornberg, A. Inorganic polyphosphate: essential for growth and survival. *Annual Review Biochemistry*, 78, 605-647, 2009, *doi*:10.1146/annurev.biochem.77.083007.093039.

[105] Brown, M. R. W. and Kornberg, A. Inorganic polyphosphate in the origin and survival of species. *Proc. Natl. Acad. Sci. U.S.A*, 101, 16085-16087, 2004, *doi*:10.1073/pnas.0406909101.

[106] Albi, T. and Serrano, A. Inorganic polyphosphate in the microbial world. Emerging roles for a multifaceted biopolymer. *World Journal of Microbiology and Biotechnology*, 32, 27, 2016, *doi*:10.1007/s11274-015-1983-2.

[107] Kulaev, I. S., Vagabov, V. M., and Kulakovskaya, E. V. *The Biochemistry of Inorganic Polyphosphates*. 2004, *ISB-Number*:0-470-85810-9, (John Wiley & Sons).

[108] Delgadillo-Mirquez, L., Lopes, F., Taidi, B., and Pareau, D. Nitrogen and phosphate removal from wastewater with a mixed microalgae and bacteria culture. *Biotechnology Reports*, 11, 18-26, 2016, *doi*:10.1016/j.btre.2016.04.003.

[109] Christ, J. J., Willbold, S., and Blank, L. M. Polyphosphate chain length determination in the range of two to several hundred P-subunits with a new enzyme assay and 31P NMR. *Analytical Chemistry*, 91, 7654-7661, 2019, *doi*:10.1021/acs.analchem.9b00567.

[110] Dürr-Mayer, T. *et al.* The chemistry of branched condensed phosphates. *Nature Communications*, 12, 5368, 2021, *doi*:10.1038/s41467-021-25668-3.

[111] Denoncourt, A. and Downey, M. Model systems for studying polyphosphate biology: a focus on microorganisms. *Current Genetics*, 67, 331-346, 2021, *doi*:10.1007/s00294-020-01148-x.

[112] Sanz-Luque, E., Bhaya, D., and Grossman, A. R. Polyphosphate: A Multifunctional Metabolite in Cyanobacteria and Algae. *Frontiers in Plant Science*, Volume 11 - 2020, 2020, *doi*:10.3389/fpls.2020.00938.

[113] Vila, T., Frases, S., and Gomes, F. M. Lessons from protozoans: Phosphate sensing and polyphosphate storage in fungi. *PLoS Pathogens*, 18, e1010298, 2022, *doi*:10.1371/journal.ppat.1010298.

[114] Borghi, F. and Saiardi, A. Evolutionary perspective on mammalian inorganic polyphosphate (polyP) biology. *Biochemical Society Transactions*, 51, 1947-1956, 2023, *doi*:10.1042/bst20230483.

[115] Gomes, F. M., Ramos, I. B., Araujo, H., Miranda, K., and Ednildo, E. A. in *Inorganic Polyphosphates in Eukaryotic Cells.* Inorganic Polyphosphate Functions and Metabolism in Insects (eds Tatiana Kulakovskaya, Evgeny Pavlov, & Elena N. Dedkova), 123-138, 2016, *doi*:10.1007/978-3-319-41073-9_9 (Springer International Publishing).

[116] Van Wazer, J. R. and Holst, K. A. Holst structure and properties of the condensed phosphate.pdf. *Journal of the American Chemical Society*, 72, 630-644, 1950.

[117] Mandala, V. S. *et al.* Bacterial Phosphate Granules Contain Cyclic Polyphosphates: Evidence from (31)P Solid-State NMR. *J Am Chem Soc*, 142, 18407-18421, 2020, *doi*:10.1021/jacs.0c06335.

[118] Glonek, T. Did Cyclic Metaphosphates Have a Role in the Origin of Life? *Origins of Life and Evolution of Biospheres*, 51, 1-60, 2021, *doi*:10.1007/s11084-021-09604-5.

[119] Achbergerová, L. and Nahálka, J. Polyphosphate - an ancient energy source and active metabolic regulator. *Microbial Cell Factories*, 10, 63, 2011, *doi*:10.1186/1475-2859-10-63.

[120] Kulaev, I. S. and Vagabov, V. M. Polyphosphate metabolism in micro-organisms. *Advances in Microbial Physiology*, 24, 83-171, 1983, *doi*:10.1016/s0065-2911(08)60385-9.

[121] Kornberg, A., Rao, N. N., and Ault-Riché, D. Inorganic polyphosphate: a molecule of many functions. *Annual Review Biochemistry*, 68, 89-125, 1999, *doi*:10.1146/annurev.biochem.68.1.89.

[122] Kulaev, I. and Kulakovskaya, T. Polyphosphate and phosphate pump. *Annual Review Microbiology*, 54, 709-734, 2000, *doi*:10.1146/annurev.micro.54.1.709.

[123] Kornberg, A. Inorganic polyphosphate: toward making a forgotten polymer unforgettable. *Journal of Bacteriology*, 177, 491-496, 1995, *doi*:10.1128/jb.177.3.491-496.1995.

[124] Tumlirsch, T., Sznajder, A., and Jendrossek, D. Formation of polyphosphate by polyphosphate kinases and its relationship to poly(3-hydroxybutyrate) accumulation in *Ralstonia eutropha* strain H16. *Applied Environmental microbiology*, 81, 8277-8293, 2015, *doi*:10.1128/aem.02279-15.

[125] Neville, N. *et al.* Modification of histidine repeat proteins by inorganic polyphosphate. *Cell Reports*, 42, 113082, 2023, *doi*:10.1016/j.celrep.2023.113082.

[126] Omelon, S. *et al.* Control of Vertebrate Skeletal Mineralization by Polyphosphates. *PLoS ONE*, 4, e5634, 2009, *doi*:10.1371/journal.pone.0005634.

[127] Morrissey, J. H. Polyphosphate: a link between platelets, coagulation and inflammation. *International Journal of Hematology*, 95, 346-352, 2012, *doi*:10.1007/s12185-012-1054-5.

[128] Christ, J. J. Novel polyphosphate analytics for the development of biotechnological polyphosphate production. PhD Thesis, RWTH Aachen University, 2020.

[129] Morya, R., Tyagi, B., Sharma, A., and Thakur, I. S. in *Biomass, Biofuels, Biochemicals.* Chapter 11 - Production and applications of polyphosphate (eds Parameswaran Binod,

Sindhu Raveendran, & Ashok Pandey), 283-307, 2021, *doi*:10.1016/B978-0-12-821888-4.00001-0 (Elsevier).

[130] EFSA, Panel on Food Additives and Flavourings (FAF) *et al.* Re-evaluation of phosphoric acid–phosphates – di-, tri- and polyphosphates (E 338–341, E 343, E 450–452) as food additives and the safety of proposed extension of use. 17, e05674, 2019, *doi*:10.2903/j.efsa.2019.5674.

[131] Rashchi, F. and Finch, J. A. Polyphosphates: A review their chemistry and application with particular reference to mineral processing. *Minerals Engineering*, 13, 1019-1035, 2000, *doi*:10.1016/S0892-6875(00)00087-X.

[132] Lewis, D. F., Grooves, K. H. M., and Holgate, J. H. Action of Polyphosphates in Meat Products. *Food Structure*, 5, 1986, *doi*: [Online]. Available: https://digitalcommons.usu.edu/cgi/viewcontent.cgi?referer=&httpsredir=1&article=1148&context=foodmicrostructure.

[133] Fu, W. *et al.* Effects of emulsifying conditions on creaming effect, mechanical properties and microstructure of processed cheese using a rapid visco-analyzer. *Bioscience, Biotechnology & Biochemistry*, 82, 476-483, 2018, *doi*:10.1080/09168451.2018.1431106.

[134] Nagyová, G. *et al.* Use of sodium polyphosphates with different linear lengths in the production of spreadable processed cheese. *Journal of Dairy Science*, 97, 111-122, 2014, *doi*:10.3168/jds.2013-7210.

[135] Lorencová, E., Vltavská, P., Budinský, P., and Koutný, M. Antibacterial effect of phosphates and polyphosphates with different chain length. *Journal of Environmental Science and Health*, 47, 2241-2245, 2012, *doi*:10.1080/10934529.2012.707544.

[136] Akhtar, S., Paredes-Sabja, D., and Sarker, M. R. Inhibitory effects of polyphosphates on *Clostridium perfringens* growth, sporulation and spore outgrowth. *Food Microbiology*, 25, 802-808, 2008, *doi*:10.1016/j.fm.2008.04.006.

[137] Molina, R. E., Bohrer, B. M., and Mejia, S. M. V. Phosphate alternatives for meat processing and challenges for the industry: A critical review. *Food Research International*, 166, 112624, 2023, *doi*:10.1016/j.foodres.2023.112624.

[138] Thangavelu, K. P., Kerry, J. P., Tiwari, B. K., and McDonnell, C. K. Novel processing technologies and ingredient strategies for the reduction of phosphate additives in processed meat. *Trends in Food Science & Technology*, 94, 43-53, 2019, *doi*:10.1016/j.tifs.2019.10.001.

[139] Hansen–Bruhn, I., Laura Craig, J., Hinge, M., and Hull, T. R. Ammonium polyphosphates: Correlating structure to application. *European Polymer Journal*, 223, 113644, 2025, *doi*:10.1016/j.eurpolymj.2024.113644.

[140] McBeath, T. M., Lombi, E., McLaughlin, M. J., and Bünemann, E. K. Polyphosphate-fertilizer solution stability with time, temperature, and pH. *Journal of Plant Nutrition and Soil Science*, 170, 387-391, 2007, *doi*:10.1002/jpln.200625166.

[141] Van Wazer, J. R. Principles of Phosphorus Chemistry. I. Some Generalities Concerning Multiple Bonding1. *Journal of the American Chemical Society*, 78, 5709-5715, 1956, *doi*:10.1021/ja01603a001.

[142] Brown, M. R. W. and Kornberg, A. The long and short of it - polyphosphate, PPK and bacterial survival. *Trends Biochemical Sciences*, 33, 284-290, 2008, *doi*:10.1016/j.tibs.2008.04.005.

[143] Urech, K., Dürr, M., Boller, T., Wiemken, A., and Schwencke, J. Localization of polyphosphate in vacuoles of *Saccharomyces cerevisiae*. *Archives of Microbiology*, 116, 275-278, 1978, *doi*:10.1007/bf00417851.

[144] Langen, P. and Liss, E. Formation and conversion of yeast polyphosphates. *Biochem Z*, 330, 455-466, 1958.

[145] Liss, E. and Langen, P. Versuche zur Polyphosphat-Überkompensation in Hefezellen nach Phosphatverarmung. *Archiv für Mikrobiologie*, 41, 383-392, 1962, *doi*:10.1007/BF00422195.

[146] Austin, S. and Mayer, A. Phosphate Homeostasis − A Vital Metabolic Equilibrium Maintained Through the INPHORS Signaling Pathway. *Frontiers in Microbiology*, 11, 1-21, 2020, *doi*:10.3389/fmicb.2020.01367.

[147] Thomas, M. R. and O'Shea, E. K. An intracellular phosphate buffer filters transient fluctuations in extracellular phosphate levels. *Proc. Natl. Acad. Sci. U.S.A.*, 102, 9565-9570, 2005, *doi*:10.1073/pnas.0501122102.

[148] Bru, S. *et al.* Polyphosphate is a key factor for cell survival after DNA damage in eukaryotic cells. *DNA Repair*, 57, 171-178, 2017, *doi*:10.1016/j.dnarep.2017.08.001.

[149] Kim, G.-D., Qiu, D., Jessen, H. J., and Mayer, A. Metabolic Consequences of Polyphosphate Synthesis and Imminent Phosphate Limitation. *mBio*, 14, e00102-00123, 2023, *doi*:10.1128/mbio.00102-23.

[150] Seufferheld, M. J., Alvarez, H. M., and Farias, M. E. Role of Polyphosphates in Microbial Adaptation to Extreme Environments. *Applied and Environmental Microbiology*, 74, 5867-5874, 2008, *doi*:10.1128/AEM.00501-08.

[151] Ohtake, H., Kato, J., Kuroda, A., Wu, H., and Ikeda, T. Regulation of bacterial phosphate taxis and polyphosphate accumulation in response to phosphate starvation stress. *Journal of Biosciences*, 23, 491-499, 1998, *doi*:10.1007/BF02936143.

[152] Freimoser, F. M., Hürlimann, H. C., Jakob, C. A., Werner, T. P., and Amrhein, N. Systematic screening of polyphosphate (poly P) levels in yeast mutant cells reveals strong interdependence with primary metabolism. *Genome Biology*, 7, R109, 2006, *doi*:10.1186/gb-2006-7-11-r109.

[153] Bru, S. *et al.* Polyphosphate is involved in cell cycle progression and genomic stability in *Saccharomyces cerevisiae*. *Molecular Microbiology*, 101, 367-380, 2016, *doi*:10.1111/mmi.13396.

[154] Rao, N. N. and Kornberg, A. Inorganic polyphosphate supports resistance and survival of stationary-phase *Escherichia coli*. *Journal of Bacteriology*, 178, 1394-1400, 1996, *doi*:10.1128/jb.178.5.1394-1400.1996.

[155] Iakovchuk, N., Fabian, J., Dellwig, O., Hassenrück, C., and Schulz-Vogt, H. N. Distinctive physiology of polyphosphate-accumulating *Beggiatoa* suggests an important role in benthic phosphorus cycling. *Applied and Environmental Microbiology*, 91, e02330-02324, 2025, *doi*:10.1128/aem.02330-24.

[156] Morawska, L. P., Hernandez-Valdes, J. A., and Kuipers, O. P. Diversity of bet-hedging strategies in microbial communities-Recent cases and insights. *WIREs Mechanisms of Disease*, 14, e1544, 2022, *doi*:10.1002/wsbm.1544.

[157] Voronkov, A. and Sinetova, M. Polyphosphate accumulation dynamics in a population of Synechocystis sp. PCC 6803 cells under phosphate overplus. *Protoplasma*, 256, 1153-1164, 2019, *doi*:10.1007/s00709-019-01374-2.

[158] Fees, J. Novel approach of P_i recycling: Conversion of waste streams to valuable polyphosphate using engineered *Saccharomyces cerevisiae*. PhD Thesis, RWTH Aachen University, 2024.

[159] Christ, J. J., Smith, S. A., Willbold, S., Morrissey, J. H., and Blank, L. M. Biotechnological synthesis of water-soluble food-grade polyphosphate with *Saccharomyces cerevisiae*. *Biotechnology and Bioengineering*, 117, 2089-2099, 2020, *doi*:10.1002/bit.27337.

[160] Ogawa, N., DeRisi, J., and Brown, P. O. New components of a system for phosphate accumulation and polyphosphate metabolism in *Saccharomyces cerevisiae* revealed by genomic expression analysis. *Molecular Biology of the Cell*, 11, 4309-4321, 2000, *doi*:10.1091/mbc.11.12.4309.

[161] Markham, E. and Byrne, W. J. UPTAKE, STORAGE AND UTILIZATION OF PHOSPHATE BY YEAST III. THE BEHAVIOUR OF PHOSPHATE-STARVED YEAST. *Journal of the Institute of Brewing*, 74, 374-378, 1968, *doi*:10.1002/j.2050-0416.1968.tb03144.x.

[162] Ljungdahl, P. O. and Daignan-Fornier, B. Regulation of Amino Acid, Nucleotide, and Phosphate Metabolism in *Saccharomyces cerevisiae*. *Genetics*, 190, 885-929, 2012, *doi*:10.1534/genetics.111.133306 %J Genetics.

[163] Krallish, I., Gonta, S., and Savenkova, L. Changes in the Pi uptake and polyP accumulation in *Saccharomyces cerevisiae* strains deficient in the synthesis of trehalose and/or glycerol. *Process Biochemistry*, 42, 434-438, 2007, *doi*:10.1016/j.procbio.2006.08.010.

[164] Yoshida, K., Ogawa, N., and Oshima, Y. Function of the PHO regulatory genes for repressible acid phosphatase synthesis in *Saccharomyces cerevisiae*. *Molecular and General Genetics MGG*, 217, 40-46, 1989, *doi*:10.1007/BF00330940.

[165] Carroll, A. S. and O'Shea, E. K. Pho85 and signaling environmental conditions. *Trends Biochemical Sciences*, 27, 87-93, 2002, *doi*:10.1016/S0968-0004(01)02040-0.

[166] Toh, E. A. and Nishizawa, M. Structure and function of cyclin-dependent Pho85 kinase of *Saccharomyces cerevisiae*. *Journal of General and Applied Microbiology*, 47, 107-117, 2001, *doi*:10.2323/jgam.47.107.

[167] Huang, D., Friesen, H., and Andrews, B. Pho85, a multifunctional cyclin-dependent protein kinase in budding yeast. *Molecular Microbiology*, 66, 303-314, 2007, *doi*:10.1111/j.1365-2958.2007.05914.x.

[168] Schneider, K. R., Smith, R. L., and O'Shea, E. K. Phosphate-Regulated Inactivation of the Kinase PHO80-PHO85 by the CDK Inhibitor PHO81. *Science*, 266, 122-126, 1994, *doi*:10.1126/science.7939631.

[169] Ogawa, N. *et al.* Functional Domains of Pho81p, an Inhibitor of Pho85p Protein Kinase, in the Transduction Pathway of Pi Signals in *Saccharomyces cerevisiae*. *Molecular and Cellular Biology*, 15, 997-1004, 1995, *doi*:10.1128/MCB.15.2.997.

[170] Huang, S., Jeffery, D. A., Anthony, M. D., and O'Shea, E. K. Functional Analysis of the Cyclin-Dependent Kinase Inhibitor Pho81 Identifies a Novel Inhibitory Domain. *Molecular and Cellular Biology*, 21, 6695-6705, 2001, *doi*:10.1128/MCB.21.19.6695-6705.2001.

[171] Waters, N. C., Knight, J. P., Creasy, C. L., and Bergman, L. W. The yeast Pho80–Pho85 cyclin–CDK complex has multiple substrates. *Current Genetics*, 46, 1-9, 2004, *doi*:10.1007/s00294-004-0501-0.

[172] Shears, S. B. Inositol pyrophosphates: Why so many phosphates? *Advances in Biological Regulation*, 57, 203-216, 2015, *doi*:10.1016/j.jbior.2014.09.015.

[173] Chabert, V. *et al.* Inositol pyrophosphate dynamics reveals control of the yeast phosphate starvation program through 1,5-IP(8) and the SPX domain of Pho81. *Elife*, 12, 2023, *doi*:10.7554/eLife.87956.

[174] Gu, C. *et al.* The Significance of the Bifunctional Kinase/Phosphatase Activities of Diphosphoinositol Pentakisphosphate Kinases (PPIP5Ks) for Coupling Inositol Pyrophosphate Cell Signaling to Cellular Phosphate Homeostasis. *Journal of Biological Chemistry*, 292, 4544-4555, 2017, *doi*:10.1074/jbc.M116.765743.

[175] Secco, D. *et al.* The emerging importance of the SPX domain-containing proteins in phosphate homeostasis. *New Phytologist*, 193, 842-851, 2012, *doi*:10.1111/j.1469-8137.2011.04002.x.

[176] Secco, D., Wang, C., Shou, H., and Whelan, J. Phosphate homeostasis in the yeast *Saccharomyces cerevisiae,* the key role of the SPX domain-containing proteins. *FEBS Letters*, 586, 289-295, 2012, *doi*:10.1016/j.febslet.2012.01.036.

[177] Auesukaree, C., Tochio, H., Shirakawa, M., Kaneko, Y., and Harashima, S. Plc1p, Arg82p, and Kcs1p, Enzymes Involved in Inositol Pyrophosphate Synthesis, Are Essential for Phosphate Regulation and Polyphosphate Accumulation in *Saccharomyces cerevisiae*. *Journal of Biological Chemistry*, 280, 25127-25133, 2005, *doi*:10.1074/jbc.M414579200.

[178] Wild, R. *et al.* Control of eukaryotic phosphate homeostasis by inositol polyphosphate sensor domains. *Science*, 352, 986-990, 2016, *doi*:10.1126/science.aad9858.

[179] Lee, Y.-S., Mulugu, S., York, J. D., and O'Shea, E. K. Regulation of a Cyclin-CDK-CDK Inhibitor Complex by Inositol Pyrophosphates. *Science*, 316, 109-112, 2007, *doi*:10.1126/science.1139080.

[180] Azevedo, C. and Saiardi, A. Eukaryotic phosphate homeostasis: The inositol pyrophosphate perspective. *Trends Biochemical Sciences*, 42, 219-231, 2017, *doi*:10.1016/j.tibs.2016.10.008.

[181] Shears, S. B. Intimate connections: Inositol pyrophosphates at the interface of metabolic regulation and cell signaling. *Journal of Cellular Physiology*, 233, 1897-1912, 2018, *doi*:10.1002/jcp.26017.

[182] Vardi, N. *et al.* Sequential Feedback Induction Stabilizes the Phosphate Starvation Response in Budding Yeast. *Cell Reports*, 9, 1122-1134, 2014, *doi*:10.1016/j.celrep.2014.10.002.

[183] Springer, M., Wykoff, D. D., Miller, N., and O'Shea, E. K. Partially Phosphorylated Pho4 Activates Transcription of a Subset of Phosphate-Responsive Genes. *PLOS Biology*, 1, e28, 2003, *doi*:10.1371/journal.pbio.0000028.

[184] Conrad, M. *et al.* Nutrient sensing and signaling in the yeast *Saccharomyces cerevisiae*. *FEMS Microbiology Reviews*, 38, 254-299, 2014, *doi*:10.1111/1574-6976.12065 %J FEMS Microbiology Reviews.

[185] Oshima, Y. The phosphatase system in *Saccharomyces cerevisiae*. *Genes & Genetic Systems*, 72, 323-334, 1997, *doi*:10.1266/ggs.72.323.

[186] Wykoff, D. D., Rizvi, A. H., Raser, J. M., Margolin, B., and O'Shea, E. K. Positive feedback regulates switching of phosphate transporters in *S. cerevisiae*. *Molecular Cell*, 27, 1005-1013, 2007, *doi*:10.1016/j.molcel.2007.07.022.

[187] Yang, S. Y., Huang, T. K., Kuo, H. F., and Chiou, T. J. Role of vacuoles in phosphorus storage and remobilization. *J Exp Bot*, 68, 3045-3055, 2017, *doi*:10.1093/jxb/erw481.

[188] Patton-Vogt, J. Transport and metabolism of glycerophosphodiesters produced through phospholipid deacylation. *Biochimica et Biophysica Acta (BBA) - Molecular and Cell Biology of Lipids*, 1771, 337-342, 2007, *doi*:10.1016/j.bbalip.2006.04.013.

[189] Xu, Y. F. *et al.* Nucleotide degradation and ribose salvage in yeast. *Molecular systems biology*, 9, 665, 2013, *doi*:10.1038/msb.2013.21.

[190] Gerasimaitė, R., Sharma, S., Desfougères, Y., Schmidt, A., and Mayer, A. Coupled synthesis and translocation restrains polyphosphate to acidocalcisome-like vacuoles and prevents its toxicity. *Journal of Cell Science*, 127, 5093-5104, 2014, *doi*:10.1242/jcs.159772 %J Journal of Cell Science.

[191] Lander, N., Cordeiro, C., Huang, G., and Docampo, R. Polyphosphate and acidocalcisomes. *Biochemical Society Transactions*, 44, 1-6, 2016, *doi*:10.1042/bst20150193.

[192] Klionsky, D. J., Herman, P. K., and Emr, S. D. The fungal vacuole: composition, function, and biogenesis. *Microbiol Rev*, 54, 266-292, 1990, *doi*:10.1128/mr.54.3.266-292.1990.

[193] Kulakovskaya, T. V., Lichko, L. P., Vagabov, V. M., and Kulaev, I. S. Inorganic polyphosphates in mitochondria. *Biochemistry (Moscow)*, 75, 825-831, 2010, *doi*:10.1134/S0006297910070035.

[194] Lichko, L., Kulakovskaya, T., Pestov, N., and Kulaev, I. Inorganic polyphosphates and exopolyphosphatases in cell compartments of the yeast *Saccharomyces cerevisiae* under inactivation of PPX1 and PPN1 genes. *Biosci Rep*, 26, 45-54, 2006, *doi*:10.1007/s10540-006-9003-2.

[195] Voříšek, J., Knotková, A., and Kotyk, A. Fine Cytochemical Localization of Polyphosphates in the Yeast *Saccharomyces cerevisiae*. *Zentralblatt für Mikrobiologie*, 137, 421-432, 1982, *doi*:10.1016/S0232-4393(82)80021-8.

[196] Gerasimaite, R. and Mayer, A. Ppn2, a novel Zn2+-dependent polyphosphatase in the acidocalcisome-like yeast vacuole. *Journal of Cell Science*, 130, 1625-1636, 2017, *doi*:10.1242/jcs.201061.

[197] Gerasimaitė, R. and Mayer, A. Enzymes of yeast polyphosphate metabolism: structure, enzymology and biological roles. *Biochemical Society Transactions*, 44, 234-239, 2016, *doi*:10.1042/bst20150213.

[198] Andreeva, N., Ryazanova, L., Dmitriev, V., Kulakovskaya, T., and Kulaev, I. Adaptation of *Saccharomyces cerevisiae* to toxic manganese concentration triggers changes in inorganic polyphosphates. *FEMS Yeast Research*, 13, 463-470, 2013, *doi*:10.1111/1567-1364.12049 %J FEMS Yeast Research.

[199] Pick, U. and Weiss, M. Polyphosphate Hydrolysis within Acidic Vacuoles in Response to Amine-Induced Alkaline Stress in the Halotolerant Alga Dunaliella salina. *Plant Physiology*, 97, 1234-1240, 1991, *doi*:10.1104/pp.97.3.1234 %J Plant Physiology.

[200] Müller, O. *et al.* The Vtc proteins in vacuole fusion: coupling NSF activity to V(o) trans-complex formation. *The EMBO Journal*, 21, 259-269, 2002, *doi*:10.1093/emboj/21.3.259.

[201] Tomashevsky, A. *et al.* VTC4 Polyphosphate Polymerase Knockout Increases Stress Resistance of *Saccharomyces cerevisiae* Cells. *Cells. Biology*, 10, 487, 2021.

[202] Liu, W. *et al.* Cryo-EM structure of the polyphosphate polymerase VTC reveals coupling of polymer synthesis to membrane transit. *EMBO Journal*, 42, e113320, 2023, *doi*:10.15252/embj.2022113320.

[203] Uttenweiler, A., Schwarz, H., Neumann, H., and Mayer, A. The vacuolar transporter chaperone (VTC) complex is required for microautophagy. *Molecular Biology of the Cell*, 18, 166-175, 2007, *doi*:10.1091/mbc.e06-08-0664.

[204] Hothorn, M. *et al.* Catalytic Core of a Membrane-Associated Eukaryotic Polyphosphate Polymerase. *Science*, 324, 513-516, 2009, *doi*:10.1126/science.1168120.

[205] Desfougères, Y., Gerasimaite, R., Jessen, H. J., and Mayer, A. Vtc5, a novel subunit of the vacuolar transporter chaperone complex, regulates polyphosphate synthesis and phosphate homeostasis in yeast. *Journal of Biological Chemistry*, 291, 22262-22275, 2016, *doi*:10.1074/jbc.M116.746784.

[206] Guan, Z. *et al.* The cytoplasmic synthesis and coupled membrane translocation of eukaryotic polyphosphate by signal-activated VTC complex. *Nature Communications*, 14, 718, 2023, *doi*:10.1038/s41467-023-36466-4.

[207] Gerasimaite, R. *et al.* Inositol Pyrophosphate Specificity of the SPX-Dependent Polyphosphate Polymerase VTC. *ACS Chemical Biology*, 12, 648-653, 2017, *doi*:10.1021/acschembio.7b00026.

[208] Langen, P. and Liss, E. Differentiation of orthophosphates of yeast cells. *Biochem. Z.*, 332, 403–406, 1960.

[209] Hürlimann, H. C. and et al. Pho91 Is a Vacuolar Phosphate Transporter That Regulates Phosphate and Polyphosphate Metabolism in *Saccharomyces cerevisiae*. *Molecular Biology of the Cell*, 18, 4438-4445, 2007, *doi*:10.1091/mbc.E07-05-0457.

[210] Andreeva, N., Trilisenko, L., Eldarov, M., and Kulakovskaya, T. Polyphosphatase PPN1 of *Saccharomyces cerevisiae*: Switching of Exopolyphosphatase and Endopolyphosphatase Activities. *PLoS ONE*, 10, 1-11, 2015, *doi*:10.1371/journal.pone.0119594.

[211] Kumble, K. D. and Kornberg, A. Endopolyphosphatases for long chain inorganic polyphosphate in yeast and mammals. *Journal of Biological Chemistry*, 271, 27146-27151, 1996, *doi*:10.1074/jbc.271.43.27146.

[212] Lichko, L. P., Kulakovskaya, T. V., Kulakovskaya, E. V., and Kulaev, I. S. Inactivation of PPX1 and PPN1 genes encoding exopolyphosphatases of *Saccharomyces cerevisiae* does not prevent utilization of polyphosphates as phosphate reserve. *Biochemistry (Moscow)*, 73, 985-989, 2008, *doi*:10.1134/S0006297908090046.

[213] Wurst, H. and Kornberg, A. A soluble exopolyphosphatase of *Saccharomyces cerevisiae.* Purification and characterization. *Journal of Biological Chemistry*, 269, 10996-11001, 1994, *doi*:10.1016/S0021-9258(19)78082-X.

[214] Persson, B. L. *et al.* Phosphate permeases of *Saccharomyces cerevisiae*. *Biochimica et Biophysica Acta (BBA) - Bioenergetics*, 1365, 23-30, 1998, *doi*:10.1016/S0005-2728(98)00037-1.

[215] Bun-Ya, M., Nishimura, M., Harashima, S., and Oshima, Y. The PHO84 gene of *Saccharomyces cerevisiae* encodes an inorganic phosphate transporter. *Molecular and Cellular Biology*, 11, 3229-3238, 1991, *doi*:10.1128/mcb.11.6.3229-3238.1991.

[216] Eskes, E., Deprez, M.-A., Wilms, T., and Winderickx, J. pH homeostasis in yeast; the phosphate perspective. *Current Genetics*, 64, 155-161, 2018, *doi*:10.1007/s00294-017-0743-2.

[217] Martinez, P. and Persson, B. L. Identification, cloning and characterization of a derepressible Na+-coupled phosphate transporter in *Saccharomyces cerevisiae*. *Molecular and General Genetics MGG*, 258, 628-638, 1998, *doi*:10.1007/s004380050776.

[218] Serra-Cardona, A., Petrezsélyová, S., Canadell, D., Ramos, J., and Ariño, J. Coregulated Expression of the Na+/Phosphate Pho89 Transporter and Ena1 Na+-ATPase Allows Their Functional Coupling under High-pH Stress. *Molecular and Cellular Biology*, 34, 4420-4435, 2014, *doi*:10.1128/MCB.01089-14.

[219] Hürlimann, H. C., Pinson, B., Stadler-Waibel, M., Zeeman, S. C., and Freimoser, F. M. The SPX domain of the yeast low-affinity phosphate transporter Pho90 regulates transport activity. *EMBO Reports*, 10, 1003-1008, 2009, *doi*:10.1038/embor.2009.105.

[220] Levy, S., Kafri, M., Carmi, M., and Barkai, N. The Competitive Advantage of a Dual-Transporter System. *Science*, 334, 1408-1412, 2011, *doi*:10.1126/science.1207154.

[221] Christ, J. J. and Blank, L. M. Analytical polyphosphate extraction from *Saccharomyces cerevisiae*. *Analytical Biochemistry*, 563, 71-78, 2018, *doi*:10.1016/j.ab.2018.09.021.

[222] Christ, J. J. and Blank, L. M. Enzymatic quantification and length determination of polyphosphate down to a chain length of two. *Analytical Biochemistry*, 548, 82-90, 2018, *doi*:10.1016/j.ab.2018.02.018.

[223] Angelova, P. R. *et al.* In Situ Investigation of Mammalian Inorganic Polyphosphate Localization Using Novel Selective Fluorescent Probes JC-D7 and JC-D8. *ACS Chemical Biology*, 9, 2101-2110, 2014, *doi*:10.1021/cb5000696.

[224] Robinson, T. E., Arkinstall, L. A., Cox, S. C., and Grover, L. M. Determining the Structure of Hexametaphosphate by Titration and 31P-NMR Spectroscopy. *Comments on Inorganic Chemistry*, 42, 47-59, 2022, *doi*:10.1080/02603594.2021.1973444.

[225] Pronk, J. T. Auxotrophic Yeast Strains in Fundamental and Applied Research. *Applied and Environmental Microbiology*, 68, 2095-2100, 2002, *doi*:10.1128/AEM.68.5.2095-2100.2002.

[226] Winzeler, E. A. *et al.* Functional characterization of the *S. cerevisiae* genome by gene deletion and parallel analysis. *Science*, 285, 901-906, 1999, *doi*:10.1126/science.285.5429.901.

[227] Deitert, A. *et al.* Rapid Fluorescence Assay for Polyphosphate in Yeast Extracts Using JC-D7. *Yeast*, 41, 593-604, 2024, *doi*:10.1002/yea.3979.

[228] Szklarczyk, D. *et al.* The STRING database in 2023: protein-protein association networks and functional enrichment analyses for any sequenced genome of interest. *Nucleic Acids Res*, 51, D638-d646, 2023, *doi*:10.1093/nar/gkac1000.

[229] Duetz, W. A. *et al.* Methods for Intense Aeration, Growth, Storage, and Replication of Bacterial Strains in Microtiter Plates. *Applied and Environmental Microbiology*, 66, 2641-2646, 2000, *doi*:10.1128/AEM.66.6.2641-2646.2000.

[230] Wahjudi, S. M. W., Engel, D., and Büchs, J. Metabolic studies of *Ogataea polymorpha* using nine different corn steep liquors. *BMC Biotechnology*, 25, 5, 2025, *doi*:10.1186/s12896-024-00927-5.

[231] Todd, R. T., Braverman, A. L., and Selmecki, A. Flow Cytometry Analysis of Fungal Ploidy. *Current Protocols in Microbiology*, 50, e58, 2018, *doi*:10.1002/cpmc.58.

[232] Verduyn, C., Postma, E., Scheffers, W. A., and Van Dijken, J. P. Effect of benzoic acid on metabolic fluxes in yeasts: a continuous-culture study on the regulation of respiration and alcoholic fermentation. *Yeast*, 8, 501-517, 1992, *doi*:10.1002/yea.320080703.

[233] Anderlei, T., Zang, W., Papaspyrou, M., and Büchs, J. Online respiration activity measurement (OTR, CTR, RQ) in shake flasks. *Biochemical Engineering Journal*, 17, 187-194, 2004, *doi*:10.1016/S1369-703X(03)00181-5.

[234] Vyas, V. K. *et al.* New CRISPR Mutagenesis Strategies Reveal Variation in Repair Mechanisms among Fungi. *mSphere*, 3, 10.1128/msphere.00154-00118, 2018, *doi*:10.1128/msphere.00154-18.

[235] Concordet, J.-P. and Haeussler, M. CRISPOR: intuitive guide selection for CRISPR/Cas9 genome editing experiments and screens. *Nucleic Acids Res*, 46, W242-W245, 2018, *doi*:10.1093/nar/gky354 %J Nucleic Acids Research.

[236] Nguyen Van, D. Untersuchungen zur Zinkanreicherung von Hefen in Abhängigkeit vom Polyphosphatstatus. Diplomarbeit, TU Berlin, 2023.

[237] Mertens, A. Deletion of the polyphosphatase Ddp1 in *Saccharomyces cerevisiae* and development of a fluorescence based screening method for polyphosphate detection. Bachelor Thesis, RWTH Aachen University, 2023.

[238] Plouviez, M. *et al.* Responses of *Chlamydomonas reinhardtii* during the transition from P-deficient to P-sufficient growth (the P-overplus response): The roles of the vacuolar transport chaperones and polyphosphate synthesis. *Journal of Phycology*, 57, 988-1003, 2021, *doi*:10.1111/jpy.13145.

[239] Shen, Q. W. and Swartz, D. R. Influence of salt and pyrophosphate on bovine fast and slow myosin S1 dissociation from actin. *Meat Science*, 84, 364-370, 2010, *doi*:10.1016/j.meatsci.2009.09.003.

[240] Wazer, J. R. V. and Campanella, D. A. Structure and Properties of the Condensed Phosphates. IV. Complex Ion Formation in Polyphosphate Solutions. *Journal of the American Chemical Society*, 72, 655-663, 1950, *doi*:10.1021/ja01158a004.

[241] Bru, S., Jiménez, J., Canadell, D., Ariño, J., and Clotet, J. Improvement of biochemical methods of polyP quantification. *Microbial cell*, 4, 6-15, 2016, *doi*:10.15698/mic2017.01.551.

[242] Christ, J. J., Willbold, S., and Blank, L. M. Methods for the analysis of polyphosphate in the life sciences. *Analytical Chemistry*, 92, 4167-4176, 2020, *doi*:10.1021/acs.analchem.9b05144.

[243] Godinot, C., Gaysinski, M., Thomas, O. P., Ferrier-Pagès, C., and Grover, R. On the use of 31P NMR for the quantification of hydrosoluble phosphorus-containing compounds in coral host tissues and cultured zooxanthellae. *Scientific Reports*, 6, 21760, 2016, *doi*:10.1038/srep21760.

[244] Aschar-Sobbi, R. *et al.* High Sensitivity, Quantitative Measurements of Polyphosphate Using a New DAPI-Based Approach. *Journal of Fluorescence*, 18, 859-866, 2008, *doi*:10.1007/s10895-008-0315-4.

[245] Streichan, M., Golecki, J. R., and Schön, G. Polyphosphate-accumulating bacteria from sewage plants with different proceses for biological phosphorus removal. *FEMS Microbiology Ecology*, 6, 113-124, 1990, *doi*:10.1111/j.1574-6968.1990.tb03931.x %J FEMS Microbiology Ecology.

[246] Gomes, F. M. *et al.* New insights into the in situ microscopic visualization and quantification of inorganic polyphosphate stores by 4',6-diamidino-2-phenylindole (DAPI)-staining. *European Journal of Histochemistry*, 57, e34, 2013, *doi*:10.4081/ejh.2013.e34.

[247] Martin, P. and Mooy, B. A. S. V. Fluorometric Quantification of Polyphosphate in Environmental Plankton Samples: Extraction Protocols, Matrix Effects, and Nucleic Acid Interference. *Applied and Environmental Microbiology*, 79, 273-281, 2013, *doi*:10.1128/AEM.02592-12.

[248] Kolozsvari, B., Parisi, F., and Saiardi, A. Inositol phosphates induce DAPI fluorescence shift. *Biochemical Journal*, 460, 377-385, 2014, *doi*:10.1042/BJ20140237 %J Biochemical Journal.

[249] Diaz, J. M. and Ingall, E. D. Fluorometric Quantification of Natural Inorganic Polyphosphate. *Environmental Science & Technology*, 44, 4665-4671, 2010, *doi*:10.1021/es100191h.

[250] Zhu, J. *et al.* A genetically validated approach for detecting inorganic polyphosphates in plants. *The Plant Journal*, 102, 507-516, 2020, *doi*:10.1111/tpj.14642.

[251] Yang, X. *et al.* Quantification of Polyphosphate in Environmental Planktonic Samples Using a Novel Fluorescence Dye JC-D7. *Environmental Science & Technology*, 58, 14249-14259, 2024, *doi*:10.1021/acs.est.4c04545.

[252] Hope, C. K., Billingsley, K., de Josselin de Jong, E., and Higham, S. M. A Preliminary Study of the Effects of pH upon Fluorescence in Suspensions of Prevotella intermedia. *PLoS ONE*, 11, e0158835, 2016, *doi*:10.1371/journal.pone.0158835.

[253] Sethuraman, A., Rao, N. N., and Kornberg, A. The endopolyphosphatase gene: Essential in *Saccharomyces cerevisiae*. *Proc. Natl. Acad. Sci. U.S.A.*, 98, 8542-8547, 2001, *doi*:10.1073/pnas.151269398.

[254] Pestov, N. A., Kulakovskaya, T. V., and Kulaev, I. S. Effects of inactivation of the PPN1 gene on exopolyphosphatases, inorganic polyphosphates and function of mitochondria in the yeast *Saccharomyces cerevisiae*. *FEMS Yeast Research*, 5, 823-828, 2005, *doi*:10.1016/j.femsyr.2005.03.002 %J FEMS Yeast Research.

[255] Andreeva, N., Lichko, L., Trilisenko, L., Kulakovskiy, I., and Kulakovskaya, T. in *Inorganic Polyphosphates in Eukaryotic Cells.* Yeast Polyphosphatases PPX1 and PPN1: Properties, Functions, and Localization (eds Tatiana Kulakovskaya, Evgeny Pavlov, & Elena N. Dedkova), 15-33, 2016, *doi*:10.1007/978-3-319-41073-9_2 (Springer).

[256] Lemire, J. M., Willcocks, T., Halvorson, H. O., and Bostian, K. A. Regulation of Repressible Acid Phosphatase Gene Transcription in *Saccharomyces cerevisiae*. *Molecular and Cellular Biology*, 5, 2131-2141, 1985, *doi*:10.1128/mcb.5.8.2131-2141.1985.

[257] van Eunen, K. *et al.* Measuring enzyme activities under standardized in vivo-like conditions for systems biology. *The FEBS Journal*, 277, 749-760, 2010, *doi*:10.1111/j.1742-4658.2009.07524.x.

[258] Breus, N. A., Ryazanova, L. P., Dmitriev, V. V., Kulakovskaya, T. V., and Kulaev, I. S. Accumulation of phosphate and polyphosphate by *Cryptococcus humicola* and *Saccharomyces cerevisiae* in the absence of nitrogen. *FEMS Yeast Research*, 12, 617-624, 2012, *doi*:10.1111/j.1567-1364.2012.00812.x %J FEMS Yeast Research.

[259] Khourchi, S., Delaplace, P., and Bargaz, A. Polyphosphate fertilizer use efficiency strongly relies on soil physicochemical properties and root-microbial activities. *Geoderma*, 429, 116281, 2023, *doi*:10.1016/j.geoderma.2022.116281.

[260] Kapuscinski, J. Interactions of nucleic acids with fluorescent dyes: spectral properties of condensed complexes. *Journal of Histochemistry & Cytochemistry*, 38, 1323-1329, 1990, *doi*:10.1177/38.9.1696951.

[261] Kapuscinski, J. DAPI: a DNA-Specific Fluorescent Probe. *Biotechnic & Histochemistry*, 70, 220-233, 1995, *doi*:10.3109/10520299509108199.

[262] Ohtomo, R., Sekiguchi, Y., Kojima, T., and Saito, M. Different chain length specificity among three polyphosphate quantification methods. *Analytical Biochemistry*, 383, 210-216, 2008, *doi*:10.1016/j.ab.2008.08.002.

[263] Saito, K., Ohtomo, R., Kuga-Uetake, Y., Aono, T., and Saito, M. Direct Labeling of Polyphosphate at the Ultrastructural Level in *Saccharomyces cerevisiae* by Using the Affinity of the Polyphosphate Binding Domain of *Escherichia coli* Exopolyphosphatase. *Applied and Environmental Microbiology*, 71, 5692-5701, 2005, *doi*:10.1128/AEM.71.10.5692-5701.2005.

[264] Lonetti, A. *et al.* Identification of an Evolutionarily Conserved Family of Inorganic Polyphosphate Endopolyphosphatases. *Journal of Biological Chemistry*, 286, 31966-31974, 2011, *doi*:10.1074/jbc.M111.266320.

[265] Sun, J. *et al.* Accumulation and Enrichment of Trace Elements by Yeast Cells and Their Applications: A Critical Review. *Microorganisms*, 10, 1746, 2022, *doi*:10.3390/microorganisms10091746

[266] Kulakovskaya, T. Inorganic polyphosphates and heavy metal resistance in microorganisms. *World Journal of Microbiology and Biotechnology*, 34, 139, 2018, *doi*:10.1007/s11274-018-2523-7.

[267] Müller, W. E. G., Schröder, H. C., and Wang, X. Inorganic Polyphosphates As Storage for and Generator of Metabolic Energy in the Extracellular Matrix. *Chemical Reviews*, 119, 12337-12374, 2019, *doi*:10.1021/acs.chemrev.9b00460.

[268] Jastrzab, R., Nowak, M., Zabiszak, M., Odani, A., and Kaczmarek, M. T. Significance and properties of the complex formation of phosphate and polyphosphate groups in particles present in living cells. *Coordination Chemistry Reviews*, 435, 213810, 2021, *doi*:10.1016/j.ccr.2021.213810.

[269] Park, Y., Malliakas, C. D., Zhou, Q., Gu, A. Z., and Aristilde, L. Molecular Coordination, Structure, and Stability of Metal-Polyphosphate Complexes Resolved by Molecular Modeling and X-ray Scattering: Structural Insights on the Biological Fate of Polyphosphate. *Environmental Science & Technology*, 55, 14185-14193, 2021, *doi*:10.1021/acs.est.1c04782.

[270] Cockrell, A. L., Holmes-Hampton, G. P., McCormick, S. P., Chakrabarti, M., and Lindahl, P. A. Mössbauer and EPR Study of Iron in Vacuoles from Fermenting *Saccharomyces cerevisiae*. *Biochemistry*, 50, 10275-10283, 2011, *doi*:10.1021/bi2014954.

[271] Nguyen, T. Q., Dziuba, N., and Lindahl, P. A. Isolated *Saccharomyces cerevisiae* vacuoles contain low-molecular-mass transition-metal polyphosphate complexes†. *Metallomics*, 11, 1298-1309, 2019, *doi*:10.1039/c9mt00104b %J Metallomics.

[272] Schröder, H. C. *et al.* Inorganic Polyphosphate: Coacervate Formation and Functional Significance in Nanomedical Applications. *International Journal Nanomedicine*, 17, 5825-5850, 2022, *doi*:10.2147/ijn.S389819.

[273] Yan, Z. *et al.* Hydrolysis Mechanism of Water-Soluble Ammonium Polyphosphate Affected by Zinc Ions. *ACS Omega*, 8, 17573-17582, 2023, *doi*:10.1021/acsomega.2c07642.

[274] Huang, Z., Zhang, X.-a., Bosch, M., Smith, S. J., and Lippard, S. J. Tris(2-pyridylmethyl)amine (TPA) as a membrane-permeable chelator for interception of biological mobile zinc†. *Metallomics*, 5, 648-655, 2013, *doi*:10.1039/c3mt00103b %J Metallomics.

[275] Anderegg, G., Hubmann, E., Podder, N. G., and Wenk, F. Pyridinderivate als Komplexbildner. XI. Die Thermodynamik der Metallkomplexbildung mit Bis-, Tris- und Tetrakis[(2-pyridyl)methyl]-aminen. *Helvetica Chimica Acta*, 60, 123-140, 1977, *doi*:10.1002/hlca.19770600115.

[276] van Wazer, J. Phosphorous and its Compounds. *Interscience*, 1958.

[277] Chen, Z. *et al.* A systematic study of regulating inorganic polyphosphates production in *Saccharomyces cerevisiae*. *Synthetic and Systems Biotechnology*, 10, 816-826, 2025, *doi*:10.1016/j.synbio.2025.04.004.

[278] Holbein, S., Freimoser, F. M., Werner, T. P., Wengi, A., and Dichtl, B. Cordycepin-hypersensitive growth links elevated polyphosphate levels to inhibition of poly(A) polymerase in *Saccharomyces cerevisiae*. *Nucleic Acids Res*, 36, 353-363, 2007, *doi*:10.1093/nar/gkm990 %J Nucleic Acids Research.

[279] Hirata, R., Graham, L. A., Takatsuki, A., Stevens, T. H., and Anraku, Y. VMA11 and VMA16 Encode Second and Third Proteolipid Subunits of the *Saccharomyces cerevisiae*

Vacuolar Membrane H+-ATPase*. *Journal of Biological Chemistry*, 272, 4795-4803, 1997, *doi*:10.1074/jbc.272.8.4795.

[280] Rühle, T. and Leister, D. Assembly of F1F0-ATP synthases. *Biochimica et Biophysica Acta (BBA) - Bioenergetics*, 1847, 849-860, 2015, *doi*:10.1016/j.bbabio.2015.02.005.

[281] Helleckes, L. M. *et al.* High-throughput screening of catalytically active inclusion bodies using laboratory automation and Bayesian optimization. *Microbial Cell Factories*, 23, 67, 2024, *doi*:10.1186/s12934-024-02319-y.

[282] Hemmerich, J., Noack, S., Wiechert, W., and Oldiges, M. Microbioreactor Systems for Accelerated Bioprocess Development. *Biotechnology Journal*, 13, 1700141, 2018, *doi*:10.1002/biot.201700141.

[283] Auesukaree, C. *et al.* Intracellular Phosphate Serves as a Signal for the Regulation of the PHO Pathway in *Saccharomyces cerevisiae*. *Journal of Biological Chemistry*, 279, 17289-17294, 2004, *doi*:10.1074/jbc.M312202200.

[284] Umeda, C. *et al.* Overexpression of polyphosphate polymerases and deletion of polyphosphate phosphatases shorten the replicative lifespan in yeast. *FEBS Letters*, 597, 2316-2333, 2023, *doi*:10.1002/1873-3468.14715.

[285] Ojima, Y., Naoi, K., Akiyoshi, R., and Azuma, M. Quantitative analysis of phosphate accumulation in PHO regulatory system-mutant strains of *Saccharomyces cerevisiae*. *Archives of Microbiology*, 205, 138, 2023, *doi*:10.1007/s00203-023-03488-x.

[286] Bowring, B. G. *et al.* Dysregulating PHO Signaling via the CDK Machinery Differentially Impacts Energy Metabolism, Calcineurin Signaling, and Virulence in *Cryptococcus neoformans*. *mBio*, 14, e03551-03522, 2023, *doi*:10.1128/mbio.03551-22.

[287] Rosenfeld, L. *et al.* The effect of phosphate accumulation on metal ion homeostasis in *Saccharomyces cerevisiae*. *JBIC Journal of Biological Inorganic Chemistry*, 15, 1051-1062, 2010, *doi*:10.1007/s00775-010-0664-8.

[288] Henk, A. Evaluation of industrial yeast for polyphosphate production in fermentation processes. Bachelor Thesis, RWTH Aachen University, 2025.

[289] Parapouli, M., Vasileiadis, A., Afendra, A. S., and Hatziloukas, E. *Saccharomyces cerevisiae* and its industrial applications. *AIMS Microbiol*, 6, 1-31, 2020, *doi*:10.3934/microbiol.2020001.

[290] Gallone, B. *et al.* Domestication and Divergence of *Saccharomyces cerevisiae* Beer Yeasts. *Cell*, 166, 1397-1410.e1316, 2016, *doi*:10.1016/j.cell.2016.08.020.

[291] van der Hoek, S. A. *et al.* Engineering the Yeast *Saccharomyces cerevisiae* for the Production of L-(+)-Ergothioneine. *Frontiers Bioengineering and Biotechnology*, 7, 262, 2019, *doi*:10.3389/fbioe.2019.00262.

[292] Salari, R. and Salari, R. Investigation of the Best *Saccharomyces cerevisiae* Growth Condition. *Electron Physician*, 9, 3592-3597, 2017, *doi*:10.19082/3592.

[293] Nielsen, J. Yeast Systems Biology: Model Organism and Cell Factory. *Biotechnology Journal*, 14, 1800421, 2019, *doi*:10.1002/biot.201800421.

[294] Pinto, J., Tavakolian, N., Li, C. B., and Stelkens, R. The relationship between cell density and cell count differs among *Saccharomyces* yeast species. *MicroPubl Biol*, 2024, 2024, *doi*:10.17912/micropub.biology.001215.

[295] Kuriyama, H. and Kobayashi, H. Effects of oxygen supply on yeast growth and metabolism in continuous fermentation. *Journal of Fermentation and Bioengineering*, 75, 364-367, 1993, *doi*:10.1016/0922-338X(93)90135-U.

[296] Westman, J. O. and Franzén, C. J. Current progress in high cell density yeast bioprocesses for bioethanol production. *Biotechnology Journal*, 10, 1185-1195, 2015, *doi*:10.1002/biot.201400581.

[297] Shen, D., He, X., Weng, P., Liu, Y., and Wu, Z. A review of yeast: High cell-density culture, molecular mechanisms of stress response and tolerance during fermentation. *FEMS Yeast Research*, 22, 2022, *doi*:10.1093/femsyr/foac050.

[298] Shojaosadati, S., Kolaei, S., Babaeipour, V., and Farnoud, A. Recent advances in high cell density cultivation for production of recombinant protein. *Iranian J. Biotechnol*, 6, 2007.

[299] Weber, A., Prokazov, Y., Zuschratter, W., and Hauser, M. J. B. Desynchronisation of Glycolytic Oscillations in Yeast Cell Populations. *PLoS ONE*, 7, e43276, 2012, *doi*:10.1371/journal.pone.0043276.

[300] Ahmad, M. R., Nakajima, M., Kojima, S., Homma, M., and Fukuda, T. The Effects of Cell Sizes, Environmental Conditions, and Growth Phases on the Strength of Individual W303 Yeast Cells Inside ESEM. *IEEE Transactions on NanoBioscience*, 7, 185-193, 2008, *doi*:10.1109/TNB.2008.2002281.

[301] Aon, J. C., Tecson, R. C., and Loladze, V. *Saccharomyces cerevisiae* morphological changes and cytokinesis arrest elicited by hypoxia during scale-up for production of therapeutic recombinant proteins. *Microbial Cell Factories*, 17, 195, 2018, *doi*:10.1186/s12934-018-1044-2.

[302] Fukuda, N. Apparent diameter and cell density of yeast strains with different ploidy. *Scientific Reports*, 13, 1513, 2023, *doi*:10.1038/s41598-023-28800-z.

[303] Postma, E., Verduyn, C., Scheffers, W. A., and Van Dijken, J. P. Enzymic analysis of the crabtree effect in glucose-limited chemostat cultures of *Saccharomyces cerevisiae*. *Applied Environmental Microbiology*, 55, 468-477, 1989, *doi*:10.1128/aem.55.2.468-477.1989.

[304] Van Hoek, P., Van Dijken, J. P., and Pronk, J. T. Effect of specific growth rate on fermentative capacity of baker's yeast. *Applied Environmental Microbiology*, 64, 4226-4233, 1998, *doi*:10.1128/aem.64.11.4226-4233.1998.

[305] van Hoek, P., de Hulster, E., van Dijken, J. P., and Pronk, J. T. Fermentative capacity in high-cell-density fed-batch cultures of baker's yeast. *Biotechnology and Bioengineering*, 68, 517-523, 2000, *doi*:10.1002/(SICI)1097-0290(20000605)68:5<517::AID-BIT5>3.0.CO;2-O.

[306] Michaillat, L. and Mayer, A. Identification of Genes Affecting Vacuole Membrane Fragmentation in *Saccharomyces cerevisiae*. *PLoS ONE*, 8, e54160, 2013, *doi*:10.1371/journal.pone.0054160.

[307] Boekhout, T. *et al.* Trends in yeast diversity discovery. *Fungal Diversity*, 114, 2021, *doi*:10.1007/s13225-021-00494-6.

[308] Vries, A. R. G. d., Pronk, J. T., and Daran, J.-M. G. Industrial Relevance of Chromosomal Copy Number Variation in *Saccharomyces* Yeasts. *Appl Environ Microbiol*, 83, e03206-03216, 2017, *doi*:10.1128/AEM.03206-16.

[309] Wilkening, S. *et al.* An evaluation of high-throughput approaches to QTL mapping in *Saccharomyces cerevisiae*. *Genetics*, 196, 853-865, 2014, *doi*:10.1534/genetics.113.160291.

[310] Bigey, F. *et al.* Evidence for Two Main Domestication Trajectories in *Saccharomyces cerevisiae* Linked to Distinct Bread-Making Processes. *Current Biology*, 31, 722-732.e725, 2021, *doi*:10.1016/j.cub.2020.11.016.

[311] Mangado, A., Morales, P., Gonzalez, R., and Tronchoni, J. Evolution of a Yeast With Industrial Background Under Winemaking Conditions Leads to Diploidization and Chromosomal Copy Number Variation. *Frontiers Microbiology*, 9, 1816, 2018, *doi*:10.3389/fmicb.2018.01816.

[312] Manoukian, L., Stein, R. S., Correa, J. A., Frigon, D., and Omelon, S. Short-chain polyphosphates: Extraction effects on migration and size estimation of *Saccharomyces cerevisiae* extracts with polyacrylamide gel electrophoresis. *Electrophoresis*, 44, 1197-1205, 2023, *doi*:10.1002/elps.202300055.

[313] Steenwyk, J. L. and Rokas, A. Copy Number Variation in Fungi and Its Implications for Wine Yeast Genetic Diversity and Adaptation. *Frontiers Microbiology*, 9, 288, 2018, *doi*:10.3389/fmicb.2018.00288.

[314] Robinson, D. *et al.* Gene-by-environment interactions influence the fitness cost of gene copy-number variation in yeast. *G3 (Bethesda)*, 13, 2023, *doi*:10.1093/g3journal/jkad159.

[315] Gallone, B. *et al.* Origins, evolution, domestication and diversity of *Saccharomyces* beer yeasts. *Current Opinion in Biotechnology*, 49, 148-155, 2018, *doi*:10.1016/j.copbio.2017.08.005.
[316] Steensels, J. and Verstrepen, K. J. Taming wild yeast: potential of conventional and nonconventional yeasts in industrial fermentations. *Annual Review of Microbiology*, 68, 61-80, 2014, *doi*:10.1146/annurev-micro-091213-113025.
[317] Morard, M. *et al.* Aneuploidy and Ethanol Tolerance in *Saccharomyces cerevisiae*. *Frontiers Genetics*, 10, 82, 2019, *doi*:10.3389/fgene.2019.00082.
[318] Legras, J.-L., Merdinoglu, D., Cornuet, J.-M., and Karst, F. Bread, beer and wine: *Saccharomyces cerevisiae* diversity reflects human history. *Molecular Ecology*, 16, 2091-2102, 2007, *doi*:10.1111/j.1365-294X.2007.03266.x.
[319] Yoon, S., Xuan, Z., Makarov, V., Ye, K., and Sebat, J. Sensitive and accurate detection of copy number variants using read depth of coverage. *Genome Res*, 19, 1586-1592, 2009, *doi*:10.1101/gr.092981.109.
[320] Dashko, S., Zhou, N., Compagno, C., and Piškur, J. Why, when, and how did yeast evolve alcoholic fermentation? *FEMS Yeast Research*, 14, 826-832, 2014, *doi*:10.1111/1567-1364.12161.
[321] Habegger, L., Rodrigues Crespo, K., and Dabros, M. Preventing Overflow Metabolism in Crabtree-Positive Microorganisms through On-Line Monitoring and Control of Fed-Batch Fermentations. *Fermentation*, 4, 79, 2018.
[322] Pfeiffer, T. and Morley, A. An evolutionary perspective on the Crabtree effect. *Frontiers Molecular Biosciences*, 1, 17, 2014, *doi*:10.3389/fmolb.2014.00017.
[323] Guo, Y. *et al.* The advances in creating Crabtree-negative *Saccharomyces cerevisiae* and the application for chemicals biosynthesis. *FEMS Yeast Research*, 25, 2025, *doi*:10.1093/femsyr/foaf014.
[324] Österlein Kück, A. Media characterization and adaptive laboratory evolution for enhanced polyphosphate production with *Saccharomyces cerevisiae*. Bachelor Thesis, RWTH Aachen University, 2023.
[325] Repin, J. Mediencharakterisierung und Bestimmung des Einflusses der Phospholipidsynthese auf die Polyphosphatproduktion mit *Saccharomyces cerevisiae*. Bachelor Thesis, RWTH Aachen University, 2024.
[326] Kullik, G. A., Waldmann, M., and Renné, T. Analysis of polyphosphate in mammalian cells and tissues: methods, functions and challenges. *Current Opinion in Biotechnology*, 90, 103208, 2024, *doi*:10.1016/j.copbio.2024.103208.
[327] Tao, Z. *et al.* Yeast Extract: Characteristics, Production, Applications and Future Perspectives. *Journal of microbiology and biotechnology*, 33, 151-166, 2023, *doi*:10.4014/jmb.2207.07057.
[328] Zhang, K. *et al.* EDTA-based adsorbents for the removal of metal ions in wastewater. *Coordination Chemistry Reviews*, 434, 213809, 2021, *doi*:10.1016/j.ccr.2021.213809.
[329] Deitert, A. *et al.* Polyphosphate Accumulation Is Determined by Zinc and Inositol in *Saccharomyces cerevisiae*. *Yeast*, 0, 1-12, 2025, *doi*:10.1002/yea.70006.
[330] Battling, S. *et al.* Novel plasmid-free *Gluconobacter oxydans* strains for production of the natural sweetener 5-ketofructose. *Microbial Cell Factories*, 19, 54, 2020, *doi*:10.1186/s12934-020-01310-7.
[331] Müller, J., Beckers, M., Mußmann, N., Bongaerts, J., and Büchs, J. Elucidation of auxotrophic deficiencies of *Bacillus pumilus* DSM 18097 to develop a defined minimal medium. *Microbial Cell Factories*, 17, 106, 2018, *doi*:10.1186/s12934-018-0956-1.
[332] Magonet, E., Hayen, P., Delforge, D., Delaive, E., and Remacle, J. Importance of the structural zinc atom for the stability of yeast alcohol dehydrogenase. *The Biochemical Journal*, 287 (Pt 2), 361-365, 1992, *doi*:10.1042/bj2870361.
[333] Bird, A. J. and Wilson, S. Zinc homeostasis in the secretory pathway in yeast. *Current Opinion Chemical Biology*, 55, 145-150, 2020, *doi*:10.1016/j.cbpa.2020.01.011.

[334] Wilson, S. and Bird, A. J. Zinc sensing and regulation in yeast model systems. *Archives of Biochemistry and Biophysics*, 611, 30-36, 2016, *doi*:10.1016/j.abb.2016.02.031.
[335] Leskovac, V., Trivić, S., and Pericin, D. The three zinc-containing alcohol dehydrogenases from baker's yeast, *Saccharomyces cerevisiae*. *FEMS Yeast Research*, 2, 481-494, 2002, *doi*:10.1111/j.1567-1364.2002.tb00116.x.
[336] Regalla, L. M. and Lyons, T. J. in *Molecular Biology of Metal Homeostasis and Detoxification: From Microbes to Man.* Zinc in yeast: mechanisms involved in homeostasis (eds Markus J. Tamas & Enrico Martinoia), 37-58, 2006, *doi*:10.1007/4735_98 (Springer Berlin Heidelberg).
[337] Vallee, B. L. and Falchuk, K. H. The biochemical basis of zinc physiology. *Physiol Rev*, 73, 79-118, 1993, *doi*:10.1152/physrev.1993.73.1.79.
[338] Henry, S. A., Kohlwein, S. D., and Carman, G. M. Metabolism and Regulation of Glycerolipids in the Yeast *Saccharomyces cerevisiae*. *Genetics*, 190, 317-349, 2012, *doi*:10.1534/genetics.111.130286.
[339] Zhao, X.-Q. and Bai, F.-w. Zinc and yeast stress tolerance: Micronutrient plays a big role. *Journal of Biotechnology*, 158, 176-183, 2012, *doi*:10.1016/j.jbiotec.2011.06.038.
[340] Andreini, C., Banci, L., Bertini, I., and Rosato, A. Zinc through the three domains of life. *Journal Proteome Research*, 5, 3173-3178, 2006, *doi*:10.1021/pr0603699.
[341] Zhao, Y.-y. *et al.* Identification of the Genetic Requirements for Zinc Tolerance and Toxicity in *Saccharomyces cerevisiae*. *G3 Genes|Genomes|Genetics*, 10, 479-488, 2020, *doi*:10.1534/g3.119.400933
[342] Kizawa, K., Aono, T., and Ohtomo, R. PHO8 gene coding alkaline phosphatase of *Saccharomyces cerevisiae* is involved in polyphosphate metabolism. *Journal of General and Applied Microbiology*, 62, 297-302, 2017, *doi*:10.2323/jgam.2016.05.006.
[343] Donella-Deana, A., Ostojić, S., Pinna, L. A., and Barbarić, S. Specific dephosphorylation of phosphopeptides by the yeast alkaline phosphatase encoded by PHO8 gene. *Biochim Biophys Acta*, 1177, 221-228, 1993, *doi*:10.1016/0167-4889(93)90044-p.
[344] Shah, A., Ganguli, S., Sen, J., and Bhandari, R. Inositol Pyrophosphates: Energetic, Omnipresent and Versatile Signalling Molecules. *Journal Indian Institute of Science*, 97, 23-40, 2017, *doi*:10.1007/s41745-016-0011-3.
[345] Shetty, A., Swaminathan, A., and Lopes, J. M. Transcription Regulation of a Yeast Gene from a Downstream Location. *Journal of Molecular Biology*, 425, 457-465, 2013, *doi*:10.1016/j.jmb.2012.11.018.
[346] Szijgyarto, Z., Garedew, A., Azevedo, C., and Saiardi, A. Influence of inositol pyrophosphates on cellular energy dynamics. *Science*, 334, 802-805, 2011, *doi*:10.1126/science.1211908.
[347] Bennett, M., Onnebo, S. M., Azevedo, C., and Saiardi, A. Inositol pyrophosphates: metabolism and signaling. *Cellular and Molecular Life Sciences*, 63, 552-564, 2006, *doi*:10.1007/s00018-005-5446-z.
[348] Qin, N. *et al.* Flux regulation through glycolysis and respiration is balanced by inositol pyrophosphates in yeast. *Cell*, 186, 748-763.e715, 2023, *doi*:10.1016/j.cell.2023.01.014.
[349] Lesaffre. *Ethanol Red®, Dry yeast for ethanol*, https://leaf-lesaffre.com/wp-content/uploads/2025/05/er_en_v6.pdf, 2025.
[350] Trivellin, C., Olsson, L., and Rugbjerg, P. Quantification of Microbial Robustness in Yeast. *ACS Synthetic Biology*, 11, 1686-1691, 2022, *doi*:10.1021/acssynbio.1c00615.
[351] Furukawa, K., Obata, H., Kitano, H., Mizoguchi, H., and Hara, S. Effect of cellular inositol content on ethanol tolerance of *Saccharomyces cerevisiae* in sake brewing. *Journal of Bioscience and Bioengineering*, 98, 107-113, 2004, *doi*:10.1016/S1389-1723(04)70250-9.
[352] Chi, Z., Kohlwein, S. D., and Paltauf, F. Role of phosphatidylinositol (PI) in ethanol production and ethanol tolerance by a high ethanol producing yeast. *Journal of Industrial Microbiology and Biotechnology*, 22, 58-63, 1999, *doi*:10.1038/sj.jim.2900603.

[353] Maas, A. E. Media development and screening of mutants for polyphosphate production with *Saccharomyces cerevisiae*. Internship report, RWTH Aachen University, 2025.

[354] Zhang, Y., Su, M., Wang, Z., Nielsen, J., and Liu, Z. Rewiring regulation on respiro-fermentative metabolism relieved Crabtree effects in *Saccharomyces cerevisiae*. *Synthetic and Systems Biotechnology*, 7, 1034-1043, 2022, *doi*:10.1016/j.synbio.2022.06.004.

[355] Malina, C., Yu, R., Björkeroth, J., Kerkhoven, E. J., and Nielsen, J. Adaptations in metabolism and protein translation give rise to the Crabtree effect in yeast. *Proc. Natl. Acad. Sci. U.S.A.*, 118, e2112836118, 2021, *doi*:10.1073/pnas.2112836118.

[356] Zimmermann, J. and Dott, W. Sequenced Bioleaching and Bioaccumulation of Phosphorus from Sludge Combustion – A New Way of Resource Reclaiming. *Advanced Materials Research*, 71-73, 625-628, 2009, *doi*:10.4028/www.scientific.net/AMR.71-73.625.

[357] Henry, S. A., Gaspar, M. L., and Jesch, S. A. The response to inositol: Regulation of glycerolipid metabolism and stress response signaling in yeast. *Chemistry and Physics of Lipids*, 180, 23-43, 2014, *doi*:10.1016/j.chemphyslip.2013.12.013.

[358] Yadav, K. K., Singh, N., and Rajasekharan, R. PHO4 transcription factor regulates triacylglycerol metabolism under low-phosphate conditions in *Saccharomyces cerevisiae*. *Molecular Microbiology*, 98, 456-472, 2015, *doi*:10.1111/mmi.13133.

[359] Yadav, K. K., Singh, N., and Rajasekharan, R. Responses to phosphate deprivation in yeast cells. *Current Genetics*, 62, 301-307, 2016, *doi*:10.1007/s00294-015-0544-4.

[360] Yang, X. *et al.* Effect of ammonium acetate on alcohol fermentation in cassava-alcohol fermentation process. *Microbiological Research*, 256, 126868, 2022, *doi*:10.1016/j.micres.2021.126868.

[361] Canadell, D., González, A., Casado, C., and Ariño, J. Functional interactions between potassium and phosphate homeostasis in *Saccharomyces cerevisiae*. *Molecular Microbiology*, 95, 555-572, 2015, *doi*:10.1111/mmi.12886.

[362] Dunn, T., Gable, K., and Beeler, T. Regulation of cellular Ca2+ by yeast vacuoles. *Journal of Biological Chemistry*, 269, 7273-7278, 1994, *doi*:10.1016/S0021-9258(17)37279-4.

[363] Breus, N. A. *et al.* Accumulation of inorganic polyphosphates in *Saccharomyces cerevisiae* under nitrogen deprivation: Stimulation by magnesium ions and peculiarities of localization. *Microbiology*, 80, 624-630, 2011, *doi*:10.1134/S002626171105002X.

[364] Strauss, U. P. and Siegel, A. COUNTERION BINDING BY POLYELECTROLYTES. VI. THE BINDING OF MAGNESIUM ION BY POLYPHOSPHATES IN AQUEOUS ELECTROLYTE SOLUTIONS1. *The Journal of Physical Chemistry*, 67, 2683-2687, 1963, *doi*:10.1021/j100806a042.

[365] Machnicka, A., Suschka, J., and Grübel, K. THE IMPORTANCE OF POTASSIUM AND MAGNESIUM IONS IN BIOLOGICAL PHOSPHORUS REMOVAL FROM WASTEWATER. 2004.

[366] Han, G. S., Wu, W. I., and Carman, G. M. The *Saccharomyces cerevisiae* Lipin homolog is a Mg2+-dependent phosphatidate phosphatase enzyme. *Journal of Biological Chemistry*, 281, 9210-9218, 2006, *doi*:10.1074/jbc.M600425200.

[367] Mendonsa, R. and Engebrecht, J. Phospholipase D function in *Saccharomyces cerevisiae*. *Biochimica et Biophysica Acta (BBA) - Molecular and Cell Biology of Lipids*, 1791, 970-974, 2009, *doi*:10.1016/j.bbalip.2009.01.013.

[368] Hanscho, M. *et al.* Nutritional requirements of the BY series of *Saccharomyces cerevisiae* strains for optimum growth. *FEMS Yeast Research*, 12, 796-808, 2012, *doi*:10.1111/j.1567-1364.2012.00830.x.

[369] Dos Santos, E. O. *et al.* Evaluation of the composition of culture medium for yeast biomass production using raw glycerol from biodiesel synthesis. *Brazilian Journal of Microbiology*, 43, 432-440, 2012, *doi*:10.1590/s1517-83822012000200002.

[370] Ehrmann, A. K. *et al.* Engineering *Saccharomyces cerevisiae* for fast vitamin-independent aerobic growth. *Metabolic Engineering*, 82, 201-215, 2024, *doi*:10.1016/j.ymben.2024.01.010.

[371] Hansen, J. Ø. *et al.* Down-stream processing of baker's yeast (*Saccharomyces cerevisiae*) – Effect on nutrient digestibility and immune response in Atlantic salmon (*Salmo salar*). *Aquaculture*, 530, 735707, 2021, *doi*:10.1016/j.aquaculture.2020.735707.

[372] Straathof, A. in *Comprehensive Biotechnology (Second Edition).* Vol. 2*,* The Proportion of Downstream Costs in Fermentative Production Processes (ed Murray Moo-Young), 811-814, 2011, *doi*:10.1016/B978-0-08-088504-9.00492-X (Academic Press).

[373] Walker, G. M. and Stewart, G. G. *Saccharomyces cerevisiae* in the Production of Fermented Beverages. *Beverages*, 2, 30, 2016, *doi*:10.3390/beverages2040030.

[374] Wu, W., Long, M. R., Zhang, X., Reed, J. L., and Maravelias, C. T. A framework for the identification of promising bio-based chemicals. *Biotechnology and Bioengineering*, 115, 2328-2340, 2018, *doi*:10.1002/bit.26779.

[375] Singh, V. *et al.* Strategies for Fermentation Medium Optimization: An In-Depth Review. *Frontiers Microbiology*, 7, 2087, 2016, *doi*:10.3389/fmicb.2016.02087.

[376] Reddy, V. S., Singh, A. K., and Rajasekharan, R. The *Saccharomyces cerevisiae* PHM8 Gene Encodes a Soluble Magnesium-dependent Lysophosphatidic Acid Phosphatase. *Journal of Biological Chemistry*, 283, 8846-8854, 2008, *doi*:10.1074/jbc.M706752200.

[377] Zheng, Z. and Zou, J. The Initial Step of the Glycerolipid Pathway: IDENTIFICATION OF GLYCEROL 3-PHOSPHATE/DIHYDROXYACETONE PHOSPHATE DUAL SUBSTRATE ACYLTRANSFERASES IN *SACCHAROMYCES CEREVISIAE*. *Journal of Biological Chemistry*, 276, 41710-41716, 2001, *doi*:10.1074/jbc.M104749200.

[378] Boer, V. M., de Winde, J. H., Pronk, J. T., and Piper, M. D. W. The Genome-wide Transcriptional Responses of *Saccharomyces cerevisiae* Grown on Glucose in Aerobic Chemostat Cultures Limited for Carbon, Nitrogen, Phosphorus, or Sulfur. *Journal of Biological Chemistry*, 278, 3265-3274, 2003, *doi*:10.1074/jbc.M209759200.

[379] Yoshida, K., Kuromitsu, Z., Ogawa, N., and Oshima, Y. Mode of expression of the positive regulatory genes PHO2 and PHO4 of the phosphatase regulon in *Saccharomyces cerevisiae*. *Molecular and General Genetics MGG*, 217, 31-39, 1989, *doi*:10.1007/BF00330939.

[380] Lenburg, M. E. and O'Shea, E. K. Signaling phosphate starvation. *Trends Biochemical Sciences*, 21, 383-387, 1996, *doi*:10.1016/S0968-0004(96)10048-7.

[381] Athenstaedt, K. and Daum, G. Biosynthesis of phosphatidic acid in lipid particles and endoplasmic reticulum of *Saccharomyces cerevisiae*. *Journal of Bacteriology*, 179, 7611-7616, 1997, *doi*:10.1128/jb.179.24.7611-7616.1997.

[382] Riekhof, W. R., Wu, J., Jones, J. L., and Voelker, D. R. Identification and Characterization of the Major Lysophosphatidylethanolamine Acyltransferase in *Saccharomyces cerevisiae*. *Journal of Biological Chemistry*, 282, 28344-28352, 2007, *doi*:10.1074/jbc.M705256200.

[383] Benghezal, M., Roubaty, C., Veepuri, V., Knudsen, J., and Conzelmann, A. SLC1 and SLC4 Encode Partially Redundant Acyl-Coenzyme A 1-Acylglycerol-3-phosphate O-Acyltransferases of Budding Yeast. *Journal of Biological Chemistry*, 282, 30845-30855, 2007, *doi*:10.1074/jbc.M702719200.

[384] Riekhof, W. R. *et al.* Lysophosphatidylcholine Metabolism in *Saccharomyces cerevisiae:* THE ROLE OF P-TYPE ATPases IN TRANSPORT AND A BROAD SPECIFICITY ACYLTRANSFERASE IN ACYLATION. *Journal of Biological Chemistry*, 282, 36853-36861, 2007, *doi*:10.1074/jbc.M706718200.

[385] Shekar, S., Tumaney, A. W., Rao, T. J., and Rajasekharan, R. Isolation of lysophosphatidic acid phosphatase from developing peanut cotyledons. *Plant Physiology*, 128, 988-996, 2002, *doi*:10.1104/pp.010654.

[386] Carman, G. M. and Han, G.-S. Regulation of phospholipid synthesis in *Saccharomyces cerevisiae* by zinc depletion. *Biochimica et Biophysica Acta (BBA) - Molecular and Cell Biology of Lipids*, 1771, 322-330, 2007, *doi*:10.1016/j.bbalip.2006.05.006.

[387] Carman, G. M. and Henry, S. A. Phospholipid biosynthesis in the yeast *Saccharomyces cerevisiae* and interrelationship with other metabolic processes. *Progress Lipid Research*, 38, 361-399, 1999, *doi*:10.1016/s0163-7827(99)00010-7.

[388] Boumann, H. A. *et al.* The Two Biosynthetic Routes Leading to Phosphatidylcholine in Yeast Produce Different Sets of Molecular Species. Evidence for Lipid Remodeling. *Biochemistry*, 42, 3054-3059, 2003, *doi*:10.1021/bi026801r.

[389] Yao, S., Kim, S.-C., Li, J., Tang, S., and Wang, X. Phosphatidic acid signaling and function in nuclei. *Progress Lipid Research*, 93, 101267, 2024, *doi*:10.1016/j.plipres.2023.101267.

[390] Nakamura, Y. Phosphate starvation and membrane lipid remodeling in seed plants. *Progress Lipid Research*, 52, 43-50, 2013, *doi*:10.1016/j.plipres.2012.07.002.

[391] Riekhof, W. R., Naik, S., Bertrand, H., Benning, C., and Voelker, D. R. Phosphate starvation in fungi induces the replacement of phosphatidylcholine with the phosphorus-free betaine lipid diacylglyceryl-N,N,N-trimethylhomoserine. *Eukaryot Cell*, 13, 749-757, 2014, *doi*:10.1128/ec.00004-14.

[392] Cooke, F. T. *et al.* The stress-activated phosphatidylinositol 3-phosphate 5-kinase Fab1p is essential for vacuole function in *S. cerevisiae*. *Current Biology*, 8, 1219-S1212, 1998, *doi*:10.1016/S0960-9822(07)00513-1.

[393] Yamamoto, A. *et al.* Novel PI(4)P 5-kinase homologue, Fab1p, essential for normal vacuole function and morphology in yeast. *Molecular Biology Cell*, 6, 525-539, 1995, *doi*:10.1091/mbc.6.5.525.

[394] Weaver, J. D., Wang, H., and Shears, S. B. The kinetic properties of a human PPIP5K reveal that its kinase activities are protected against the consequences of a deteriorating cellular bioenergetic environment. *Biosci Rep*, 33, 2013, *doi*:10.1042/bsr20120115.

[395] Wang, H., Falck, J. R., Hall, T. M., and Shears, S. B. Structural basis for an inositol pyrophosphate kinase surmounting phosphate crowding. *Nat Chem Biol*, 8, 111-116, 2011, *doi*:10.1038/nchembio.733.

[396] Azevedo, C., Livermore, T., and Saiardi, A. Protein polyphosphorylation of lysine residues by inorganic polyphosphate. *Molecular Cell*, 58, 71-82, 2015, *doi*:10.1016/j.molcel.2015.02.010.

[397] Carman, G. M. and Henry, S. A. Phosphatidic Acid Plays a Central Role in the Transcriptional Regulation of Glycerophospholipid Synthesis in *Saccharomyces cerevisiae*. *Journal of Biological Chemistry*, 282, 37293-37297, 2007, *doi*:10.1074/jbc.R700038200.

[398] Carman, G. M. and Han, G.-S. Regulation of phospholipid synthesis in yeast. *Journal of Lipid Research*, 50, S69-S73, 2009, *doi*:10.1194/jlr.R800043-JLR200.

[399] Santos-Rosa, H., Leung, J., Grimsey, N., Peak-Chew, S., and Siniossoglou, S. The yeast lipin Smp2 couples phospholipid biosynthesis to nuclear membrane growth. *The EMBO Journal*, 24, 1931-1941, 2005, *doi*:10.1038/sj.emboj.7600672.

[400] Han, G.-S., O'Hara, L., Carman, G. M., and Siniossoglou, S. An Unconventional Diacylglycerol Kinase That Regulates Phospholipid Synthesis and Nuclear Membrane Growth. *Journal of Biological Chemistry*, 283, 20433-20442, 2008, *doi*:10.1074/jbc.M802903200.

[401] Park, Y., Han, G.-S., Mileykovskaya, E., Garrett, T. A., and Carman, G. M. Altered Lipid Synthesis by Lack of Yeast Pah1 Phosphatidate Phosphatase Reduces Chronological Life Span. *Journal of Biological Chemistry*, 290, 25382-25394, 2015, *doi*:10.1074/jbc.M115.680314.

[402] Pascual, F., Soto-Cardalda, A., and Carman, G. M. PAH1-encoded phosphatidate phosphatase plays a role in the growth phase- and inositol-mediated regulation of lipid synthesis in *Saccharomyces cerevisiae*. *Journal of Biological Chemistry*, 288, 35781-35792, 2013, *doi*:10.1074/jbc.M113.525766.

[403] Sasser, T. *et al.* Yeast lipin 1 orthologue pah1p regulates vacuole homeostasis and membrane fusion. *Journal of Biological Chemistry*, 287, 2221-2236, 2012, *doi*:10.1074/jbc.M111.317420.

[404] Perli, T., Wronska, A. K., Ortiz-Merino, R. A., Pronk, J. T., and Daran, J. M. Vitamin requirements and biosynthesis in *Saccharomyces cerevisiae*. *Yeast*, 37, 283-304, 2020, *doi*:10.1002/yea.3461.

[405] White, M. J., Lopes, J. M., and Henry, S. A. in *Advances in Microbial Physiology.* Vol. 32*,* Inositol Metabolism in Yeasts (eds A. H. Rose & D. W. Tempest), 1-51, 1991, *doi*:10.1016/S0065-2911(08)60004-1 (Academic Press).

[406] Ambroziak, J. and Henry, S. A. INO2 and INO4 gene products, positive regulators of phospholipid biosynthesis in *Saccharomyces cerevisiae*, form a complex that binds to the INO1 promoter. *Journal of Biological Chemistry*, 269, 15344-15349, 1994, *doi*:10.1016/S0021-9258(17)36612-7.

[407] Donahue, T. F. and Henry, S. A. myo-Inositol-1-phosphate synthase. Characteristics of the enzyme and identification of its structural gene in yeast. *Journal of Biological Chemistry*, 256, 7077-7085, 1981, *doi*:10.1016/S0021-9258(19)69102-7.

[408] Villa-García, M. J. *et al.* Genome-wide screen for inositol auxotrophy in *Saccharomyces cerevisiae* implicates lipid metabolism in stress response signaling. *Molecular Genetics Genomics*, 285, 125-149, 2011, *doi*:10.1007/s00438-010-0592-x.

[409] Dean-Johnson, M. and Henry, S. A. Biosynthesis of Inositol in Yeast: Primary structure of myo-inositol-1-phosphate synthase (EC 5.5.1.4) and functional analysis of its structural gene, the INO1 locus. *Journal of Biological Chemistry*, 264, 1274-1283, 1989, *doi*:10.1016/S0021-9258(19)85082-2.

[410] Nikawa, J., Tsukagoshi, Y., and Yamashita, S. Isolation and characterization of two distinct myo-inositol transporter genes of *Saccharomyces cerevisiae*. *Journal of Biological Chemistry*, 266, 11184-11191, 1991, *doi*:10.1016/S0021-9258(18)99146-5.

[411] Lai, K. and McGraw, P. Dual control of inositol transport in *Saccharomyces cerevisia*e by irreversible inactivation of permease and regulation of permease synthesis by INO2, INO4, and OPI1. *Journal of Biological Chemistry*, 269, 2245-2251, 1994, *doi*:10.1016/S0021-9258(17)42160-0.

[412] Nikawa, J., Hosaka, K., and Yamashita, S. Differential regulation of two *myo*-inositol transporter genes of *Saccharomyces cerevisiae*. *Molecular Microbiology*, 10, 955-961, 1993, *doi*:10.1111/j.1365-2958.1993.tb00967.x.

[413] Konopka, J. B. Plasma Membrane Phosphatidylinositol 4-Phosphate Is Necessary for Virulence of *Candida albicans*. *mBio*, 13, e0036622, 2022, *doi*:10.1128/mbio.00366-22.

[414] Schneider, S. Inositol transport proteins. *FEBS Letters*, 589, 1049-1058, 2015, *doi*:10.1016/j.febslet.2015.03.012.

[415] Patton-Vogt, J. L. and Henry, S. A. GIT1, a gene encoding a novel transporter for glycerophosphoinositol in *Saccharomyces cerevisiae*. *Genetics*, 149, 1707-1715, 1998, *doi*:10.1093/genetics/149.4.1707 %J Genetics.

[416] United Nations. The Sustainable Development Goals Report 2016. *Department of Economic and Social Affairs (DESA)*, 2016, [Online]. Available: https://unstats.un.org/sdgs/report/2016/the%20sustainable%20development%20goals%20report%202016.pdf.

[417] Brownlie, W., Sutton, M. A., Heal, K., Reay, D., and Spears, B. The Our Phosphorus Future Report. *UK Centre for Ecology & Hydrology, Edinburgh*, 2022, *doi*:10.13140/RG.2.2.17834.08645.

[418] Our Phosphorus Future project (OPF). The Helsinki Declaration. 2019, [Online]. Available: https://www.opfglobal.com/helsinki-declaration (accessed Sep. 04, 2025).

[419] The International Court of Justice. Obligations of states in respect of climate change - Advisory Opinion. 2025, [Online]. Available: https://www.icj-cij.org/sites/default/files/case-related/187/187-20250723-adv-01-00-en.pdf.

[420] Bourazza, A., H. Sidikou, A., Fenta, B. A., and Hirich, A. Restoration of phosphate mined lands: literature review with insights from Morocco. *Frontiers in Environmental Science*, 13, 2025, *doi*:10.3389/fenvs.2025.1519868.

[421] Zhang, J., Liu, M., and Song, Y. Human-Dominated Land Use Change in a Phosphate Mining Area and Its Impact on the Water Environment. *Water*, 14, 1074, 2022, *doi*:10.3390/w14071074.

[422] Gale, S. The mined-out phosphate lands of Nauru, equatorial western Pacific. *Australian Journal of Earth Sciences*, 63, 333-347, 2016, *doi*:10.1080/08120099.2016.1206621.

[423] German Federal Ministry for Economic Cooperation and Development (BMZ). Mining and biodiversity. *Deutsche Gesellschaft für Internationale Zusammenarbeit (GIZ) Gmb*, 2021, [Online]. Available: https://rue.bmz.de/resource/blob/101918/briefing-note-biodiversity.pdf.

[424] Tian, J., Wang, X., Tong, Y., Chen, X., and Liao, H. Bioengineering and management for efficient phosphorus utilization in crops and pastures. *Current Opinion in Biotechnology*, 23, 866-871, 2012, *doi*:10.1016/j.copbio.2012.03.002.

[425] Geissler, B., Hermann, L., Mew, M. C., and Steiner, G. Striving Toward a Circular Economy for Phosphorus: The Role of Phosphate Rock Mining. *Minerals*, 8, 395, 2018, *doi*:10.3390/min8090395.

[426] Murray, C. *et al.* Past, Present and Future Eutrophication Status of the Baltic Sea. *Frontiers in Marine Science*, 6, 2019, *doi*:10.3389/fmars.2019.00002.

[427] Kubier, A., Wilkin, R. T., and Pichler, T. Cadmium in soils and groundwater: A review. *Applied Geochemistry*, 108, 104388, 2019, *doi*:10.1016/j.apgeochem.2019.104388.

[428] Pizzol, M., Smart, J. C. R., and Thomsen, M. External costs of cadmium emissions to soil: a drawback of phosphorus fertilizers. *Journal of Cleaner Production*, 84, 475-483, 2014, *doi*:10.1016/j.jclepro.2013.12.080.

[429] Taylor, M. *et al.* in *Phosphorus in Agriculture: 100 % Zero.* Trace Element Contaminants and Radioactivity from Phosphate Fertiliser (eds Ewald Schnug & Luit J. De Kok), 353, 2016, *doi*:10.1007/978-94-017-7612-7_12 (Springer Dordrecht).

[430] Shahid, M., Dumat, C., Khalid, S., Niazi, N. K., and Antunes, P. M. C. Cadmium Bioavailability, Uptake, Toxicity and Detoxification in Soil-Plant System. *Reviews Environmental Contamination Toxicology*, 241, 73-137, 2017, *doi*:10.1007/398_2016_8.

[431] Kouzbour, S. *et al.* Comparative analysis of industrial processes for cadmium removal from phosphoric acid: A review. *Hydrometallurgy*, 188, 222-247, 2019, *doi*:10.1016/j.hydromet.2019.06.014.

[432] The European Parliament and the Council of the European Union. REGULATION (EU) 2019/1009 OF THE EUROPEAN PARLIAMENT AND OF THE COUNCIL of 5 June 2019 laying down rules on the making available on the market of EU fertilising products and amending Regulations (EC) No 1069/2009 and (EC) No 1107/2009 and repealing Regulation (EC) No 2003/2003. *Official Journal of the European Union*, 2019, [Online]. Available: https://eur-lex.europa.eu/eli/reg/2019/1009/oj/eng.

[433] Christiansen, B., Denda, A., and Christiansen, S. Potential effects of deep seabed mining on pelagic and benthopelagic biota. *Marine Policy*, 114, 103442, 2020, *doi*:10.1016/j.marpol.2019.02.014.

[434] Yao, W. *et al.* Development of deep-sea mining and its environmental impacts: a review. *Frontiers in Marine Science*, 12, 2025, *doi*:10.3389/fmars.2025.1598584.

[435] Screen - Solutions for CRitical Raw materials. FACTSHEETS UPDATES BASED ON THE EU FACTSHEETS 2020 - PHOSPHATE ROCK AND PHOSPHORUS. *European Union's Horizon 2020 research and innovation programme under grant agreement No 958211*, 2020, [Online]. Available: https://scrreen.eu/wp-content/uploads/2023/01/PHOSPHATE-ROCK-AND-ELEMENTAL-PHOSPHORUS_CRM_2020_Factsheets_critical_Final.pdf.

[436] Rami, A. O. The supply behaviour of state mining enterprises: A case study of the Jordanian phosphate industry. *Resources Policy*, 33, 196-202, 2008, *doi*:10.1016/j.resourpol.2008.04.001.

[437] Zhang, W. *et al.* Efficiency, economics, and environmental implications of phosphorus resource use and the fertilizer industry in China. *Nutrient Cycling in Agroecosystems*, 80, 131-144, 2008, *doi*:10.1007/s10705-007-9126-2.

[438] Elsayed, D. in *Corruption in the MENA Region. Political Corruption and Governance.* Corruption in North Africa: Monopoly of Power and Widespread Ignorance (eds Dan Hough & Paul M. Heywood), 165-234, 2020, *doi*:10.1007/978-3-030-55314-2_7 (Palgrave Macmillan).

[439] Allan, J. and Ojeda-García, R. Natural resource exploitation in Western Sahara: new research directions. *The Journal of North African Studies*, 27, 1107-1136, 2022, *doi*:10.1080/13629387.2021.1917120.

[440] Special Committee on Decolonization. Report of the Special Committee on the Situation with regard to the Implementation of the Declaration on the Granting of Independence to Colonial Countries and People. *United Nations General Assembly*, 1963, [Online]. Available: https://docs.un.org/en/A/5446/Rev.1.

[441] Mohammed, S. Evaluating the dynamic interaction between the defence / security policy of the US, UN, and Western Sahara. *International Journal of Civilizations Studies & Tolerance Sciences*, 1, 94-98, 2024, *doi*:10.54878/p8xpj3314421.

[442] Environmental Research of the Federal Ministry for the Environment, Nature Conservation and Nuclear Safety. OekoRess II: Country Case Study IV - Morocco/Western Sahara: Phosphate (Bou Craa). Demel, C. *et al.*, *German Environment Agency*, 2018, [Online]. Available: https://www.umweltbundesamt.de/sites/default/files/medien/1410/publikationen/5-06_20200117_oekoressii_morocco_western_sahara_case_study_final_v2.pdf.

[443] The Legal Counsel. Letter dated 29 January 2002 from the Under-Secretary-General for Legal Affairs, the Legal Counsel, addressed to the President of the Security Council. Correl, H., *United Nations Security Council*, 2002, [Online]. Available: https://www.arso.org/Olaeng.pdf.

[444] European Parliament. Answer given by Vice-President Mogherini on behalf of the Commission. 2015, [Online]. Available: https://www.europarl.europa.eu/doceo/document/E-8-2015-004499-ASW_EN.pdf.

[445] U.S. Geological Survey. Phosphate rock statistics and information. Jasinski, S. M., 2024, [Online]. Available: https://pubs.usgs.gov/periodicals/mcs2025/mcs2025-phosphate.pdf.

[446] Geissler, B., Mew, M. C., and Steiner, G. Phosphate supply security for importing countries: Developments and the current situation. *Science of the Total Environment*, 677, 511-523, 2019, *doi*:10.1016/j.scitotenv.2019.04.356.

[447] NORGE MINING PLC. JORC resource at Storeknuten doubles to almost 2 billion tonnes. *Press release*, 2023, [Online]. Available: https://kommunikasjon.ntb.no/pressemelding/18007583/norge-mining-plc-norge-mining-or-the-company-jorc-resource-at-storeknuten-doubles-to-almost-2-billion-tonnes?publisherId=90063.

[448] Berg, E., Kverndokk, S., and Rosendahl, K. E. Gains from cartelisation in the oil market. *Energy Policy*, 25, 1075-1091, 1997, *doi*:10.1016/S0301-4215(97)00096-7.

[449] Nassar, N. T. *et al.* Evaluating the mineral commodity supply risk of the U.S. manufacturing sector. *Science Advances*, 6, eaay8647, 2020, *doi*:10.1126/sciadv.aay8647.

[450] Weikard, H.-P. Phosphorus recycling and food security in the long run: a conceptual modelling approach. *Food Security*, 8, 405-414, 2016, *doi*:10.1007/s12571-016-0551-4.

[451] Liu, X., Zhang, Y., Cheng, M., Jiang, S., and Yuan, Z. Recycling phosphorus from waste in China: Recycling methods and their environmental and resource consequences.

Resources, Conservation and Recycling, 188, 106669, 2023, *doi*:10.1016/j.resconrec.2022.106669.

[452] Cui, R., Zhang, Y., Guo, J., Guo, Z., and Xiao, Y. Development Strategy of Phosphate Rock in China Under Global Allocation of Resources. *Chinese Journal of Engineering Science*, 21, 128, 2019, *doi*:10.15302/J-SSCAE-2019.01.018.

[453] Wang, J., Zhang, Z., and Liu, Y. Spatial shifts in grain production increases in China and implications for food security. *Land Use Policy*, 74, 204-213, 2018, *doi*:10.1016/j.landusepol.2017.11.037.

[454] Hu, Y. and Liu, Y. Impact of fertilizer and pesticide reductions on land use in China based on crop-land integrated model. *Land Use Policy*, 141, 107155, 2024, *doi*:10.1016/j.landusepol.2024.107155.

[455] Mariev, O. and Blueschke, D. Interplay of Chinese rare earth elements supply and European clean energy transition: A geopolitical context analysis. *Renewable Energy*, 238, 121986, 2025, *doi*:10.1016/j.renene.2024.121986.

[456] Schmid, M. Rare Earths in the Trade Dispute Between the US and China: A Déjà Vu. *Intereconomics*, 54, 378-384, 2019, *doi*:10.1007/s10272-019-0856-6.

[457] European Parliament. Commission must tackle China's export restrictions on rare earth elements. Cosijn, L., *European Parliament*, 2025, [Online]. Available: https://www.europarl.europa.eu/pdfs/news/expert/2025/7/press_release/20250704IPR29456/20250704IPR29456_en.pdf.

[458] U.S. Department of Agriculture. Impacts and Repercussions of Price Increases on the Global Fertilizer Market. Jones, K. and Nti, F., 2022, [Online]. Available: https://www.fas.usda.gov/sites/default/files/2022-09/IATR%20Fertlizer%20Final.pdf.

[459] Leal Filho, W. *et al.* Reinvigorating the sustainable development research agenda: the role of the sustainable development goals (SDG). *International Journal of Sustainable Development & World Ecology*, 25, 131-142, 2018, *doi*:10.1080/13504509.2017.1342103.

[460] Sachs, J. D. *et al.* Six Transformations to achieve the Sustainable Development Goals. *Nature Sustainability*, 2, 805-814, 2019, *doi*:10.1038/s41893-019-0352-9.

[461] Kumar, V., Sinha, A. K., Makkar, H. P. S., and Becker, K. Dietary roles of phytate and phytase in human nutrition: A review. *Food Chemistry*, 120, 945-959, 2010, *doi*:10.1016/j.foodchem.2009.11.052.

[462] Bohn, L., Meyer, A. S., and Rasmussen, S. K. Phytate: impact on environment and human nutrition. A challenge for molecular breeding. *Journal Zhejiang University Science B*, 9, 165-191, 2008, *doi*:10.1631/jzus.B0710640.

[463] Masum Akond, A., Crawford, H., Berthold, J., Talukder, Z. I., and Hossain, K. Minerals (Zn, Fe, Ca and Mg) and Antinutrient (Phytic Acid) Constituents in Common Bean. *American Journal Food Technology*, 6, 235-243, 2011, *doi*:10.3923/ajft.2011.235.243.

[464] Herrmann, K. R., Ruff, A. J., and Schwaneberg, U. Phytase-Based Phosphorus Recovery Process for 20 Distinct Press Cakes. *ACS Sustainable Chemistry & Engineering*, 8, 3913-3921, 2020, *doi*:10.1021/acssuschemeng.9b07433.

[465] Romano, N. and Kumar, V. in *Enzymes in Human and Animal Nutrition.* Chapter 4 - Phytase in animal feed (eds Carlos Simões Nunes & Vikas Kumar), 73-88, 2018, *doi*:10.1016/B978-0-12-805419-2.00004-6 (Academic Press).

[466] Pasalari, H., Farzadkia, M., Khosravani, F., Ganachari, S., and Aminabhavi, T. M. Phosphorous recovery from sewage sludge via chemical and thermal technologies. *Chemical Engineering Journal*, 496, 153869, 2024, *doi*:10.1016/j.cej.2024.153869.

[467] Amara, N. I., Chukwuemeka, E. S., Obiajulu, N. O., and Chukwuma, O. J. Yeast-driven valorization of agro-industrial wastewater: an overview. *Environmental Monitoring and Assessment*, 195, 1252, 2023, *doi*:10.1007/s10661-023-11863-w.

[468] Cordell, D. and White, S. Peak Phosphorus: Clarifying the Key Issues of a Vigorous Debate about Long-Term Phosphorus Security. *Sustainability*, 3, 2027-2049, 2011, *doi*:10.3390/su3102027.

[469] Ben Hassen, T. and El Bilali, H. Impacts of the Russia-Ukraine War on Global Food Security: Towards More Sustainable and Resilient Food Systems? *Foods*, 11, 2301, 2022, *doi*:10.3390/foods11152301.

[470] Brownlie, W. *et al.* Phosphorus price spikes: A wake-up call for phosphorus resilience. *Frontiers in Sustainable Food Systems*, 7, 1088776, 2023, *doi*:10.3389/fsufs.2023.1088776.

[471] Koga, D. in *Phosphorus Recovery and Recycling.* Struvite Recovery from Digested Sewage Sludge (eds H. Ohtake & Satoshi Tsuneda), 255-264, 2019, *doi*:10.1007/978-981-10-8031-9_17 (Springer Nature Singapore Pte Ltd).

[472] Cai, T. *et al.* Cell-free chemoenzymatic starch synthesis from carbon dioxide. *Science*, 373, 1523-1527, 2021, *doi*:10.1126/science.abh4049.

[473] Sun, M., Cao, X., Liu, X., Cao, T., and Zhu, Q. The Russia-Ukraine conflict, soaring international energy prices, and implications for global economic policies. *Heliyon*, 10, e34712, 2024, *doi*:10.1016/j.heliyon.2024.e34712.

[474] Davison, B. H. and Lievense, J. SBE supplement: Commercializing industrial biotechnology - technology challenges and opportunities. *AIChE's Society for Bio-logical Engineering*, 112, 2016.

[475] Liu, D., Ding, L., Sun, J., Boussetta, N., and Vorobiev, E. Yeast cell disruption strategies for recovery of intracellular bio-active compounds - A review. *Innovative Food Science & Emerging Technologies*, 36, 181-192, 2016, *doi*:10.1016/j.ifset.2016.06.017.

[476] Eliodório, K. P. *et al.* Physiology of *Saccharomyces cerevisiae* during growth on industrial sugar cane molasses can be reproduced in a tailor-made defined synthetic medium. *Scientific Reports*, 13, 10567, 2023, *doi*:10.1038/s41598-023-37618-8.

[477] Ikram-ul, H., Ali, S., Qadeer, M. A., and Iqbal, J. Citric acid production by selected mutants of Aspergillus niger from cane molasses. *Bioresource Technology*, 93, 125-130, 2004, *doi*:10.1016/j.biortech.2003.10.018.

[478] Wheals, A. E., Basso, L. C., Alves, D. M. G., and Amorim, H. V. Fuel ethanol after 25 years. *Trends in Biotechnology*, 17, 482-487, 1999, *doi*:10.1016/S0167-7799(99)01384-0.

[479] Helm, T. *et al.* Introducing molasses as an alternative feedstock into itaconate production using Ustilago sp. *New Biotechnology*, 77, 30-39, 2023, *doi*:10.1016/j.nbt.2023.06.003.

[480] Wohlers, A. E. Regulating genetically modified food. Policy trajectories, political culture, and risk perceptions in the U.S., Canada, and EU. *Politics Life Sci*, 29, 17-39, 2010, *doi*:10.2990/29_2_17.

[481] Bruetschy, C. The EU regulatory framework on genetically modified organisms (GMOs). *Transgenic Research*, 28, 169-174, 2019, *doi*:10.1007/s11248-019-00149-y.

[482] The European Parliament and the Council of the European Union. Directive 2001/18/EC of the European Parliament and of the council of 12 March 2001 on the deliberate release into the environment of genetically modified organisms and repealing Council Directive 90/220/EEC. *Off. J. Eur. Union*, 2001, [Online]. Available: https://eur-lex.europa.eu/legal-content/EN/TXT/PDF/?uri=CELEX:02001L0018-20210327.

[483] Metson, G. S., Bennett, E. M., and Elser, J. J. The role of diet in phosphorus demand. *Environmental Research Letters*, 7, 044043, 2012, *doi*:10.1088/1748-9326/7/4/044043.

[484] Chen, M. and Graedel, T. E. A half-century of global phosphorus flows, stocks, production, consumption, recycling, and environmental impacts. *Global Environmental Change*, 36, 139-152, 2016, *doi*:10.1016/j.gloenvcha.2015.12.005.

[485] Starck, T., Fardet, T., and Esculier, F. Phosphorus recycling from human excreta in French agroecosystems and potential for food self-sufficiency. *Nutrient Cycling in Agroecosystems*, 129, 411-425, 2024, *doi*:10.1007/s10705-024-10367-4.

[486] De Boer, M. A., Romeo-Hall, A. G., Rooimans, T. M., and Slootweg, J. C. An Assessment of the Drivers and Barriers for the Deployment of Urban Phosphorus Recovery Technologies: A Case Study of The Netherlands. *Sustainability*, 10, 1790, 2018, *doi*:10.3390/su10061790.

[487] Shilton, A. N. and Blank, L. M. Phosphorus biotechnology. *Current Opinion in Biotechnology*, 23, 830-832, 2012, *doi*:10.1016/j.copbio.2012.09.007.

[488] The European Parliament and the Council of the European Union. REGULATION (EC) No 1333/2008 OF THE EUROPEAN PARLIAMENT AND OF THE COUNCIL of 16 December 2008 on food additives. *Official Journal of the European Union*, 2008, [Online]. Available: https://eur-lex.europa.eu/legal-content/EN/TXT/PDF/?uri=CELEX:32008R1333.

[489] Wang, H. *et al.* Identification of novel umami peptides from yeast extract and the mechanism against T1R1/T1R3. *Food Chemistry*, 429, 136807, 2023, *doi*:10.1016/j.foodchem.2023.136807.

[490] Podpora, B., Swiderski, F., Sadowska, A., Rakowska, R., and Wasiak-Zys, G. Spent brewer's yeast extracts as a new component of functional food. *Czech Journal of Food Sciences*, 34, 554-563, 2016, *doi*:10.17221/419/2015-CJFS.

[491] nova-Institut GmbH. Naturwissenschaftlich-regulatorische Einordnung Biopolyphosphate. Hark, N. and Dammer, L., 2024.

[492] Bundesinstitut für Risikobewertung. Intake of Phosphates: Babies, infants and children can exceed the health guidance values. *BfR Communication*, 2019, [Online]. Available: https://www.bfr.bund.de/cm/349/babies-infants-and-children-can-exceed-the-health-guidance%20values.pdf.

[493] Ritz, E., Hahn, K., Ketteler, M., Kuhlmann, M. K., and Mann, J. Phosphate additives in food-a health risk. *Dtsch Arztebl Int*, 109, 49-55, 2012, *doi*:10.3238/arztebl.2012.0049.

[494] Jacob, F., Striegel, L., Rychlik, M., Hutzler, M., and Methner, F.-J. Yeast extract production using spent yeast from beer manufacture: influence of industrially applicable disruption methods on selected substance groups with biotechnological relevance. *European Food Research and Technology*, 245, 1169-1182, 2019, *doi*:10.1007/s00217-019-03237-9.

[495] Kaelle, G. *et al.* Diet digestibility and palatability and intestinal fermentative products in dogs fed yeast extract. *Italian Journal of Animal Science*, 21, 802-810, 2022, *doi*:10.1080/1828051X.2022.2054733.

[496] Zhang, J., Reddy, J., Buckland, B., and Greasham, R. Toward consistent and productive complex media for industrial fermentations: Studies on yeast extract for a recombinant yeast fermentation process. *Biotechnology and Bioengineering*, 82, 640-652, 2003, *doi*:10.1002/bit.10608.

[497] Baker, L. M., Kraft, J., Karnezos, T. P., and Greenwood, S. L. Review: The effects of dietary yeast and yeast-derived extracts on rumen microbiota and their function. *Animal Feed Science and Technology*, 294, 115476, 2022, *doi*:10.1016/j.anifeedsci.2022.115476.

[498] Patterson, R., Rogiewicz, A., Kiarie, E. G., and Slominski, B. A. Yeast derivatives as a source of bioactive components in animal nutrition: A brief review. *Frontiers Veterinary Science*, 9, 1067383, 2022, *doi*:10.3389/fvets.2022.1067383.

[499] Shi, H. and Kim, I. H. Dietary yeast extract complex supplementation increases growth performance and nutrient digestibility of weaning pigs. *Livestock Science*, 230, 103850, 2019, *doi*:10.1016/j.livsci.2019.103850.

[500] Pan, L. *et al.* Yeast extract could be used as a partial substitute for spray-dried porcine plasma in diets for weaned pigs. *Livestock Science*, 224, 20-25, 2019, *doi*:10.1016/j.livsci.2019.04.002.

[501] van Dijk, A. J., Everts, H., Nabuurs, M. J. A., Margry, R. J. C. F., and Beynen, A. C. Growth performance of weanling pigs fed spray-dried animal plasma: a review. *Livestock Production Science*, 68, 263-274, 2001, *doi*:10.1016/S0301-6226(00)00229-3.

[502] Fathima, S., Shanmugasundaram, R., Sifri, M., and Selvaraj, R. Yeasts and yeast-based products in poultry nutrition. *Journal of Applied Poultry Research*, 32, 100345, 2023, *doi*:10.1016/j.japr.2023.100345.

[503] Frohn, L. *et al.* Yeast extract improves growth in rainbow trout (Oncorhynchus mykiss) fed a fishmeal-free diet and modulates the hepatic and distal intestine transcriptomic profile. *Aquaculture*, 579, 740226, 2024, *doi*:10.1016/j.aquaculture.2023.740226.

[504] Gaspar, L. R., Camargo, F. B., Gianeti, M. D., and Maia Campos, P. M. B. G. Evaluation of dermatological effects of cosmetic formulations containing *Saccharomyces cerevisiae* extract and vitamins. *Food and Chemical Toxicology*, 46, 3493-3500, 2008, *doi*:10.1016/j.fct.2008.08.028.

[505] Bentley, J. P. *et al.* Peptides from live yeast cell derivative stimulate wound healing. *Archives of Surgery*, 125, 641-646, 1990, *doi*:10.1001/archsurg.1990.01410170089019 %J Archives of Surgery.

[506] Kim, K. S. and Yun, H. S. Production of soluble β-glucan from the cell wall of *Saccharomyces cerevisiae*. *Enzyme and Microbial Technology*, 39, 496-500, 2006, *doi*:10.1016/j.enzmictec.2005.12.020.

[507] Vysoka, M. *et al.* Oleaginous Yeast Extracts and Their Possible Effects on Human Health. *Microorganisms*, 11, 492, 2023, *doi*:10.3390/microorganisms11020492.

[508] Mirzaei, M. *et al.* Bioactive peptides from yeast: A comparative review on production methods, bioactivity, structure-function relationship, and stability. *Trends in Food Science & Technology*, 118, 297-315, 2021, *doi*:10.1016/j.tifs.2021.10.008.

[509] Waszkiewicz-Robak, B. in *Lipid Metabolism.* Spent Brewer's Yeast and Beta-Glucans Isolated from Them as Diet Components Modifying Blood Lipid Metabolism Disturbed by an Atherogenic Diet (ed Rodrigo Valenzuela Baez), 2013, *doi*:10.5772/51530 (IntechOpen).

[510] Xi, Q., Lai, W., Cui, Y., Wu, H., and Zhao, T. Effect of Yeast Extract on Seedling Growth Promotion and Soil Improvement in Afforestation in a Semiarid Chestnut Soil Area. *Forests*, 10, 76, 2019, *doi*:10.3390/f10010076.

[511] Du, L. *et al.* Hyperuricemia and its related diseases: mechanisms and advances in therapy. *Signal Transduction and Targeted Therapy*, 9, 212, 2024, *doi*:10.1038/s41392-024-01916-y.

[512] Zare, F. *et al.* Uric acid, a nucleic acid degradation product, down-regulates dsRNA-triggered arthritis. *Journal of Leukocyte Biology*, 79, 482-488, 2005, *doi*:10.1189/jlb.0805426 %J Journal of Leukocyte Biology.

[513] Hou, C. *et al.* Guidelines for purine extraction and determination in foods. *Food Frontiers*, 2, 557-573, 2021, *doi*:10.1002/fft2.100.

[514] Coelho, M. O. C. *et al.* High dietary nucleotide consumption for one week increases circulating uric acid concentrations but does not compromise metabolic health: A randomised controlled trial. *Clinical Nutrition ESPEN*, 49, 40-52, 2022, *doi*:10.1016/j.clnesp.2022.04.022.

[515] Trevelyan, W. E. Determination of uric acid precursors in dried yeast and other forms of single-cell protein. *Journal of the Science of Food and Agriculture*, 26, 1673-1680, 1975, *doi*:10.1002/jsfa.2740261108.

[516] Alim, A. *et al.* Changes in the perception of bitter constituents in thermally treated yeast extract. *Journal of Food and Agriculture*, 99, 4651-4658, 2019, *doi*:10.1002/jsfa.9705.

[517] Benavides, D., Boehmwald, F., Illanes, A., Guerrero, C., and Urrutia, P. Debittering yeast extract from spent brewer's yeast by adsorption of iso-α-acids onto macroporous resin. *LWT*, 227, 117977, 2025, *doi*:10.1016/j.lwt.2025.117977.

[518] Jaeger, A., Arendt, E. K., Zannini, E., and Sahin, A. W. Brewer's Spent Yeast (BSY), an Underutilized Brewing By-Product. *Fermentation*, 6, 123, 2020, *doi*:10.3390/fermentation6040123.

[519] Zheng, Y. *et al.* Investigating characteristics and possible origins of off-odor substances in various yeast extract products. *Journal of Food Biochemistry*, 44, e13184, 2020, *doi*:10.1111/jfbc.13184.

[520] Rakowska, R., Sadowska, A., Dybkowska, E., and Świderski, F. Spent yeast as natural source of functional food additives. *Rocz Panstw Zakl Hig*, 68, 115-121, 2017.

[521] Tomé, D. Yeast Extracts: Nutritional and Flavoring Food Ingredients. *ACS Food Science & Technology*, 1, 487-494, 2021, *doi*:10.1021/acsfoodscitech.0c00131.

[522] Frohnmeyer, H., Kodra, N., and Elling, L. Advanced enzymatic multigram-scale production of nucleotide sugars in a continuous fed-batch membrane reactor. *Journal of Biotechnology*, 395, 1-11, 2024, *doi*:10.1016/j.jbiotec.2024.09.001.

[523] Dutta, A. and Trivedi, A. Waste to Wealth: Utilization of Slaughterhouse Wastes as Phosphate Fertilizer in India. *National Academy Science Letters*, 45, 467-471, 2022, *doi*:10.1007/s40009-022-01152-4.

[524] Fernández-Delgado, M., del Amo-Mateos, E., García-Cubero, M. T., Coca, M., and Lucas, S. Phosphorus recovery from organic waste for its agronomic valorization: technical and economic evaluation. *J Chem Technol Biotechnol*, 97, 167-178, 2022, *doi*:10.1002/jctb.6926.

[525] Yu, J. *et al.* Polyphosphate-enriched algae fertilizer as a slow-release phosphorus resource can improve plant growth and soil health. *Journal of Integrative Agriculture*, 24, 3656-3670, 2025, *doi*:10.1016/j.jia.2025.02.004.

[526] Johnson, W. *et al.* Safety Assessment of Phosphoric Acid and Its Salts as Used in Cosmetics. *International Journal of Toxicology*, 40, 34S-85S, 2021, *doi*:10.1177/10915818211014499.

[527] Hug, K. Genetically modified organisms: do the benefits outweigh the risks? *Medicina (Kaunas)*, 44, 87-99, 2008.

[528] European Commission. EU's rules on New Genomic Techniques. *Publications Office of the European Union*, 2025, *doi*:10.2875/1144622.

[529] EFSA, Panel on Genetically Modified Organisms *et al.* In vivo and in vitro random mutagenesis techniques in plants. 19, e06611, 2021, *doi*:10.2903/j.efsa.2021.6611.

[530] Lee, S. and Kim, P. Current Status and Applications of Adaptive Laboratory Evolution in Industrial Microorganisms. *Journal of microbiology and biotechnology*, 30, 793-803, 2020, *doi*:10.4014/jmb.2003.03072.

[531] Arora, N., Yen, H.-W., and Philippidis, G. P. Harnessing the Power of Mutagenesis and Adaptive Laboratory Evolution for High Lipid Production by Oleaginous Microalgae and Yeasts. *Sustainability*, 12, 5125, 2020, *doi*:10.3390/su12125125.

[532] Fukuda, N. Crossbreeding of Yeasts Domesticated for Fermentation: Infertility Challenges. *International Journal Molecular Sciences*, 21, 2020, *doi*:10.3390/ijms21217985.

[533] Judgment of the Court (Grand Chamber). Reference for a preliminary ruling - Deliberate release of genetically modified organisms into the environment - Mutagenesis - Directive 2001/18/EC - Articles 2 and 3 - Annexes I A and I B - Concept of 'genetically modified organism' - Techniques/methods of genetic modification conventionally used and deemed to be safe - New techniques/methods of mutagenesis - Risks for human health and the environment - Discretion of the Member States when transposing the directive - Directive 2002/53/EC - Common catalogue of varieties of agricultural plant species - Herbicide-tolerant plant varieties - Article 4 - Acceptability of genetically modified varieties obtained by mutagenesis for inclusion in the common catalogue - Human health and environmental protection requirement - Exemption., *Court reports*, 2018, [Online]. Available: https://eur-lex.europa.eu/legal-content/EN/TXT/PDF/?uri=CELEX:62016CJ0528.

[534] Hauschild, M. Z. in *CIRP Encyclopedia of Production Engineering.* Life Cycle Assessment (eds Sami Chatti, Luc Laperrière, Gunther Reinhart, & Tullio Tolio), 1034-1043, 2019, *doi*:10.1007/978-3-662-53120-4_16814 (Springer Berlin Heidelberg).

[535] Technical Committee ISORC 207. ISO 14040: Environmental management – Life cycle assessment – Principles and framework. *International Organization for Standardization*, 1997.

[536] Remy, C. and Kraus, F. in *Phosphorus Recovery and Recycling.* Life Cycle Assessment of Processes for P Recycling (eds Hisao Ohtake & Satoshi Tsuneda), 59-73, 2019, *doi*:10.1007/978-981-10-8031-9_4 (Springer Singapore).

[537] Becker, M., Ziemińska-Stolarska, A., Markowska, D., Lütz, S., and Rosenthal, K. Comparative Life Cycle Assessment of Chemical and Biocatalytic 2'3'-Cyclic GMP-AMP Synthesis. *ChemSusChem*, 16, e202201629, 2023, *doi*:10.1002/cssc.202201629.

[538] Dossow, M., Eyberg, V., Dieterich, V., Fendt, S., and Spliethoff, H. CESTEA: The TUM Chair of Energy Systems Techno-Economic Analysis Method. *TUM-CES White Paper Series "Energy System in Transition"*, 42, 2024, *doi*:10.14459/2024md1743206.

[539] Lynch, M. D. The bioprocess TEA calculator: An online technoeconomic analysis tool to evaluate the commercial competitiveness of potential bioprocesses. *Metabolic Engineering*, 65, 42-51, 2021, *doi*:10.1016/j.ymben.2021.03.004.

Curriculum Vitae

Personal Information

Name:	Alexander Deitert
Born:	18th January, 1996 in Bonn, North Rhine-Westphalia, Germany
Nationality:	German
Mobile	+491778704710
E-Mail:	alexander.deitert@rwth-aachen.de

Education

12/2021 – 11/2025
PhD candidate
RWTH Aachen University – Institute of Applied Microbiology
Contributions to a circular phosphate economy –
Polyphosphate production in *Saccharomyces cerevisiae*
Supervision: Prof. Dr.-Ing. Lars M. Blank

04/2018 – 09/2021
Molecular and Applied Biotechnology, M.Sc.
RWTH Aachen University
Final grade: 1.0
Master thesis: Development and implementation of an *in situ* adsorption process for purification of fermentation broths from biorefinery processes
Supervision: Dr. Johannes Pastoors, Prof. Dr.-Ing. Jochen Büchs, Prof. Dr.-Ing. Andreas Jupke

10/2014 – 03/2018
Molecular and Applied Biotechnology, B.Sc.
RWTH Aachen University
Final grade: 1.4
Bachelor thesis: Ames RAMOS test: Investigating the influence of different media components and optimizing the process performance in the RAMOS and µRAMOS device
Supervision: Dr. Kira Kauffmann, Prof. Dr.-Ing. Jochen Büchs, Prof. Dr. rer. nat. Henner Hollert

08/*2006 – 06/2014*
Abitur
Geschwister-Scholl-Gymnasium Stadtlohn
Final grade: 1.0

Practical Experience

02/2020 – 09/2020
Voluntary Research Internship Abroad
Enhanced butanol production in the integrated fed-batch fermentation process with pervaporation
Prof. Dr. Lars Rehmann, Department of Chemical and Biochemical Engineering, University of Western Ontario, Canada

09/2019 – 01/2020
Voluntary Research Internship
Working with spore-forming microorganisms and defining media requirements
Dr. Jennifer Goldmanns, Institute of Biochemical Engineering, RWTH Aachen University

09/2018 – 01/2020
Research Assistant for Fermentation Processes
Institute of Biochemical Engineering, RWTH Aachen University

04/2017 – 07/2017	**Voluntary Research Internship** Boosting the performance of a protease in the presence of two model polymers Dr. Martin Thiele, Schwaneberg Group, RWTH Aachen University
12/2016 – 03/2017	**Voluntary Research Internship** iGEM continue project Dr. Martin Thiele, Schwaneberg Group, RWTH Aachen University
09/2015 – 10/2016	**iGEM Team Aachen** RWTH Aachen University
08/2013	**Voluntary Internship Abroad** Bewital Nutrición España SL, Madrid, Spain Subsidiary of Bewital Petfood GmbH & Co. KG

Research Papers

Deitert, A.[§], Fees, J.[§], Mertens, A., Nguyen Van, D., Maares, M., Haase, H., Blank, L. M., and Keil, C. Rapid Fluorescence Assay for Polyphosphate in Yeast Extracts Using JC-D7. *Yeast*, 41, 593-604, 2024, doi: 10.1002/yea.3979.

Deitert, A., Baier, M., Eerlings, R., Fees, J., Österlein Kück, A., Repin, J., Demling, P., and Blank, L. M. Polyphosphate Accumulation Is Determined by Zinc and Inositol in *Saccharomyces cerevisiae*. *Yeast*, 0, 1–12, 2025, doi: 10.1002/yea.70006.

Battling, S., Pastoors, J., **Deitert, A.**, Götzen, T., Hartmann, L., Schröder, E., Yordanov, S., and Büchs, J. Development of a novel defined minimal medium for *Gluconobacter oxydans* 621H by systematic investigation of metabolic demands. *Journal of Biological Engineering*, 16, 31, 2022, doi: 10.1186/s13036-022-00310-y.

Demling, P., Baier, M., **Deitert, A.**, Fees, J., and Blank, L. M. Biotechnological polyphosphate as an opportunity to contribute to the circularization of the phosphate economy. *Current Opinion in Biotechnology*, 87, 103107, 2024, doi: 10.1016/j.copbio.2024.103107

Forsten, E., Finger, M., Scholand, T., **Deitert, A.**, Kauffmann, K., and Büchs, J. Inoculum cell count influences separation efficiency and variance in Ames plate incorporation and Ames RAMOS test. *Science of the Total Environment*, 905, 167035, 2023, doi: 10.1016/j.scitotenv.2023.167035

Goldmanns, J., Röhling, G. A., Lipa, M. K., Scholand, T., **Deitert, A.**, May, T., Haas, E. P., Boy, M., Herold, A., and Büchs, J. Development of a chemically defined medium for *Paenibacillus polymyxa* by parallel online monitoring of the respiration activity in microtiter plates. *BMC Biotechnology*, 23, 25, 2023, doi: 10.1186/s12896-023-00793-7

Kauffmann, K., Werner, F., **Deitert, A.**, Finklenburg, J., Brendt, J., Schiwy, A., Hollert, H., and Büchs, J. Optimization of the Ames RAMOS test allows for a reproducible high-throughput mutagenicity test. *Science of the Total Environment*, 717, 137168, 2020, doi: 10.1016/j.scitotenv.2020.137168

Pastoors, J., **Deitert, A.**, Michel, C., Günster, K., Finger, M., Hofstede, J., Deischter, J., Biselli, A., Viell, J., Palkovits, R., Jupke, A., and Büchs, J. *In situ* adsorption of itaconic acid from fermentations of *Ustilago cynodontis* improves bioprocess efficiency. *Biotechnology for Biofuels and Bioproducts*, 16, 181, 2023, doi: 10.1186/s13068-023-02433-w

Pastoors, J., Baltin, C., Bettmer, J., **Deitert, A.**, Götzen, T., Michel, C., Deischter, J., Schroll, I., Biselli, A., Palkovits, R., Rose, M., Jupke, A., and Büchs, J. Respiration-based investigation of adsorbent-bioprocess compatibility. *Biotechnology for Biofuels and Bioproducts*, 16, 49, 2023, doi: 10.1186/s13068-023-02297-0

Plouviez, M., Demling, P., **Deitert, A.**, Fees, J., Baier, M., Karmainski, T., Blank, L. M., and Guieysse, B. Coming to Terms: The Mechanisms of Overplus and Luxury Phosphorus Uptake for Polyphosphate Storage in Microalgae and Yeast. *Biotechnology and Bioengineering*, 0, 1–10, 2025, doi: 10.1002/bit.70061.

Oral presentations

Deitert, A.[§], Fees, J.[§], Demling, P., and Blank, L. M. Establishing a circular phosphate economy – Polyphosphate production in *Saccharomyces cerevisiae*. Himmelfahrtstagung on Bioprocess Engineering 2022 – Future Bioprocesses for a Sustainable Industry, 23rd-25th May, 2022, Mainz, Germany.

Deitert, A., Fees, J., Baier, M., Demling, P., and Blank, L. M. Contributing to a circular phosphate economy – Polyphosphate production in *Saccharomyces cerevisiae*. FEBS workshop Polyphosphate: The Actual Biology of an Ancient Polymer, 09th-12th May, 2023, Cádiz, Spain.

Deitert, A., Demling, P., Fees, J., Baier, M., Christ, J. J., and Blank, L. M. Bioprocess development for the production of polyphosphate-rich yeast extract as a novel food additive. 34th VH Yeast Conference, 15th-16th May, 2023, Vienna, Austria.

Posters

Deitert, A.[§], Völker, F.[§], Teucher, P., Demling, P., and Blank, L. M. Food4Root – Development of a slow-release fertilizer based on the biopolymers poly-γ-glutamic acid and polyphosphate. The 7th Applied Synthetic in Biology in Europe (ASBE7), 06th-08th November, 2024, Brno, Czech Republic.

Deitert, A., Demling, P., Baier, M., Karmainski, T., Fees, J., and Blank, L. M. Bioprocess development for the production of polyphosphates with novel applications. 8. BioProcessingDays 2025, 24th-26th February, 2025, Recklinghausen, Germany.

Deitert, A., Baier, M., Fees, J., Demling, P., Karmainski, T., and Blank, L. M. Bioprocess development to produce polyphosphate-rich yeast extract as a novel food additive. PolyP-2025, the third international Conference on Polyphosphate Biology, 20th-23rd May, 2025, Ann Arbor, MI, USA.

Baier, M., Demling, P., Fees, J., **Deitert, A.**, and Blank, L. M. Metabolic engineering of *S. cerevisiae* for polyphosphate production. 8th Conference on Physiology of Yeast and Filamentous Fungi (PYFF), 05th-08th June, 2023, Cork, Ireland.

Baier, M., Fees, J., **Deitert, A.**, Karmainski, T., Demling, P., and Blank, L. M. Metabolic engineering of *S. cerevisiae* for polyphosphate production. Metabolic Engineering 16, 15th-19th June, 2025, Copenhagen, Denmark.

Demling, P., Fees, J., **Deitert, A.**, Jensen, P. E., Worberg, A., Sudarsan, S., and Blank, L. M. Bioprocess development for the production of polyphosphates with novel applications. Recent Advances In Fermentation Technology (RAFT), 05th-09th November, 2022, Bonita Springs, Florida, USA.

Demling, P.§, **Deitert, A.**§, Fees, J.§, Mertens, M., Nguyen Van, D., Maares, M., Haase, H., Blank, L. M., and Keil, C.§. Easing Polyphosphate Detection in Yeast Extracts through JC-D7 Fluorescence Assay. 36th VH Yeast Conference. 22nd-23rd May, 2025, Düsseldorf, Germany.

Demling, P., Karmainski, T., Baier, M., **Deitert, A.**, Fees, J., and Blank, L. M. Synergistic approach for the biotechnological production of polyphosphates in baker's yeast. Himmelfahrtstagung on Bioprocess Engineering 2025, 26th-28th May, 2025, Bremen, Germany.

Fees, J., **Deitert, A.**, Baier, M., Demling, P., and Blank, L. M. Biotechnological polyphosphate production by *Saccharomyces cerevisiae* using phosphate-rich waste streams. FEBS workshop Polyphosphate: The Actual Biology of an Ancient Polymer, 09th-12th May, 2023, Cádiz, Spain.

Karmainski, T., Demling, P., Baier, M., **Deitert, A.**, Willing, K., Regestein, L., and Blank, L. M. Process-guided strain engineering enables efficient fermentation. 36th VH Yeast Conference. 22nd-23rd May, 2025, Düsseldorf, Germany.

Karmainski, T., Demling, P., Baier, M., **Deitert, A.**, Willing, K., Regestein, L., and Blank, L. M. Polyphosphate production in baker's yeast – Process-guided strain engineering enables efficient fermentation. Himmelfahrtstagung on Bioprocess Engineering 2025, 26th-28th May, 2025, Bremen, Germany.

Keil, C.§, **Deitert, A.**§, Fees, J.§, Mertens, M., Nguyen Van, D., Maares, M., Haase, H., and Blank, L. M. Easing Polyphosphate Detection in Yeast Extracts through JC-D7 Fluorescence Assay. 38th Annual Meeting of the German Society for Minerals and Trace Elements (GMS) jointly with the Annual Meeting of the Society for Magnesium Research, 24th-26th October, 2024, Munich, Germany.

§ The authors share the first author.

- Additional co-authorship of several conference presentations (oral and poster).
- Co-authorship of three grant proposals.